# Contents

## S16 Session 16: Radiation in the environment
Oral presentations


**S16-01** **Regularities of long-term changes in artificial radionuclides content in the Barents Sea ecosystem** . . . . . 2337
Matishov, Gennady; Matishov Dmitry; Solatie Dina; Kasatkina Nadezda; Leppänen Ari-Pekka

**S16-02** **Human dose pathways from forests contaminated by atmospheric radionuclide deposition** . . . . . 2345
Rantavaara, Aino; Ammann, Michael

**S16-03** **Occurrence of plutonium in the terrestrial environment at Thule, Greenland** . . . . . 2356
Roos, Per; Jernström, Jussi; Nielsen, Sven P.

**S16-04** **Environmental radioactivity assessment at nuclear legacy sites in the Republic of Tajikistan** (ABSTRACT) . . . . . 2362
Nalbandyan, Anna; Hosseini, Ali

**S16-05** **Improved model for estimation of fallout from atmospheric nuclear testing** (ABSTRACT) . . . . . 2363
Pálsson, Sigurdur Emil; Howard, Brenda J.; Ikäheimonen, Tarja K.; Nielsen, Sven P.

**S16-06Y** **Reduction of radioxenon emissions from radiopharmaceutical facilities – A pilot study** . . . . . 2364
Braekers, Damien; Camps, Johan; Paridaens, Johan; Saey, Paul R. J.; van der Meer, Klaas

**S16-07Y** **Public exposure by natural radionuclides in drinking water – Models for effective dose assessment and implications to guidelines** . . . . . 2374
Gruber, Valeria; Maringer, Franz Josef

# Contents

## P16 Topic 16: Radiation in the environment
Poster presentations


P16-01 **Impact of facilities under the nuclear fuel cycle on the public health: SUE "Hydro Metallurgical Plant" (LPO "ALMAZ") case study** . . . . . 2383
Titov, A. V.; Tukov, A. R.; Bogdanova, L. S.; Yatsenko, V. N.; Korzinkin, M. B.

P16-02 **Modelling with a CFD code the near-range dispersion of particles unexpectedly released from a nuclear power plant** . . . . . 2392
Gallego, Eduardo; Barbero, Rubén; Cuadra, Daniel; Domingo, Jerónimo; Iranzo, Alfredo

P16-03 **Inspection Plan for the detection of contamination at a Nuclear Fuel Cycle facility** . . . . . 2401
Pérez Fonseca, Agustín; Ortiz Trujillo, Diego

P16-04 **Establishment of a special radiological surveillance programme at the "El Cabril" solid radioactive waste disposal facility** . . . . . 2407
Ortiz, Teresa; Fuentes, Luis; Pinilla, José Luis

P16-05 **Monitoring of radionuclides in the vicinity of Czech nuclear power plants** . . . . . 2418
Svetlik, Ivo; Fejgl, Michal; Beckova, Vera; Pospichal, Jiri; Striegler, Rostislav; Tomaskova, Lenka

P16-06 **$^{14}$C in biological samples from the vicinity of NPP Krško** . . . . . 2428
Obelić, Bogomil; Krajcar Bronić, Ines; Barešić, Jadranka; Horvatinčić, Nada; Sironić, Andreja; Breznik, Borut

P16-07 **Uranium and long-lived decay products in water of the Mulde River** . . . . . 2436
Bister, Stefan; Koenn, Florian; Bunka, Maruta; Birkhan, Jonny; Lüllau, Torben; Riebe, Beate; Michel, Rolf

P16-08 **$^{129}$I in Finnish waters** (ABSTRACT) . . . . . 2445
Räty, Tero; Lehto, Jukka; Hou, Xiaolin; Possnert, Göran; Paatero, Jussi; Flinkman, Juha; Kankaanpää, Harri

P16-09 **Monitoring and assessment of radioactivity in the Baltic Sea coordinated by HELCOM** (ABSTRACT) . . . . . 2446
Nielsen, Sven P.; Ikäheimonen, Tarja K.; Outola, Iisa; Vartti, Vesa-Pekka; Herrmann, Jürgen; Kanisch, Günter; Suplinska, Maria; Zalewska, Tamara; Vilimaite-Silobritiene, Beata; Stepanov, Andrey; Osokina, Anna; Lüning, Maria; Osvath, Iolanda; Jakobson, Eia

P16-10 **Results obtained in monitoring programmes and environmental studies carried out during more than 40 years in the sea areas surrounding the Finnish NPPs** . . . . . 2448
Ilus, Erkki

P16-11 **Tritium level along Romanian Danube river sector** . . . . . 2458
Varlam, Carmen; Stefanescu, Ioan; Vagner, Irina; Faurescu, Ionut; Faurescu, Denisa

P16-12 **Radioactivity monitoring of sediments in rivers in Serbia during the period 2005–2009** . . . . . 2465
Eremic-Savkovic, Maja; Pantelic, Gordana; Vuletic, Vedrana; Tanaskovic, Irena; Javorina, Ljiljana

P16-13 **Radiocarbon and tritium activity in the environment of the National Park Plitvice Lakes** (ABSTRACT) . . . . . 2471
Horvatinčić, Nada; Barešić, Jadranka; Krajcar Bronić, Ines; Obelić, Bogomil

P16-14 **$^{137}$Cs concentrations in Saimaa ringed seals during 2003–2009** . . . . . 2472
Ylipieti, Jarkko; Solatie, Dina

P16-15 **Radioactivity of $^{210}$Po in oysters collected in Taiwan** . . . . . 2480
Lee, Hsiu-wei; Wang, Jeng-Jong; Chang, Bor-Jing

P16-16 **Natural alpha emitting radionuclides in bottled drinking water, mineral water and tap water** . . . . . 2487
Benedik, Ljudmila; Jeran, Zvonka

# Contents


P16-17 **Radiation protection of the public and the environment: long-term, large-scale radioecological monitoring by spruce needles** (ABSTRACT) . . . . . 2495
Seidel, Claudia; Gruber, Valeria; Maringer, Franz Josef

P16-18 **Slovenian experience with inconsistencies in the global contamination monitoring results** . . . . . 2496
Cindro, Michel; Vokal Nemec, Barbara; Križman, Milko

P16-19 **Problems connected to measuring a valid Peak-to-valley ratio in field gamma spectrometry** (ABSTRACT) . . . . . .2503
Östlund, Karl; Samuelsson, Christer

P16-20 **Interception of wet deposition of radiocaesium and radiostrontium by *Brássica napus*** . . . . . 2504
Rosén, Klas; Bengtsson, B. Stefan

P16-21 **Variation of dietary intake of radioactive cesium after the Chernobyl fallout in Finland** . . . . . 2509
Kostiainen, Eila; Outola, Iisa; Huikari, Jussi; Solatie, Dina

P16-22 **Investigation of $^{137}$Cs redistribution within urban ecosystem** . . . . . 2518
Seleznev, Andrian A.; Yarmoshenko, Ilia V.; Ekidin, Alexey A.

P16-23 **Radioactivity in the environmental samples around the Cernavoda NPP** . . . . . 2523
Popoaca, Simona; Bucur, Cristina; Simionov, Vasile

P16-24 **Radionuclides activity concentration in soil in Serbia** . . . . . 2530
Pantelić, Gordana; Eremić Savković, Maja; Vitorović, Gordana; Vuletić, Vedrana; Tanasković, Irena; Javorina, Ljiljana

P16-25 **Monte Carlo calculation of ambient dose equivalent and effective dose from natural radionuclides in the soil of Vojvodina district in Serbia** . . . . . 2534
Spasic Jokic, Vesna; Gordanic, Vojin

P16-26 **Interpretation of radionuclide concentrations near the detection limit for dose calculations** . . . . . 2541
Črnič, Boštjan; Korun, Matjaž; Zorko, Benjamin

P16-27 **Environmental tritium monitoring techniques applied for a tritium removal facility** (ABSTRACT) . . . . . 2549
Dobrin, Relu; Dulama, Cristian; Toma, Alexandru;
Ciurduc Todoran, Germizara Anca; Varlam, Carmen; Pavelescu, Mihai

P16-28 **Radioecological studies in the Barents Sea (results of expedition in 2007–2009)** . . . . . 2550
Leppänen, Ari-Pekka; Kasatkina, Nadezda; Matishov, Gennady; Solatie, Dina

P16-29 **Experimental study of the radionuclides transport in soil and plants from waste dump** . . . . . 2555
Bragea, Mihaela; Aldave de las Heras, Laura; Cristache, Carmen; Carlos Marquez, Ramon; Toro, Laszlo

P16-30 **HYDRUS-computer simulation of radionuclide migration in groundwater due to clearance of low-level waste from decommissioning** . . . . . 2561
Merk, Rainer

P16-31 **Radioactivity in Trinitite – a review and new measurements** . . . . . 2569
Pittauerová, Daniela; Kolb, William M.; Rosenstiel, Jon C.; Fischer, Helmut W.

P16-32 **External exposure of a representative individual at selected sites of the peaceful underground nuclear explosions in Russia** . . . . . 2579
Ramzaev, Valery; Repin, Victor; Medvedev, Alexander; Khramtcov, Evgeny; Timofeeva, Maria; Mishin, Arkady

# Regularities of long-term changes in artificial radionuclides content in the Barents Sea ecosystem

Matishov, Gennady[1]; Matishov Dmitry[1]; Solatie Dina[2];
Kasatkina Nadezda[1]; Leppänen Ari-Pekka[2]
[1] Murmansk Marine Biological Institute of the Kola Science Center of RAS, RUSSIA
[2] STUK – Radiation and Nuclear Safety Authority, Regional Laboratory in Northern Finland, FINLAND

## Abstract
The comparative analysis is performed for the radiation contamination of the Barents Sea ecosystem in the 1980s and 1990s and in the first decade of the 21st century. Natural purification processes in the marine environment are the main factors of the decrease in the intensity level of artificial radioactive isotopes. These processes include repeated dilution, nuclear decay, sorption by sediments and suspended solid material, and accumulation by aquatic inhabitants. A stable decreasing trend is observed for the intensity level of artificial radioactive isotopes in the Barents Sea.

## Introduction
The phenomenon of artificial radioactivity has been observed for the natural environment since the first nuclear tests in 1940s and continues at present. The disposal and dumping of both solid and liquid nuclear waste were typical for the Arctic and the northern seas. Radiological hazard sites can be observed in the coastal area, which are concentrated in Kola and Motovsky bays; the city of Murmansk, as well as towns: Severomorsk, Polyarny, and Gadzhievo; and the following fjords: Saida, Olenya, Pala, Zapadnaya Litsa, Ura, and Ara. Gaseous, liquid, and solid nuclear wastes are being stored there. The European reprocessing plants are the most significant producers of nuclear waste in the Arctic Ocean. The Sellafield factory (Great Britain) is the biggest one amongst them. The total activity of radionuclides discharged by these plants was $160\times10^{15}$ Bq. Around 10–20% of $^{137}$Cs discharged in Sellafield and around 30% of $^{90}$Sr enter the Barents Sea. The plume of west European discharges crosses the shelf area of the Barents Sea and reaches the Central Polar Basin in six years (Nikitin et al., 1991; Nies, Nielsen, 1996; Matishov, Matishov, 2004). The input of Chernobyl accident provided from 10 to 20% of the radioactive pollution of the Kara and Barents seas in the 1990s.

The concentration of radioactivity has decreased an order of magnitude in the Arctic marine ecosystems from the 1960s to the 1990s as a result of water self-purification, natural decay of $^{90}$Sr and $^{137}$Cs, and the reduction of nuclear waste

dumping. At the same time, with the time passed after the Chernobyl accident and the moment nuclear tests on the Novaya Zemlya and adjacent shelf were ceased, it is reasonable to follow the evolution of anthropogenic radioisotopes in the first decade of the 21st century. Of vital importance are also the problems of radiation safety, ecological standardization and forecast of the long-term effect of low doses on the marine biota. Not less important is the forecast of ecological security in case of nuclear energy installations' application while oil and gas development and extraction on shelf, in particular, at the Stockman gas condensate deposit.

Murmansk Marine Biological Institute of the Kola science center of the Russian academy of sciences (MMBI KSC RAS) has been carrying out regular monitoring of artificial radionuclides in the environment and organisms of the West Arctic seas since 1990 (Matishov 1994, 1995, 1996; Smith et al. 1995; Matishov, Matishov, 2004). In 1992-1999 radiation monitoring was carried out by MMBI in co-operation with Radiation and Nuclear Safety Authority (STUK, Finland). This co-operation got new development in 2006-2007.

## Material and methods

Materials for radioecological investigations were collected during both coastal and marine multi-disciplinary expeditions of MMBI KSC RAS.

Preliminary concentration of cesium isotopes from water samples (100 l volume each) were performed by the cellulose-inorganic sorbent *ANFEZH*. The measurements of $^{137}$Cs, $^{40}$K, and $^{226}$Ra activity were made by the *Canberra* gamma-spectrometer. To determine the specific activity of $^{90}$Sr oxalate-radiochemical preparation was applied with subsequent measurement of counting sample at the *Beckman LS-6500* alpha-beta-scintillation counter by Cherenkov radiation of daughter radionuclide $^{90}$Y. The anion exchange method was applied to analyze the Pu isotopes, when $^{242}$Pu was used as a tracer agent. To determine Polonium samples were treated by tracer $^{209}$Po and isotope $^{210}$Po was deposited on a silver disk (Vesterbacka, Ikäheimonen, 2005). The activity of $^{238}$Pu, $^{239,240}$Pu, and $^{210}$Po isotopes was measured by the alpha-spectrometer *Canberra Alpha Analyst.* The standard *Genie-2000* software was used for spectrum analysis.

The gamma-emitting isotopes and $^{90}$Sr activity were measured at the certified radioecological laboratory of MMBI KSC RAS. The $^{238}$Pu, $^{239,240}$Pu isotope activity was measured at the laboratory of STUK. The inter-calibration, which gave good concordance of results obtained at two laboratories, was carried out during the joint activities.

## Results and Discussion

The radioecological pattern of the Barents Sea at the end of the twentieth century was quite patchy. The $^{137}$Cs activity concentration in the waters was relatively high at the end of the 1980s, from 10 to 40-90 Bq/m$^3$. The concentration of this isotope decreased in the middle of the 1990s an order of magnitude and did not reach more than 2-15 Bq/m$^3$. The content of $^{137}$Cs in the waters of the Zapadnaya Litsa Fjord was 4.9 Bq/m$^3$, of the Ara Fjord – 4.7 Bq/m$^3$, in the entrance of the Kola Bay to the Barents Sea – 8 Bq/m$^3$. The volumetric activity of $^{90}$Sr varied from 1 to 7 Bq/m$^3$ in the 1990s. The $^{239,240}$Pu activity decreased from 13-18 to 6-11 Bq/m$^3$ from the 1980s to the 1990s. The waters close to

the radioactive waste treatment plant RTP «*Atomflot*» were enriched by $^{239,240}$Pu of 18-70 Bq/m$^3$ at the end of the 1990s (Matishov et al. 1996, 1997; Matishov, Matishov, 2004).

The specific activity of $^{137}$Cs in the bottom sediments of the Barents Sea varied from 10 to 30 Bq/kg dry weight. The coastal areas of Spitsbergen, the Kola Peninsula, Novaya Zemlya, Franz Josef Land, and the shallow waters of the Pechora Sea were characterized by lower activity of $^{137}$Cs, from 0.6-3.0 to 6.0 Bq/kg. Relatively higher concentrations of $^{137}$Cs (5-11 Bq/kg) are typical for bottom sediments in all troughs and trenches in the open areas of the shelf. Clayish sediments covering the bottom of the Central Trench (300-380 m deep) contained 5-9 Bq/kg of $^{137}$Cs and 0.2-0.8 Bq/kg of $^{90}$Sr (Matishov et al. 1994, 1995, 1996; Matishov, Matishov, 2004). $^{239,240}$Pu was found everywhere in the sediments of the Barents Sea shelf, from 0.1 to 20 Bq/kg. The distribution of this isotope depends on the sediment type and geographical distance to the nuclear weapons range. The silts of the Central Trench contain from 0.9 to 3.2 Bq/kg of $^{239,240}$Pu. The concentration of this isotope is quite low in sands and aleurites of the shallow waters (0.1-1.0 Bq/kg); it may increase up to 3.2–4.3 Bq/kg in some trenches and downwarpings, and it is as high as 13 Bq/kg in the South-Novozemelskaya Trench to the south of Chernaya Guba (Matishov, Matishov, 2004). The bottom sediments of the Zapadnaya Litsa, Saida, Pala fjords (Kola and Motovskii bays) are characterized by a concentration of 2 to 9 Bq/kg of $^{239,240}$Pu, and higher concentrations of $^{137}$Cs (30-120 Bq/kg) and $^{60}$Co (from 4-10 to 80 Bq/kg) (Matishov et al. 1996; Matishov, Matishov, 2004). These fjords are the nuclear-power submarine depot complexes.

Macroalgae, mostly *Fucus* spp. and *Laminaria* spp., accumulate the isotopes in the coastal waters. The maximal activity of $^{137}$Cs was found in the early 1980s (up to 10 Bq/kg) and after the Chernobyl event (up to 7 Bq/kg) (Matishov 1995; Matishov, Matishov, 2004). In the 1980s and 1990s, the macrophytes contained up to 0.4-5.0 Bq/kg of $^{137}$Cs, 0.3-3.0 Bq/kg of $^{90}$Sr, and 0.02-0.3 Bq/kg of $^{239,240}$Pu. The local contamination was focused on the water area close to the vessel «Lepse» belonging to RTP «Atomflot». This vessel is used as a spent-fuel storage; the concentration of isotopes in the macrophytes here was as high as 20–46 Bq/kg of $^{137}$Cs, 1.2 Bq/kg of $^{134}$Cs, 1.6 Bq/kg of $^{60}$Co, and 4.6 Bq/kg of $^{152}$Eu (Matishov, Matishov, 2004). However, this contamination is several orders lower than that observed in other areas after the Chernobyl event.

To ascertain the contemporary degradation regularities of anthropogenic radioactive substances, the Barents Sea water, bottom sediments, and algae – bio-indicators of radioactive contamination – were analyzed in 2005-2009. It is quite obvious that a natural decrease of artificial radionuclides' content is typical of all elements of marine ecosystem for the last decade (Matishov et al. 2004, 2005, 2007). Obviously, all the ecosystem elements are characterized by decrease in the anthropogenic isotope concentrations for the last decade.

The volumetric activity of the radionuclide $^{137}$Cs in the Barents Sea in 2005-2007 is quite equable for all the investigated areas. The isotope activity is low and varies from 1-2 to 3.6 Bq/m$^3$, decreasing an order of magnitude compared to the 1970s. The maximal $^{137}$Cs content of 6.5 Bq/m$^3$ was registered in Kola Bay waters near the area of RTP «Atomflot» outfall. Relatively high concentrations were found in the coastal area on the way of the Murmansk costal current. The activity of $^{137}$Cs in Dalnezelenetskaya and Teriberskaya bays varied about 3.4-3.6 Bq/m$^3$. The activity of the same isotope constituted about 2 Bq/m$^3$ in the waters off the Novaya Zemlya western coast and, thus,

was close to average for the Barents Sea. The $^{90}Sr$ comes from the Norwegian Sea by the warm currents, according to the data of 2005-2009. The Atlantic warm waters are characterized by increased concentration of $^{90}Sr$, reaching up to 6-8 Bq/m$^3$. The concentration of $^{90}Sr$ is several times lower and is about 1-4 Bq/m$^3$ in the south-eastern sector of the Barents Sea, where the waters are already transformed. The activity of this isotope is 1.2-3.9 Bq/m$^3$ along the Novaya Zemlya coast.

The present-day contamination level of the bottom sediments in the Barents Sea is quite low. The average specific activity of $^{137}Cs$ is 1-3 Bq/kg and $^{90}Sr$ is 0.2-2.0 Bq/kg in the bottom sediments for the period of 2005-2009 (Fig 1a). The predictable activity of the isotopes is usual for all the bottom sediments of the Barents Sea with some exceptions for the coastal areas. The minimal activities of $^{137}Cs$ (0.5-2.9 Bq/kg) and $^{90}Sr$ (0.1-2.0 Bq/kg) were found in the open areas of the sea, where quartz is the main rock-forming mineral. Quartz is characterized by a low sorption capacity. The local increase of $^{137}Cs$ activity (5-8 Bq/kg) was observed in troughs near the Franz Josef Land. The bottom sediments there are mostly formed by silts. The bottom sediments off the Novaya Zemlya coast contained up to 4.7 Bq/kg of $^{137}Cs$. The specific activity of $^{238}Pu$ in bottom sediment along the standard section No. 6 was 0.02-0.04 Bq/kg. $^{239}Pu$ activity was 0.4-1.3 Bq/kg. The analyzed ratio $^{238}Pu/^{239}Pu$ in the sediment samples showed that the plutonium is from global fallout from the atmospheric nuclear weapons testing.

The main part of system radioecological studies is the establishment of balance mathematical models. The obtained data on radionuclide distribition in waters was applied to calculate the current balance of artificial radionuclides in the Barents Sea. The calculation results show that the input of $^{137}Cs$ and $^{90}Sr$ is largely determined by the radionuclides exchange on the western boundaries of the Sea, where the resulting transfer is always directed from the Norwegian Sea to the Barents Sea. The contribution of atmospheric fallout and river runoff into the total radionuclides input is negligible at present as compared to radionuclide input with the Atlantic waters which is about 64 TBq/year of $^{137}Cs$ and 271 TBq/year $^{90}Sr$.

The bottom sediments sampled from the station on the north-western slope of the Murmansk Bank, which is affected by the Norwegian Current, were characterized by the presence of $^{125}Sb$ (half-life period 2.77 years). This anthropogenic radionuclide, together with $^{99}Tc$, is usually associated with liquid discharges of the nuclear industry plants. Its presence in the Barents Sea indicates that a small amount of radioactive wastes of the Sellafield Plant comes with Atlantic waters.

Some of the Barents Sea coastal areas, including Kola Bay, are characterized by increased concentration of the anthropogenic radionuclide in the bottom sediments. These areas belong to the local sources of pollution, such as numerous depot complexes of atomic submarines and icebreakers, the places of the moorings and waste reclamation of these vessels, and radioactive waste storage sites. Bottom sediments within the territory of RTP «Atomflot» are characterized by the highest levels of $^{137}Cs$ up to 20 Bq/kg (Fig 1b). Besides $^{137}Cs$ and $^{90}Sr$ some other anthropogenic radionuclides, such as $^{152}Eu$, $^{60}Co$, $^{134}Cs$, were found in this sample. The presence of these isotopes is not typical for the open parts of the Barents Sea.

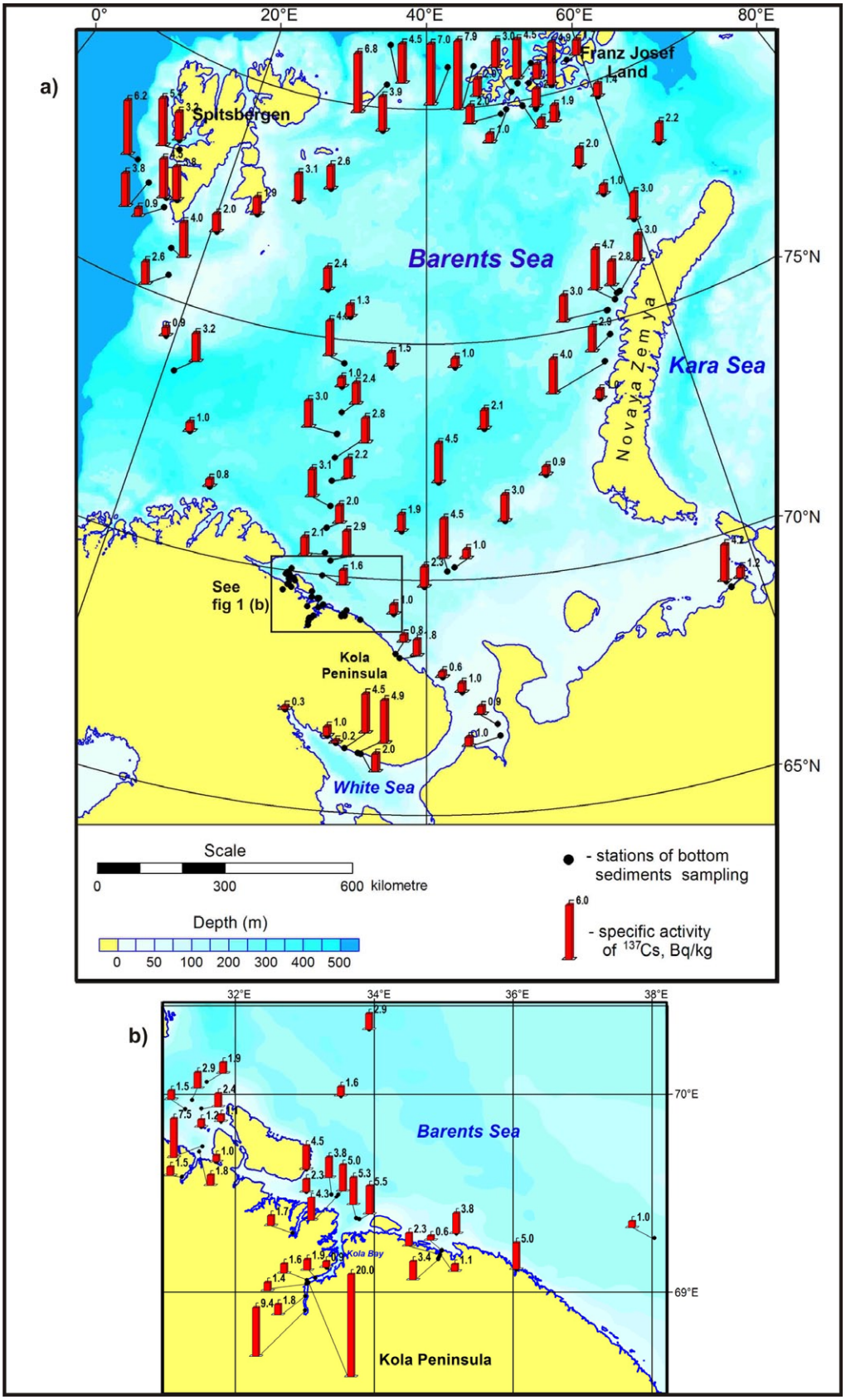


**Fig. 1. Specific activity of $^{137}$Cs in bottom sediments of the Barents, Greenland and White Seas, 2005-2009.**

The activity of $^{137}Cs$ in contemporary macrophytes (Fucus vesiculosus. being mainly studied) varied from 0-1.2 to 8.4 Bq/kg dry weight and 90Sr, from 0.6 up to 4.0 Bq/kg (Table 1, predominantly *Fucus vesiculosus*). The maximal concentration of $^{137}Cs$ of 8.4 Bq/kg was found for the littoral macrophytes near the settlement of Mishukovo close to «Atomflot» Enterprise.

**Table 1. Specific activity of artificial and natural radionuclides in *Fucus vesuculosus* of the Barents Sea, 2007.**

| Sampling area | Coordinates | | Specific activityof of radionuclide, Bq/kg dry weight | | |
|---|---|---|---|---|---|
| | N | E | $^{137}Cs$ | $^{90}Sr$ | $^{40}K$ |
| Kola Bay, Abram-Mys settlement | 68° 58' 53" | 33° 01' 41" | <1,2 | 0,8±0,3 | 958±51 |
| Kola Bay, Retinskoe settlement | 69° 06' 48" | 33° 22' 00" | 4,7±1,0 | 2,3±0,9 | 591±70 |
| Kola Bay, Min'kino settlement | 69° 59' 36" | 33° 01' 36" | <1,27 | – | 840±100 |
| Kola Bay, Belokamenka settlement | 69° 04' 34" | 33° 10' 13" | <1,86 | 1,6±0,5 | 661±80 |
| Upper part of Kola Bay | 68° 54' 27" | 33° 01' 32" | 4,7±1,3 | 1,8±0,4 | 930±109 |
| Teriberskaya Bay | 69° 10' 48" | 35° 10' 57" | <1,35 | – | 717±83 |
| Dalnezelenetskaya Bay | 69° 07' 01" | 36° 04' 11" | <1,56 | 0,8±0,3 | 837±37 |
| Kola Bay, Roslyakovo settlement | 69° 03' 39" | 33° 12' 30" | <1,07 | 2,4±0,8 | 722±28 |
| Kola Bay, town of Severomorsk | 69° 05' 00" | 33° 25' 42" | <2,1 | 0,6±0,3 | 748±9 |
| Kola Bay, Mishukovo settlement | 69° 02' 39" | 33° 02' 42" | 8,4±1,7 | 1,8±0,7 | 707±9 |
| Ura-Guba | 69° 18' 08" | 32° 50' 43" | <1,66 | 4,0±0,5 | 558±68 |

Radioecological studies of the Barents Sea commercial fish showed that the present-day activity of artificial radionuclides is extremely low. All investigated species (Atlantic cod, haddock, long rough dab, spotted wolfish) contained $^{137}Cs$ of less than 0.2 Bq/kg raw weight. Thus, the radioactivity of the Barents Sea ichthyofauna nowadays is primarily determined by the presence of natural radionuclide $^{40}K$.

Temporal changes in the $^{137}Cs$ content have been best studied in Atlantic cod from the Barents Sea (Fig. 2). The average $^{137}Cs$ concentrations are known for the period beginning from 1979. The maximum $^{137}Cs$ content in cod (2.2 Bq/kg raw weight) was observed in 1982, which may have been accounted for discharges from radiochemical enterprises of the Western Europe. The maximum $^{137}Cs$ content in cod from the Barents Sea was delayed by four to five years with respect to the maximum amount of this nuclide in water (Matishov et al. 2001). The $^{137}Cs$ content in cod of the Barents Sea after 1982 was diminished exponentially with a seven-year half-life period. In 2005-2009, the $^{137}Cs$ concentration in cod did not exceed 0.2 Bq/kg raw weight. Taking into account the current composition of food consumed by human beings, the dose of radioactive cesium received through eating fish falls into the «radioactively safe zone».

In summary, the present-day concentrations of the anthropogenic isotopes in the ecosystem elements are evidence of the absence of high-energy sources of artificial radioactivity after the cessation of nuclear weapons tests on Novaya Zemlya and the adjacent shelf in 1950-1960s and the Chernobyl global emission in 1986.

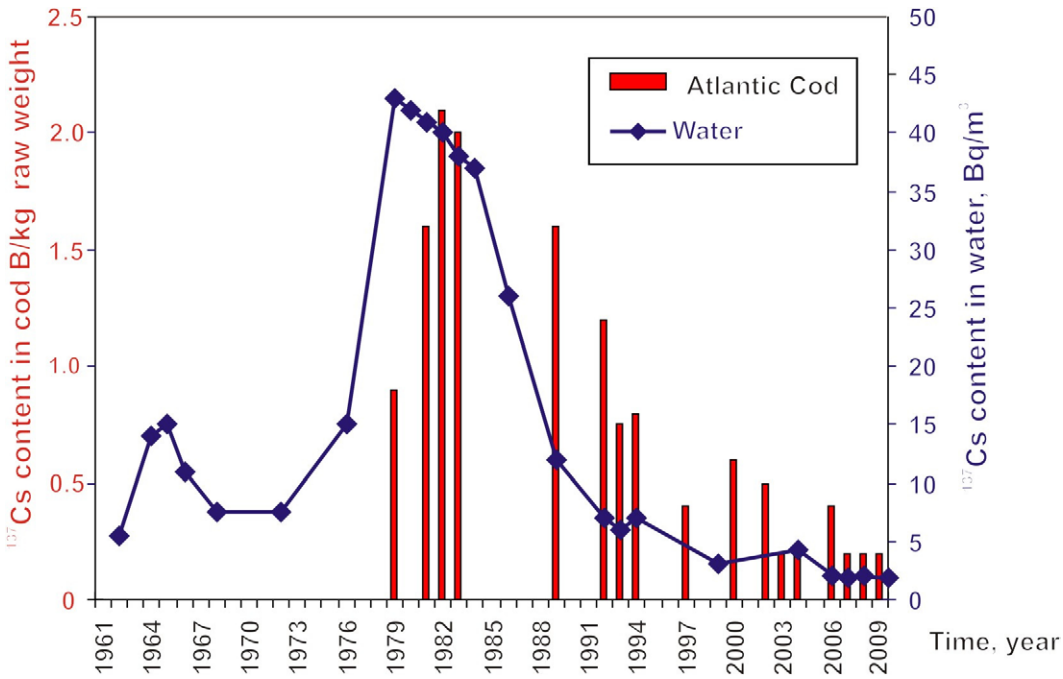


**Fig. 2. Average $^{137}$Cs concentration in water and in Atlantic cod from the Barents Sea (1979-2009).**

## Conclusions

The major source of the present-day radioactive pollution in the Russian Western Arctic are still the long-living isotopes of $^{137}$Cs, $^{90}$Sr, and $^{239,240}$Pu, emitted during nuclear weapons tests in the middle of the twentieth century. Some artificial radionuclides originating from the Sellafield factory are coming with the Atlantic waters. The impact of local atomic power fleet and transport complexes is registered in sites 10-20 km apart.

Natural purification processes in the marine environment, such as repeated dilution, nuclear decay, sorption by sediments and suspended solid material, and accumulation by aquatic inhabitants, are the main factors of the decrease in the intensity level of artificial radioactive isotopes. Against the background of radioactive pollution decrease, studies on other natural previously unexamined radionuclides ($^{40}$K, $^{226}$Ra, $^{228}$Th, $^{210}$Po and others) may become a question of interest.

## References

Matishov D.G., Matishov G.G. Radioecology in Northern European Seas. Springer, Heidelberg. 2004. 335 p.

Matishov D.G., Matishov G.G., Kasatkina N.E., Usyagina I.S. Dynamics of the radioactive pollution of bottom sediments of the Barents, White, and Azov seas. Dokl. Earth Sci. 2004; 396 (4): 560–562.

Matishov D.G., Matishov G.G., Rissanen K. et al. Radionuclides in the West Arctic seas. Izv. Akad. Nauk. Ser. Geogr. 1995; 6: 36–42 [in Russian].

Matishov D.G., Matishov G.G., Rissanen K. Radioactive contamination of the Kola Bay of the Barents Sea. Dokl. Akad. Nauk. 1996; 351 (4): 571–573 [in Russian].

Matishov D.G., Usyagina I.S., Kasatkina N.E., Pavel'skaya E.V. Accumulation Peculiarities of Artificial Radionuclides in the Elements of Coastal Ecosystems on the Kola Peninsula. Dokl. Earth Sci. 2007; 413A (3): 448–451.

Matishov G.G., Matishov D.G., Kasatkina N.E. et al. Analysis of Distribution of Artificial Radionuclides in the Ecological System of Barents Sea. Dokl. Biological Sci. 2005; 404: 375–378.

Matishov G.G., Matishov D.G., Namyatov A.A. Artificial radionuclides in the Barents Sea fish tissues // Ecology of the Barents Sea Commercial Fish Species. Izd. Kol'sk. Nauch. Tsentra Ros. Akad. Nauk, Apatity. 2001: 217–228 [in Russian].

Matishov G.G., Matishov D.G., Namyatov A.A. Levels and conditions of anthropogenic radionuclides accumulation in the Kola and Motovsky Bays. Dokl. Akad. Nauk. 1997; 357 (6): 812–814 [in Russian].

Matishov G.G., Matishov D.G., Schipa E., Rissanen K. Radionuclides in the ecosystem of the region of the Barents and Kara Seas. Izd. Kol'sk. Nauch. Tsentra Ros. Akad. Nauk, Apatity. 1994. 237 p. [in Russian].

Nies H., Nielsen S. P. Radioactivity in the Baltic Sea // Radionuclides in the Oceans, Inputs and Inventories. Les Ulis, France. 1996: 219–231.

Nikitin A.I., Katrich I.Yu., Kabanov A.I. et. al. Radioactive contamination of the Arctic Ocean by the results of observations in 1985–1987. At. Energ. 1991; 71 (2): 169–172 [in Russian].

Smith J. N., Ellis K. M., Naes K., Matishov D., Dahle S. Sedimentation and mixing rates of radionuclides in Barents Sea sediments off Novaya Zemlya. Deep-Sea Res. 1995; 6: 1471–1493.

Vesterbacka P. and Ikäheimonen T. Optimization of $^{210}$Pb Determination via Spontaneous Deposition of $^{210}$Po on a Silver Disk. Anal. Chim. Acta. 1997; 545: 252–261.

# Human dose pathways from forests contaminated by atmospheric radionuclide deposition

Rantavaara, Aino; Ammann, Michael
STUK – Radiation and Nuclear Safety Authority, FINLAND

## Abstract

After radionuclide contamination of forests, the potential health risk of both the early and late phase radiation exposure of people using forests needs to be assessed. Radionuclides vary in their exposure characteristics. Short-lived $^{131}$I can be a significant source of internal and external radiation in the first weeks. Long-lived $^{137}$Cs may call for long-lasting surveillance of forest products, and $^{134}$Cs contributes to human doses for a few years. $^{90}$Sr is seldom a significant contributor to the radiation doses from forests unless there is a high surface contamination of berry plants and mushrooms. Radiation doses depend on the ways people use forests and forest products. Consumption rates of wild foods and the time spent in forest vary by countries and population groups. Dose pathways that need attention are the ingestion of wild foods, the handling and use of wood ash, and the exposure to external radiation in forests particularly in the first weeks after radionuclide deposition.

A hypothetical contamination scenario was used to demonstrate the importance of the different pathways to the human doses. The forest food chain and dose model of RODOS, a European emergency response system, was used for scenario assessment. The assessments show that the highest annual doses arise from the ingestion of wild foods from the first harvest after deposition of $^{131}$I, $^{134}$Cs, $^{137}$Cs and $^{90}$Sr in early July. Exposure of adults to external radiation from $^{131}$I in forest vegetation and ground is important in the first weeks. Small scale users of fuel wood are exposed via an additional dose pathway through the use of contaminated ash for enrichment of garden soil. Regular ash fertilization accumulates $^{137}$Cs in soil year by year. A maximum annual dose of 60 µSv a$^{-1}$ was estimated to residents due to stay in ash-fertilized garden, as late as seventy years after the hypothetical contamination event (100 kBq m$^{-2}$). Of course, actual doses will depend on the details of exposure situation. Nevertheless, the presented assessment may help in understanding the relevant pathways. Such an understanding is important when giving advice on the safe use of contaminated forests as are regionally adapted assessment models and knowledge of the local forestry practices.

## Introduction

Atmospheric release and the consequent distribution and deposition of radioactive material in rural areas may present a threat to radiation safety of people using forests. The deposition pattern can vary substantially due to the characteristics of the release, weather conditions during the passage of the plume, and the distance from the source of release. Environmental and ecosystem related processes change the initial distribution of radionuclides in forests. In addition, radioactive decay reduces the overall activity in forest.

Radionuclide contamination of forests has been a concern of experts on radioecology, radiation protection and forestry since the Chernobyl accident in 1986. In recent decades long retention times of radioactive caesium in the nutrient cycle of forest became evident. Only insignificant losses of radionuclides through surface runoff or fixation in soil minerals were detected in boreal forests on podzolic soil horizons (Tikhomirov and Shcheglov 1994; Bergman 1994, Dahlgaard et al. 1994). Relatively high uptake of radioactive caesium from soil to forest vegetation and further to wild foods was also confirmed (Aarkrog 1994; Rantavaara 1990).

The aim of the present study was to clarify human dose pathways after radionuclide contamination of forests. Comparative model predictions of the potential doses to different users of forests were assessed and factors modifying the doses were referred to.

## Dose pathways from contaminated forest

Radionuclides distributed in trees, understory, ground layer vegetation and soil are sources of external exposure to people spending time in contaminated forests. Sawn timber and logs used as building material can expose people to external radiation in residential and working environments. Living year-round (7000 h $a^{-1}$) in a wooden house made of 15-20 cm thick logs requires that the activity concentration of $^{137}Cs$ is less than 1700-2000 Bq $kg^{-1}$(80% dry matter) in order that the dose from building material to residents remains below 1 mSv $a^{-1}$. For sawn timber used in a timber-framed detached house the respective $^{137}Cs$ concentration level would be 2400 Bq $kg^{-1}$ (80% dry matter). The dose assessment model MATERIA (Markkanen 1995) was used for this estimation. Various other wood products in residential environments, for instance furniture, are causing considerably lower doses than wood used as building material (IAEA 2003).

Wood ash concentrates those radionuclides that are not released to the atmosphere during combustion, e.g. isotopes of Cs and Sr. The concentration factor for the combustion of wood ranges from 50 to 200, and corresponds to mass ratio of dry fuel and ash. Workers involved in disposal and recycling of ash may receive the highest individual doses amongst the workers in the production chain of wood energy (Vetikko et al. 2004).

Ingestion of radionuclides in wild berries, mushrooms and game meat is often the most significant dose pathway from forest, mostly due to the consumption of large amounts of wild foods. Mostly minor doses are received from the inhalation of airborne radionuclides during the passage of a radioactive cloud or from resuspended particles, soil or ash dust, if the instructions for protection of workers and the public are followed.

## About assessment data

The radiological significance of a contaminating event depends on the characteristics of deposited radionuclides, their decay rates, type and energy of radiation and their chemical behaviour in natural ecosystems and human metabolism. Site conditions and forest management practices govern the radionuclide dynamics in forests.

The dose that is received within the first year depends crucially on the season during which the radionuclide deposition occurred. Furthermore, the time from deposition to the actual radiation exposure needs to be taken into account. The longer the delay, the lower is the dose contribution from short-lived nuclides and from foliar contamination of plants. The ways people are using forests and forest products varies and requires surveying. For instance, berry and mushroom pickers und hunters have distinctive consumption patterns. Forestry workers were assumed to be exposed to radiation during working in forest only; they may still belong to other subgroups of users of forests.

It is challenging to quantify radionuclide flow in forests, a continuously changing ecosystem with a rotation period of about 80 years in Central Europe and even longer in sub-arctic conditions. Of great value to radioecology has been the experience gained in forest research and the collaboration with organizations that have comprehensive knowledge of forest. State-of-the-art sampling methods are essential for obtaining reliable field data on radionuclides in forest (Aro et al. 2009). There exist several assessment models for forests. The validity of some of them was compared in the BIOMASS programme of IAEA and reviewed by Shaw et al. (2005).

Two nuclear accidents in the past caused widespread contamination and had also an impact on forests in boreal and temperate Eurasia and America. These were the accident at the Chernobyl nuclear power plant in Ukraine in 1986 and the chemical explosion in the nuclear fuel processing plant Mayak near Kyshtym, Cheliabinsk province, Siberia in 1957 (Trabalka et al. 1980; Jones 2008). These accidents were widely studied and provided important radioecological field data on radionuclide behaviour in forests. Another valuable data source were studies related to the global fallout from atmospheric nuclear testing during 1945-1980. Also some smaller events have contaminated forests, albeit on a limited scale, and were subject to radioecological studies (Auerbach 1987). Radionuclide transfer in forests was one of the topics in a literature review published by IAEA (2009) and in a handbook on transfer parameters (IAEA 2010), which, regarding forests, was summarized by Calmon et al. (2009).

## Dose assessment model

The forest food chain and dose assessment model FDMF, which is part of the European emergency response system RODOS, was used for the dose assessments (Rantavaara et al. 2001). The parameters of FDMF were derived from Finnish and other European data from experimental field studies, survey data on people's outdoor activities and consumption of wild foods. The compartment structure and transfer processes considered in FDMF allow assessment of the radionuclide flow in forests (Fig. 1).

Using the RODOS system, predictions for large affected areas can be provided. Through regional parameters the assessment results represent the conditions in calculation area. During dry weather the time-integrated air concentrations are used in

the calculation of the initial activity densities of radionuclides on different surfaces within the forest. These surfaces are the forest soil, understory vegetation, and crown and trunk of trees. The deposition onto these surfaces during rain depends on the development stage of the canopy, the amount of rain and the total deposited activity. The result of a prognosis calculation depends on the choices made during the setup of a model run. The choices can be, e.g. the type of forest, the population group, the species of plants and animals providing wild foods, the type of fuel wood and the details of the use of wood ash. The model takes into account height and biomass density of the forest type chosen, regional consumption rates of wild foods and losses of radionuclides during cooking.

FDMF calculates the time-dependent radionuclide contents in forest compartments, activity concentrations in forest products and radiation doses to various population groups (hunters, pickers, public). The need for intervention and availability of acceptable wood and wild food products can be further assessed with another RODOS model, LCMforest (Rantavaara, Ammann 2005).

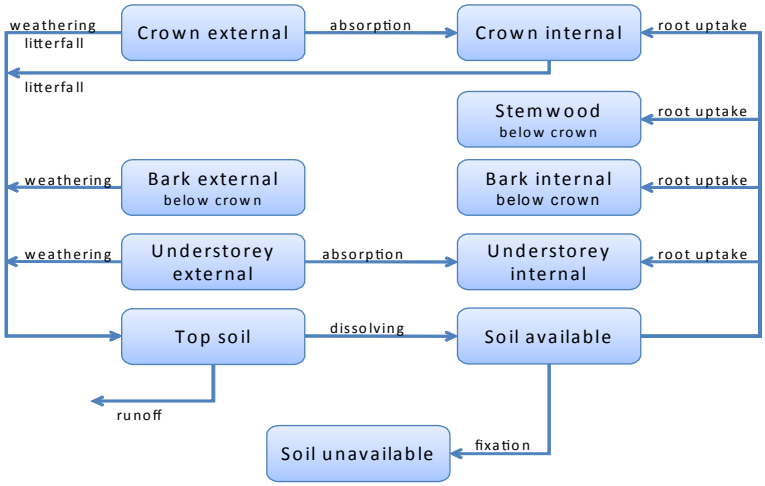


**Fig. 1. Compartments of the dynamic module of the forest model FDMF and the processes changing their radionuclide content with time.**

## Calculation scenario

A hypothetical contamination of two forest types was assumed to have happened in July. The activity inventories of the forests contained the following four radionuclides: $^{90}$Sr, $^{131}$I, $^{134}$Cs and $^{137}$Cs (Table 1). The initial contamination exceeded manyfold the average activity densities of these radionuclides in most countries after the Chernobyl accident. The activity ratios of the radionuclides were roughly those found in Fennoscandia in early May 1986. Dry deposition was assumed to happen on the 8th of July. An advanced Scots pine *(Pinus sylvestris L.)* forest was chosen to represent the Northern Europe and a coniferous forest type the Central Europe.

Wild food species were blueberry *(Vaccinium myrtillus L.)*, moose *(Alces alces)* and mushrooms corresponding to an aggregated transfer coefficient of 0.05 m$^2$ kg$^{-1}$ for

isotopes of Cs. For Central Europe this uptake category included *Cantharellus cibarius, Boletus edulis, Collybia sp.*, several *Lactarius* sp., *Leccinum* sp. etc. and for Northern Europe *Cantharellus tubaeformis Cratellus cornucopioides*, some of the *Russula sp.* etc.

**Table 1. Radionuclides included in the assessment, their half lives and activity inventories in forest at the end of radionuclide deposition.**

| Radionuclide | Half life[1)] | Inventory (Bq $m^{-2}$) |
|---|---|---|
| $^{90}Sr$ | 28.79 y | $10^3$ |
| $^{131}I$ | 8.02 d | $5\times10^5$ |
| $^{134}Cs$ | 2.065 y | $5\times10^4$ |
| $^{137}Cs$ | 30.07 y | $10^5$ |

[1)] Chu SYF, Ekström LP, Firestone RB. The Lund/LBNL Nuclear Data Search, Version 2, February 1999.

Potential doses of adults from external radiation exposure were calculated from air kerma in boreal Scots pine forest. In FDMF the conversion from kerma to effective dose of an adult takes into account the source compartments in forest and a correction for the size of a subject to obtain effective dose for a five years old child. Doses from ingestion of wild foods were estimated for Central Europe (CE) and Finland (FI).

Activity concentrations in timber for building (logs, sawn timber) and fuel wood (split firewood) were assessed. The dose pathway of using wood ash for soil enrichment was assessed with FDMF. Doses to residents were derived from $^{134}Cs$ and $^{137}Cs$ accumulating in soil due to a regular distribution of ash from fireplace to kitchen garden. The fuel wood from an affected area was used. Other assumptions were:

- delay since felling of trees until distribution of ash: 1 year
- ash application rate: 0.2 kg $m^{-2}$ in a year
- surface soil was managed after each ash application, denoting a radiation attenuation factor of 0.3
- exposure time of adult residents to radiation from ash in garden: 300 h/year.

## Results of scenario calculations

In the first week after radionuclide deposition $^{131}I$ in crown layer and in the entire forest contributed to the dose rate more than $^{134}Cs$ and $^{137}Cs$ together (Figs. 2 and 3). After the first week the ground layer contributed most to the dose rates in forest.

The activity concentrations in logs and split firewood (Fig. 4), the activity density accumulating in garden soil via regular ash application (Fig. 5) and the annual effective dose from additional $^{134}Cs$ and $^{137}Cs$ in garden (Fig. 6) due to ash mixed in soil indicate a gradual increase of the annual doses to residents during decades. The dose from the external exposure to radionuclides in ash distributed in the garden soil was approaching 0.04 mSv $a^{-1}$ forty years after the deposition. The contribution of $^{134}Cs$ to the dose was negligible. The maximum annual dose to adult residents was estimated to be 0.06 mSv $a^{-1}$ about seventy years after deposition.

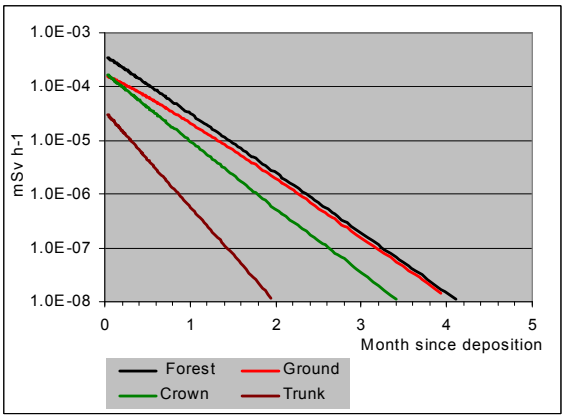


**Fig. 2. Effective dose rate (mSv $h^{-1}$) due to radiation from $^{131}I$ in ground, trunk and crown layers, and the total dose rate in forest. Region FI.**

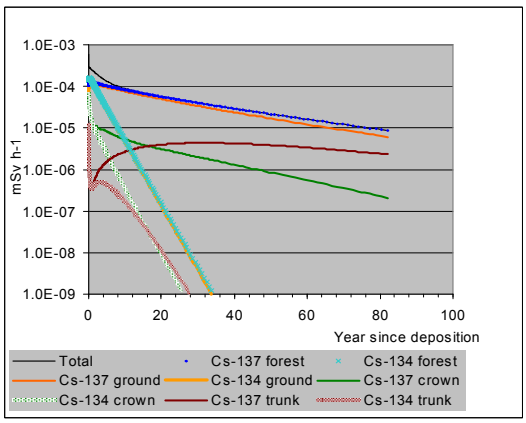


**Fig. 3. Effective dose rate (mSv $h^{-1}$) due to radiation from $^{134}Cs$ and $^{137}Cs$ in ground, trunk and crown layers, and the total dose rate in forest. Region FI.**

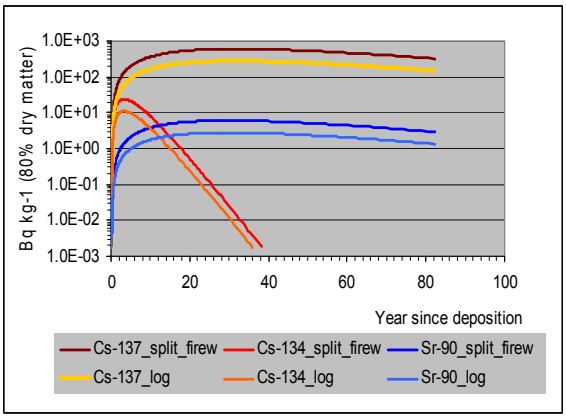


**Fig. 4. Activity concentration in timber(Bq $kg^{-1}$, 80% dry matter) for building (logs) and in split firewood.**

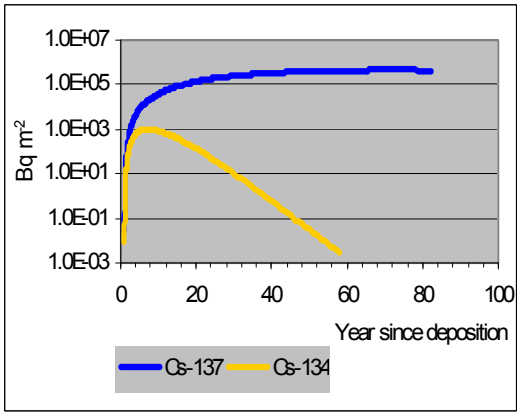


**Fig.5. Activity density of $^{134}Cs$ and $^{137}Cs$ in kitchen garden due to soil enrichment with wood ash.**

The doses to adults from external exposure in forests (Fig. 6) were used to give an idea of the differences between population groups. Adults in Central Europe received 33% and hunters and pickers 44% of the dose that adults in Finland would receive. Within the Finnish population the doses to different population groups were, again compared to adults, 33% for children (5 years of age), 140% for hunters and 110% for pickers. Forest workers were assumed to work 150 hours per month in forest without shielding from a harvester or other machines. Annual doses during 11 months per year were 15-fold compared to the dose of an adult (Fig. 6).

Wild foods contributed to the dietary dose significantly more in Northern (Fig. 7) than in Central Europe (Fig. 8). The doses differed mainly because of lower consumption rates in Central Europe (Fig. 9). Children (5 y) were not assumed to consume wild foods or go to the forest in CE. Radionuclides deposited on plant surfaces close to harvest or hunting seasons contributed significantly to the first year doses from blueberry and moose meat.

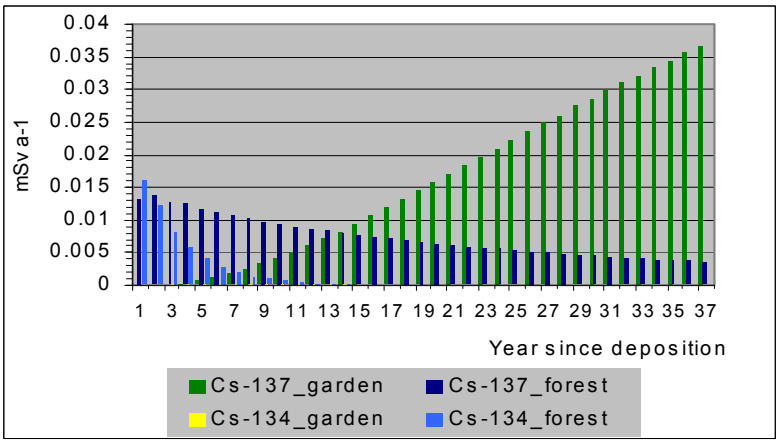


**Fig. 6. Annual effective dose to an adult due to radiation from ash distributed in kitchen garden, compared to dose received in forest. Region FI.**

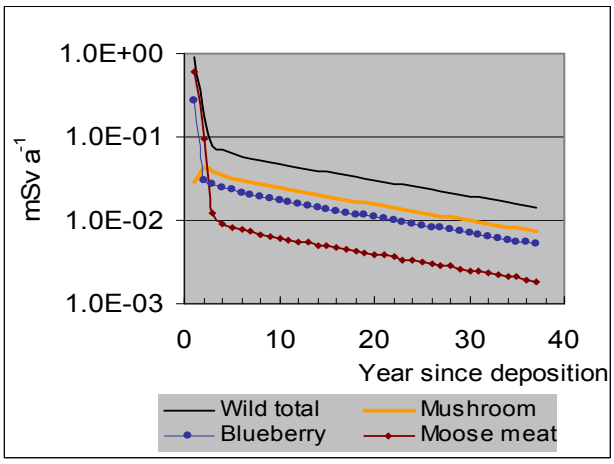


**Fig. 7. Effective dose commitment to adults from annual ingestion of radionuclides in wild foods, region FI.**

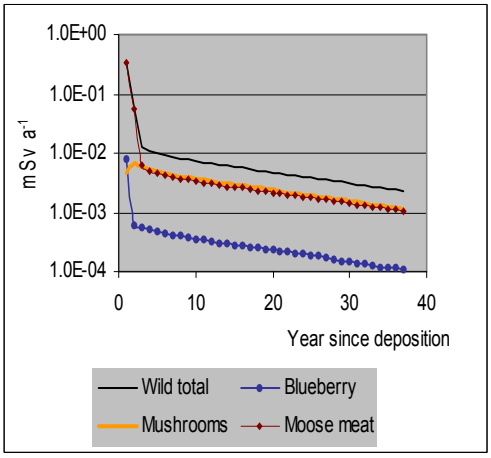


**Fig. 8. Effective dose commitment to adults from annual ingestion of radionuclides in wild foods, region CE.**

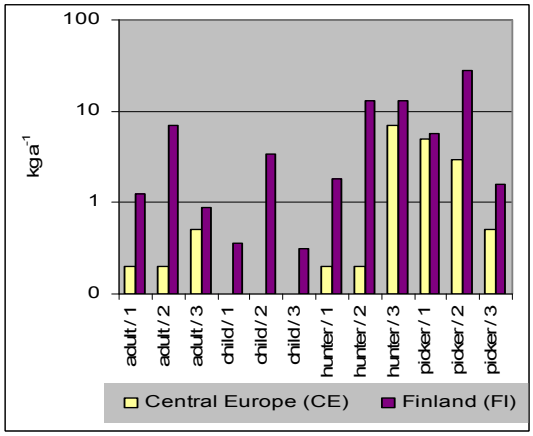


**Fig.9. Consumption rate of mushrooms (1), berries (2) and game meat (3) by population group in two regions.**

## Discussion

The various dose pathways contribute to the human dose from forests in relation to radionuclide, region, population group, and the time since forest contamination. The ways people use forests and forest products are changing in time. Consumption rates of wild foods and the time people spend in forests should be surveyed regionally at intervals of a decade or so. A suitable survey methodology should be used, the types and species of wild foods specified and cultural and other sources of regional variation considered. All parameters determining the effective dose from external radiation or dose commitment from radionuclides ingested in wild foods are important independent of the nature of data.

Natural processes and forest management are changing the radionuclide distribution in forest vegetation and soil. Together with consumption rates they are contributing to temporal variation in radiation doses received from wild foods. The dominant dietary pathway to the public is seldom via forest during the first years after a contaminating event. Later this may change, and the exposure to slowly declining $^{137}$Cs concentrations in wild foods will prevail while other foodstuffs are practically clean. An example on such changes was obtained via assessment of systematic foodstuff surveillance data collected in Finland in 1960-2005. Percentage contributions of terrestrial wild foods to dietary $^{137}$Cs increased in time during periods of global nuclear fallout and after the Chernobyl accident (Rantavaara 2008). Essential was the simultaneous decrease in the total dietary intake, caused mostly by environmental processes in agricultural production systems. Substantial dietary changes did not hide the effect of environmental processes on doses from ingestion of $^{90}$Sr and $^{137}$Cs during these periods. The doses received in the first year after radionuclide deposition were the higher the closer to consumption of foodstuffs of the season the deposition occurred.

Timber used for building, actually stemwood, is the least contaminated part of a harvested tree, whereas fuel wood can contain also more contaminated parts of a tree. Particularly wood ash needs attention of experts on radiation protection, energy industry and small scale use of firewood. Bioenergy production based on forest biomass as fuel can be a pathway of concern in the future. Intensive harvesting of felling residues has been supposed to involve detrimental removal of mineral nutrients from forest. If carried out, a condition would develop where increased root uptake of radioactive caesium and strontium occurs, whereas returning nutrients to forest floor through wood ash fertilization could have a reducing effect on $^{137}$Cs contamination of forest vegetation (Rantavaara and Aro 2009).

Radiation safety guidance is needed in energy industry for protection of workers handling with wood ash. The wood ash surveys in the 1990's (Rantavaara and Moring 1999) and early 2000's (Vetikko et al. 2004) clarified the need for site-specific measurements of industrial ash in Finland. The studies probably facilitated safe handling of ash and following the related radiation safety guide (STUK 2003).

## Conclusions

Radionuclide contamination of a forested area should be assessed for the potential health risk. Providing local people and other concerned population groups with information and advice can help avoiding unnecessary radiation doses. Due to the complexities in radionuclide contamination of forests assessment models are needed to prepare the preliminary advice. Nevertheless, decisions on remedial measures and restrictions for the use of forests need to be based on qualified measurements because of their socio-economic consequences. For correct interpretation of the measurement results scientific design of measurement and sampling strategies are fundamental. Experts on forestry should be involved in the planning and implementation of intervention programmes.

Stem wood will be contaminated with delay, slowly accumulating long-lived isotopes $^{137}$Cs and $^{90}$Sr, and is the least contaminated part of a tree. Timber that is used for buildings and originates in other than the most contaminated areas of Europe is not supposed to cause to residents an effective dose higher than 1 mSv $a^{-1}$.

Doses from the treatment, transport and use of wood ash can occasionally exceed 1 mSv $a^{-1}$ to e.g. long-range truck drivers. The small scale users of contaminated fuel wood and ash may need guidance to avoid unnecessary radiation exposure.

## Acknowledgements

The European Union partially financed the development of the forest modules of RODOS during past Fission Safety programmes. P. Calmon, IRSN, Institut de Radioprotection et de Sûreté Nucléaire, France, participated in the development of the first version of the model. M.I. Balonov, A.N. Barkovski and V. Yu. Golikov from the Institute of Radiation Hygiene, St. Petersburg, Russia, derived the algorithms for air kerma in forest.

## References

Aarkrog A. Doses from Chernobyl accident to the Nordic populations via diet intake. In: Dahlgaard H, (Ed.) Nordic Radioecology. The Transfer of Radionuclides through Nordic Ecosystems to Man. Amsterdam: Elsevier; 1994. p. 433–456.

Aro L, Plamboeck AH, Rantavaara A, Strålberg E, Vetikko V. Sampling in forests for radionuclide analysis - General and practical guidance. NKS-183. Roskilde, Denmark; 2009. p. 49. http://www.nks.org/download/pdf/NKS-Pub/NKS-183.pdf

Auerbach SI. Comparative behaviour of three long-lived radionuclides in forest ecosystems. Conf-8609191--2, DE-87 001836, Oak Ridge National Laboratory, Oak Ridge, Tennessee, USA. 1987.

Bergman R. The distribution of radioactive caesium in boreal forest ecosystems. In: Dahlgaard H (Ed). Nordic Radioecology – The transfer of radionuclides through Nordic ecosystems to man. Studies in Environmental Science. Elsevier, Amsterdam, 1994; Vol. 62: 335-379.

Calmon P, Thiry Y, Zibold G, Rantavaara A, Fesenko S. Transfer parameter values in temperate forest ecosystems: A Review. Journal of Environmental Radioactivity 2009; 100: 757-766.

Dahlgaard H, Notter M, Brittain J, Strand P, Rantavaara A, Holm E. General summary and conclusions. In: Dahlgaard H, (Ed.). Nordic radiecology – The transfer of

radionuclides through Nordic ecosystems to man. Studies in Environmental Science. Amsterdam: Elsevier, 1994; 62: 7-20.

IAEA. Handbook of parameter values for the prediction of radionuclide transfer in terrestrial and freshwater environments. Technical reports series No. 472, Vienna: International Atomic Energy Agency; 2010.

IAEA. Quantification of radionuclide transfer in terrestrial and freshwater environments for radiological assessments. TECDOC-1616, Vienna: International Atomic Energy Agency; 2009.

IAEA. Assessing radiation doses to the public from radionuclides in timber and wood products. IAEA-TECDOC-1376, Vienna: International Atomic Energy Agency; 2003.

Jones S. Windscale and Kyshtym: a double anniversary. Journal of Environmental Radioactivity 2008; 99: 1-6.

Markkanen M. Radiation dose assessments for materials with elevated natural radioactivity. STUK-B-STO 32. Helsinki: Painatuskeskus Oy, 1995: 1-40.

Rantavaara A. Ingestion doses in Finland due to $^{90}$Sr, $^{134}$Cs and $^{137}$Cs from nuclear weapons testing and the Chernobyl accident. Applied Radiation and Isotopes 2008; 66: 1768-1774.

Rantavaara A. Transfer of Radiocesium through Natural Ecosystems to Foodstuffs of Terrestrial Origin in Finland. In: Transfer of Radionuclides in Natural and Seminatural Environments. Desmet G, Nassimbeni P, Belli M. (Eds.) New York: Elsevier Science Publishers Ltd., 1990, pp. 202-209.

Rantavaara A, Ammann M. Forest models of the RODOS system as assessment tools for intervention after radionuclide contamination of forests. In: Valentin J. et al. (eds). Proceedings of the XIV Regular Meeting of the Nordic Society for Radiation Protection, NSFS – Rättvik, Sweden, 27–31 August 2005. SSI Report 2005:15. Stockholm: Swedish Radiation Protection Authority; 2005. p. 339-342.

Rantavaara A, Aro L.J. Radiological impact of using forest tree biomass for energy and recycling the ash. Radioprotection 2009; 44 (5): 927-932.

Rantavaara A, Calmon P, Wendt J, Vetikko V. Forest food chain and dose model (FDMF) for RODOS. Model description. STUK-A178. Helsinki: Radiation and Nuclear Safety Authority; 2001:1-65.

Rantavaara AH, Moring KM. Contaminated tree biomass in energy production – potential need for radiation protection. In: Linkov I, Schell WR. (eds.). Contaminated Forests, Kluwer Academic Publishers, Dordrecht, The Netherlands, 1999: 303-310.

Shaw G, Venter A, Avila R, Bergman R, Bulgakov A, Calmon P, Fesenko S, Frissel M, Goor F, Konoplev A, Linkov I, Mamikhin S, Moberg L, Orlov A, Rantavaara A, Spiridonov S, Thiry Y. Radionuclide migration in forest ecosystems - results of a model validation study. Journal of Environmental Radioactivity 2005; 84: 285-296.

STUK, The radioactivity of building materials and ash. Guide ST 12.2 Helsinki; Radiation and Nuclear Safety Authority (STUK); 2003.

Trabalka JR, Eyman LD, Auerbach SI. Analysis of the 1957-1958 Soviet nuclear accident. Science 1980; 209: 345-353.

Tikhomirov FA, Shcheglov A.I. Main investigation results on the forest radioecology in the Kyshtym and Chernobyl accident zones. The Science of the Total Environment 1994; 157: 45-57.

Vetikko V, Valmari T, Oksanen M, Rantavaara A, Klemola S, Hänninen R. Radioactivity of wood ash in energy industry and its radiation effects. STUK-A200. Helsinki; 2004. (In Finnish.)

# Occurrence of plutonium in the terrestrial environment at Thule, Greenland

Roos, Per; Jernström, Jussi; Nielsen, Sven P.
Risø National Laboratory for Sustainable Energy, Technical University of Denmark, P.O. Box 49, DK-4000 Roskilde, DENMARK

## Abstract
Samples of air, resuspended particles, water, soil and precipitation were collected in an area 10 km south of the Thule 1968 impact point and analysed for their content of $^{241}$Am and plutonium. The results from the soil sampling show a very inhomogeneous distribution with hot spots ranging up to several hundred kBq per m$^2$ of Pu. Although concentrations in surface soil can be very high the concentration in analysed air filter samples and passive aerosol collectors are very low. Exposure to plutonium due to inhalation of airborne plutonium particles in the area is of little importance according to this study. To further assess the risk of inhaling resuspended material particles isolated from the different hot areas have been subject to investigation on stability and leaching behaviour.

## Introduction
On the 21 of January 1968 an American B52 bomber carrying nuclear weapons crashed on the sea ice in Bylot Sound, about 15 km west of Thule Air Base, northwest Greenland, Fig.1. On impact the plane caught fire and the jet fuel as well as the weapon's chemical high explosives detonated causing a local dispersion of radioactive material. Part of the weapons plutonium was distributed over some square kilometres of the ice in the explosive fire that followed. Plutonium-contaminated ice was recovered and shipped back to the US, as was the plutonium-contaminated wreck. The underlying sea sediments received a fraction of the weapons plutonium when the sea ice melted the following summer and probably also during the accident as the impact caused the ice to break up (U.S. Air Force, 1970).

Flames from the fire reached heights of around 850 m and the smoke pillar even higher. Based on observations from eyewitnesses, metrological data and radar observations it was concluded that the contaminated cloud from the fire drifted south to southwest. At the time of the accident an inversion layer existed at around 830 m and the atmosphere was thermally stable up to around 2200 m. At a height of 1000 m the winds came from the north, higher up, at 3500 m winds were from the west. Wind speed was around 3 m s$^{-1}$ at all heights. It was anticipated that from these observations, finer particles from the fire could have been transported far away from the crash site

and reached land south of Bylot Sound, although at low concentrations. It was consequently expected that measurable concentrations of contamination could be found in the direction of the Inuit settlement site Narsaarsuk on the coast some 8 km south of the crash site and further in on land. Contaminated material on the crash site was also anticipated to have been resuspended and dispersed westwards towards Sounders Island due to the storm which followed on the 24 and 29th of January (U.S. Air Force, 1970).

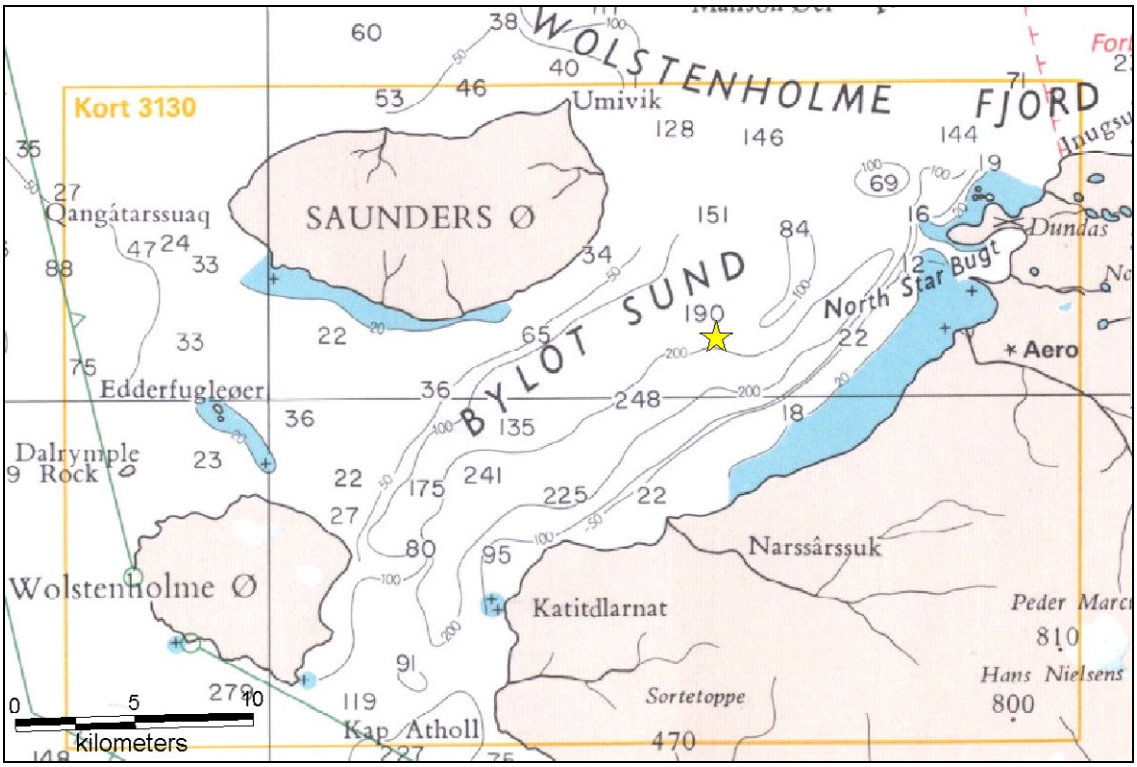


**Fig. 1. Map of Bylot Sound showing the site of the aircraft accident (star).**

Due to the frequent storms, melting snow and running surface water the contaminated material initially residing on the snow surface may to some extent have been redistributed in the months and even years following the accident. This redistribution may be anticipated to have taken place locally.

The distribution of plutonium on land was initially investigated only weeks following the accident by the analysis of snow samples. In general two zones with contaminated material was identified, one in direction towards south of the crash site, the primary fallout zone, and one towards west which most likely was due to redistributed resuspended material from the crash site in connection with the violent winds following the accident. The contaminated areas on land south of Bylot Sound showed maximum levels of around 9 kBq $m^{-2}$ close to Narsaarsuk.

In connection with the Thule-2003 project concerning investigation of plutonium in the environment around Thule (Nielsen og Roos, 2006) soil samples were collected from 8 localities at Narsaarsuk. At all 8 sites plutonium from the accident could be quantified at different levels in the top soil layers. The spatial variation in plutonium

concentrations is very un-even due to the presence of small particles. Detailed analysis of the soil samples collected in 2003 have shown particles with a $^{239,240}$Pu content up to 150 Bq. In connection with a pilot study carried out in august 2006 at Narsaarsuk, soil samples were collected which further confirmed the presence of weapons plutonium as well as a large spatial variation of the contamination.

Occupancy at Narsaarsuk, where elevated plutonium levels have been found on the ground, may include a risk of inhaling radioactive particles if these are resuspended from the ground. This resuspension may be caused either by wind or by some mechanical action of the soil. Depending on the level of exposure to these radioactive particles there is a potential risk to human health.

## Material and methods

During 2006-2008 a comprehensive field expedition was conducted in the Kap Atholl area at Thule. Soil samples were collected using a 10 cm diameter PVC-tube. At each sampling location 5 individual samples were taken in order to assess deposition variability. A total of about 500 soil-samples were collected over an area of about 20 km2. Overview of the $^{241}$Am deposition in the area was obtained using a portable NaI-detector system. Air sampling was done using a Staplex air sampler with a flow rate of about 1 $m^3$/min. Passive collectors ('sticky vinyl') were placed on wooden frames or on to walls of the shacks in Narssarssuk in order to further assesse the presence of plutonium in air. Rain was collected using a 0.25$m^2$ funnel located close to the air sampler. Assessment of resuspension of plutonium from soil was done using a simple vacuum-cleaner on areas of about 1 $m^2$. In the laboratory soil samples were screened in 5-15g aliquots to quantify the total amount of $^{241}$Am in each soil sample. The presence of particles and thus inhomogeneous soil samples made this procedure necessary. Passive collectors were analysed first using a digital autoradiography system and later analysed by radiochemical methods and solid state alpha spectrometry for Pu-isotopes. Air filters and rain samples were first analysed by gamma spectrometry and later by solid state alpha spectrometry for Pu-isotopes.

## Results

The results from analysed soil samples shows that the Pu contamination is very unevenly distributed over the Kap Atholl area. Several so called 'hot spots' ranging from less than a meter in size to several tens of meter exist in the area around Narssarssuk. Deposition density of Pu in these areas are in the order of 10-100 kBq $m^{-2}$ or even more but is difficult to determine due to the areal Pu density in many cases being determined by a few larger particles. Outside the high deposition areas concentration of Pu is more likely to be found in the 0.1-1 kBq $m^{-2}$ range. A figure showing the frequency distribution of Pu from analysed soil samples are shown in figure 2.

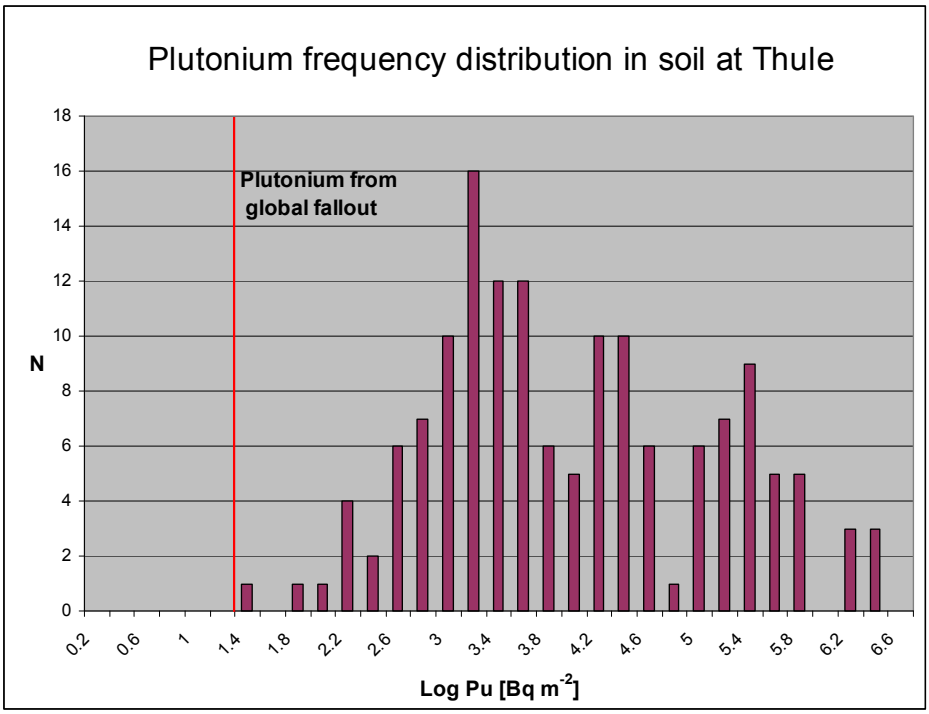


**Fig. 2. Frequency distribution of Pu from analysed soil samples.**

Results from the resuspension experiments using a simple vacuum-cleaner shows that Pu can be found in nearly all samples (figure 3). In spite of the relatively large amount of resuspended material even during a single exposure to vacuum cleaning the levels of plutonium in air was found to be very low during this study. From the air filters analysed no concentration higher than 5 nBq $m^{-3}$ was observed. Similarly the passive particle collectors showed no sign on digital autoradiography of particles attached during the exposure period. Radiochemical analysis of plutonium on the passive collectors resulted in concentrations in the range 0.1-3 mBq. The conversion of these numbers to corresponding air concentrations is not straightforward and has been omitted.

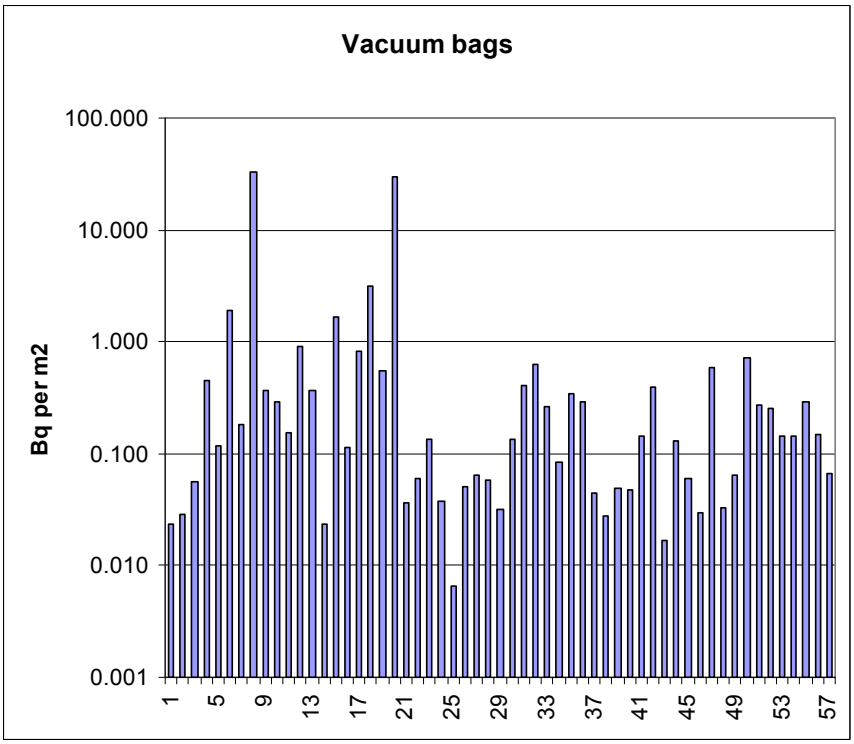


**Fig. 3. Results of $^{241}$Am from analysed vacuum cleaning bags. Corresponding $^{239}$Pu levels can be obtained by multiplying the numbers by six ($^{239}$Pu/$^{241}$Am ratio in the Thule material is about 6).**

## Discussion

The deposition density of plutonium found in the terrestrial environment south of the impact point is of the same order of magnitude as the most contaminated sediments in Bylot Sound. While relocation of contaminated sediments to accumulation bottoms is an important process explaining the spatial distribution of plutonium in Bylot Sound similar mechanisms probably can explain the spatial variability of plutonium on land in the Narssarssuk area. The Thule area is classified as an arctic desert and large areas in the Kap Atholl peninsula is stony, rocky or sand terrain. The annual amount of precipitation is very low and in combination with violent storms it is evident that areas not sheltered from wind will be heavily eroded. Any material initially deposited on such areas will thus likely reside there only for a short time before being relocated successively to areas with wind shelter and/or areas having a high water content or vegetation. Since most areas with vegetation receive their water through nearby deposited snow melting during the summer a view over the area showing pockets of snow in summertime also reveal the potential areas where redistributed plutonium has finally ended up. Probably most of the initially deposited material on snow was relocated to their final destinations during the storm that took place a few days after the accident. All the hot spots identified in the Narssarssuk area are located close to snow patches but not all snow patches are associated to elevated plutonium areas.

The risk of resuspending the deposited material is depending on surface properties such as presence of vegetation, water and how exposed the area is for wind. Although the landscape has been exposed to more than 40 y of strong winds it is clear that the risk of resuspending deposited plutonium is significant according to data in figure 3. Air

filter data however showed very low concentrations and the maximum observation of 5 nBq $m^{-3}$ corresponds to doses due to the inhalation pathways which is in the order of 1 nSv $y^{-1}$. Possibly ingestion may be the dominating pathway of the terrestrial Thule plutonium to man in the area.

## Conclusions

Although locally deposition densities of plutonium in the Narssarssuk area may reach close to 1 MBq $m^{-3}$ concentrations of plutonium in air is very low and does not constitute any severe health problems according to this study.

## References

Nielsen, Sven P. & Per Roos (May 2006). *Thule-2003 – Investigation of Radioactive Contamination*. Roskilde: Radiation Research Deptartment, Risø National Laboratory. ISBN 87-550-3508-6.

Project Crested Ice: A joint Danish-American report on the crash near Thule Air Base on 21 January 1968 of a B-52 bomber carrying nuclear weapons. Vol 65, Part 2. Danish Atomic Energy Commission. February 1970.

# Environmental radioactivity assessment at nuclear legacy sites in the Republic of Tajikistan

Nalbandyan, Anna; Hosseini, Ali
Norwegian Radiation Protection Authority, Emergency Preparedness and Environm. Radioactivity, NORWAY

## Abstract

The impressive number of extant nuclear and radiological sources in the Central Asia is a major environmental concern as they pose a potential threat of radioactive contamination to the whole region. Key sources of concern are technologically enhanced levels of naturally occurring radionuclides (TENORM) due to uranium mining and milling. Uranium ore mining and processing in the former Soviet Republic of Tajikistan resulted in origination of huge amounts of uranium tailing materials and waste rock deposits, often dumped near inhabited areas. Given the absence of a proper waste management in most of those areas, there is a considerable potential for the spread of contamination beyond existing contaminated sites. A joint field mission to Tajikistan was conducted in 2008 as part of the project: Environmental impact assessment of radionuclide contamination of selected sites in Kazakhstan, Kyrgyzstan and Tajikistan, coordinated by the Norwegian University of Life Sciences. The present work focuses on the assessment of radiation exposure and radioactivity levels in the former uranium mining and tailing sites at Taboshar, and Digmai, both located in northern part of Tajikistan. Gamma-dose rate surveys were carried out on each site. Generally, the dose rates measured at the uranium mining site in Taboshar varied between 0.70 and 4.4 µGy/h. However, this excludes some hot spots where dose-rates as high as 20 µGy/h were measured. On the tailing site which contains 1.2 mln tons of radioactive wastes the measured dose rates varied 0.7 – 1,9 µGy/h. It is noteworthy that the tailing site lies just 1 km far from the local school in Taboshar where we also did measurements. The highest level of radioactivity was exhibited by Digmai – 18.8 µGy/h. From each site soil samples were taken for subsequent lab analyses for radioactivity and track detectors placed on-site for determination of Rn concentration. The analyses are in progress and the results will be available by the end of 2009.

# Improved model for estimation of fallout from atmospheric nuclear testing

Pálsson, Sigurdur Emil[1]; Howard, Brenda J.[2]; Ikäheimonen, Tarja K.[3]; Nielsen, Sven P.[4]
[1] Icelandic Radiation Safety Authority, ICELAND
[2] Centre for Ecology and Hydrology, Bailrigg, Lancaster, UNITED KINGDOM
[3] STUK – Radiation and Nuclear Safety Authority, FINLAND
[4] Risø National Laboratory for Sustainable Energy, Technical University of Denmark, DENMARK

## Abstract

Estimation of global fallout is still important when establishing background values for many radionuclides. Even where deposition measurements have been made, there is a limit for how comprehensive they can be or can have been. Using a model makes it possible to put the available data in a better framework. Two types of models for global fallout have often been used, one assuming that the variation in deposition is a function of latitude, the other assuming that the deposition can be described as the product of radionuclide concentration in precipitation and the amount of precipitation. The former has a meteorological basis for dividing global data into latitude bands and the quantitative estimate is based on the UNSCEAR compilation of deposition data, even though the original sources clearly state that the compilation is for the latitude band as such and should not be used as a model for individual sites. The latter has been used successfully for individual countries and regions, but the same parameters cannot be expected to hold for all conditions. The global model presented here uses the concentration function as a basis, but includes also latitude dependency and contribution of dry deposition through making the average annual deposition one of the parameters used in the model. The parameters of this new model have been determined using the data from the comprehensive global EML network and the model was validated with good results using data from other networks and data from the Nordic countries.

# Reduction of radioxenon emissions from radiopharmaceutical facilities – A pilot study

Braekers, Damien[1]; Camps, Johan[1]; Paridaens, Johan[1];
Saey, Paul R. J.[2]; van der Meer, Klaas[1]
[1] Belgian Nuclear Research Centre (SCK•CEN), BELGIUM
[2] Vienna University of Technology, Atomic Institute of the Austrian Universities, AUSTRIA

## Abstract

The Comprehensive Nuclear-Test-Ban Treaty Organization (CTBTO) is building an International Monitoring System (IMS) in order to verify that the state signatories of the treaty fulfil their commitments of not performing any kind of nuclear explosion. The atmospheric noble gas monitoring is a part of this verification system and focuses on the measurement of short-lived radioxenon isotopes in the atmosphere. In order to improve the sensitivity of the IMS noble gas network, the radioxenon background should be decreased. Previous research has shown that a very limited number of radiopharmaceutical facilities are responsible for the major part of the radioxenon background [Saey 2009]. In addition xenon routine releases from such facilities can hide the release of radiological more important nuclides like iodine during on- or off-site gas monitoring. Reduction of radioxenon release will consequently decrease the global background and enhance the basic safety of such nuclear facilities.

This study reports on several techniques that could be installed in a radioisotope production facility to reduce the discharge of radioxenon in the atmosphere. This pilot study was centred on the Institute for Radioelements (IRE) facility in Fleurus, Belgium – the worldwide third largest Mo-99 producer. Each production step was analysed to determine the amount and the isotopic composition of a possible xenon release. Many techniques (e.g. adsorption on solid materials, cryogenic processes…) will be discussed in terms of performance and practical aspects for the filtration and/or delay of xenon fission gas emissions.

It has been demonstrated in this work that significant reductions of radioxenon atmospheric discharges from Mo-99 production facilities are theoretically possible. Nevertheless it requires a complete inventory of each pathway of xenon release during separation and purification steps of medical radionuclides.

## Introduction

The Comprehensive Nuclear-Test-Ban-Treaty Organisation (CTBTO) is operating for verification purposes an International Monitoring System (IMS) based on four different techniques (seismic, hydroaccoustic, infrasound and radionuclide (particulate and noble

gas) measurements) to detect if an explosion in nature is nuclear or not. The objective of the IMS is, according to the CTBT: "…At least 90% detection capability within 14 days after a nuclear explosion in the atmosphere, underwater or underground for a 1 kton nuclear explosion". The global monitoring of noble gases measures the activity concentration in air of four radioxenon isotopes (Xe-133, Xe-133m, Xe-135 and Xe-131m) with a limit of detection below 1mBq/m$^3$ for Xe-133 [Saey 2007]. However the global radioxenon background which has mainly an anthropogenic origin (nuclear power plants, hospitals and radiopharmaceutical facilities) is in certain areas up to 2 orders of magnitude above the detection limit of the IMS network. It has been demonstrated that the largest contribution to the radioxenon global background by far is coming from the four most important medical radioisotopes production plants that are producing 95% of the Mo-99 world demand by neutron irradiation of highly enriched uranium [Saey 2009]. Mo-99 is the precursor of Tc-99m which is used in 80% of the medical applications with radioisotopes involved world-wide. By consequence, reduction of the radioxenon discharges from these radiopharmaceutical production plants will decrease the global radioxenon background and thus increase considerably the sensibility of the noble gas monitoring network.

On the other hand reducing the radioxenon routine discharges of such kind of nuclear facilities can have another interesting impact regarding the nuclear safety of these installations. Even if the radioxenon nuclides are not important from the radiological point of view, the huge noble gas activity released can mask other more dangerous nuclides such as iodine during on- or off-site gas monitoring. Reduction of radioxenon emissions will consequently decrease the global background and enhance the basic safety of such nuclear facilities in case of an accident but also during the routine monitoring.

This pilot study of the reduction of radioxenon discharges coming from a radiopharmaceutical facility was focused on the case of the Institute for Radioelements at Fleurus in Belgium which is one of the largest Mo-99 producers.

## Review of the noble gases retention-scrubber techniques

Xenon is part of the group of noble gases - its interactions with other elements or matter are, therefore, very limited. Except a few uncommon chemical reactions with strong reagents, xenon is chemically "inert". Xenon interactions with matter or other elements are limited to the van der Waals forces (more specific dispersion or London forces). Consequently only physical separation processes have been proposed and investigated for the recovery of radioxenon from gaseous effluents like adsorption on solid material, cryogenic distillation or diffusion through membranes. The cryogenic distillation process has already been studied extensively and tested for the treatment of krypton and xenon present in the off-gases coming from a nuclear waste reprocessing plant [Collard et al. 1982]. This technique is said to be promising, however it has been rejected because of the higher operational costs and the potential fire hazard caused by ozone accumulation [Geens et al. 1985]. Gas diffusion through thin polymer membranes technology has been already studied in the nuclear sciences field for the purification of a reactor building contaminated air with radioactive noble gases [Stern et al. 1980]. Despite the high efficiency of a multi-stage permeation system, this technique hasn't been selected because of its lower throughput and the sensibility of the thin membranes

to the chemically reactive substances that could be present in the off-gas (e.g. iodine, volatile acids, nitrogen oxides…).

The adsorption process on activated carbons (A.C.) or zeolites is an easy-to-install and reliable process with limited expected operational costs. Several authors have already studied and tested this technique for the treatment of radioactive noble gases effluents coming from different nuclear installations [Moeller et al. 1981, Mondino et al. 2002]. Despite the fire hazard in presence of $NO_x$, activated carbons are a very effective type of adsorbents for the retention of xenon until the radioactive decay has reduced sufficiently the radioxenon activity at the output of the system. The off-gas from a radiopharmaceutical facility contains several radioactive gases (Xe, Kr, I and Rb) as well as non-radioactive gases (Xe, Kr, $N_2$, $O_2$, $NO_x$, $CO_2$, iodine and water vapour) that requires a multi component adsorption approach [Munakata 1999]. Moreover, a pre-treatment of the carrier gas will be necessary in order to remove the most important impurities (water vapour, iodine and carbon dioxide) that could interfere with xenon for the adsorption. Noble gas adsorption depends mainly on several parameters as nature and flow rate of carrier gas, temperature and pressure that can be optimized to obtain the maximal retention time for radioxenon. Finally, xenon breakthrough curve models taking into account the radioactive decay [Lee et al. 1971, Madey et al. 1981] or with an advanced description of the dynamic process [Munakata et al. 2001] can be used on a set of experimental data to extract some important parameters like effective adsorption coefficient and/or diffusion coefficients. In our study these models have been used as a prediction tool to determine the xenon retention time and the decontamination factor of a given adsorption system with the help from experimental data already published in the literature.

## Pilot study → The Institute for Radioelements

The main radionuclides currently produced from irradiated uranium targets (up to 93% of U-235) at the IRE institute are Mo-99, I-131, Xe-133 and Y-90. About 15-20% of the worldwide production of Tc-99m is performed in the Fleurus radiopharmaceutical plant [Kidd 2008].

In order to understand the xenon discharges into the atmosphere by such a facility in detail, a complete analysis of the chemical processes of separation and purification of radionuclides is required. Furthermore, the quantitative simulation of fission products with the ORIGEN code based on target and irradiation specifications can allow us to estimate the amount of radioxenon released for each discharge pathway during the production.

### Investigation of the xenon emissions during the radiochemical process of separation and purification of radionuclides

The chemical processes for the recovery and the purification of the medical radioisotopes play a major role in the dynamics of the radioxenon emissions in the atmosphere from a radionuclides production plant. For the clarity of the following discussion, the radioxenon released has been split in two categories:

- Xenon from dissolution is the xenon accumulated in the targets (by direct fission production or decay) at the time of dissolution and released during the targets dissolution step.

- Xenon from decay is coming from the radioactive decay of the other uranium fission product like iodine or tellurium after the dissolution step.

The isotopic ratio of these two categories is different with a important contribution to the xenon total activity of shorter half-life radionuclides (Xe-135 and Xe-135m) for the xenon from dissolution while Xe-133, Xe-133m and Xe-131m account for the major part of the activity released by radioactive decay of the other fission products. The general process taking place in the IRE institute for the separation and the purification of the medical radioisotopes is based on [Salacz 1985]. The flow sheet is shown in Fig.1 and the critical steps of the process in terms of potential radioxenon emissions are presented in yellow.

The target dissolution by a sodium hydroxide solution releases all fission gases that have been produced during the irradiation and the cooling time over a short period of time. There are about 30h between the end of irradiation and the beginning of the dissolution. Radioactive noble gases such as xenon and krypton account for the major part of the gaseous inventory and are carried out of the dissolver by a helium flow to a cryogenic trap at liquid nitrogen temperature for the recovery of Xe-133. An additional charcoal trap also working at low temperature is installed after the first one to reduce the radioxenon discharges in the ventilation system. The trapped xenon is transferred to MDS Nordion for purification and concentration by gas chromatography. The efficiency of the xenon recovery line and the purification step has been estimated by monitoring at 99% [Verboomen et al. 2009].

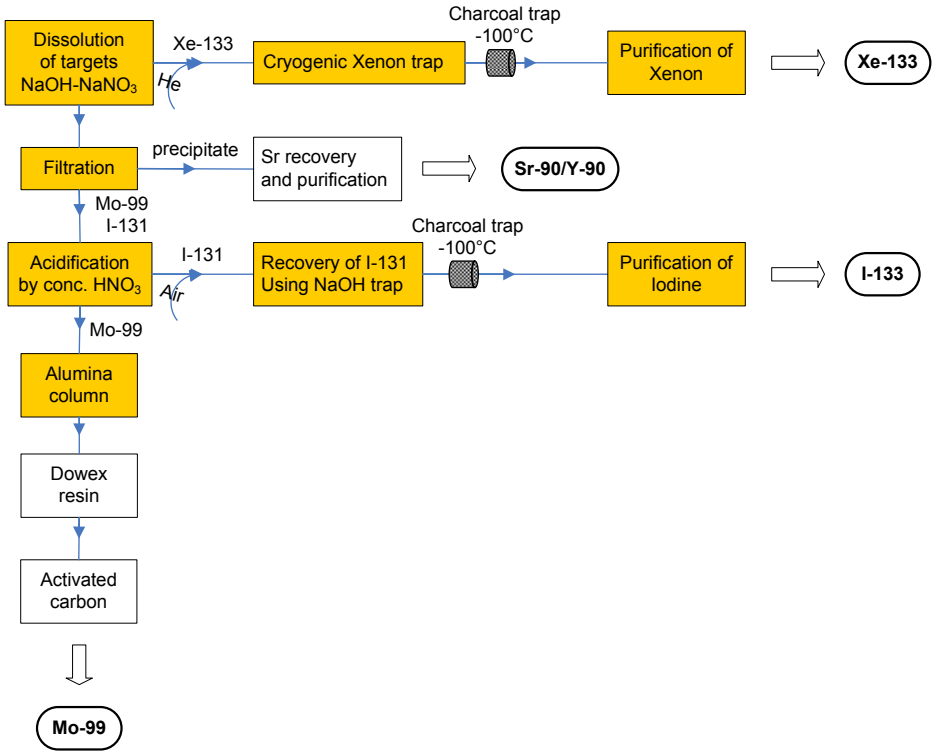


**Fig.1. The process flow sheet for the recovery and the purification of Y-90, Mo-99, I-131 and Xe-133 medical radioisotopes at the Institute for Radioelements.**

The precipitate containing the unfissioned uranium and some insoluble fission products like strontium is removed from the liquid phase by filtration. Radioxenon that is still present in the dissolver after the dissolution is released during this step. The next phase of the recovery and the purification of Sr-90 from the solid residue can be considered as free of radioxenon because of the time interval of years between the filtration and the beginning of the strontium production. However the precipitate continues to release radioxenon that is still contained in the solid material but also from the radioactive decay of iodine and tellurium traces.

The oxidation of $I^-$ into $I_2$ by nitric acid induces the release of iodine in the gas phase. Iodine is trapped on a sodium hydroxide trap and stored until its purification. To reduce the discharge of xenon, a small charcoal trap has been installed after the iodine trap. The efficiency of the iodine recovery is maximum 90% [Salacz 1985]. About 10% of the total amount of iodine stays in the liquid phase and will be transferred on the first chromatography column for the continuation of the Mo-99 purification. The time between the end of the acidification and the beginning of the iodine purification is about 7 days for reaching the good isotopic ratio between I-131 and I-133. During this 7-days interval, the radioactive decay of iodine is producing continuously radioxenon (mainly Xe-133 and Xe-131m). The first alumina chromatography column of the Mo-99 purification step is also a potential source of radioxenon emission because iodine and tellurium traces are removed from the bulk solution and sent in the liquid waste tanks.

Finally, the liquid waste tanks and charcoal filters of the ventilation system that are containing iodine which has not been trapped or treated before, continuously produce some radioxenon isotopes by radioactive decay.

The profile of the radioxenon emissions from a radionuclide production facility is very complex because of the diversity of the emission sources in the process with a xenon isotopic ratio changing over the time. Contrary to a nuclear fuel reprocessing plant where the Kr-85 is mostly discharged all at once during the cutting and the dissolution of the fuel rods [Winger et al. 2005], the treatment of off-gases released only during the dissolution won't be good enough for obtaining a significant radioxenon decontamination factor. All the other critical steps in terms of potential radioxenon emissions in the process also have to be taken into account.

### Estimation of the xenon source term using Origen code simulation

The quantification of the xenon contained in the uranium targets after irradiation has been done by using the Origen code simulation tool [Bowman et al. 1999]. The irradiation of the high enriched uranium targets used by the IRE is actually performed in three different research reactors: in the BR-2 reactor at Mol (Belgium), in the HFR reactor at Petten (the Netherlands) and in the OSIRIS Reactor at Saclay (France). The average irradiation conditions of the uranium targets in these three facilities are shown in Table 1.

**Table 1. Input data for Origen calculations.**

| | |
|---|---|
| **Target type** | U-Al alloy (93% U-235) |
| **Amount of U-235** | 4 g per target |
| **Irradiation time** | 150h |
| **Thermal Neutron flux** | 1.5 $10^{14}$ n/cm$^2$.s |
| **Cooling time** | 30h |

Actually, 12 targets (48g of U-235) are irradiated and treated in one batch per production and there are 3 productions per week [Verboomen et al. 2009]. The time dependence of the activity for the main five radioxenon isotopes after the end of the irradiation is shown in Fig.2. The total xenon activity that is released from the targets during the dissolution step has been estimated to 438 TBq. If we consider an efficiency of 99% for the Xe-133 recovery and purification lines, a discharge of 4.4 TBq of "fresh" radioxenon (xenon from dissolution) per dissolution can be expected. The main contributions to this activity are coming from the Xe-133 and the short half-live xenon isotopes (Xe-135 and Xe-135m). This graph shows clearly that the xenon isotopic ratio of a discharge happening during the dissolution of the targets can be very different of one coming during the iodine purification step (7 days later). All the radioxenon discharges (puffs and constant releases) that are coming from different places in the facility at different times since the end of the irradiation merge together in the ventilation and reach the atmosphere by the same stack. The complete attribution of each signal detected by a single monitoring system at the level of the stack is virtually impossible because of the overlapping of all kind of radioxenon emissions.

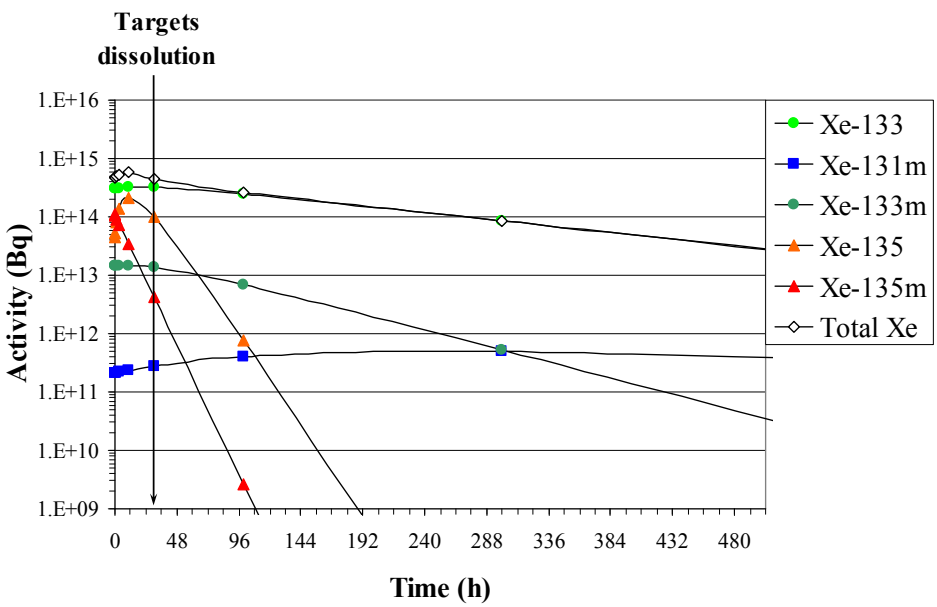


**Fig. 2. Activity (Bq) versus time (h) for the main xenon radioisotopes produced during the irradiation period.**

Another interesting point is to compare the contribution of the xenon activity released during the dissolution to the xenon activity produces by radioactive decay of

the other fission products. The evolution of the xenon activity in function of time is shown in Fig.3. in terms of the sum of both types of xenon emissions. The xenon activity that can be released from fission products decaying is about 32 TBq after 100 hours. This contribution accounts for 12.5% of the total activity if all xenon is discharged at that moment. Although this part of radioxenon is generated over several days and probably not released during a short period of time, the amount produced from these decay chains is split during the acidification step between the first Mo-99 purification column (10%) and the purification of iodine (90%) (See Fig.1.). At the end about 10% of the xenon activity produced by radioactive decay of the fission products (3.2 TBq over 4 days) is sent to the liquid wastes storage facility. It illustrates clearly that an untreated xenon discharge can rapidly account for several percents of the total radioxenon emissions and thus can mask the effort put in treating other release pathways.

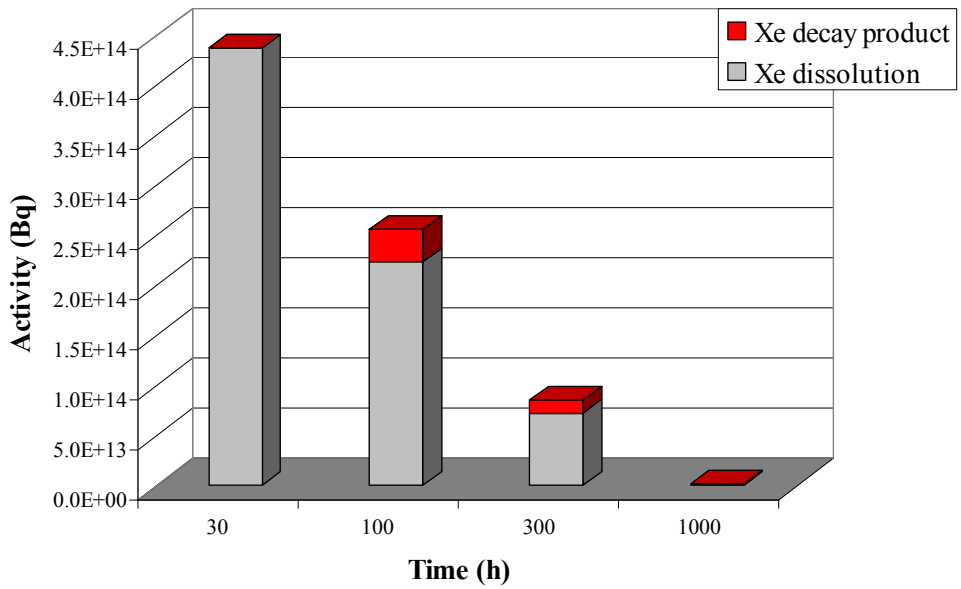


**Fig. 3. Evolution of xenon activity (Bq) in function of time (h) (grey: Xenon released during dissolution; red: Xenon produced by radioactive decay).**

## Example of a xenon adsorption delay system

The scheme of the example presented below is shown in Fig.4. This system has been designed for the treatment of gaseous effluents with a relative small flow rate (up to 4l/min) and helium is used as the carrier gas to minimize its influence. Two preconditioning steps have been planned to remove most of the impurities before contact with the adsorbent bed. The first one is relative to the removing of nitrogen oxide by catalytic reduction with ammonia. The second is a pressure swing adsorption (PSA) system for the elimination of water vapour and the carbon dioxide. Four activated carbon packed bed columns (length=100cm, radius=10cm) installed in parallel are the adsorption part for the retention of the xenon.

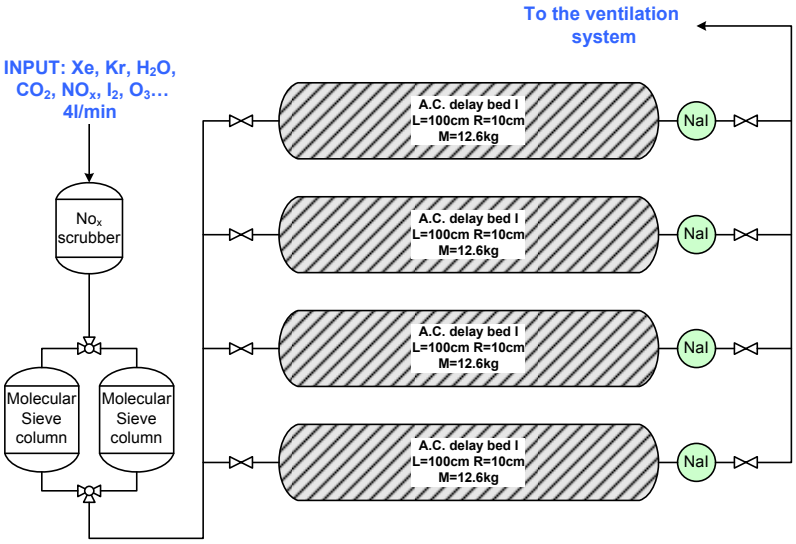


**Fig. 4. Example of a xenon delay system for the treatment of contaminated gaseous effluents up to 4l/min.**

A parallel multi-column adsorption system has two advantages:

- To reduce the linear velocity of the carrier gas in each column, which is an important parameter that can seriously affect the retention time;
- Increase the basic safety of the installation with the principle of redundancy.

The monitoring of the radioxenon activity is done by a sodium iodine detector on top of each column and each column can be isolated for decay if needed. The input and output parameters of the xenon breakthrough curve simulation, based on the experimental data of [Munakata et al. 2001], are listed in table 2.

**Table 2. Input and output parameters for the breakthrough curve simulation of the example.**

| Parameters | Value |
|---|---|
| **Flow rate** | 4 liters/min. |
| **Temperature** | 195K |
| **Column length** | 100cm |
| **Column radius** | 10cm |
| **Linear velocity** | 0.53 mm/s in each column |
| **Bed density** | 0.40g/cm$^3$ |
| **Amount of A.C.** | 12.6kg/column → 50.4kg |
| **Xenon partial pressure** | 100 Pa |
| **Effective adsorption coef.** | ~6500 cm$^3$/g |
| **Retention time** | 56.7 days |
| **Decontamination factor (Xe-133)** | > 1000 |

This example has shown that a small system with only 50kg of A.C. is able to treat a helium flow contaminated with radioxenon up to 4liters/min. We can imagine

that each critical step, pointed out from Fig.1, can be treated with this system or that all the contaminated gaseous phases will be sent into a single tank connected to the delay system for a global treatment to reduce the operational costs.

From the radioprotection point of view, this kind of retention system can raise some problems for the protection of workers because of the high specific activities of short-life radioxenon isotopes and the important amount of radioxenon which is going to accumulate inside the adsorption beds.

## Conclusions

The possible reduction of the atmospheric radioxenon discharges from a radioisotope production facility like the Institute for Radioelements at Fleurus, Belgium has been investigated. The review of the noble gases filtration/mitigation processes has pointed out that the adsorption on activated carbon is the most suitable technique for this purpose. The analysis of separation and purification steps of the radioisotopes, combined with quantitative estimation by using the ORIGEN code have shown that the dynamics of the xenon emissions are very complex and can not be attributed to only one process but to the entire process flow taking place in the facility.

A small adsorption system working at low temperature has been designed with four parallel activated carbon columns for the retention of radioxenon. Breakthrough curve models have shown that a decontamination factor of more than 1000 for Xe-133 can be expected. However the installation of such a system for the treatment of all possible sources of radioxenon from inside the facility could raise some problems of radioprotection due to the high radioxenon activity present.

## Acknowledgments

The authors would like to thanks Dr. H. Miley and Dr. J.C. Hayes from the Pacific Northwest National Laboratory (PNNL) for their advices all through this research. We are grateful to Dr. B. Verboomen, Dr. B. Deconninck, Mr. N. Paquet and Dr. J.-Y. Binamé from the Institute for Radioelements (IRE) for their help and their permanent support.

## References

Bowman S.M., Leal L.C., Hermann O.W., Parks C.V. Origen-ARP, A Fast and Easy-to-Use Source Term Generation Tool, Proceeding of the Ninth International Conference on Radiation Shielding (ICRS-9). 1999 Oct 17-22; Tsukuba, Japan.

Collard G., Goossens W.R.A, Vaesen J., Glibert R., Baetsé L.H. Cryogenic Distillation Unit for Krypton and Xenon Removal from Gaseous Effluents. Transactions of the American Nuclear Society 1982; 40:122-124.

Geens L.P., Collard G., Goossens W.R.A., Baetsé L.H. Krypton recovery from Reprocessing Off-gases by Cryogenic Distillation. Radioactive Waste management and Environmental Restoration 1985; 6(3-4):219-235.

Kidd L. Curies for patients. Nuclear Engineering International 2008; 53(648): 26-32.

Lee K.B., Madey R. The transmission of Xenon-133 through Activated Carbon Adsorber Beds. Nuclear Science and Engineering 1971; 43:27-31.

Madey R., Huang J.-C., Pflumm E. Transmission of a Gaseous Radioactive Isotope Though an Adsorber Bed. Nuclear Science and Engineering 1981; 78:205-210.

Moeller D.W., Underhill D.W. Review and Evaluation of Factors Affecting Noble-Gas Adsorption on Activated Carbon. Nuclear Safety 1981; 22(5):599-611.

Mondino A.V., Manzini A.C., Cerutti G.L., Iglicki F.A., Novello N.A. Retention of fission xenon in air by activated carbon at 2 °C. Journal of Radioanalytical and Nuclear Chemistry 2002; 253(2):205-208.

Munakata K., Fukumatsu T., Yamatsuki S., Tanaka K., Nishikawa M. Adsorption Equilibria of Krypton, Xenon, Nitrogen and Their Mixtures on Molecular Sieve 5A and Activated Charcoal. Journal of Nuclear Science and Technology 1999; 36(9):818-829.

Munakata K., Tanakata K., Yamatsuki S., Fukumatsu T., Kanjo S., Yokoyama Y., Nishikawa M. Dynamics of Adsoprtion of Kr and Xe on MS5A and Activated Charcoal. Journal of Chemical Engineering of Japan 2001; 37(7):853-861.

Saey P.R.J. Ultra-Low-Level Measurements of Argon, Krypton and Radioxenon for Treaty Verification Purposes. Esarda Bulletin 2007; 36:42-56.

Saey P.R.J. The influence of radiopharmaceutical isotope production on the global radioxenon background. Journal of Environmental Radioactivity 2009; 100:396-406.

Salacz J. Reprocessing of irradiated Uranium-235 for the production of Mo-99, I-131, Xe-133 radioisotopes. Revue IRE 1985; 9(3):22-28.

Stern S.A., Wang S.-C. Permeation Cascades for the Separation of Krypton and Xenon from Nuclear Reactor Atmospheres. AIChE Journal 1980; 26(6):891-901.

Verboomen B., Deconninck B., Paquet N., Binamé J.-Y. Pers. Communication. Institute for Radioelements (IRE), Begium 2009.

Winger K., Freichter J., Kalinowski M.B., Sartorius H., Schlosser C. A new compilation of the atmospheric $^{85}$krypton inventories from 1945 to 2000 and its evaluation in a global transport model. Journal of Environmental Radioactivity 2005; 80:183-215.

# Public exposure by natural radionuclides in drinking water – Models for effective dose assessment and implications to guidelines

Gruber, Valeria[1,2]; Maringer, Franz Josef[2,3]
[1] European Commission – Joint Research Centre, Institute for Environment and Sustainability, Radioactivity Environmental Monitoring Group, ITALY
[2] BOKU - University of Natural Resources and Applied Life Science, Low Level Counting Laboratory Arsenal, AUSTRIA
[3] BEV – Federal Office of Metrology and Surveying, AUSTRIA

## Abstract

In Austria the legal framework to "Exposure by natural radionuclides in drinking water" is the Austrian Drinking Water Ordinance (Trinkwasserverordnung BGBl. II 304/2001) which implements exactly the European Drinking Water Directive 98/83/EC. The minimum requirements on the quality of drinking water and water intended for human consumption are appointed in it. For radioactivity two indicative standard parameter limits are established – tritium activity concentration of 100 Bq/l and total indicative dose TID (effective dose from radionuclides in drinking water except $^{3}$H, $^{40}$K, radon and radon progenies) of 0.1 mSv/a. The appointment and the evaluation of the TID are specified in the Austrian Standard OENORM S 5251:2005. Generally only the radionuclides $^{226}$Ra and $^{228}$Ra, dose conversion factors for adults and a yearly water consumption of 730 l are taken into account for dose calculation.

In the paper the estimation of the TID according to the drinking water directive and the OENORM standard is compared to dose estimations for other age groups and other nuclides based on measurements carried out in Upper Austria. The dose contributions of $^{210}$Po and $^{210}$Pb clearly preponderate the dose contributions of the radium isotopes. An alternative model for dose estimations has been developed, which takes into account a daily water intake and a continuous excretion of activity from the body. The presented dose assessment clearly yields lower annual effective doses for the population. Present regulations and guidelines for drinking water monitoring and surveillance are discussed and evaluated with regard to the results of this study.

Disagreement persists on methods and applied parameters for estimating total doses caused by natural radionuclides in drinking water within Europe, its individual countries and experts. This paper contributes supporting facts and feasibilities to yield a good basis for future guidelines.

## Introduction

Drinking water is the most important food. Therefore its availability, quality and regulation are delicate and important topics. For this purpose it is fundamental to have an overview and hence reasonable regulations about natural radioactivity in drinking water. In the European Drinking Water Directive 98/83/EC (European Commission, 1998) a minimum requirement on the quality of drinking water and water intended for human consumption is appointed. For radioactivity two indicative standard parameter limits are established – Tritium activity concentration of 100 Bq/l and total indicative dose TID (effective dose from radionuclides in drinking water except $^{3}$H, $^{40}$K, radon and radon progenies) of 0.1 mSv/a.

Radon and the radon progenies are excluded from the European directive (European Commission, 1998). The European commission (European Commission, 2001) recommends for $^{222}$Rn, that a reference level should be appointed above an activity concentration of 100 Bq/l, and with radon activity concentrations above 1000 Bq/l measures are justified. For the radon progenies $^{210}$Pb and $^{210}$Po the Commission recommends (European Commission, 2001) that above an activity concentration of 0.2 Bq/l and 0.1 Bq/l respectively, it should be tested whether any measures are necessary.

$^{238}$U were not taken into account in the European commission recommendations, but the World Health Organisation (WHO) recommends a guidance level of 15 µg/l natural uranium, which corresponds to a 0.19 Bq/l $^{238}$U activity concentration in the drinking water guidelines (WHO, 2004). These guidance levels are applied to chemo-toxic effects of uranium, not on the radioactive exposure. The WHO defines guidance levels for several radionuclides in drinking water (artificial and natural) and says that no deleterious radiological health effects are expected from consumption of drinking water if the concentrations of radionuclides are below the guidance levels (equivalent to a committed effective dose below 0.1 mSv/a). This corresponds with the European directive 98/83/EC (European Commission, 1998).

For radon the WHO guidelines recommend that controls should be implemented if the radon concentration of drinking-water for public water supplies exceeds 100 Bq/l, which corresponds basically with the European Commission recommendation (European Commission, 2001) but is stricter.

All these recommendations afford high responsibilities of the countries to establish their individual and detailed limitations and regulations.

In Austria the legal framework for exposure from natural radionuclides in drinking water is the Drinking Water Regulation – TWV (Republic of Austria, 2001) which implements exactly the European Drinking Water Directive 98/83/EC (European Comission, 1998). The appointment and the evaluation of the TID are specified in the Austrian Standard OENORM S 5251 (OENORM, 2005). The required measurement techniques (e.g. detection limit), sampling site and the evaluation methods including examples are specified there. Generally only the radionuclides $^{226}$Ra and $^{228}$Ra with dose conversion factors for adults and a consumption rate of 730 l/a are taken into account for dose calculation of drinking water in Austria. Beside this standard there is a lack of regulation concerning other radionuclides e.g. $^{222}$Rn, $^{210}$Po and $^{210}$Pb.

For taking of an inventory of radionuclides in drinking water a drinking water pilot study was carried out in Austria. Based on these measurements dose calculations

were implemented according to the Austrian Standards and compared with other dose models and evaluated. The paper yields to provide a basis for further discussions because of disagreement on methods and applied parameters for estimating total doses caused by natural radionuclides in drinking water within Europe, its individual countries and experts.

## Material and methods

A drinking water research project was carried out between 2004 and 2006 in Upper Austria (area: 12 000 km$^2$, population: 1.4 million) funded by the Government of Upper Austria in which 350 water samples were taken in water supplies, wells and at consumers' houses. All water samples were analyzed for different radionuclides ($^{222}$Rn, $^{226}$Ra, $^{3}$H, $^{238}$U) and gross-alpha-beta-activity concentration by LSC and ICP-MS. A collection of the water samples were additionally analyzed for $^{228}$Ra, $^{210}$Po and $^{210}$Pb by LSC. The detailed sampling methods and the project in whole is discussed in (Gruber et al., 2007, Gruber, 2009) and the detailed measuring procedures are also given in Landstetter & Katzlberger (2005).

For the analyzed radionuclides activity concentrations in the water samples ($c_i$) dose calculations were carried out. The total indicative dose (TID) was calculated according to the Austrian Standard OENORM S 5251 (OENORM, 2005). The total dose is the sum of the dose contributions of the single radionuclides ($GD_i$) (according to OENORM S 5251 basically only $^{226}$Ra and $^{228}$Ra), which are calculated from the activity concentrations ($c_i$) with the legal valid dose conversion factors ($h(g)_i$) for adults (age >17a) respectively and an annual consumption ($KM$) of 730 l/a (according to OENORM S 5251) (Formula 1). Activity concentrations below detection limit are set to zero. Uncertainties are calculated by error propagation without taking into account an uncertainty contribution of consumption and dose conversion factors.

$$GD = \sum_i GD_i = \sum_i h(g)_i \cdot c_i \cdot KM \qquad (1)$$

For the compliance of a reference value for the total indicative dose ($RGD$ – e.g. the total indicative dose (TID) according to the drinking water directive (Republic of Austria, 2001)) the following requirement has to be proved, whereas $\Delta GD$ is the uncertainty of the total dose (Formula 2).

$$RGD \geq GD - \Delta GD \qquad (2)$$

The total dose (Formula 1) was additionally calculated regarding other measured nuclides ($^{238}$U) and also for nuclides excluded in the drinking water directive (European Commission, 1998) like $^{210}$Pb, $^{210}$Po. Besides the dose contribution of the different radionuclides and the total dose were estimated with dose conversion factors for other age groups (babies, children), because they are applied for dose assessments in some countries and this topic is still under discussion within the experts. The dose conversion factors are the values of the committed effective dose per unit intake via ingestion for members of the public at different age groups according to the Basic Safety Standards (IAEA, 1996, see Table 1). The annual water intake values were chosen by the Article 31 working party on radioactivity in drinking water after overview of different intake

values by different organisations, including the WHO. The age group 12–17 a was not considered for dose calculation because of no defined water intake for that age group (Risica & Grande, 2000).

**Table 1. Dose conversion factors for different age groups and nuclides (IAEA, 1996) and annual water intake (European Commission (1998), Risica & Grande (2000)).**

| Age group | Dose conversion factors (Sv/Bq) | | | | | Annual water intake (l) |
|---|---|---|---|---|---|---|
| | $^{228}$Ra | $^{226}$Ra | $^{238}$U | $^{210}$Pb | $^{210}$Po | |
| <1 | 3.0 E-5 | 4.7 E-6 | 3.4 E-7 | 8.4 E-6 | 2.6 E-5 | 250 |
| 1–2 | 5.7 E-6 | 9.6 E-7 | 1.2 E-7 | 3.6 E-6 | 8.8 E-6 | 350 |
| 2–7 | 3.4 E-6 | 6.2 E-7 | 8.0 E-8 | 2.2 E-6 | 4.4 E-6 | 350 |
| 7–12 | 3.9 E-6 | 8.0 E-7 | 6.8 E-8 | 1.9 E-6 | 2.6 E-6 | 350 |
| (12–17 | 5.3 E-6 | 1.5 E-6 | 6.7 E-8 | 1.9 E-6 | 1.6 E-6) | |
| >17 | 6.9 E-7 | 2.8 E-7 | 4.5 E-8 | 6.9 E-7 | 1.2 E-6 | 730 |

Additional dose assessments were carried out based on a model by Bronzovic et al. (2006) taking into account a continuous daily water intake and a continuous excretion of the radionuclides from the body. Therefore the m(t) value according to IAEA (2004) was applied, which describes the fraction of a unit intake retained in the whole body at time t after intake. The major part of the radionuclide is excreted from the body within a few days after the intake (e.g. for Ra, Figure 1). A daily total radionuclide activity in the body was calculated for different radionuclides by a daily 2 litre drinking water intake with a constant activity concentration and a daily excretion specified by the m(t) value. The effective dose for the total body (without distinguishing between tissues and organs, related to a 70 kg reference person) was estimated taking into account the absorbed fraction, the energy emitted in the body by the radionuclides and the radiation weighting factors.

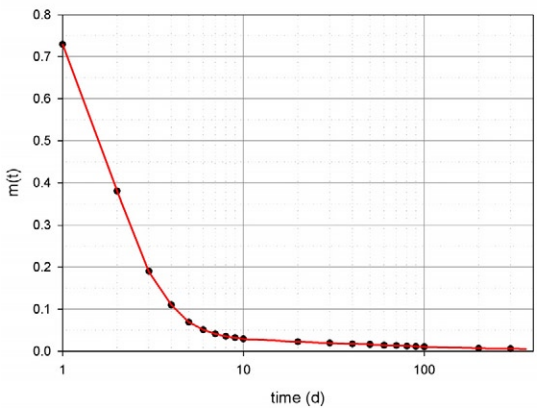


**Fig. 1. The fraction of a unit intake retained in the whole body at time t after intake (m(t) value, for one year) for the radionuclides $^{226}$Ra and $^{228}$Ra.**

## Results and discussion

The calculated total dose according to formula (1) according to the Austrian standard OENORM S 5251 (OENORM, 2005) – considering only $^{226}$Ra and $^{228}$Ra is below the parametric value of total indicative dose (TID) of 0.1 mSv/a for all analyzed drinking waters in Upper Austria (Fig.2). Corresponding to the cumulative frequency distribution in Figure 2 for 90 % of the Upper Austrian drinking waters a total dose below 0.01 mSv/a is expected.

The dose calculations considering other nuclides show, that the dose contribution of $^{238}$U is in general insignificant, but preponderate the dose contribution of $^{226}$Ra and $^{228}$Ra in some particular samples. The total dose caused by the radon progenies $^{210}$Pb and $^{210}$Po is clearly higher and 10 % of the water samples exceed the parametric value of the total indicative dose of 0.1 mSv/a (Figure 3). These radionuclides should therefore not be disregarded in guidelines and regulations for radiation protection purposes.

Only samples with both activity concentrations above detection limit (DL) are displayed in the figures.

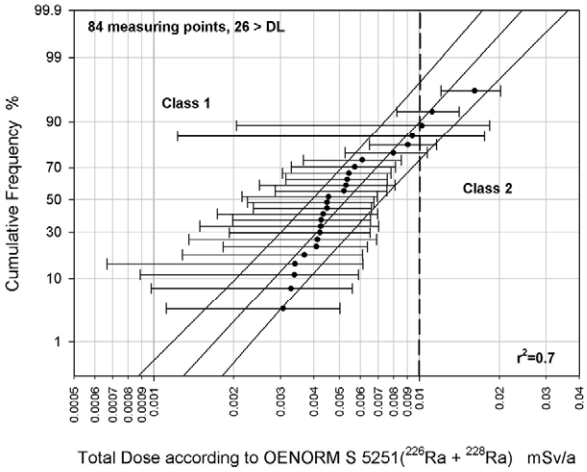


**Fig. 2. Cumulative frequency of the total dose according to OENORM S 5251 (OENORM, 2005).**

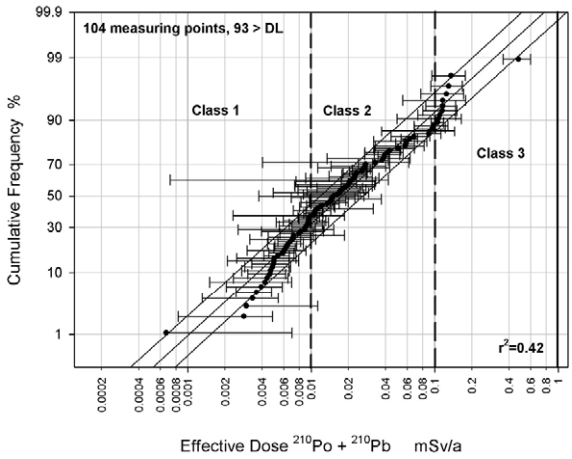


**Fig. 3. Cumulative frequency of the total effective dose by $^{210}$Po and $^{210}$Pb calculated for adults.**

The total doses for $^{226}$Ra and $^{228}$Ra are also clearly below the parametric value of 0.1 mSv/a for the other age groups (children). For about 10 % of the Upper Austrian drinking waters a dose above 0.1 mSv/a is expected for babies (< 1a) (Fig.4). No analyzed water sample has a dose caused by $^{238}$U higher than 0.1 mSv/a for all age groups. The dose caused by $^{210}$Pb and $^{210}$Po for babies (< 1 a) exceeds 0.1 mSv/a for about 50 % of the analyzed Upper Austrian drinking waters. Also for the other age groups doses above 0.1 mSv/a occur for these nuclides (Figure 5).

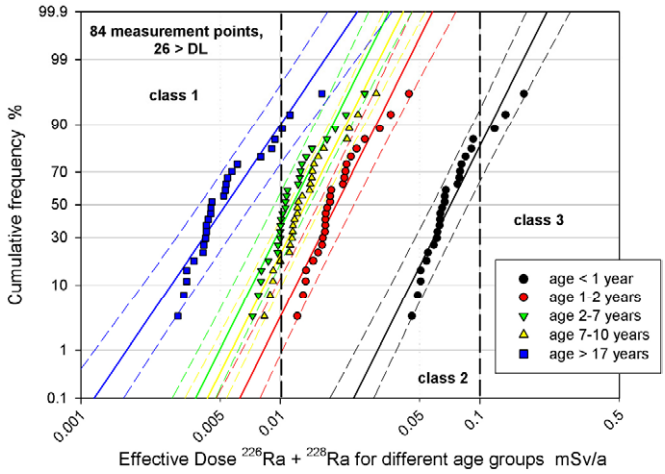


**Fig. 4. Cumulative frequency distribution of the sum of the effective doses in drinking water caused by $^{226}$Ra and $^{228}$Ra for different age groups.**

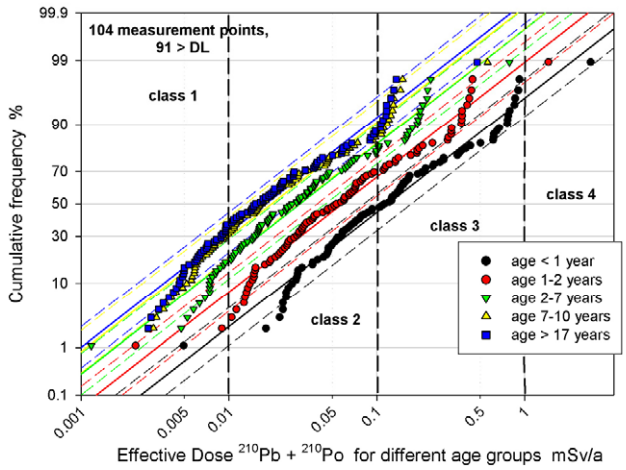


**Fig. 5. Cumulative frequency distribution of the sum of the effective doses in drinking water caused by $^{210}$Pb and $^{210}$Po for different age groups.**

Figure 6 illustrates the dose contribution of each nuclide to the annual total dose for adults (> 17a) estimated for each analyzed drinking water sample. For most of the samples the dose contribution of $^{210}$Po dominates (up to 80-100 %) because of its high dose conversion factor (Table 1). The activity concentration of $^{228}$Ra is below detection limit for most of the samples, but if the activity concentration is above detection limit, it contributes clearly to the total dose because of its high dose conversion factor (Table 1).

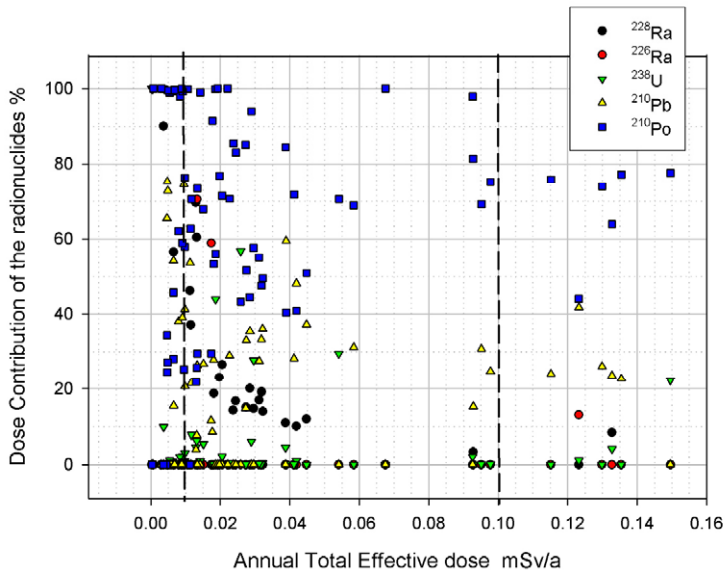


**Fig. 6. Dose contributions of the nuclides to the annual total effective dose for adults (>17a).**

The effective doses calculated with the above discussed alternative method, taking into account a daily water intake and a continuous excretion of the radionuclides from the body (m(t) value) are at least 2 magnitudes lower for adults than calculated with the conventional method (formular (1), Austrian Standards Institute, 2005) with the same activity concentration in drinking water. So it has to be proofed, if dose calculations according to formula (1) overestimate the radiation exposure of the public caused by radionuclides in drinking water and if the parametric value of the total indicative dose of 0.1 mSv/a is too conservative.

## Conclusions

Dose assessments of radionuclides in drinking water are an issue of steady discussion within countries of the European Union and others and also within experts of one country. There are discussions about the legislative regulation and implementation of dose parameters or of reference activity concentrations. As discussed and explained in this paper, the European drinking water directive (European Commission, 1998) only states a total indicative dose and a tritium activity concentration, which was one-to-one adopted in various national laws (like Austria and Germany for example). For other radionuclides like the radon progenies $^{210}$Po and $^{210}$Pb only (activity concentration related) recommendations exists. As shown above the dose caused by $^{210}$Po and $^{210}$Pb is not negligible compared to the dose contribution of the radium isotopes. So these nuclides should be taken into account in applied regulations and dose calculations.

The survey in this paper should illustrate that in Upper Austria risk for the population caused by natural radioactivity in drinking waters only occurs in individual cases and for most of the Upper Austrian drinking waters no hazards for the population exist. Nevertheless drinking water should be controlled and surveyed regarding radioactivity, but drinking waters with little enhanced radioactivity concentrations according to different standards, recommendations and guidelines should not be set disabled for drinking water purposes without further surveys and dose assessments. For

this purpose guideline values were developed in the framework of this project to simplify and standardize experts' activities in drinking water affairs. These recommendations are already adopted and published in the "Austrian food and drinking water codex", Codex alimentarius Austriacus, Chapter B, drinking water (BMGFJ, 2008) and are based on a differentiation between a monitoring level (indicative parameter of TID 0.1 mSv/a) and an intervention level of a total indicative dose of 1 mSv/a. If this intervention level is exceeded appropriate remedial actions should be recommended. In the codex also intervention levels for the activity concentration of $^{222}$Rn (1000 Bq/l) and its progenies $^{210}$Pb (2 Bq/l) and $^{210}$Po (1 Bq/l) are included. The codex is not a regulation, but an important implement which proclaims terms and definitions, technical names and research in Austria. The worked out recommendation could also yield an extension of the Austrian drinking water regulations.

## References

Bronzovic, M., Marovic, G., Vrtar, M. Public Exposure to Ra-226 in Drinking Water, Arh Hig Rada Toksikol (57): 39-44, 2006

Bundesministerium für Gesundheit, Familie und Jugend (BMGFJ). Österreichisches Lebensmittelbuch (Codex alimentarius Austriacus). 4. Auflage, Kapitel B, Trinkwasser, Vienna, 2008

European Commission. Council Directive 98/83/EC of 3 November 1998 on the quality of water intended for human consumption. Official Journal L 330; 05.12.1998, p.0032-0054, 1998

European Commission. Commission Recommendation of 20 December 2001 on the protection of the public against exposure to radon in drinking water supplies. 2001/982/Euratom, L344/85, 2001

Gruber, V., Maringer, F.J., et al. Strahlenexposition durch Trinkwasser in Oberösterreich – 2004 bis 2006, Teilprojekt Bevölkerungsexposition. Final Report; Linz; Amt der oberösterreichischen Landesregierung, Umwelt- und Anlagentechnik; 2007

Gruber, V. Radiation Exposure by Natural Radionuclides in Drinking Water in Upper Austria – A Radioanalytical and Hydrogeological Research and Evaluation in an International Context. Ph.D. thesis; Universität für Bodenkultur; Vienna; 2009

International Atomic Energy Agency (IAEA). International Basic Safety Standards for Protection against Ionizing Radiation and for the Safety of Radiation Sources. Safety Report Series, No. 115, Vienna, 1996

International Atomic Energy Agency (IAEA). Methods for Assessing Occupational Radiation Doses Due to Intakes of Radionuclides. Safety Reports Series, No.37, Vienna, 2004

C. Landstetter, C. Katzlberger. Rapid method for determining natural radionuclides in drinking water. Proceedings Book of the 2005 International Liquid Scintillation Conference, Katowice, Radiocarbon, 2005, pp.181-190

OENORM S 5251. Bestimmung und Bewertung der Gesamtdosis durch Radionuklide im Trinkwasser. Vienna; Austrian Standards Institute; 2005

Republik Österreich. 304. Verordnung des Bundesministers für soziale Sicherheit und Generationen über die Qualtität des Wassers für den menschlichen Gebrauch (Trinkwasserverordnung – TWV). BGBl. II, Nr. 304. Vienna, 2001

Risica, S., Grande, S. Council Directive 98/83/EC on the Qualtiy of Water Intended for Human Consumption: Calculation of Derived Activity Concentrations. Rapporti ISTISAN 00/16, Roma, 2000

World Health Organization (WHO). Guidelines for Drinking Water Quality. 3rd edition; Geneva; 2004

# Impact of facilities under the nuclear fuel cycle on the public health: SUE "Hydro Metallurgical Plant" (LPO "ALMAZ") case study

Titov, A. V.; Tukov, A. R.; Bogdanova, L. S.; Yatsenko, V. N.; Korzinkin, M. B.
Burnasyan Federal Medical Biophysical Center, Moscow, RUSSIA

## Abstract

Over the full period of the nuclear power engineering and industry development, comprehensive radio-ecological inspections are carried out in the Russian Federation to reveal and evaluate potential negative consequences of past activity of facilities under the Nuclear Fuel Cycle (NFC).

The Project No 3003 of the International Science and Technological Centre (ISTC) «Radiation Impact of the Facilities under the Russian Nuclear Energy Complex on the Environment and Human. Development of the Scientific Basis for Radiation Protection of the Environment» integrated efforts of several key international organizations involved in the radiation safety examinations. The Burnasyan Federal Medical Biophysical Centre under the FMBA of Russia (ex-Institute of Biophysics) is one of the participants of this project. The Centre accumulated the great experience in evaluation of the public doses originated from radioactive discharges and effluents; it also developed some methods for assessment of radiation impact on the human health. Following this work, the available results of the radiation situation monitoring have been summarized and analyzed; doses resulted from man-made radiation exposure to the public living nearby the Krasnoyarsk Mining Chemical Combine (MCC), LPO "Almaz" and Novovoronezh NPP have been assessed, and their contribution has been evaluated into dose due to the natural background at such areas.

At the same time, epidemiological inspection was being performed to identify potential connection between the radiation situation at the area of the facility impact and the public health. Data on incidence of malignant neoplasms have been collected over the period from 1991 to 2006 in respect to the residents of the areas studied. The special attention was paid to leukemia, which is the first response to over-exposure. The development took into account indexes of patients with cancer of lymphoid, blood-forming (hematoplastic) and their nested tissues, as well as cancers of other critical human organs. Finally, the database on epidemiological data has been arranged and treated.

Analysis of morbidity with malignant neoplasms helped to reveal significant differences in the morbidity statistics of male and female residents of Lermontov city

situated at the area of the LPO "Almaz" impact, in comparison with the control area in respect of common morbidity and incidence of the trachea, bronchus and lung cancers.

## Material and methods

Three methods are used in epidemiology to answer the question about potential association between radiation situation at the area inspected and malignant neoplasms of the residents at this area. These are: *cohort examination*, when the morbidity risk of persons under radiation exposure is being evaluated in comparison with the control group; *case-control study* – risk connected with exposure is calculated by means of comparison of the diseased person group ("cases") with that of healthy individuals ("control") by their radiation exposure index; *territorial comparison*, when areas are chosen with different radiation exposure level.

Generally, case-control studies are less reliable than randomized control examinations or cohort ones.

The main requirement for application of the cohort or "case-control" study is availability of the personal dose data for each resident studied. Today, it is impossible to provide such kind of information. Therefore, we applied the method of territorial comparison in this work.

Obninsk city was selected as the control territory and its population was under examination. The town-forming facility is located in Obninsk – the Institute of Physics and Power Engineering (IPPE) equipped with the first Russian nuclear power plant – nevertheless, inspection aimed at risk assessment of leukemia incidence in the IPPE experts being carried out by V K Ivanov ea. [1], did not find any excessive risk, so the conclusion can be made on its absence for the rest residents of the city as well. In addition, «…long-term experience of nuclear facility operation in Obninsk shows that man-made radioactivity is low and does not impact significantly on doses to the public and environmental species» [2].

Having in mind that leukemia is generally the first response to over-exposure, our development included firstly indexes of the number of persons diseased with cancers of lymphoid, blood-forming and their nested tissues, as well as cancers of other critical human organs which are more frequent at the areas inspected.

The database arranged includes the areas being inspected over the period from 1991 to 2006. To improve the information validity, data have been treated by two-year cycles of study. For this purpose, all absolute indexes were being summed each two years.

Intensive indexes of morbidity were calculated according to the equation:

$$P=\frac{a \cdot k}{n}, \quad (1)$$

where P – intensive index,
$a$ – number of persons diseased,
$n$ – number of the relevant serviced contingent,
$k$ –for malignant neoplasms = 100 000.

The standard error is calculated for the intensive indexes (m) according to the equation:

$$m = \pm \sqrt{\frac{P \cdot Q}{n}}, \quad (2)$$

where $m$ – standard error,
$P$ – intensive index,
$Q = k - P$,
$n$ – number of the relevant serviced contingent.

The standard error is included into the lists of the intensive indexes. Then, tables of morbidity indexes are being arranged for different nosologies and cycles of study.

To evaluate validity of difference between two indexes (the t – Student criterion), the mean error of this difference has been calculated, equal the square root from the sum of squares of the mean errors for these indexes

$$s.e.difference = \sqrt{(s.e.C_1)^2 + (s.e.C_2)^2} \quad (3)$$

If difference ($C_1$-$C_2$) is at least twice higher than its mean error, then some to the some extent we can say that the difference in the indexes is valid (non-random) and depends on some certain reason. If otherwise, this difference is less than twice higher than its mean error, then this difference is not valid (random).

The confidence probability specifies result reliability of the sampling study. We use 95% confidence probability in this work.

## Results and Discussion

In the course of operation of the hydro-metallurgical plant (HMP), maximum doses originated from the current effluents took place near Ostrogorka village, subsidiary plots of which located near the border of the health protection zone. Table 1 shows annual effective dose to the residents of Ostrogorka village via each pathway of effluent-induced exposure over 1979 - 1991, being calculated according to [3].

**Table 1. annual effective dose to the residents of Ostrogorka village originated from the current effluents, μSv.**

| Yar | | | | | | | | | | | | | |
|---|---|---|---|---|---|---|---|---|---|---|---|---|---|
| 1978 | 1979 | 1980 | 1981 | 1982 | 1983 | 1984 | 1985 | 1986 | 1987 | 1988 | 1989 | 1990 | 1991 |
| 2,8 | 1,9 | 0,8 | 2,6 | 2,6 | 2,6 | 2,6 | 4,0 | 4,0 | 4,1 | 3,3 | 2,4 | 2,7 | 0,12 |

Data from Table 1 confirm that radionuclide release into atmosphere during the uranium ore milling at the HMP did not impact significantly on the public living to the leeward relating to the effluent sources. Internal exposure due to ingestion radionuclide intake via the local foods made the main contribution into annual effective dose to the public - 98 %. $^{210}$Pb and $^{210}$Po made the highest contribution into internal dose due to ingestion.

*Effective doses of potential internal and external exposure to the public because of contamination of water in the surface ponds with the mine water*

Self-leaked mine water from Gallery 32 at Beshtau hill passes to Zolotushka River and left tributary of Podkumok River through discharge 5. In summer, the residents use water from discharge 5 without purification to irrigate their gardens and vegetable gardens located close to the gallery. In addition, contamination of water reservoirs with mine water causes the external exposure to the public in the course of swimming and staying at the parts of contaminated floodplain.

The internal public doses have been evaluated hypothetically assuming that food intake received from the personal gardens was 211 kg/year for 1 person. In addition, in some cases small cattle is ranched at the subsidiary plots (goats, sheep, pigs, nutrias, rabbits, birds etc.), and fishing is undertaken in the ponds. Taking into account these factors of potential radionuclide intake via foods, the calculations included milk and meat intake at the 10% level of the value averaged over the Stavropol Territory, i.e. 20.3 l/year and 5.3 kg/year, respectively, while fish intake- at 5% level of the averaged value – 0.56 kg/year.

Table 2 includes assessment of effective internal doses to the critical population group due to food intake issued from the subsidiary plots, while Table 3 includes effective external doses originated from staying at the contaminated soils (plots) and swimming in the ponds.

**Table 2. Internal public doses, mSv/year.**

| Radionucide | Fish | Potato and other agricultural products | Meat | Milk | Gross dose |
|---|---|---|---|---|---|
| $^{238}U$ | 1,6E-04 | 2,3E-03 | 6,1E-05 | 3,5E-04 | 2,9E-03 |
| $^{234}Th$ | 1,1E-04 | 4,4E-06 | 1,2E-06 | 1,1E-07 | 1,1E-04 |
| $^{230}Th$ | 1,5E-02 | 3,3E-03 | 2,1E-04 | 2,1E-05 | 1,9E-02 |
| $^{226}Ra$ | 2,8E-03 | 7,3E-04 | 6,4E-03 | 6,0E-03 | 1,6E-02 |
| Gross dose over all radionuclides | 1,8E-02 | 6,3E-03 | 6,7E-03 | 6,4E-03 | 3,8E-02 |

For the part of residents who provide themselves fully with meat and milk from personal domestic animals, internal doses can reach 0,16 mSv/year. Internal doses to the critical group - «fishmen», who intake fish from the local ponds in 100 % volume, will be 0,39 mSv/year.

**Table 3. External doses, mSv/year.**

| Radonuclide | Swimming | Staying at the area of the floodplain | Gross dose due to both exposure pathways |
|---|---|---|---|
| $^{234}Th$ | 1,5.10-6 | 2,5.10-9 | 1,5.10-6 |
| $^{230}Th$ | 0 | 2,2.10-5 | 2,2.10-5 |
| $^{226}Ra$ | 1,0.10-5 | 3,2.10-3 | 3,2.10-3 |
| Gross dose over all radionuclides | 1,2.10-5 | 3,2.10-3 | 3,2.10-3 |

In case of permanent living at this territory and full provision with the agricultural products, meat and milk originated from such personal plots, effective internal doses will be 1,7-2,5 mSv/year. At that, only 7-10 % of this dose are resulted from irrigation

of the personal gardens with the mine water. External dose from radionuclides containing in soil will be 0,84 mSv/year.

The area of the village sitting is considered as radon hazardous territory. Additional exposure to the public can be resulted from inhalation intake of radon fission products, airborne in dwellings. Direct measurements of the radon EEC in the village are not being carried out. However, there are data on the neighbor Lermontov city. The more representative data [4, 7] are from the FMBC (ex-SRC Institute of Biophysics) experts under the FMBA of Russia and CSEN under MSCh-101. They carried out their measurements in 213 dwellings over the period since April 1995 till March 1996. The findings of inspections showed high EEC levels in the cottage-type houses, and revealed the season dependency of the radon EEC in dwellings. The EEC levels over the autumn-winter period were 2 and more times higher than those in summer. The evaluated annual effective doses to the residents of individual design dwellings were about 28 mSv. At that maximum doses about three times differed from the mean values. According to measurements of 2006, the mean radon EEC value was 230 Bq/m$^3$ in the cottage-type houses (85 measurements); this corresponds to about 17 mSv annual effective doses to the public.

Having in mind that the lung cancer is generally the first response to over-exposure of radon and its daughter products, our development included firstly the persons diseased with this nosology, as well as cancers of other human organs, which are more frequent at the areas inspected (Table 4)

**Table 4. Distribution of persons diseased with malignant neoplasms over Lermontov and Obninsk cities by different nosologies and sex.**

| Sitting of malignant neoplasm | Sex | Totl number of diseases registered | |
|---|---|---|---|
| | | Lermontov | Obninsk |
| 1 | 2 | | |
| Malignant neoplasms – total including: | M | 838 | 2528 |
| | F | 823 | 2955 |
| Ventricle | M | 75 | 343 |
| | F | 60 | 254 |
| Trachea, bronchus, lung | M | 240 | 458 |
| | F | 38 | 59 |
| Breast | F | 143 | 615 |
| Lymphoid, кроветворнойblood-forming and their nested tissues | M | 38 | 169 |
| | F | 30 | 162 |
| Leukemia | M | 21 | 70 |
| | F | 20 | 57 |
| Leukemia except for CLL | M | 12 | 51 |
| | F | 14 | 36 |

Figure 1 demonstrates dynamics of total morbidity with malignant neoplasms of the male residents of the cities by the examination periods

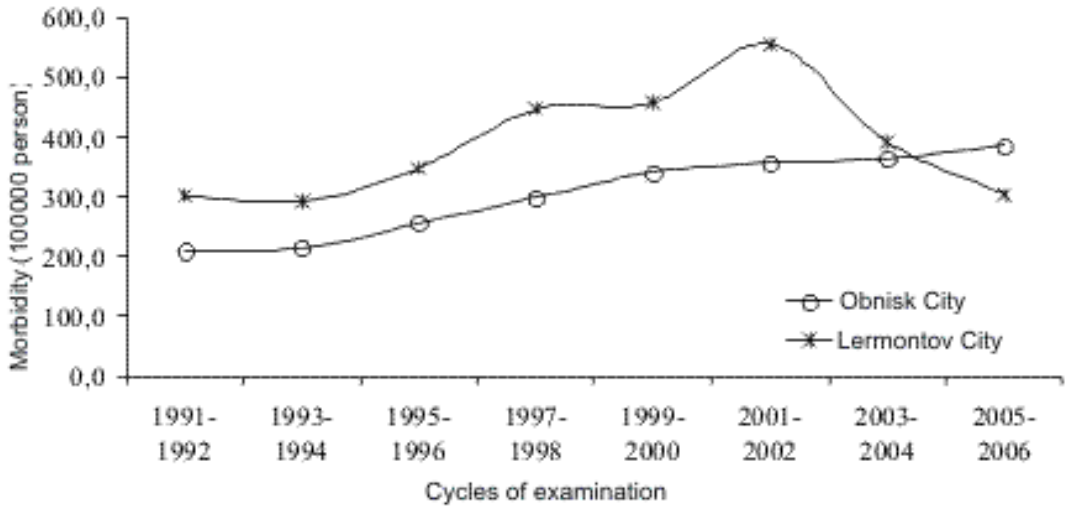


**Figure 1. Dynamics of malignant neoplasm morbidity of male residents of Lermontov and Obninsk cities, by the examination cycles.**

Such data demonstrate increasing index of common morbidity with malignant neoplasms of males with years in Obninsk city from 208,99 to 385,29 per 100000 males, i.e., 84 %. The indexes for the boundary periods for Lermontov city, such increasing has not been registered, but, for some cycles of examination, they reached rather high values – up to 554,59 per 100000 males over 2001-2002.

Over all periods of surveillance except for 2005-2006, male morbidity indexes for Lermontov are higher than the similar indexes for Obninsk city, and valid differences have been found for 6 cycles of examination of 8: 1991-1992, 1993-1994, 1995-1996, 1997-1998, 1999-2000, 2001-2002.

The most interesting is morbidity with cancer of trachea, bronchus and lung of males over Obninsk city increased with years a bit, while over Lermontov city it has increased up to 2001-2002 inclusively, reaching 153,13 per 100000, but over two last cycles of examination it decreased to 85,5 and 72,6 respectively.

Over each cycle of examination, the male morbidity indexes over Lermontov city were higher in comparison with those over Obninsk, and differences in the indexes were valid, except for two last cycles of examination (2003-2004 and 2005-2006).

The morbidity trend with cancer of lymphoid, blood-forming and their nested tissues was unstable both for Obninsk and for Lermontov. It has increasing tendency for Obninsk data, while for Lermontov it firstly increased, then decreased up to 4,27 per 100000 males over the last cycle of examination (2005-2006).

Comparison of indexes by cities showed that generally there were not valid differences by the cycles of examination.

Male morbidity with leukemia in Obninsk was wavelike. As for Lermontov, increasing morbidity is registered with years of inspection; rather high indexes of morbidity have ben registered over 2003-2004: it reached 27,01 per 100000 male residents of the city, nevertheless over the next period, 2005-2006, there were not registered leukemia events among them.

The most interest can be connected with data on leukemia morbidity except for the CLL, because they confirm unhealthy radiation impact of the environmental factors

on the population. Over males in Lermontov, such kind of pathology has not been registered in 3 cycles of examination.

In two cycles (2001-2002, 2003-2004 гг.), the morbidity indexes over Lermontov city were higher than the similar values over Obninsk, but number of diseased persons was small, so differences in the morbidity indexes were invalid.

Thus, of all examined indexes of male morbidity with malignant neoplasms over Lermontov city in comparison with the Obninsk population, higher total cancer morbidity has been found as well as morbidity with the trachea, bronchus and lung cancers.

The female cancer morbidity in all malignant neoplasms both over Lermontov and over Obninsk generally trends for increasing with years of examination. It became 68 % higher for Lermontov, and 78 % for Obninsk.

Figure 2 demonstrates the comparative assessment of malignant neoplasm morbidity for females of Lermontov and Obninsk cities by the cycle of examination (per 100000 females).

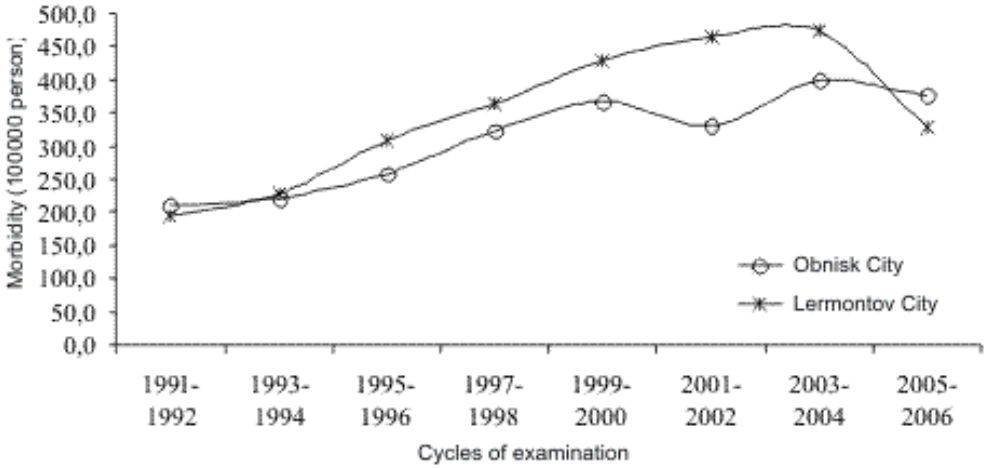


**Figure 2. Dynamics of the female malignant neoplasm morbidity over Lermontov and Obninsk cities, by the cycles of examination.**

Over some cycles of examination, the morbidity over Lermontov is a bit higher than over Obninsk, except for the last period. Differences in common malignant neoplasm morbidity is invalid, except for 2001-2002 period, when such difference is significant. Recently, the morbidity in Lermontov became lower in comparison with the Obninsk one.

Morbidity with the trachea, bronchus and lung cancers in both cities varies over the cycles of examination; this is more evident for Lermontov.

Over all cycles of examination, indexes for Lermontov are higher that for Obninsk. Differences in indexes are valid in two cycles – 1995-1996 and 2003-2004.

Comparative assessment of the breast cancer of females in Lermontov and Obninsk by the cycles of examination demonstrates their unstable difference by the cycles of examination.

For Obninsk, the morbidity increased slowly from 45,2 to 98,1 per 100000 females, while for Lermontov it reached maximum of 95,7 (period 1999-2000) and decreased significantly over the following cycles of examination up to 25,3 (2005-

2006). Regardless the fact that over two cycles (1997-1998 and 1999-2000) the breast cancer morbidity over Lermontov was higher than the similar index over Obninsk, this difference is invalid.

The female morbidity with the lymphoid, blood-forming and their nested tissues cancers is instable by the cycles of examination in both cities.

There were no valid differences of such kind of pathology over cities.

The excessive leukemia morbidity has been registered of females in Lermontov in comparison with that of Obninsk over 2001-2004, but because of small number of female diseased with leukemia this difference in indexes is invalid.

The female morbidity with leukemia except for the CLL has the same trends as the leukemia morbidity, but at the lower digital level, and over three cycles of examination in Lermontov such kind of disease has not been registered at all.

Thus, comparative analysis of female morbidity with all forms of malignant neoplasms in Lermontov demonstrated exceeding of this index in comparison with the similar index for Obninsk. Valid difference between them has been found only for the cycle of examination 2001-2002. The trachea, bronchus and lung cancer morbidity is notable in Lermontov, where in two cycles of examination (1995-1996, 2003-2004) in validly differs from that for Obninsk.

The above mentioned enables to make the following conclusions:

Morbidity with malignant neoplasms (by all analyzed forms) of residents in Lermontov city, especially the trachea, bronchus and lung cancer is higher than the similar indexes over the control area.

Excessive morbidity with malignant neoplasms (common by the analyzed forms) of the Lermontov population, especially the trachea, bronchus and lung cancer in comparison with the similar indexes over the Obninsk population can be explained by radiation exposure originated both from excessive contents of airborne radon and its daughter decay products during work of males in mines, and from living and staying in dwellings and public buildings being constructed over 1950-70s using the constructive materials with excessive contents of natural radionuclides.

## Conclusions

Dose evaluation of man-made radiation exposure to the public living at the LPO "Almaz" impact area demonstrated that maximum effective dose via the meat and milk chain is 2,5 mSv/year. $^{226}$Ra is the main dose-forming radionuclide in both cases; its contribution for both exposure pathways exceeds 90%. Maximum potential internal public dose due to intake of foods being produced at the subsidiary plots and gardens varies from 37 µSv/year to 470 µSv/year. On another hand, results of radiation survey in the city demonstrated the presence of high levels of radon and its progenies contents in dwellings of the city, especially in the cottage-type buildings. The evaluated annual effective doses to the public living in the individual design houses were 28 mSv over 1995-1996; according to measurements of 2006 - 17 mSv. Comparative analysis of doses demonstrates prevailing of the natural component above the man-made.

The above mentioned permits to conclude that inhalation intake of radon and its decay products is the main radiation factor affecting the public health in Lermontov city.

The analysis of malignant neoplasm morbidity helps to find some statistical domination over male and female residents of Lermontov in comparison with the

similar index over Obninsk city in respect to common cancer morbidity and morbidity with the trachea, bronchus and lung cancer.

We think that such domination of the morbidity with malignant neoplasms of residents in Lermontov is induced by ionizing radiation due to radon release from the earth surface and due to residence and staying in dwellings and public buildings being constructed over 1950-70s using the constructive materials with excessive contents of natural radionuclides, that is confirmed by the higher level of the female morbidity with the trachea, bronchus and lung cancer in Lermontov [2, 5].

In addition, in past, males have been subjected to direct radiation exposure when mining the uranium ore under underground conditions, especially over the first after-war years, when work conditions of miners were being specified by excessive level of the quartz containing dust, radon and its progeny [6]. Taking into account long latent period in case of the lung cancer incidence, these factors could result in the increased morbidity of the population with such pathology.

Nevertheless, in data of the state medical report, it is impossible to identify miners in common population of Lermontov under service, therefore in the course of continuing study, it is reasonable to develop the register with personal data.

## References

1. Ivanov, V. K., A. F. Tsyb, et al. “Cancer incidence among nuclear workers in Russia based on data from the Institute of Physics and Power Engineering: a preliminary analysis.” Radiat. Res. 2001, v. 155(6), P. 801-808.
2. Vakulovskiy S.M., Kryshev I.I. Radiation Situation in Obninsk. J.Nuclear Energy, v. 99, No 3, 2005, p. 214-221 (in Russian).
3. Guidace for establishment of the permissible radioactive releases into atmosphere. DV-98. M., 1999, ….. c.
4. Serebryakov I.S., Brykin S.N., Zemlenukhin V.I., Kosova O.E. ea. Assessment of the radio-ecological situation and environmental quality control in the vicinity of the typical industrial facilities. Volume 1. Assessment of the radio-ecological situation and environmental quality control at the state unitary enterprise "Hydro Metallurgical Plant" (HMP). M., International Centre of Environmental Safety under Minatom of Russia, 2001, 86 pp.
5. Verejko S.P. «Radiation hygienic assessment of work and life conditions in Lermontov city located close to the uranium deposition» Dissertation abstract for cand.med.sci., M. 1998, 15 pp.
6. Gneusheva G.I., Shalaev I.Ya., Glushinskiy M.V. «Quantitative evaluation of occupational cancer risk induced by the lung cancer under conditions of underground uranium mining». Medical radiology and medical safety, 2004, vol. 49, No 2, p. 13-16.
7. Izhevskiy P.V., Saurov M.M., Zykova A.S., Gneusheva G.I., ea. Assesment of medical demographical situation in Lermontov city in terms of birth rates, death rates and life duration and resolution on the disposition for incidence of negative pregnancy deliverable and cancer pathology of the persons under examination. Certificate on the metrological attestation. Draft recommendations for health and hygienic situation improvement in the city". M., 1996, IBPh Report, 56 pp.

# Modelling with a CFD code the near-range dispersion of particles unexpectedly released from a nuclear power plant

Gallego, Eduardo[1]; Barbero, Rubén[2]; Cuadra, Daniel[2];
Domingo, Jerónimo[2]; Iranzo, Alfredo[2]
[1] Nuclear Engineering Department, E.T.S. Ingenieros Industriales,
Universidad Politécnica de Madrid, SPAIN
[2] Análisis-DSC (Dynamic and Security Computations), Madrid, SPAIN

## Abstract

An event in November 2007 in Ascó-1 nuclear power plant (Spain) originated the release of a significant amount of hot metallic particles through the discharge stack. Particles were dispersed and deposited in roofs and neighbouring areas within the NPP controlled area. However, the event was not detected until March 2008. More than 1,300 hot points with radioactive particles were found, 94% located inside the double fenced controlled area and 6% within the exclusion area; 5 particles were out of the exclusion area, across the river.

To provide additional insights on the potential consequences of the release, a computational fluid dynamics (CFD) code, Ansys-CFX-11, has been used to simulate the near-range atmospheric dispersion and deposition of the particles. The purpose of the analysis was to assess the distance travelled by particles of different sizes. A very detailed model of the site was built, taking into account the buildings and the terrain features including the river valley and the surrounding hills. The modelled domain was 3.2 x 5.2 km, with the atmospheric layer up to 4 km height. The atmospheric conditions recorded during different periods of time were classified into 37 representative categories.

In general, the distribution of the particles found was adequately reproduced. Particles larger than 100 microns could not travel beyond the double fence. Particles between 50 and 100 microns could have been deposited mainly within the exclusion area, with a small probability of travelling farther. Smaller particles could have travelled beyond, but also should have been deposited in the nearby area, while the majority of particles found are larger, thus indicating that the size of the released particles should be above 50 microns.

The detailed CFD simulation allowed answering relevant questions concerning the possibility of having an impacted region larger than the exclusion area.

## Introduction

An incident classified as level 2 on the INES scale happened at the Ascó I nuclear power plant in Spain, consisting of the release of radioactive particles with activated corrosion product isotopes. This occurred due to the contamination of the fuel building ventilation system with water originating from the cleaning of the fuel transfer canal at the end of the refueling outage of the reactor, as a result of a combination of incorrect practices and noncompliance with the operating standards (CSN, 2009a).

The detection of the release and its subsequent notification took place over four months after the occurrence of the event, since it became evident not because of the available automatic radiological control systems but through a site radiological surveillance walkthrough. This was due mainly to the fact that these systems are designed to detect homogeneous radioactive emissions and not discrete particles such as those involved in the event. On March 14$^{th}$ 2008, hot particles were first detected in the containment hatch area. A further increase in radiological surveillance activities in the following days lead to discover several hot points on the roofs of the buildings adjacent to the NPP stack (see figure 1). On April 4$^{th}$ a report was released to the regulatory authority, the Nuclear Safety Council (CSN), which was followed by press releases and official statements to the public, as well as a wide campaign to check more than 2,700 persons through the whole body radiological counter, including workers and visitors. No person was found contaminated. A team of experts from the European Commission's General Directorate of Energy and Transport visited Ascó on April 29$^{th}$ and verified the radiological protection control methodology which confirmed the non-radiological significance of the event and endorsed the technology employed to guarantee the control measures from the operative, administrative and quality points of view.

**Fig. 1. Photograph of the Ascó I reactor building and the adjacent buildings of the nuclear power plant. The release of particles took place through the stack.**

The event was investigated and the conclusion was that the release of hot particles to the atmosphere started on November 29th 2007, when the ventilation system was switched from filtered mode to normal mode (without filtration). As a consequence, particles were dragged out through the stack and then dispersed via the stack to the roofs of Unit I buildings.

An exhaustive active particle location programme was soon accomplished on the plant site, by the licensee in the area under its control and by the CSN in off-site areas, with more than 1,300 particles collected with a total activity of 409 MBq, subsequently calculated on November 26th 2007 (CSN, 2009b). As a comparison, the cleaning of the ventilation system allowed to recover a total of 37,6 GBq. 94% of the particles were located inside the double fenced controlled area and 6% within the exclusion area; 5 particles were out of the exclusion area, across the river (figure 2).

To provide additional insights on the potential consequences of the release, a computational fluid dynamics (CFD) code, Ansys-CFX-11, has been used to simulate the near-range atmospheric dispersion and deposition of the particles. The purpose of the analysis was to assess the distance travelled by particles of different sizes (and activities) and the probability that they have been deposited at a given location.

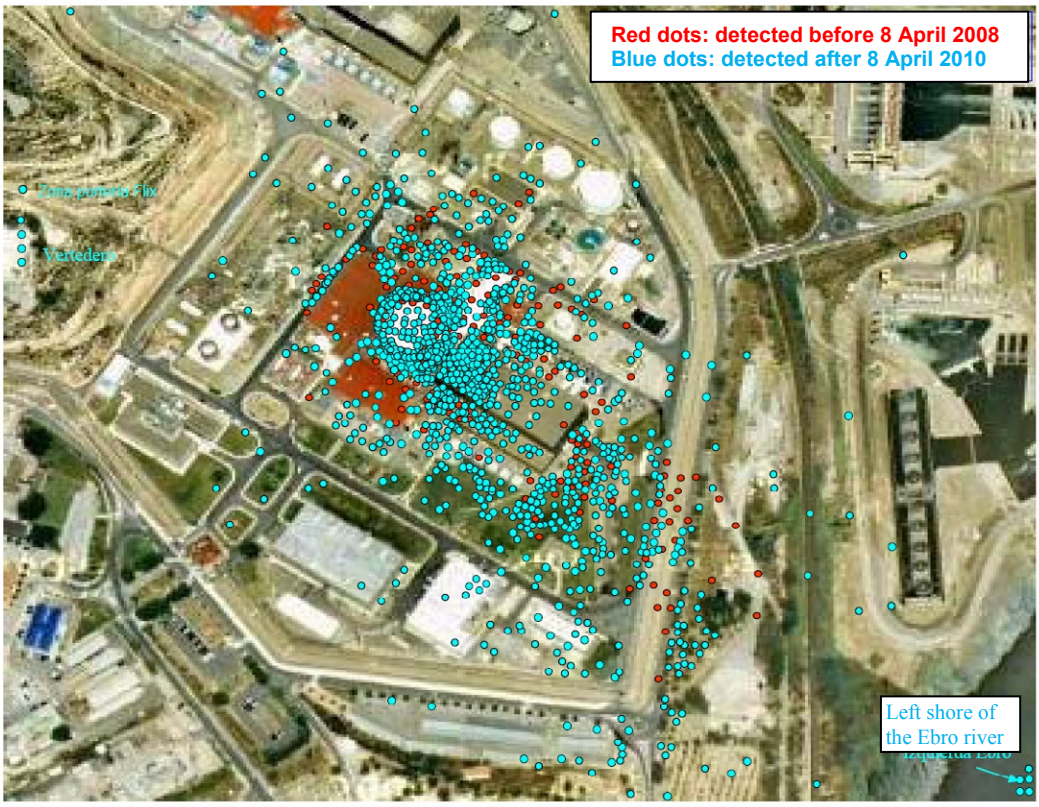


**Fig. 2. Aerial view of Ascó I site showing the locations where hot particles were collected.**

## Material and methods

The modelled fluid flow presents two well differenced phases: a continuous phase of air mixed with steam and a dispersed phase, constituted by solid particles. Consideration of steam was necessary due to the presence of the forced and natural flow cooling towers.

Turbulent phenomena in the air flow have been included in the simulation by means of the SST model (Shear Stress Transport), widely used for industrial applications where limit layer effects in contact with surfaces are relevant. Therefore, the flow characterization is performed by solving the three equations of momentum for gases in *x*, *y* and *z*; the continuity or mass conservation equation; the energy conservation equation; the two equations of the turbulence model: for turbulent kinetic energy and frequency of turbulent structures; and the transport equations for steam. Also, the equations relative to particle transport which are solved by means of a lagrangian model coupled to the fluid flow model (one-way coupling).

A very detailed numerical model of the site was built, taking into account the buildings and the terrain features including the river valley and the surrounding hills. The modelled domain was 3.2 x 5.2 km, with the atmospheric layer up to 4 km height. The atmospheric conditions recorded during different periods of time were classified into 37 representative categories.

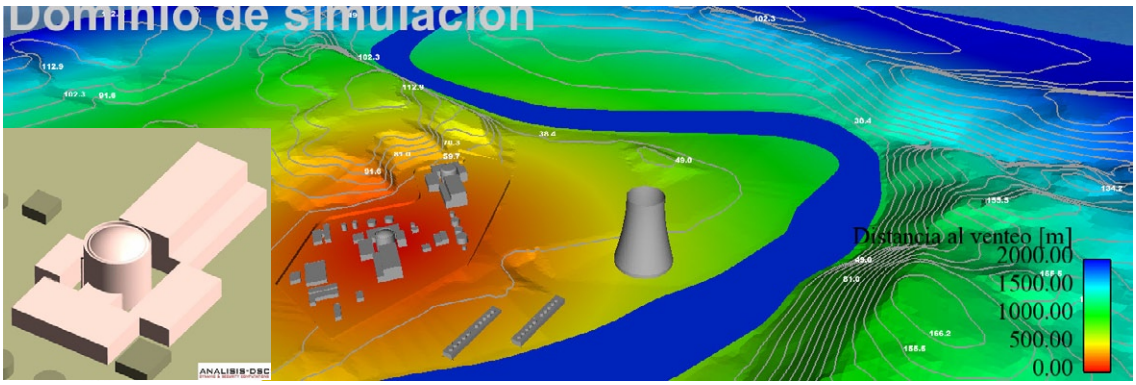


**Fig. 3. Overall view of the geometric model of Ascó I site. On the left, a detail of the main buildings of the plant.**

The steps followed in the study were the following:

1. Generation and adjustment of a 3-D detailed model for Ansys-CFX based on the terrain elevation (digital map of the area) and the dimensions of the buildings. The building geometries are less detailed for those that are farther from the release point. The general view of the geometric model can be seen in figure 3. The nodalization and mesh structure of the model is based in tetrahedrical finite volumes complemented by prismatic volumes near the surfaces. It is shown with some details in figure 4. Near the surfaces, the size of the cells is small enough as to adequately capture the behaviour in the interface.
2. Analysis of the meteorological data recorded at the site between 29 November 2007 and 31 January 2008. Data have been recorded at 10, 24.5 and 60 m above ground at 15 minutes intervals. The analysis of these data has lead to classify the different atmospheric conditions in a total of 37 categories as reasonably representative of the local meteorology during the period under study. There was a compromise between the need for realistic calculations and the computational resources needed for each simulation. In practical terms, the combination of these 37 categories, with adjusted frequencies, allowed to reasonably represent the atmospheric conditions in the following periods: 29/Nov/2007; from 29/Nov/2007

to 31/Dec/2007; from 29/Nov/2007 to 31/Jan/2008 (one day, one month and two months from the change in the ventilation system to non-filtered mode).

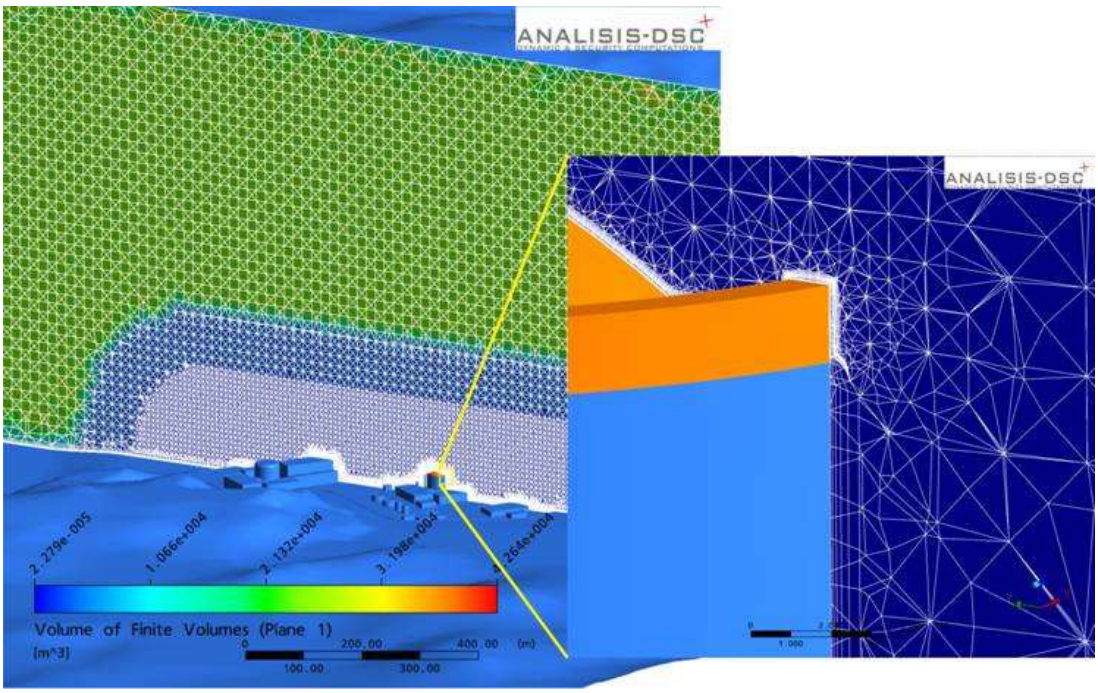


**Fig. 4. Details of the nodalization of the atmosphere around the reactor building and in the mid-range distances along the site and up in the atmosphere.**

3. Simulation of the 37 categories, with specific conditions of temperature gradient and atmospheric stability, relative humidity, wind speed and direction. The temperature gradient chosen was the typical for the atmospheric stability (Snell, 1994) and the most frequent temperature was chosen as representative for each category. Wind speed profiles with height were adjusted by considering a potential law dependent on the atmospheric stability (Hanna, 1982). The air flow released from the stack is 37 $m^3/s$ with a temperature 20ºC. 3-D effects in the air flow around the site were very relevant, due to the irregular terrain features and the influence of the cooling towers.
4. Seven classes of particles were taken into account in the simulations: 1–25 µm; 25–50 µm; 50–75 µm; 75–100 µm; 100–150 µm; 150–250 µm; 1–250 µm. For bigger sizes, their behaviour is dominated by inertial forces and their distribution is similar. Larger particles could not leave the stack, as demonstrated with a preliminary study of balance of forces in the released flow. The particles density was taken as 7 $g/cm^3$, as it corresponds to metallic compounds from corrosion of the reactor primary cooling circuit.
5. Parametric study to get a probability of deposition of particles of different size in a given zone, taking into account the atmospheric dispersion. Combination of results for each of the 37 categories with their frequencies during each time period.

## Results

The particle deposition map (fig. 2) is the result of the atmospheric dispersion and deposition of the particles released through the stack plus the later processes of resuspension and deposition by wind, transport by rain water runoff and other weathering factors which cannot be simulated in the model. It is therefore reasonable to see some differences with respect to the calculated deposition patterns. It is also necessary to remind that the collection of particles started in April 2008, while the release took place from 29 November 2007.

In order to give a useful representation of the deposition pattern, the number of simulated particles was 10,000 for each size range of 25 microns. To represent it, we have multiplied it by 100 so we have a number of $10^6$ particles and the graphical representation displays the number of particles deposited (per $m^2$) per million particles released. The minimum representation limit is 1 particle per $m^2$. For the global case comprising 1–250 µm the number of particles assumed was $10^7$.

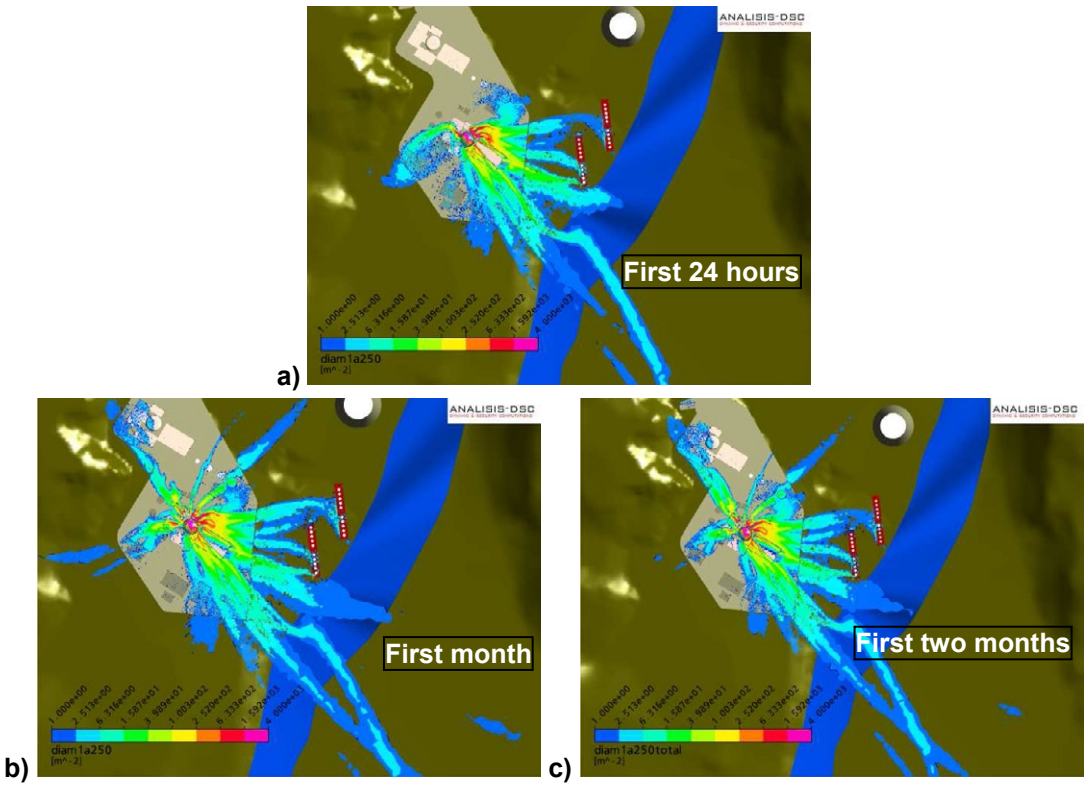


**Fig. 5. Results of the simulated deposition of particles of diameters 1–250 µm considering the atmospheric conditions in three different time periods. The patterns represent the particle density per $m^2$ assuming a release of $10^7$ particles.**

There is a preferential deposition in the South East area, partly due to the higher frequency of winds in that direction, combined with the effect of the forced flow cooling towers which force humid air to go upwards and which cause some entrainment of particles in that direction. By comparing the three periods considered in the calculations, the conclusion is that a release during the first 24 hours (fig. 5-a) cannot explain alone the pattern of particles found. However, the deposition reached in the period from 29 November 2007 to 31 December 2007 (fig. 5-b) is very similar to the

one if the period extended up to 31 January 2008 is considered (fig. 5-c). This result suggests that the release could have taken place most likely in the first month after the change of the ventilation system to normal mode.

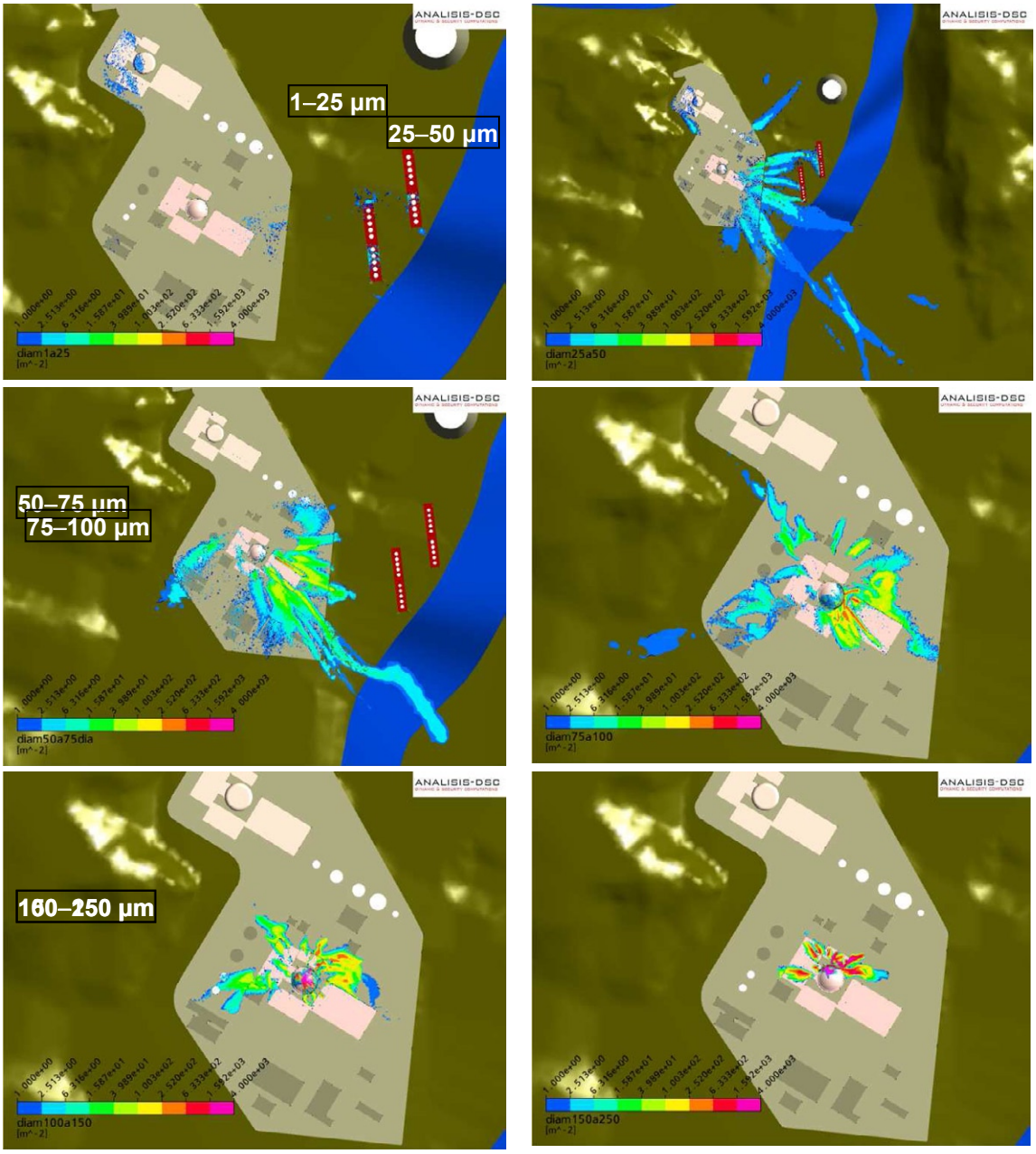


**Fig. 6. Results of the simulated deposition of particles of different diameter ranges considering the weather conditions during the first month after the change of the ventilation system to normal mode (29/Nov/2007 to 31/Dec/2007). The patterns represent the particle density per m$^2$ assuming a release of 10$^6$ particles.**

Fig. 6 displays the deposition patterns of particles of different size. Small particles (1–25 µm), of very low activity compared to the large ones, would be able to travel out of the calculation domain. They could also deposit, in small concentrations, around the stack and in other points of the site, with influence of the forced flow cooling towers.

However, in the radiological survey such small particles were not found, and therefore this result suggests that, if present, their fraction in the total should have been extremely low.

Particles of larger size (25–50 μm) show a distribution through a very large area, and their deposition density should be very small, with a likely deposition within the site, but also off-site. A significant fraction of such particles is leaving the calculation domain.

For particles with size between 50–75 μm, the larger fraction should be deposited within the site, although some of them could travel a bit out and cross the river. This could explain why 5 particles were found in that zone after a careful radiological survey. The radial-like deposition pattern seen in the figure is a reflection of the way in which the calculation has considered wind directions, with fixed angle in each category and a weighted combination of the results obtained.

When larger particles are considered, with sizes between 75–100 μm, they hardly seem able to leave the site, and they are deposited mainly along the dominant wind directions, towards E and SE as commented above.

Particles with size between 100–150 μm would be totally deposited within the plant fence, dominantly towards E and NE, because of the influence of the buildings in the local wind flow patterns. The majority of particles found did have sizes of this range, which could have been altered with time due to the particle "life" in the environment. In fact, many particles show a composition which is not purely metallic but associated with carbonates or silicates.

The biggest particles, with diameter larger than 150 μm, relatively very heavy and active, would deposit totally in short distances around the stack, many of them in the roofs of the reactor building and the surrounding buildings: auxiliary equipment building; fuel management and storage building; turbine building. Some of them would be trapped by the main wind flow and be able to go beyond the buildings, but certainly not far from the plant due to their high inertia. Later, resuspension or runoff phenomena could have transported them farther.

## Discussion

This study had as starting point the distribution of the deposited particles, after about four months of weathering in the site. However, it has been affected by some uncertainties impossible to exclude; two of them were fundamental:

- Knowledge of the precise moments at which the release of particles took place.
- The particle size.

The study has tried to overcome these uncertainties by undertaking a wide parametric study covering a full range of particle sizes, from very small to the largest particles able to exit through the stack at the existing flow dynamic conditions, together with a variety of atmospheric conditions, 37 in total, which covered a high percentage of those existing during the likely emission periods.

Based on those considerations, the study has given valuable information with regard to the likely deposition pattern of particles of different sizes in different release periods, concluding that particles of all sizes could have been found within the inspected area where the hot particles were found. Particles larger than 100 μm could have not travel beyond the fenced area of the plant. A small fraction of particles sized

between 50–75 µm could have leave the fenced area travelling towards the SE direction, where some particles were effectively found across the river. Small particles could in principle have travel far from the site, but they should also have deposited on site, and this was not the actual finding. Given their origin and the spread of particles found it is not very likely that these small particles were abundant in the release.

## Conclusions

The main conclusion is about the usefulness of this study in order to better assess the radiological importance of the event. The great capability of CFD models to simulate very local effects –like the flow perturbation by the forced cooling towers, the buildings of the plant or the surrounding hills–, has proven essential to accurately interpret the behaviour of particles of different sizes. In summary, the detailed CFD simulations allowed answering relevant questions concerning the possibility of having an impacted region larger than the nuclear power plant exclusion area.

However, to give realistic results, these models need a significant effort in terms of modelling the site features, terrain elevation and geometry of the buildings and installations which could alter the overall wind flow. Also, current computational capacities in general do not allow simulating dynamic sequences with changing weather; therefore, we have chosen a representative set of "static" sequences and have weighted the results in order to obtain a realistic pattern of the likely deposition of the leaked particles.

In general these methods would be recommended only when the geometry and dispersion conditions of the site are very complex as well as in the case of particles whose dispersion is better simulated with lagrangian models.

## Acknowledgements

We deeply acknowledge the support received from "Asociación Nuclear Ascó-Vandellós II", and their supply of data for the simulations.

## References

CSN. Spanish Nuclear Safety Council report to the Parliament. Year 2008 Summary (in English). Madrid: Consejo de Seguridad Nuclear; 2009a.

CSN. Suceso de liberación de partículas radiactivas en C.N. Ascó I. Descripción y consecuencias radiológicas. Madrid: Consejo de Seguridad Nuclear; 2009b.

Hanna S.R., Briggs, G.A., Hosker, R.P. Handbook on Atmospheric Diffusion. DOE/TIC-11223. Washington D.C.: Technical Information Center. U.S. Department of Energy; 1982.

Snell W. Nuclear Regulatory Commission Staff Computer Programs for Use with Meteorological Data. NUREG-0917. Washington D.C.: U.S. Nuclear Regulatory Commission; 1994.

# Inspection Plan for the detection of contamination at a Nuclear Fuel Cycle facility

**Pérez Fonseca, Agustín; Ortiz Trujillo, Diego**
ENUSA Industrias Avanzadas, SPAIN

## Introduction

A number of incidents related to the finding of contamination spots outside main operation buildings were detected at different nuclear sites in Spain over 2008. In response to these incidents, the CSN (Spanish Nuclear Regulatory Body) issued requirements demanding all the operators the execution of the site's comprehensive inspection plans in order to ensure that no contamination spots would be found out of control.

The ENUSA's Fuel Fabrication Plant at Juzbado is a nuclear fuel cycle facility whose specific features make it different to the rest of Spanish nuclear installations, provided that only Low Enriched Uranium (5% maximum) is handled as process material. Therefore, the inventory of isotopes consists only of U-isotopes and their daughters. These isotopes can be found in Nature in different amounts, depending on the geologic characteristics of the area, amongst others. Therefore, the natural background itself can contain spots of the contaminant, and must be taken into account for the preparation of the inspection plan adding complexity to its implementation. The criteria to distinguish background from non background values must be set (impacted and non impacted areas).

To implement the inspection plan at the Juzbado Plant, the MARSSIM methodology was chosen for the Scope & Characterization Surveys, following the Data Quality Objective (DQO) process. Derived Concentration Guideline Levels (DCGL) were not used: comparison between background values versus field values was used instead.

MARSSIM (Multi-Agency Radiation Survey and Site Investigation Manual) is a tool to conduct radiation surveys and investigation of contaminated sites. This method is used by different agencies and it is a reference for NRC, amongst others, being described on NUREG 1575.

## Material and methods

Following the MARSSIM approach, there are six steps in the Radiation Survey Process:

a) Site Identification.
b) Historical Site Assessment.
c) Scoping Survey.
d) Characterization Survey.
e) Remedial Action Support Survey.

f) Final Status Survey.

As this is a facility that is not going to be decommissioned, only steps a) to d) will be performed.

To prepare the inspection plan, a review of all the activities that took place on site has been done. This, History Site Assessment (HSA using MARSSIM vocabulary), give us a map where contaminated material has been handled. The contaminated material has only been handled in the main building and radioactive liquid treatment facilities.

**Fig 1. Map of Juzbado facility. Red spots indicate areas where contamination could be found.**

After the review of the activities has been done, the other main conclusion at this point is that the only radioactive material handled was low enriched uranium, in the form of oxides (no $UF_6$).

With this information, we have a clear idea of what and where we have to found in order to prepare the characterization plan. No scoping survey will be done, we will try to perform only one characterization survey, using the regular periodic inspection that have been done in the facility as an scope.

The first part in the characterization survey is to classify the zones first in land areas or structures areas, because the types of surveys are different. After this, a risk based classification will be done. The areas with higher risk of contamination will be classified as class 1, and the areas with lower risk will be classified as class 3. To act in a conservative way, all the areas were considered as impacted areas, so all the areas must be surveyed.

The land areas we have in the facility according to the classification are included in the following map. The criteria used to classify each area is that areas where contaminated material was handled are classified as class 1, areas surrounding areas class 1 are class 2 and the rest is class 3.

**Fig 2. Land areas. Green area is class 3 and blue areas area class 2.**

The type of survey necessary to inspect each area was selected using the DQO (Data Quality Objective) process. These areas must be inspected by a scanning process and a simple measurement. For the scanning part, gamma measurement will be done, using portable equipment (INa monitor). For the single measurement a soil sample will be taken, and later alpha spectroscopy of the soil will be done, where $^{234}U$ and $^{238}U$ will be compared. For material with enriched uranium, the amount of $^{234}U$ is higher than what we can found in nature. To conclude if an area is contaminated or not, we compare the ratio $^{238}U$:$^{234}U$ (sample) vs $^{238}U$:$^{234}U$ (background). If the mean $^{238}U$:$^{234}U$ concentration in samples collected from a survey area is greater than the mean ratio from an equivalent number of samples randomly selected from the available background sample population + a substantial difference (S) of 2 times the full background sample population standard deviation determined, then decide enriched uranium contamination is present. Otherwise decide the uranium present is natural background. A summary of the process for class 1 areas is included on this table:

**Table 1. Example of measures for the land areas, class 1.**

| Land Area | Scanning | Field Screening | Measurement/ Sampling |
|---|---|---|---|
| Class 1 | Perform medium density (50%) gamma surface scans of all accessible surfaces in each Class 1 survey area. | Pause and investigate any locations with gamma radiation levels distinguishable from background.<br><br>Mark investigative locations for potential judgmental sampling. | Use an statistics application to determine the sample size for each survey unit<br><br>The input parameters, using the Wilcoxon Rank Sum (WRS) planning mode are:<br>False Rejection Rate: 0.05%<br>False Acceptance Rate: 0.05 or 0.10%<br>Lower Bound of the Gray Region: 1.033<br>Specified Difference of True Means or Medians: 1.205<br>Estimated Standard Deviation: 0.086<br>NOTE: The WRS test mode is used for determining sample size. The non-parametric statistical test will be the Wilcoxon Mann-Whitney test. |

Later, to analyze the data, Wilcoxon Mann-Whitney Test will be used, taking both sample and background data.

For the structures area, a map of the facility was taken, and every building or road was assumed to be a significant area. The criteria used to classify areas as class 1, 2 or 3 is the same as before. If contaminated material was handled, then the area is class 1. All areas surrounding class 1 are class 2. Once the area is classified, it splits on different cells, each one with a maximum surface, depending on the classification.

**Table 2. Maximum surface allowed on every area.**

| Type of area | Maximum surface of the cell |
|---|---|
| Class 1 | 100 m2 |
| Class 2 | 1000 m2 |
| Class 3 | No limit. |

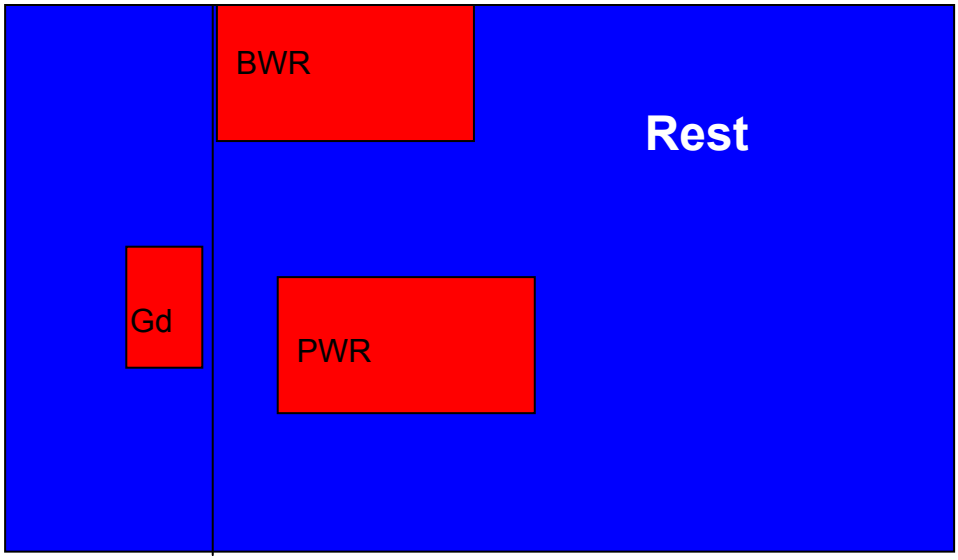


**Fig 3. Example of survey plan on the roof. Areas around the stacks are red (class 1). The rest of areas are class 2 because they are near areas class 1.**

The type of survey that will be performed on every area is also a scan or an static measurement, both with portable monitor able to measure alpha radiation. The measure will be done without any background subtraction, and will be compared to different background of different materials. If the mean cps (counts per second) in the survey area is higher than the mean of the cps from any equivalent number of background simple randomly selected from the available population + the equivalent value in cps of 0.04 Bq /cm$^2$, then it is determined there is contamination due to uranium. Otherwise, decide that area do not have contamination. In this step Wilcoxon Rank Sum Test will be used.

**Fig 3. Device used to scan surfaces in order to find contamination spots.**

**Table 3. Example of measures for structures areas, class 1.**

| Structure Areas | Scanning | Field Screening | Measurement/ Sampling |
|---|---|---|---|
| Class 1 | Perform high density scan (100%) in all the accesible surfaces | Pause and investigate any locations with radiation higher than background.<br><br>Mark investigative locations for potencial judgmental sampling. | Use an statistic application to determine the sample size for each survey unit. The input parameters using WRS will be, for the surfaces used in background (concrete and asphalt):<br>False Rejection Rate: 0.05%<br>False Acceptance Rate: 0.05%<br>Lower Bound of the Gray Region: (0.35 ó 0.44)<br>Specified Difference of True Means or Medians: (1.41 y 1.50)<br>Estimated Standard Deviation: (0.076 y 0.08)<br>NOTA: The WRS will be used. |

## Conclusions

The MARSSIM methodology it is a powerful tool. It can be used for different projects, mainly decommission projects, but also for characterization purposes. For this reason the steps related to final status survey (that uses the data that support the decision for release of an area) is very well detailed in the NUREG 1575. On the other hand, characterization survey (or scoping survey) is not detailed as good as final status survey.

This plan intends to use all the steps of MARSSIM approach, for a characterization survey, using some of the analysis methods proposed for the final status survey.

With this plan, all the areas inside the fence of the facility will be scanned in order to prove that there is no contamination risk. The requisites asked by the regulator will also be fulfilled.

If contamination is detected over the limits specified in the regulations, will be cleared, explaining all the actions taken in the report that is going to be sent to the regulator.

## References

ANSI/HPS N13.59-2008 Characterization in Support of Decommissioning Using The Data Quality Objectives Process.

Guidance for Comparing Background and Chemical Concentrations in Soil for CERCLA Sites. EPA 540-R-01-003, OSWER 9285.7-41, September 2002

NUREG 1575 Multi Agency Radiation Survey and Site Investigation Manual (MARSSIM)

# Establishment of a special radiological surveillance programme at the "El Cabril" solid radioactive waste disposal facility

Ortiz, Teresa; Fuentes, Luis; Pinilla, José Luis
ENRESA, SPAIN

## Abstract

Due to a requirement by the Nuclear Safety Council, the Spanish regulatory authority, a special radiological surveillance plan (SRSP) has been developed at the low and intermediate level Radioactive Waste Disposal Facility (El Cabril centre) in Spain. The objective of this plan, which covers outdoor areas on the site, is to identify and remediate possible contaminated areas, including exterior ground, walls, roofs or terraces, the walls of buildings, drains, channels, paths and roads.

The RSP has been developed in accordance with the MARSSIM methodology and includes an historical analysis of the facility and an initial radiological characterisation of the protected area.

## Objective and scope

In response to a requirement by the Nuclear Safety Council, the Spanish Regulatory Authority, a special radiological surveillance programme (SRSP) has been developed at the Low and Intermediate Level Solid Radioactive Waste Disposal Facility (El Cabril ), located in the province of Córdoba (Spain), covering outdoor areas of the protected zone of the Site, the aim being to identify and eliminate any possible contamination.

In accordance with the instructions given by the Nuclear Safety Council, the programme has addressed the following requirements:

- Analysis of practices that may have given rise to the presence of contamination at the Site.
- Special attention to the existence of points at which sludges are accumulated or concentrated.
- The entire surface area of the Site will be covered, with a more detailed and precise systematic approach being adopted for areas identified as presenting the highest risk of contamination.

The SRSP has been applied to the entire outdoor area of the protected zone of the Site. The study areas have included outdoor paved areas, walls, the roofing and/or terraces and walls of buildings, gardens, forested areas and external structures exposed to the weather, such as slabs, drains, channels, roads and paths, etc.

As regards the radiological surveillance of walls, it was decided that this would be carried out only if contamination were detected in areas in which the presence of contamination might be suspected.

The SRSP has been carried out in accordance with the MARSSIM methodology, including a historical analysis of the Facility and the initial radiological characterisation of its protected zone.

## Development of the special radiological surveillance programme (SRSP)

The SRSP has been carried out by the Radiological Protection and Environmental Service of the El Cabril, with support from the ENRESA Radiological Protection Technical Unit and Safety Department. In addition, there has been support from an expert in spectrometry and instrumentation. Performance of the measures was undertaken by an external company, with a Senior Technician and two field measurement systems Operators.

The SRSP was performed between September 16$^{th}$ and October 8$^{th}$ 2009. The first task consisted of analysing the initial situation of the outdoor areas, as a basis for planning of the programme. As a result of this analysis, the protected zone was divided into Impacted and Non-Impacted Areas, these being defined as follows:

Non-impacted areas: those in which there has been no relation with radioactive materials during the operating lifetime of the Facility.

Impacted area: those in which there may have been a relation with radioactive materials as a result of the operating lifetime of the Facility. These are divided into three classes:

- Class 1: areas in which the existence of residual radioactivity is highly probable.
- Class 2: areas in which the existence of residual activity is a possibility.
- Class 3: areas in which the probability of residual activity is low.

The SRSP identified only the existence of class 2 and 3 Impacted Areas, no class 1 Impacted Areas were detected.

## Definition of surveillance units (SU)

So–called Surveillance Units (SU) were defined for all the areas classified as being Impacted. These consisted of known surfaces of a specific area with a similar history and homogeneous radiological characteristics; in other words, the unit is constituted of the same material (concrete, natural terrain, gravel, etc.) and the spatial distribution of the contamination should be approximately homogeneous.

As regards size, the areas defined were larger or smaller depending on their radiological classification:

- SU's defined for outdoor areas (asphalt and concrete): 10 SU's between250 m$^2$ and 24,114 m$^2$.
- SU's defined for the vertical outdoor walls of buildings (concrete): 3 SU's of 500 m$^2$.
- SU's defined for the roofing of buildings (concrete, metallic sheeting and gravel): 6 SU's between 660 m$^2$ and 1,471 m$^2$.

## Assessment of the radioactive background and identification of reference areas

In order to determine the radioactive background of the Site, Reference Background Areas (RBA) have been identified in non-impacted areas on the site. Given that the reference areas should have physical, chemical, biological and radiological characteristics similar to those of the areas in which the radiological surveillance is to be performed, a reference background area has been selected for each type of material in the areas to be characterised (asphalt, concrete, natural terrain and roofing gravel).

Thus, each SU has associated with it a non-impacted area known as the RBA that serves to establish the levels of investigation of the initial surveillance phase, on the basis of the radioactive background of the Site.

The measurements for characterisation of the RBA's were carried out using the same procedures and equipment as used for the Surveillance Units (SU's). In each RBA several scans were performed, each with a minimum of 30 data, and 30 stationary measurements were carried in different locations. In each RBA the average and typical deviation has been determined, this being used to determine the Background Estimator and Minimum Detectable Concentration for each measuring technique in each type of material.

## Reference levels

In order to determine whether any point at the Facility presented a level of residual activity, different reference levels were established, these being classified as action levels (AL) and investigation levels (IL).

**Action Levels:** The action levels used are those established in the CRL for surface concentration on building surfaces (63FR222) and those for mass concentration in soils (64FR234). The levels of action for the key radionuclides Co-60 and Cs-137 are show in table 1.

**Table 1. Action levels.**

| Type of surface | Action Level | |
|---|---|---|
| | Co-60 | Cs-137 |
| Permeable soil: earth, gravel, gardens | 0.14 Bq/g | 0.41 Bq/cm$^2$ |
| Low permeability surfaces: concrete, asphalt | 1.18 Bq/g | 4.67 Bq/cm$^2$ |

**Investigation Levels:** For each SU the applicable investigation levels are determined taking into account: the applicable action level, the background in the RBA associated with the SU, the classification of the SU / (class 1, 2, 3) and the measurement method (scanning, static measurement or sample). The levels of investigation established are in table 2.

**Table 2. Investigation levels.**

| SU Class | Scan | Static measurement or sampling |
|---|---|---|
| Class 1 | > 10 NA | > 10 NA |
| Class 2 | > NA | > NA |
| Class 3 | > NA | > 0.5 NA |

Once the investigation levels were defined, these were determined in the equipment measurement units. For the UCRM-II equipment, the investigation levels were determined in cpm, since this is the unit in which the results of the measurement are obtained.

## Measuring methods used

The wastes arising from the operation and dismantling of Nuclear Power Plants constitute the largest part of the total waste stored at the El Cabril, in terms of volume and activity, this being represented to the largest extent by Co-60 and Cs-137. These are, therefore, the radionuclides to be characterised. However, if the spectrometric measurements provide evidence of the existence of other significant radionuclides, these will also be evaluated.

The measurement methods used have been as follows:

- Scanning with the UCRM-II equipment.
- Static measurement with the UCRM-II equipment.
- Static measurement with the ISOCS equipment.
- Sampling and laboratory analysis.

The scanning measurements with the UCRM-II equipment have been performed to detect potential areas of activity. Two types of scanning were performed: systematic scanning in accordance with a determined itinerary and specific scanning carried out in areas with the highest probability of presenting residual activity. At those points static measurements were performed for confirmation.

The Inspector 1000 has been used to locate areas with higher count rates in those areas in which investigation levels have been recorded in scanning.

The static measurements with ISOCS and the sampling have been performed to determine the average activity of the SU.

The number of measurements performed has been as follows:

- Scanning: 10% of the surface of SU's of class 3, 50% for SU's of class 2 and 100% for SU's of class 1.
- Static measurements with UCMR-II: Whenever an investigation level has been detected in scanning.
- Static measurement with ISOCS: 5 measurements per SU (an initial point selected at random and the remainder in accordance with the pattern of the apexes of a W). Static measurements have also been performed using ISOCS at those points where a stationary investigation level has been confirmed with UCMR-II.
- Specific sampling in rainwater collection boxes and at rainwater pond discharge points. Samples have also been taken where the measuring equipment was inaccessible or in areas with high background levels.

## Selection of measuring equipment

The detection and measuring equipment used in performance of the Special Surveillance Plan was as follows:

a) Radiological measurement field unit (UCMR-II)
The UCMR-II is a system that has been developed to cover radiometric requirements in the field, in scenarios with difficult access. It is a 2"x2" Ina detector connected to a CPU, both being incorporated on a transport carriage.
The equipment is made up of: a central processing unit; keyboard and LCD screen; data acquisition system; GPS unit; three-wheel transport carriage with metallic structure and collimating shielding.

b) ISOCS equipment (In Situ Object Counting System)
Is a system for the measurement of objects by spectrometry, made up of: coaxial germanium detector characterised by means of the Montecarlo modelling code; shielding assembly; Inspector 2000 MCA; ISOCS software and Genie-2000 data acquisition programme and three-wheel metallic structure transport carriage.

c) INSPECTOR 1000 equipment
Is a multi-channel analyser that allows for the measurement of dose and dose rate and for the acquisition and analysis of gamma spectra.
The equipment incorporates an internal Geiger-Müller detector for high dose rate measurement and a probe with a INa (Tl) scintillation detector. The equipment has been used in scan mode for the location of hot spots.

All the equipment used was calibrated "in situ" or had calibration certificates in accordance with the respective calibration procedures approved by ENRESA.

## Analysis and evaluation of results

This section analyses and evaluates the results obtained in performing the SRSP for each of the Surveillance Units. In table 3 the main characteristics of the SU and the measurements carried out are shown.

### Outdoor areas of the site. Paved areas

a) Building area yard (Zone 11)
<u>Surveillance Unit UV-A-VIG-11</u>
Asphalted section located between the Transitory Reception, General Services, Conditioning, Active Laboratory and Auxiliary Conditioning Buildings.

Scans were performed in one scan an Investigation Level was detected. This was verified by way of a one-off measurement and a sample was taken for analysis in the laboratory. The results of this analysis did not reveal any activity above the detection thresholds.

In the static measurements performed at random locations no activity was detected.

Specific sample of sediments from the rainwater collection box was taken. The results did not reveal any activity.

This area, which was initially classified as class 3, was reclassified as non-impacted.

Surveillance Unit UV-A-VIG-33

This belongs to unit UV-A-VIG-11 and was created as an intermediate unit between the class 3 UV-A-VIG-11 and UV-A-VIG-12, reclassified as class 1 after the initial measurements.

No investigation levels were recorded in gamma scans performed.

No activity was detected above the detection thresholds in statics measurements.

This Surveillance Unit, initially classified as class 2, was reclassified as class 3 since no activity was detected above the detection thresholds.

**Table 3. Characteristics of SU and measurements performed.**

| Surveillance unit | Area ($m^2$) | Initial classification | Gamma scans | | | Number static measurements | Number samples |
|---|---|---|---|---|---|---|---|
| | | | Number | Area ($m^2$) | % | | |
| UV-A-VIG-11 | 8,560 | Class 3 | 21 | 874 | 10.2 | 5 | 2 |
| UV-A-VIG-33 | 577 | Class 2 | 6 | 305 | 53 | 5 | - |
| UV-A-CON-12 | 945 | Class 2 | 14 | 945 | 100 | 5 | 1 |
| UV-A-VIA-17 | 24,114 | Class 3 | 37 | 2,647 | 11 | 15 + 5 | 1 |
| UV-A-PLA-18 | 1,930 | Class 3 | 7 | 280 | 11 | 5 | - |
| UV-A-PLA-19 | 1,930 | Class 3 | 8 | 218 | 11 | 5 | - |
| UV-K-VIG-26 | 1,114 | Class 2 | 23 | 617 | 55 | 15 + 5 | 1 |
| UV-K-VIG-27 | 1,965 | Class 3 | 5 | 213 | 11 | 5 | - |
| UV-K-VIG-28 | 513 | Class 3 | 2 | 108 | 21 | 5 | 3 |
| UV-K-VIA-31 | 2,852 | Class 3 | 16 | 1,158 | 39 | 5 | - |
| UV-K-VIA-32 | 250 | Class 3 | 1 | 75 | 30 | 2 + 5 | - |
| UV-C-01 | 1,270 | Class 3 | 5 | 152 | 12 | 5 | 2 |
| UV-C-02 | 660 | Class 2 | 21 | 376 | 57 | - | 5 |
| UV-C-03 | 1,100 | Class 2 | | | | 15 + 5 | 3 + 15 |
| UV-C-04 | 1,471 | Class 2 | 32 | 786 | 53 | 5 | 6 + 4 |

b) Parking area (Zone 12)

Surveillance Unit UV-A-CON-12

This is an asphalted area for the transitory parking of trucks carrying radioactive wastes.

In specific gamma scans 7 points above the Investigation Level were detected. 6 points above the Investigation Level were verified by static measurement. One point with a high Cs-137 count rate was confirmed by means of a specific measurement. In view of the results, this Surveillance Unit was reclassified as class 1, 100% of its surface area was investigated by gamma scanning.

In the static measurements at random locations, no activity was detected above the detection thresholds.

A sample was taken at the location with the high count rate. The result gave a value 10 times higher than the Action Level. This area was cleaned and a new soil sample was taken, the result was below the Action Level.

This Surveillance Unit, initially classified as class 3, was reclassified as a non-impacted area.

c) Access road to North Platform and South Platform (Zone 17)

Surveillance Unit UV-A-VIA-17

Asphalted area corresponding to the access road to the radioactive waste Disposal Platforms zone.

In gamma scans performed 5 Investigation Levels were obtained. Static measurements were performed at these 5 locations, no activity was detected above the detection threshold.

No activity was detected above the detection thresholds in statics measurements at random locations.

Specific samples of sediments from the rainwater collection box were taken, no activity was detected.

This Surveillance Unit, initially classified as class 3, was reclassified as a non-impacted area.

d) Temporary ISO container disposal facility to the south of the South Platform (Zone 18)

Surveillance Unit UV-A-PLA-18

This is an asphalted area located to the south of the South Platform where ISO containers with radioactive wastes from different incidents (Acerinox and others) are kept.

Any point above the Investigation Level was detected in gamma scans.

In static measurements at random locations, no activity above the detection thresholds was detected.

This Surveillance Unit, initially classified as class 3, was reclassified as a non-impacted area.

e) Temporary ISO container disposal facility to the north of the South Platform (Zone 19)

Surveillance Unit UV-A-PLA-19

This is an asphalted area located to the north of the South Platform where ISO containers with radioactive wastes from different incidents (Acerinox and others) are kept.

No points above the Investigation Level were detected in gamma scans.

In static measurements at random locations, no activity above the detection thresholds was detected.

This Surveillance Unit, initially classified as class 3, was reclassified as a non-impacted area.

f) Outdoor area to the west of the Modules and Technology Building (Zone 26)
Surveillance Unit UV-K-VIG-26
This is a concrete area located to the west of the Technology Building and the temporary radioactive waste storage Modules.

In gamma scans performed 15 Investigation Levels were detected. Static measurements were performed at these locations; no activity was detected above the detection threshold.

In static measurements no activity was detected above the detection thresholds.

Samples of sediments from the rainwater collection box were taken. The results for the sample showed background values.

This Surveillance Unit, initially classified as class 2, was reclassified as class 3.

g) Outdoor area to the east of the Modules and Technology Building (Zone 27)
Surveillance Unit UV-K-VIG-27
This is an outdoor concrete area located to the east of the Technology Building and the temporary radioactive waste storage Modules. It also includes the areas between the Modules.

In gamma scans performed, 21 Investigation Levels were detected. A checking was made and it was considered that these values were due to the influence of a high background resulting from the radioactive wastes contained in these Modules.

The static measurements showed that no activity was detected above the detection thresholds.

This Surveillance Unit, initially classified as class 3, was reclassified as a non-impacted area.

h) Outdoor area to the east of the Technology Building and the east and south of the Modules (Zone 28)
Surveillance Unit UV-K-VIG-28
This is an area of earth located to the east and south of the temporary radioactive waste storage Modules.

In gamma scans performed 3 areas exceeding the Investigation Level were detected. Samples were taken and no activity was detected.

No activity was detected above the detection thresholds in static measurements.

This Surveillance Unit, initially classified as class 3, was reclassified as a non-impacted area.

i) Access road to Cell 29 (Zone 30) and road between the Technology Building and Cell 29 (Zone 31)
Surveillance Unit UV-K-VIA-31
This is an asphalted area providing access to Cell 29.

A large number of alarms above the Investigation Level were registered, in gamma scans, due to natural radionuclides in the ground surrounding the road.

No activity was detected above the detection thresholds in static measurements.

This Surveillance Unit, initially classified as class 3, was reclassified as a non-impacted area.

j) Band of ground between zones 11 and 13 (Zone 32)
Surveillance Unit UV-K-VIA-32
This is an area of land bounding Surveillance Units UV-A-CON-12, UV-A-VIG-11 and UV-A-VIA-17.

A single gamma scan was performed along the entire Surveillance Unit, 2 Investigation Levels were detected and confirmed by static measurements. Two samples were taken from these locations, no activity above the Detection Threshold was detected.

The measurement of the 5 random points was performed by sampling. The values obtained were those habitually found in the soils in the area.

This Surveillance Unit, initially classified as class 3, was reclassified as a non-impacted area.

k) Outdoor areas in the zone surrounding the rainwater collection pools
The radiological surveillance of these areas was performed by taking samples and analysing sediments at the outlet from the buildings and platforms rainwater pools. The two samples gave values of Cs-137 similar to those of the soils in the area due to fallout.

### Roofs of buildings

a) Roof of the Auxiliary Conditioning Building
Surveillance Unit UV-C-01
This is a concrete roof with a weatherproofing sheet and a final layer of gravel. It is a surface not considered to be affected by the discharge of gaseous effluents, for this reason was classified as the area in which it is located.

During scanning 2 investigation levels were registered, both confirmed by specific measurements.

The measurements performed at the 5 random points showed two points with values of CS-137 activity above the AMD/2 detection threshold, but below the actions levels. The specific samples taken at the two points did not show Cs-137 or Co-60 activity in either the coarse gravel fraction or the fraction of fine materials above the detection thresholds.

This Surveillance Unit, initially classified as class 3, was reclassified as a non-impacted area.

b) Roof of the Active Laboratory
Surveillance Unit UV-C-02
This is a concrete roof with a weatherproofing sheet and a final layer of gravel. It is a surface considered to be affected by the discharge of gaseous effluents.

During performance of the scans, 3 investigation levels were registered. The specific measurements performed did not confirm the alarms.

The measurements at the 5 random sampling points were performed by sampling due to difficulties in accessing the roof with the equipments. The results pointed to the no existence of residual activity above the detection thresholds.

This Surveillance Unit, initially classified as class 2, was reclassified as a class 3 area. However, it might be reclassified as a non-impacted area since no residual activity above the detection thresholds was detected in the random samples performed.

c) Roof of the Conditioning Building

This is considered to be affected by the discharge of gaseous effluents, for which reason it was initially classified as class 2.

Surveillance Unit UV-C-03

This includes the part of the rood of the Conditioning Building located to the west of the general ventilation duct. This is a concrete roof with a weatherproofing sheet and a final layer of gravel.

Systematic scanning was performed and 51 investigation levels were registered, both in the window for Cs-137 and Co-60, although expected due to the foreseeable influence of the contents of the Conditioning Building. A triangular mesh of 15 points, for specific samples, was designed additionally to the 5 points already established corresponding to the random ones.

In three of the statics measurements, activity above the action level was registered. These results show a more intense influence of the background which corresponds to the location of the containers shed. Samples were taken at these three points for laboratory analysis.

The analysis of the 15 specific samples and the three samples from random points reveals that in none of the 18 samples measured were Cs-137 or Co-60 activity values registered in excess of the detection thresholds.

This Surveillance Unit, initially classified as class 2, was reclassified as a class 3 area.

Surveillance Unit UV-C-04

This includes the part of the roof of the Conditioning Building located to the east of the general ventilation duct. This is a concrete roof with a weatherproofing sheet and a final layer of gravel.

The scans were performed in front of the stack emission points and the general ventilation duct, 8 investigation levels were detected. Of these 8 investigation levels, 6 were confirmed by specific measurements due to the confirmed influence of the interior of the building. Samples were taken at these six points for analysis.

The measurements at the random sampling points were performed using the ISOCS equipment but in four cases samples were taken due to the equipment was not operative.

The analysis of the results of the samples indicates that no Cs-137 or Co-60 activity was detected above the detection thresholds.

This Surveillance Unit, initially classified as class 2, was reclassified as a class 3 area.

d) Roofs of Modules and Technology Building
Surveillance Units UV-C-05 and UV-C-06
The radiological surveillance was not performed in these surveillance units, belonging to the roofs of the Temporary Storage Modules and Technology Building, respectively. In accordance with the initial analysis, the fact that these roofs are affected by the discharge of effluents constitutes a risk factor. However, since the Technology Building had not initiated its operation as of the date of performance of the programme, they were classified in the same class as the outdoor area in which they are located (class 3).

Consequently, in view of the results of the surveillance corresponding to the outdoor area, their reclassification as non-impacted might be assessed.

### Vertical outer walls of buildings

The radiological surveillance of the surveillance units on walls (UV-P-01, UV-P-02 and UV-P-03) has not been carried out since no contamination was detected in the outdoor areas in which they are located.

## Conclusions

- The methodology used in this SRSP is adequate for the purpose and will serve for the performance of later routine surveillance at the site of the El Cabril disposal facility.
- All the outdoor areas may be classified as non-impacted areas, with the exception of UV-A-VIG-33, which was reclassified as class 3.
- All the roofs of buildings were reclassified as class 3 areas. Nevertheless, they might be reclassified as non-impacted, since no residual activity above the detection thresholds was detected in the specific or random samples performed.
- All the vertical exterior walls of buildings might be reclassified as non-impacted or class 3 areas, since no contamination was detected in the outdoor areas in which they are located.

# Monitoring of radionuclides in the vicinity of Czech nuclear power plants

Svetlik, Ivo[1,2]; Fejgl, Michal[2]; Beckova, Vera[2]; Pospichal, Jiri[3]; Striegler, Rostislav[4]; Tomaskova, Lenka[1]
[1] DRD, Nuclear Physics Institute AS CR, CZECH REPUBLIC
[2] National Radiation Protection Institute, CZECH REPUBLIC
[3] NPP Temelin, CZECH REPUBLIC
[4] NPP Dukovany, CZECH REPUBLIC

## Abstract
The monitoring in the surrounding environment of Czech nuclear power plants (NPPs) Dukovany and Temelin consists from routine determinations, performed by NPP's staff, and also extended, supervisory, sampling performed by research institutions. In our contribution several results of this monitoring are briefly discussed and summarized.

## Introduction
At present, the most significant artificial sources of radiocarbon in the environment are effluents from nuclear power facilities, even though it is a minor contribution in comparison with its natural production. Nevertheless, radiocarbon makes a major contribution to the collective effective dose from all radionuclides released by nuclear power plants (NPP) with light-water pressurized reactors (LWPR) during normal operation (UNSCEAR, 2000). Although $^{3}H$ is not considered to be a particularly radiotoxic radionuclide and releases by commercial nuclear power plants have traditionally been well below regulatory limits, control and monitoring are important because of the sensitivity of the public to issues of radioactive material release and the potential of radiation exposure (Harris et al. 2008; Andersen 1995; Liu et al. 2003). The radionuclides $^{3}H$ and $^{14}C$ require special consideration because of their high mobility in the environment and the fundamental nature of hydrogen and carbon cycles in the biosphere (UNSCEAR 2000). Tritium produced by NPPs with LWPR can be released into the environment through waste discharge in either airborne or liquid forms (Kim & Han 1999; Harris et al. 2008). In general, normalized $^{3}H$ gaseous and liquid releases from LWPR are about 1.5 and 20 TBq GWyear$^{-1}$, respectively (Luykx & Frazel 1986). Tritium released to the atmosphere occurs in two forms: tritiated hydrogen (HT) and tritiated water vapour (HTO). HTO is subject to the same wet and dry deposition processes as other nuclides, but it can also diffuse into the soil pore space and the leaf stomates (Belot et al. 1979; Garland 1979). Tritium which is not returned to the atmosphere by evaporation moves through the soil primarily by the mass flow of liquid

water (UNSCEAR 2000). The Czech Republic has two LWPR equipped NPPs, Temelin and Dukovany, with the installed power output 2x1000 MW and 4x440 MW, respectively. The monitoring in the surrounding environment of Czech nuclear power plants (NPPs) Dukovany and Temelin consists from routine determinations, performed by NPP's staff, and also extended sampling which is performed by several research institutions. Systematical monitoring of HTO in the air of NPPs surrounding was launched there by the National Institute of Radiation Protection in 2008. Systematic sampling of biota and agricultural products for $^{14}C$ activity monitoring was started in 2002 by Nuclear Physics Institute in the cooperation with National Institute of Radiation Protection (Svetlik et al. 2007, 2008). Environmental monitoring, performed by staff of NPPs, includes these determinations: gamma spectrometry, $^{90}Sr$, $^{3}H$ (in surface and underground water), gross alpha and beta, and dose rate (ETE 2010, EDU 2010). Still other institutes are involved in the specialized monitoring of Czech NPPs surrounding, namely: Water Research Institute T.G.M. in Prague – HTO and $^{137}Cs$ in connected surface water (Hanslik et al. 2009a, b); Czech Technical University, Faculty of Nuclear Sciences and Physical Engineering, Department of Dosimetry – gamma spectrometry and dose rate in the NPPs vicinity (Thinova & Trojek 2009; Thinova & Kluson 2008).

## Material and methods

As a part of project SÚJB 5/2008 "Monitoring and evaluation of nuclear power plants discharges containing tritium" tritium activity concentration in the air humidity was also determined. Air humidity samples were collected in surroundings of the two Czech nuclear power plants (Malatova & Hulka 2008). A sampling method using sorption of the air humidity on dried silica gel was developed. The method operates in two different time regimes utilizing both static (sampling period of about four weeks) and dynamic sampling applying Dwarf aerosol sampler for point sampling with duration of about 10 minutes (Fejgl et al. 2009). Tritiated water was recovered from silica gel by means of freeze-drying. Tritium activity concentrations were measured by low-background liquid scintillation spectrometers. Four outdoor HTO sampling campaigns at the vicinity of the Dukovany power plant and one outdoor sampling expedition to the vicinity of the Temelin power plant were performed during the years 2008 and 2009. During these sampling campaigns 112 air humidity samples were collected. Sampling around power plant Dukovany was emphasised because of elevated tritium activity concentration in cooling water (hundreds Bq per liter), therefore tritium could be discharged from the power plant not only via ventilation stack but also via cooling towers (Fejgl et al. 2009a). 10 sampling points for dynamic sampling and 17 sampling points for static samplings were laid out in distance between 100 and 900 meters from the cooling towers, see Fig. 1.

Monitoring of $^{14}C$ in surrounding of the Czech NPPs and in reference localities is performed utilizing biota samples, see fig 2. This type of monitoring is restricted on the part of vegetation period. Time interval of $^{14}C$ activity record depends on period of biomass cumulation in a given plant. $^{14}C$ activity in the sampling points can be locally influenced (lowered) by anthropogenic $CO_2$ emissions from fossil fuel combustion (traffic, heating of buildings). Fossil carbon (without significant $^{14}C$ amount) causes dilution of $^{14}C$ in carbon isotopic mixture (Suess effect). Local component of Suess

effect can be observed namely in the vicinity of greater roads, cities, and other greater fossil $CO_2$ sources (Suess, 1955; Kuc & Zimoch 1998).

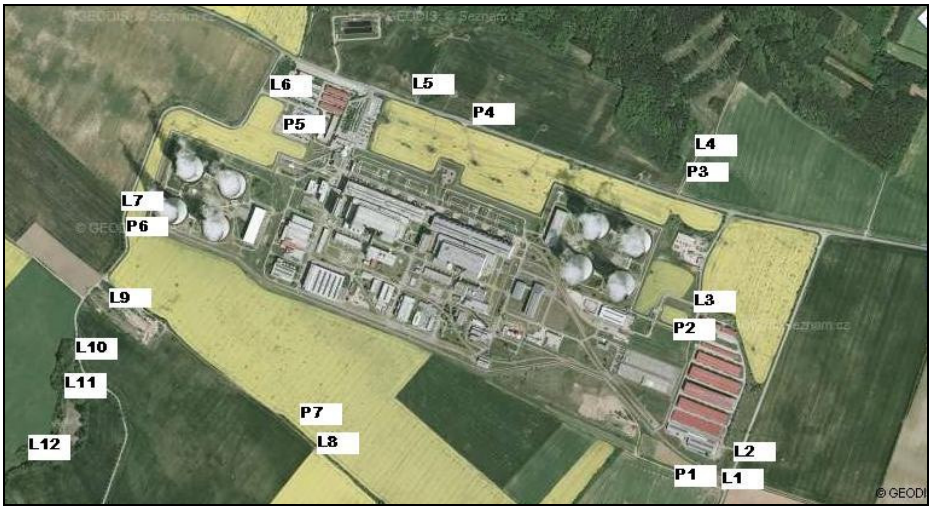


**Fig. 1. Nearest sampling points around NPP Dukovany for HTO activity monitoring in air moisture. P – prompt sampling, L – long term period of sample cumulation.**

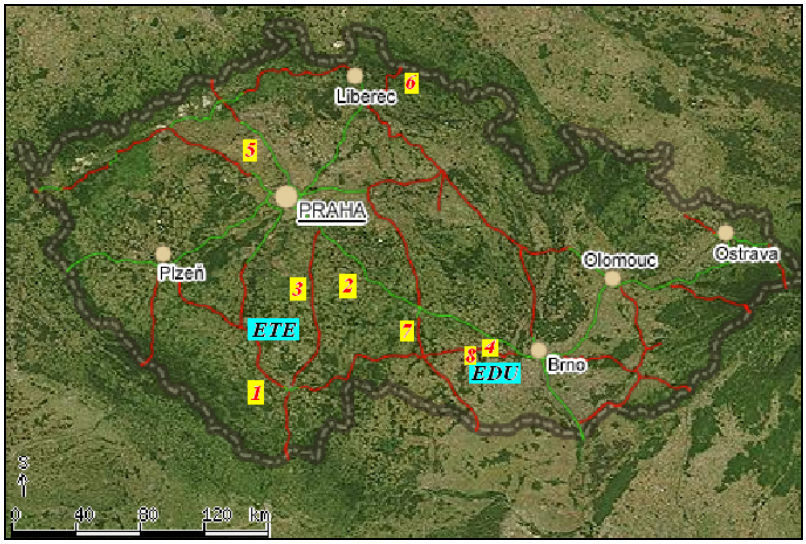


**Fig. 2. $^{14}C$ sampling points in the area of the Czech Republic: NPP Dukovany – EDU; NPP Temelin – ETE; 1-8 reference sampling points in localities with smaller load of fossil fuel combustion.**

Prevailing part of biota samples were leaves of deciduous trees, analogically to published studies performed in the vicinity of other NPPs. Leaves of *Sambucus nigra L.* (pipe tree) were preferred, because this tree is widespread in the Czech Republic, and it can be easy identified. Smaller part of samples collected were agricultural plants (spikes of wheat and barley). Dusty biota samples were washed by 10% HCl and distilled water, dried (105 $^{o}$C) and homogenized. Washing by diluted HCl was suspended if presence of dust on sample surface was not evident. Dried samples were combusted and resulting $CO_2$ was purified. In the NPI AS CR a routine of sample processing based on benzene synthesis was followed (Gupta & Polach, 1985). $^{14}C$ activity was measured by

liquid scintillation spectrometer Quantulus 1220 in 3 ml low-background Teflon vials. Total counting time was about 2000 minutes per sample. Benzene distributed by Sigma-Aldrich (spectrophotometric grade) was used as a blank sample. Calibration was performed using oxalic acid NIST (NBS) HOX II, SRM 4990-C (Schneider et al., 1995). Combined uncertainties include the individual uncertainties of measured sample, blank sample, calibration, quenching corrections, and uncertainty of the $\delta^{13}C$ value (Curie 1995). In the vicinity of NPPs Temelín and Dukovany several roads are situated and there also are some smaller cities and villages. The influence of local Suess effect could be estimated/quantified with difficulties, as data about local fuel combustion and density of traffic are absent. To compare $^{14}C$ activities in the NPPs surrounding with actual $^{14}C$ activity level in the environment two types of areas with different load of Suess effect were selected. It can be supposed that actual size of Suess effect influencing in NPPs surrounding will be in the interval demarked by the two types of reference areas (Svetlik et al. 2007). (A) Localities, in greater distances from fossil carbon sources, where only small local influence of Suess effect was supposed (Košetice, Kleť, Sudoměřice u Bechyně, Krokočín). (B) Localities where medium local Suess effect influence can be expected (bordering parts of Prague).

Staff of nuclear power plants Temelin and Dukovany is monitoring radionuclides in the NPPs vicinity following internal documents (programs of Environmental Monitoring in the Vicinity of NPPs Temelin and Dukovany). All gamma, alpha and liquid scintillation spectrometry measurements ($^{90}Sr$, HTO) of radionuclides were performed applying metrologically validated and calibrated instruments (Czech Metrology Institute - Inspectorate for Ionizing Radiation). Most of the utilized analytical methods are a subject of accreditation (Czech Accreditation Institute). The environmental monitoring of radionuclides includes these sample types: (1) Aerosols (13 sampling points in the distances from 2 to 26 km, flow rate about 40 $m^3$ per hour, one week exposition – determinations: gamma emitting radionuclides and $^{90}Sr$), monitoring of $^{131}I$ for each NPP is also performed at distance from NPP Temelin 5 km (one point) and Dukovany, 6 points at distances 3-11 km (flow rate 4 $m^3$ per hour, one week of iodine cartridge exposition); (2) bulk atmospheric deposition (8 sampling points in distances from 2 to 11 km to NPP, sampling area 0.5 $m^2$, one month sampling period – determinations: gamma emitting radionuclides); (3) atmospheric precipitation (7 points, sampling period is one month, in distances from NPP Temelin and Dukovany from 1 to 11 km, respectively – determination HTO); (4) surface water in surrounding lakes (7 sampling points) and corresponding river profiles 10 of Vltava and Jihlava (one month sampling period – determinations: gross alpha and beta, gamma spectrometry, HTO), from each profile and sampling point also determination of $^{90}Sr$ is annually performed; (5) underground water, 25 boreholes in distances from NPPs Temelin and Dukovany from 1 to 3 km - determinations: gamma spectrometry, HTO); (6) drinking water (at least samples from 11 sampling points of tap and well water - determinations: gross alpha and beta, gamma spectrometry, HTO, $^{90}Sr$); (7) milk (3 pieces of 3 litre samples in one month period (minimally) for gamma spectrometry measurement, subsequently are samples cumulated and $^{90}Sr$ determination is performed annually); (8) sediments and soils, annual quantity is about 16 sampling points (surface layers till 10 cm, fraction below 2 mm, gamma spectrometry measurement); (9) 12 agricultural and forest products (gamma spectrometry measurement) are processed annually.

## Results

Basic statistical parameters of HTO monitoring in air humidity in the vicinity of Czech NPPs and background areas are reported in Table 1.

**Table 1. Mean values of observed HTO activity concentration in air moisture and supporting data (prompt sampling/long term sample cumulation).**

| | NPP Dukovany | NPP Temelin | Background samples [c] |
|---|---|---|---|
| Median, Bq $L^{-1}$ [a] | 2.60 / 2.53 | 2.19 / 1.82 | 2.81 |
| Number of values below significance level [b] | 5 / 17 | 0 / 1 | 6 |
| Number of outlying values | 2 / 4 | 0 / 0 | 0 |
| Number of observations | 32 / 50 | 7 / 5 | 23 |

[a] Excluding outlying values in the case of NPP Dukovany.
[b] Decision threshold was calculated for 5% probability of the first kind error and was in the range 0.8 to 1.3 Bq $L^{-1}$.
[c] Background sampling was performed only for long term sample collection.

During period 2002 – 2005, 77 biota samples for $^{14}C$ analyses were collected in the vicinity of NPPs Dukovany (EDU) and Temelín (ETE). Likewise, 30 samples were collected in reference areas influenced with slight (A) and extended (B) local Suess effect. Basic statistical parameters of results (EDU, ETE, A, B) are reported in Table 2. Standard deviations of couples EDU-B, ETA-A, and ETE-B are equal on the base of F-tests performed (Fischer-Snedecor test). In the next step results from each type of area were compared utilizing t-test (student test, unpaired, probability of first kind of observation error 1%), see Table 3.

**Table 2. Basic statistical parameters of biota samples collected in the vicinity of NPPs Dukovany (EDU), Temelín (ETE) and in reference localities with slight (A) and extended (B) local Suess effect. Sampling period 2002 – 2008. Activities are reported in ‰ of $\Delta^{14}C$ (Stuiver & Polach, 1977).**

| | EDU | ETE | Ref. localities A | Ref. localities B |
|---|---|---|---|---|
| Average | 60.1 | 61.0 | 56.2 | 47.4 |
| Median | 58.3 | 60.4 | 56.2 | 45.7 |
| Standard deviation ($\sigma$) | 13.2 | 9.0 | 6.5 | 7.3 |
| Variation | 173 | 81 | 42.1 | 53.5 |
| Number of observations | 27 | 50 | 21 | 9 |
| Observed maximum | 95.9 | 84.4 | 67.9 | 58.7 |
| Observed minimum | 39.8 | 41.7 | 44.0 | 38.0 |

**Table 3. Comparisons of activities of observed results from each type area (group of the data), values of T reported in table: $T_o$ (observed) and $T_c$ (critical); t-test, unpaired, probability of first kind of observation error 1%.**

| Couple compared | $T_o$ | $T_c$ | *t-test enclosures* |
|---|---|---|---|
| A-B | 2.621 | 3.106 | $T_o < T_c \Rightarrow$ *difference is not significant* |
| EDU-A | 1.479 | 2.712 | $T_o < T_c \Rightarrow$ *difference is not significant* |
| EDU-B | 2.507 | 2.037 | $\boldsymbol{T_o > T_c \Rightarrow}$ ***difference is significant*** |
| ETE-A | 2.336 | 2.651 | $T_o < T_c \Rightarrow$ *difference is not significant* |
| ETE-B | 3.913 | 2.668 | $\boldsymbol{T_o > T_c \Rightarrow}$ ***difference is significant*** |
| EDU-ETE | 0.272 | 2,712 | $T_o < T_c \Rightarrow$ *difference is not significant* |

## Discussion

HTO activity concentrations in the air humidity from background reference sites fall in the range from <1.2 up to 3.5 Bq/L. All the samples from NPP Temelín vicinity and most of the samples from the NPP Dukovany vicinity do not exceed the same range. In some of the samples significantly increased tritium activity concentrations were found. An increase was found in the samples from the sampling point L5 (10.57 ± 0.53 Bq $L^{-1}$, September 2008) for long-term sampling and P4 for instant sampling (11.37 ± 0.57 Bq $L^{-1}$, September 2008). Both these sampling points are placed near the wastewater pipe outfall; the increase can be explained by a local evaporation of the wastewater. Another increased activity concentration was found in the sample from September 2008 from the sampling point P7 for instant sampling (7.90 ± 0.62 Bq $L^{-1}$). This point is placed 100 meters to the south from the grounds of NPP Dukovany. It was raining during the sampling and the wind blew southwards. This increase is the only one which is explainable as a sorption of tritiated water evaporated from the cooling tower (Fejgl et al. 2009). Other increases were found in the samples from the dam Mohelno vicinity from September 2008 and September 2009 i.e. 13.28 ± 0.51 and 7.03 ± 1.08 Bq $L^{-1}$, respectively. Probable reason is the evaporation from the dam reservoir (tritium volume activity concentration ranges between tens and hundreds Bq per litre), see Fig. 3. Related increase was also observed in the sample collected near the Jihlava River (8.77 ± 0.91 Bq $L^{-1}$, September 2008).

Comparison of two air humidity sampling methods sorption on silica gel versus cold trap method (air flow-rate 30 L $hour^{-1}$, temperature -20 $^{o}$C, sampling period a month) at the same place shows systematically augmented tritium activity concentrations in samples collected by sorption on silica gel. With respect to the fact that chemical laboratories of NRPI process highly tritiated water samples (up to 100 kBq $L^{-1)}$, the cross-contamination seems to be the most probable reason of tritium activity concentration increase. An experiment with very low tritium activity water was performed off the premises. The water vapour was sorbed into silica gel, this was lyophilized and subsequently the tritium activity concentration in the sample was determined. The found value was 1.22 ± 0.59 Bq/l. This result confirms possibility of

cross contamination during sample processing in the lab. Contamination of the dried silikagel just after it has been dried an before it is filled in the storage vessel seems most likely. Some precautions were applied in order to reduce cross-contamination risk. Processing time was shortened and the drying temperature was enhanced from 105 to 130 °C, the drying time was extended to 8 hours, what ensures extrusion of lasting humidity. For final evaluation of precautions it is necassary to get more data, therefore the monitoring of the samples from the background reference sites will continue.

Results of statistical comparison confirmed significantly greater $^{14}C$ activity level in surrounding biota from both NPPs in the comparison with reference area B with greater load from fossil fuel combustion (bordering parts of Prague). Nevertheless, if these tests were performed for probability of first kind of error 5% (a), significant differences were found also between reference localities A and B. The difference of $^{14}C$ activity level between biota from NPP Temelín vicinity and biota from reference area A (small local fossil fuel combustion) was found to be statistically significant also, see Table 2. In the point of view of local loads from fossil fuel combustion, it can be supposed that relevant reference $^{14}C$ activity level for NPPs surroundings with relatively frequented roads is allocated in the interval between reference areas A and B. Observed $^{14}C$ activity values for each type of locality are charged by relatively greater variations, namely in samples from NPPs surroundings, probably caused by local Suess effect from surrounding roads especially. Other reason of fluctuation can be given also by relatively short time interval of biomass cumulation in leaves of deciduous trees (about the first third of vegetation period). At this part of year activity of atmospheric $^{14}CO_2$ changes rather quickly (Levin & Kromer 2004; Levin et al. 1995, 2008, 2010; Molnár et al. 2007) and biomass of plants is cumulated in the dependence of the local microclimatic parameters (atmospheric precipitation, soil moisture, sunlight exposure). Local microclimatic differences can cause small time shift of atmospheric $^{14}CO_2$ intake period. Additional reason of $^{14}C$ activity variations in NPPs surroundings is given by relatively greater distances from NPPs stacks (below 9 km) in certain sample collection localities. Potentially influenced zones around NPPs can be probably found in the distance till 2 km, on the basis of $^{14}C$ dissipation model, (Rousel-Debet et al., 2006). Also the direct results of $^{14}C$ in biota monitoring performed in the vicinity of NPPs with boiling water reactors (BWR)[1] in Sweden confirm similar distances from stacks for maximal surplus of $^{14}C$ activity in biota (Stenström et al. 1996; Stenström et al. 1998).

On the basis of environmental monitoring performed by staff of NPPs Temelin and Dukovany during year 2009, there were observed activities of HTO enhanced above background level in surface water, see fig. 3. These activities are given by liquid releases of $^{3}H$, which did not exceed authorized limits given by State Office for Nuclear Safety. In the case of NPP Dukovany surrounding, there were observed also several increased HTO activities in underground water, which did not exceed 60 Bq $L^{-1}$. Origin of such HTO is probably connected with cooling towers, which are evaporating water from Mohelno reservoir, see fig. 3. Analogically to previous years, during 2009, no activities exceeding reference activity values were observed in the environmental

[1] In the comparison with LWPR contain releases from BWR considerably greater percentage of $^{14}CO_2$, above 90% (Kunz 1995). This chemical form of released $^{14}C$ can be assimilated by plant photosynthesis and hence greater $^{14}C$ activity excess can be observed in the surrounding biota of NPPs with BWR.

surrounding of both NPPs (ETE 2010, EDU 2010). By direct field measurements or on the basis of laboratory determinations performed in laboratories of NPPs, the only radionuclides of artificial (possible artificial) origin measurable in the surrounding environment are $^{3}H$ and $^{137}Cs$. Dominant source of $^{137}Cs$ in the environment of the Czech Republic was accident of Chernobyl NPP in 1986 and no increased activity level of this radionuclide (in the comparison with background values) was observed in the vicinity of both NPPs.

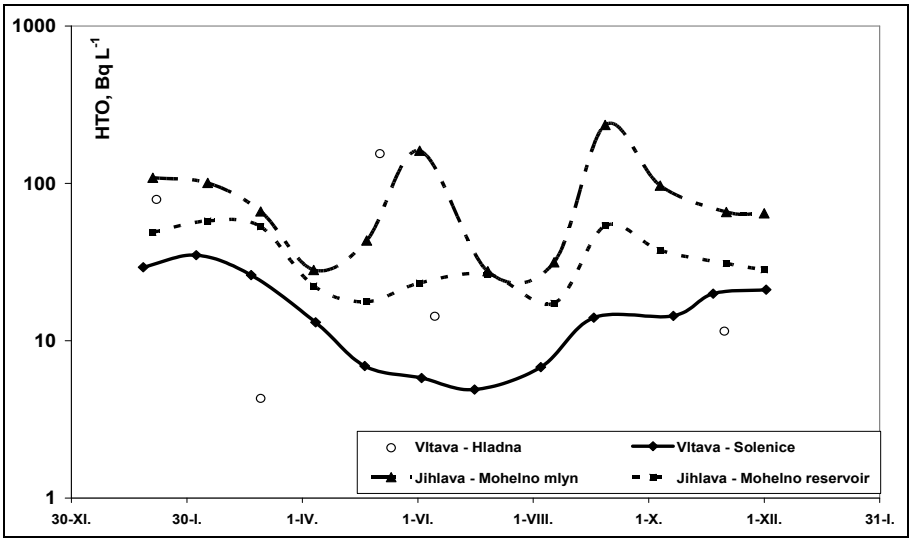


**Fig. 3. Year 2009. Time course of HTO activity concentration in profiles Hladna (about 5 km downstairs from releasing channel of NPP Temelin in Korensko) and Solenice (below barrier of the great river reservoir Orlik, about 50 km downstairs from the releasing channel). Increrased HTO activities in the profile Hladna can be observed only several days after discontinuous discharges from the NPP Temelin, in other cases are activities below 3 Bq $L^{-1}$. Liquid releases from NPP Dukovany are exhausted into Mohelno reservoir. River profile Jihlava-mlyn is about 1500 m downstairs from Mohelno reservoir barrier.**

## Conclusions

A brief summary of the monitoring performed by several institutions in the vicinity of NPPs Temelin and Dukovany was assembled. In the point of view of HTO monitoring in air moisture in the vicinity of NPP Dukovany, only several samples with significantly increased HTO activities were collected. Nevertheless, our sampling method based on silica gel sorption did not allow fine resolution and will be modified and validated. Results of $^{14}C$ activity monitoring, utilizing leaves of deciduous trees and agricultural products, in the surrounding of both NPPs highlights small probable surplus in the surrounding of NPP Temelin (about 5‰ $\Delta^{14}C$). Enhancement of $^{14}C$ activity was not statistically significant in the vicinity of NPP Dukovany.

Enhanced HTO activities in rivers Vltava and Jihlava, where liquid releases are exhausted, have been observed by staff of NPPs within the frame of routine environmental monitoring. In the case of NPP Dukovany, HTO activities in the connected underground and well water have also been observed above actual environmental background, but deeply below limit of 100 Bq $L^{-1}$, given by Czech legislative. Significant, measurable, presence of other radionuclides originated from

NPPs has not been observed by monitoring performed by staff of nuclear power plants in the surrounding, although susceptible measuring methods were applied.

## Acknowledgments

This work was funded by internal grant of the Nuclear Physics Institute AS CR (No. AV0Z 10480505) and by National Radiation Protection Institute (grants No. JC 03/2006 and JC 05/2008).

## References

Andersen RL. Criteria for radiological releases. In: Maletskos CJ, ed. Radiation protection at nuclear reactors. In: Health Physics Society 1995 Summer School. Madison, WI: Medical Physics Publishing; 1995: 21–44.

Belot Y, Ganthier K, Camus H, Caput C. Prediction of the flux of tritiated water from the air to plant leaves. Health Physics 1979; 37:575-583.

CEZ group (EDU 2010) Radiation situation in the surrounding of NPP Dukovany, 2009. (Radiační situace okolí JE Dukovany, rok 2009) Report D57. CEZ group; 2010. (in Czech)

CEZ group (ETE 2010) Results of monitoring effluents and radiation situation in the surrounding of NPP Temelin in 2009. (Výsledky monitorování výpustí a radiační situace okolí jaderné elektrárny Temelín za rok 2009.) Report D02. CEZ group; 2010. (in Czech)

Curie LA. Nomenclature in Evaluation of Analytical Methods Including Detection and Quantification Capabilities. (IUPAC Recommendation 1995). Pure & Appl. Chem. 1995; 67(10):1699-1723.

Fejgl M, Světlík I, Filgas R, Michálek V. (2009): Monitorování aktivit tritia v atmosféře v okolí jaderných elektráren České Republiky. In: Hanslik E, Pecinova A (Eds.). Proc. Konference radiologické metody v hydrosféře. 2009 May 5-6; Žďár n. Sázavou, Czech Republic. Ekomonitor; 2009:10-15. (in Czech)

Garland JA. Transfer of tritiated water vapour to and fromland surfaces. p. 349-359 in:Behaviour of Tritiumin the Environment. STI/PUB/498. Vienna: IAEA; 1979.

Gupta SK, Polach HA. Radiocarbon dating practices at ANU. Canberra: ANU; 1985.

Hanslík E, Ivanovová D, Jedináková-Křížová V, Juranová E, Šimonek P. Concentration of radionuclides in hydrosphere affected by Temelín nuclear power plant in Czech Republic. Journal of Environmental Radioactivity 2009; 100(7):558-563.

Hanslík E, Ivanovová D, Juranová E, Šimonek P, Jedináková-Křížová V. Monitoring and assessment of radionuclide discharges from Temelín Nuclear Power Plant into the Vltava River (Czech Republic). Journal of Environmental Radioactivity 2009; 100(2):131-138.

Harris JT, Miller DW, Foster DW. Tritium recapture behavior at a nuclear power reactor due to airborne releases. Health Physics August 2008; 95(2): 203-212.

Kim CK, Han MJ. Dose assessment and behavior of tritium in environmental samples around Wolsong nuclear power plant. Appl. Radiat. Isot. 1999; 50:783–791.

Kuc T, Zimnoch M.. Changes of the $CO_2$ sources and sinks in a polluted urban area (southern Poland) over the last decade, derived from the carbon isotope composition. Radiocarbon 1998; 40(1):417-423.

Kunz C. Carbon-14 discharge at three light-water reactors.Health Phys. 1985; 49:25-35.

Levin I, Graul R, Trivett NBA. Long-term observations of atmospheric $CO_2$ and carbon isotopes at continental sites in Germany. Tellus 1995; 47B:23–34.

Levin I, Hammer S, Kromer B, Meinhardt F. Radiocarbon observations in atmospheric $CO_2$: Determining fossil fuel $CO_2$ over Europe using Jungfraujoch observations as background. Science of the Total environment 2008; 391(2-3):211–216.

Levin I, Kromer B.. The tropospheric $^{14}CO_2$ level in mid-latitudes of the northern hemisphere (1959–2003). Radiocarbon 2004; 46(3):1261–1272.

Levin I, Naegler T, Kromer B, Diehl M, Francey RJ, Gomez-Pelaez AJ, Steele LP, Wagenbach D, Weller R, Worthy DE. Observations and modelling of the global distribution and long-term trend of atmospheric $^{14}CO_2$. Tellus B 2010

Liu CC, Chao JH, Lin CC. Tritium release from nuclear power plants in Taiwan. Health Physics 2003; 84:361–367.

Luykx F, Fraser G. Tritium releases from nuclear power plants and nuclear fuel processing plants. Radiation Protection Dosimetry 1986; 16:31–36.

Malátová I, Hůlka J. Research program of NRPI: Tritium from effluente from NPP. In. Proc. Conference XXX. Days of Radiation Protection. 2008 November 24-28; Lipt. Ján, Slovakia; 2008. p. 201-202.

Roussel-Debet S, Gontier G, Siclet F, Fournier M. Distribution of carbon 14 in the terrestrial environment close to French nuclear power plants. Journal of Environmental Radioactivity 2006; 87:246-259.

Schneider RJ, McNihol AP, Nadeau MJ, Reden KF. Measurements of the Oxalic Acid II/Oxalic Acid I Ratio as a Quality Control Parameter at NOSAMS. Radiocarbon 1995; 37(2):693-696.

Stenström K, Erlandsson B, Hellborg R, Wiebert A, Skog G. Environmental levels of carbon-14 around a Swedish nuclear power plant measured with accelerator mass spektrometry. Nuclear Instruments and Methods in Physics Research B 1996; 113:474-476.

Stenström K, Skog G, Thornberg C, Erlandsson B, Hellborg R, Mattsson S, Persson P. $^{14}C$ levels in the vicinity of two Swedish nuclear power plants and at two „clean-air“ sites in southernmost Sweden. Radiocarbon 1998; 40(1):433-438.

Stuiver M, Polach H. Reporting of $^{14}C$ data. Radiocarbon 1977; 19(3):355-363.

Suess HE. Radiocarbon concentration in modern wood. Science 1955; 122:415-417.

Světlík I, Michálek V, Tomášková L. Stanovení úrovně aktivity $^{14}C$ v biotě okolí JE. (Determination of $^{14}C$ activity level in the vicinity of nuclear power plants.) Bezpečnost jaderné energie 2008; 16(3-4):82-88. (in Czech)

Světlík I, Molnár M, Svingor E, Rinyu L, Futó I, Michálek V. Biomonitoring of $^{14}C$ in the vicinity of NPPs. In: Regional and Global Aspects of Radiation Protection. 2007 September 24-28; Brasov, Romania. IRPA; 2007.

Thinova L, Kluson J. Irradiation of population in the surrounding area of nuclear power plant Temelin. Natural Radiation Environment 2008; 1034:513-516.

Thinova L, Trojek T. Data analysis from monitoring of radionuclides in the nuclear power plant Temelin ecosystem area. Applied Radiation and Isotopes 2009; 67(7-8):1503-1508.

United Nations Scientific Committee on the Effects of Atomic Radiation to the General Assembly (UNSCEAR). Exposures from natural and manmade sources of radiation. Report 1. UNSCEAR; 2000.

# $^{14}C$ in biological samples from the vicinity of NPP Krško

Obelić, Bogomil[1]; Krajcar Bronić, Ines[1]; Barešić, Jadranka[1]; Horvatinčić, Nada[1]; Sironić, Andreja[1]; Breznik, Borut[2]
[1] Rudjer Bošković Institute, Zagreb, CROATIA
[2] Nuclear Power Plant Krško, Krško, SLOVENIA

## Abstract

Monitoring $^{14}C$ activity in the atmospheric $CO_2$ and in biological samples (fruits and vegetables) in the close vicinity of the NPPK was performed regularly since 2006 to estimate the possible influence of the plant on environmental $^{14}C$ levels and the possible contribution to the effective dose of local population through food chain.

Mean values of $^{14}C$ activity in atmospheric $CO_2$ in the years when the refuelling was not performed represent a barely visible increase in relation to the activities of $^{14}C$ in the atmosphere at the control point. Immediately after refuelling the atmospheric $^{14}C$ activity was increased for a short period of time. Spatial distributions of $^{14}C$ activities in biological samples show the dependence on distance and orientation. In all campaigns the highest activities were obtained at the same locations in the SW-NE direction that coincided with the most pronounced wind directions. Estimated contribution of $^{14}C$ released by NPPK to the natural dose is less than 1 μSv.

## Introduction

$^{14}C$ is formed in upper layers of the atmosphere in a reaction of neutrons from the cosmic rays and nitrogen atoms. All carbon isotopes take part in chemical reactions, hence $^{14}C$ is also oxidized into $^{14}CO_2$ and distributed uniformly throughout the atmosphere. Plants assimilate $^{14}CO_2$ through the photosynthesis process, and animals are fed by plants, thus the $^{14}C$ isotope is a part of the natural carbon cycle. In the past, the equilibrium between radioactive decay of $^{14}C$ and its production rate has been established, and the natural $^{14}C$ concentration, or better to say, specific activity of $^{14}C$, in the Earth's atmosphere and biosphere is approximately constant and it equals 226 Bq/kg of carbon. Assuming atmospheric $CO_2$ concentration of 370 ppm, this equilibrium specific activity of $^{14}C$ in the atmosphere corresponds to 0.037 Bq/m$^3$ of air.

In the second half of the 20$^{th}$ century the natural $^{14}C$ distribution was disturbed by atmospheric bomb tests and in 1963 the atmospheric $^{14}C$ specific activity reached maximum of twice the natural activity. After the ban of atmospheric bomb tests the present-day atmospheric $^{14}C$ activity approaches the natural (non-disturbed) values.

$^{14}C$ is produced also in nuclear power plants. The emitted $^{14}CO_2$ enters the carbon cycle, and through food chain it may contribute to the dose of the local population. The aim of this study was to determine distribution of $^{14}C$ in a close vicinity of the Nuclear Power Plant Krško (NPPK) in Slovenia close to the border with Croatia, and to estimate possible contribution of NPPK to the effective dose of local population through food chain.

## Sampling and measurements

Atmospheric $CO_2$ was collected at two locations inside the NPPK area, marked as **A** and **B** in Figure 1, close to the release point of the plant ventilation system. Integral samples were collected since 2006 on a regular bimonthly basis by absorption of $CO_2$ in saturated NaOH solution. $Na_2CO_3$ thus produced was in the laboratory dissolved in HCl, and the obtained $CO_2$ was used for benzene synthesis. Benzene samples were measured by a liquid scintillation counter *Quantulus* (Horvatinčić et al. 2004).

Specific $^{14}C$ activity of biological samples (apples, corn, cereals, borecole, grass) was measured in immediate vicinity (locations **C**, **D**, **E**, **I**, **J**, **L** and **R**, 200 – 400 m from the NPPK release point), and in a wider environment (locations **F**, **G**, **H**, **K**, **M**, **N**, **O**, **P** and **Q**, about 1000 m) of NPPK (Fig. 1). As a control site, where no influence of the plant is expected, we have chosen village Dobova, about 10 km SE from NPPK. Two sampling campaigns have been performed each year since 2006, in June/July and in September/October. Samples were dried, carbonized (pyrolysis at 600°C), and combusted in a stream of oxygen. The obtained $CO_2$ was absorbed in a mixture of Carbosorb®E and Permafluor®E. $^{14}C$ activity was measured by the LSC *Quantulus 1220* (Horvatinčić et al, 2004; Krajcar Bronić et al, 2009).

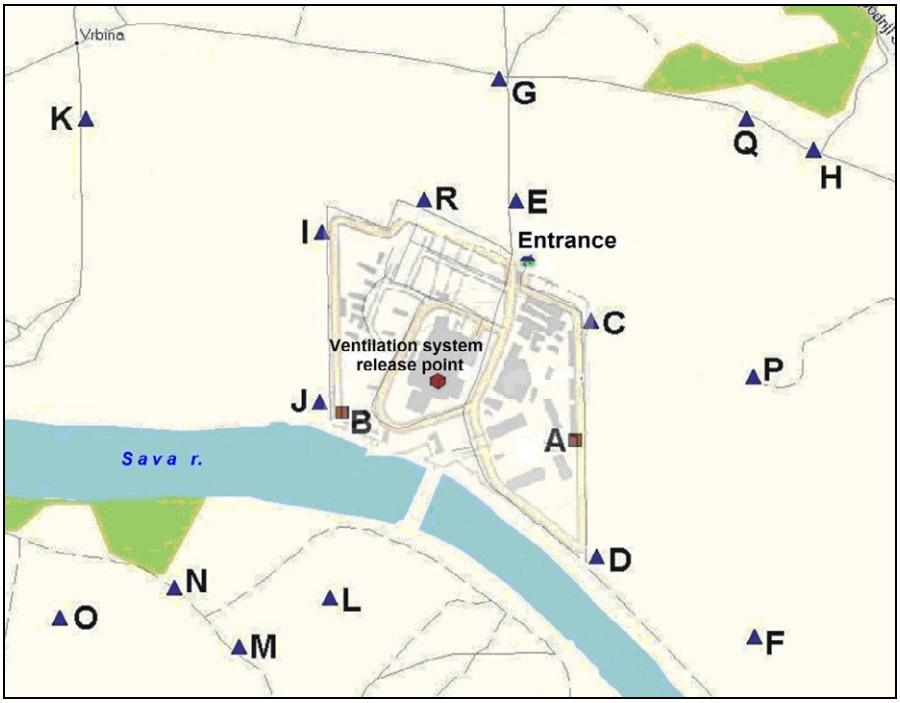


**Fig. 1. Sampling locations in the vicinity of Nuclear Power Plant Krško. Locations A and B for atmospheric $CO_2$. Locations C – R for biological samples.**

## Results

The results are usually expressed as the relative specific activity $a^{14}C$, defined as the ratio of the specific activity of the sample and that of the atmosphere undisturbed by anthropogenic influence, in "percent of Modern Carbon", or pMC. Consequently, relative specific activity of 100 pMC corresponds to specific activity of 226 Bq/kgC or to the $^{14}CO_2$ activity concentration of 0.037 Bq/m$^3$ of air.

### Activity in atmospheric $^{14}CO_2$

$^{14}C$ activity concentrations in the atmosphere at two locations (**A**, **B**) inside the NPPK are shown in Figure 2. For comparison, a part of long-term atmospheric $^{14}C$ data in the city of Zagreb is shown (Krajcar Bronić et al, 2009), as well as the integrated monthly $^{14}C$ activities released through the plant ventilation system. Atmospheric $^{14}C$ activity at the location **B** is always slightly higher than that at the location **A**. This difference can be explained by the position of location **B** relative to the release point and the local prevailing wind direction SW – NE (Fig. 3), and is particularly evident in the refuelling outage periods and immediately thereafter. The half-life of the released $^{14}C$ in the atmosphere is estimated to app. 1.5 months. During the refuelling in October 2007 higher a$^{14}C$ values at the site **B** were observed (102 mBq/m$^3$) than during the refuelling in April 2009 (69 mBq/m$^3$) probably due to the of shorter sampling period (ten days in 2007 in comparison to three weeks in 2008), which coincided better to the highest $^{14}C$ release to the atmosphere.

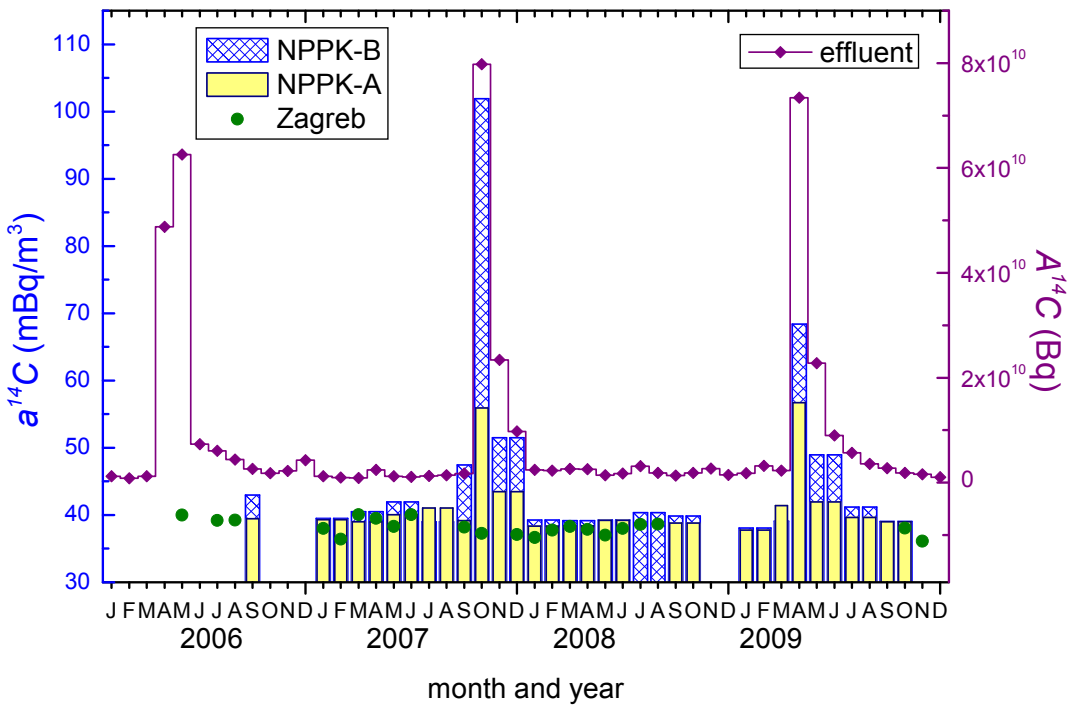


**Fig. 2. $^{14}C$ activity concentration in atmospheric $CO_2$ at locations A and B and comparison with the results obtained in Zagreb (40 km E) (left ordinate). Monthly $^{14}C$ activity in effluent released through the plant ventilation system (right ordinate).**

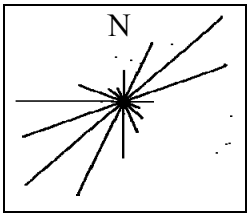


**Fig. 3. Wind rose in the vicinity of NPPK, measured on a 10 m high column (according to the Environmental Agency of the Republic of Slovenia)**

Mean values of $a^{14}C$ in atmospheric $CO_2$ in the years when the refuelling was performed (2007 and 2009) are 41.7 and 41.5 mBq/m$^3$ at the location **A**, and 47.9 and 44.2 mBq/m$^3$ at the location **B**. In 2008, when no refuelling was performed these values were 38.7 (location **A**) and 39.6 mBq/m$^3$ (location **B**). They represent a barely visible increase in relation to the activities of $^{14}C$ in the atmosphere measured in Zagreb (38.3 mBq/m$^3$ in 2007 and 37.8 mBq/m$^3$ in 2008), where the effect of reducing $^{14}C$ atmospheric activity is possible due to combustion of fossil fuels.

## Activity in biological samples

In Figure 4. we present the spatial distributions of measured $^{14}C$ activities (expressed as specific activities in pMC) for all eight sampling campaigns, as well as the corresponding polar diagrams that show the dependence on distance and orientation. In polar diagrams we have separated closer locations **C**, **D**, **E**, **I**, **J**, **L** and **R** (inner circle) and farther locations **F**, **G**, **H**, **K**, **M**, **N**, **O**, **P** and **Q** (outer circle), and have also shown $a^{14}C$ values at the control point Dobova. Increased activities were observed in all sampling campaigns in SW – NE direction of most pronounced winds. As expected, higher activities of $^{14}C$ were measured in biological material which used $CO_2$ in the refuelling outage period which was performed during and immediately after the vegetation period. In 2006 and 2009 the power plant was refuelled in spring period, so the apples, having their vegetation period immediately afterwards, collected more active $CO_2$. Therefore, at all locations the highest $^{14}C$ activity was in July 2006 and June 2009, since both campaigns were performed after the refuelling in April of the corresponding year. At the other hand, in 2007 the refuelling was in autumn after the apples were harvested, and the mean $^{14}C$ activities in both sampling periods in 2007 (July and September) were similar to the activity measured at the control point Dobova (Table 1).

Based on predetermined spatial distribution of $^{14}C$ activities in biological samples around the plant, it is clear that important results could be obtained only within a few hundred meters distance from the plant (Breznik et al, 2008). This close distance is not very convenient for testing the dispersion model but enabled to detect higher activities in a shorter time interval.

**Table 1. Mean values of $a^{14}C$ (pMC) in biological samples in all eight sampling campaigns. Inner circle – locations C, D, E, I, J, L and R. Outer circle – locations F, G, H, K, M, N, O, P and Q. * Measurements of samples from 9/2009 have not yet been completed.**

| Collection time | $a^{14}C$ (pMC) Inner circle | $a^{14}C$ (pMC) Outer circle | $a^{14}C$ (pMC) Control point |
|---|---|---|---|
| 07 / 2006 | 120.6 ± 11.0 | 108.3 ± 3.0 | 103.2 ± 1.5 |
| 10 / 2006 | 112.3 ± 12.0 | 105.1 ± 2.0 | 104.0 ± 1.5 |
| 07 / 2007 | 103.7 ± 3.9 | 103.7 ± 2.8 | 105.6 ± 1.9 |
| 09 / 2007 | 106.8 ± 1.7 | 105.7 ± 2.6 | 103.8 ± 1.8 |
| 07 / 2008 | 109.6 ± 3.5 | 107.3 ± 1.7 | 104.1 ± 2.3 |
| 10 / 2008 | 109.1 ± 3.3 | 109.1 ± 3.0 | 104.4 ± 2.7 |
| 06 / 2009 | 117.0 ± 11.2 | 110.5 ± 2.0 | 105.4 ± 1.4 |
| 09 / 2009 | 115.9 ± 11.4* | 103.2 ± 2.3* | 102.0 ± 1.4 |

## Discussion

Equivalent annual dose $E$ received by an average adult person by ingestion of food of specific $^{14}C$ activity $a^{14}C$ (Bq/kgC) can be estimated as

$$E = e \times a^{14}C \times m \times t$$

where $t$ is a 1-year period (365 days), $m$ is a mass of carbon ingested daily by food (0.3 kg, ICRP, 1996), $a^{14}C$ is measured $^{14}C$ specific activity (Bq/kg C), and $e$ is the ingestion dose coefficient for $^{14}C$, i.e., expected effective dose per unit $^{14}C$ activity, $5.8 \times 10^{-10}$ Sv/Bq (ICRP, 1996).

It is difficult to realistically estimate a possible increase of the annual dose in case of ingestion of fruit grown in the vicinity of NPPK. As we have shown here, there are spatial and temporal variations in $a^{14}C$. It is also difficult to estimate the fraction of total ingested food that originates from the close vicinity of NPPK. It is reasonable to assume that the local products are dispersed in the general food supply system, and not all consumed by local population. The simplest and the most conservative model of ingestion takes "the most exposed adult person" who would consume only apples from the close environment of NPPK throughout the year. In that case, and for the year 2006 (highest mean $^{14}C$ activity) the increase of the total annual dose is about 0.1%. Since this the most conservative estimate is unrealistic and not probable, we propose the following more realistic although still rather conservative model. We suppose that: i) in the daily consume of 0.3 kg of carbon, one half comes from the fruits; ii) 6 months the fruits from the environment of NPPK are not available, and during this period one can ingest only the food which has $a^{14}C$ as it is at the control site; iii) during the other 6 months, ⅓ of the total ingested carbon comes from fruits from any point of the monitored area around the NPPK, and the rest ⅔ come from the control site. Therefore, this model is equivalent to the assumption of ingestion of the apples from the vicinity of the power plant during 1 month in a year, while during the rest of the year carbon comes from the wider area. Taking into account these assumptions, we can calculate the increase of the equivalent $^{14}C$ dose relative to the natural $^{14}C$ dose measured at the control point, as well as relative to the total natural dose in our country (1.22 mSv). The results for each year since 2006 are shown in Table 2.

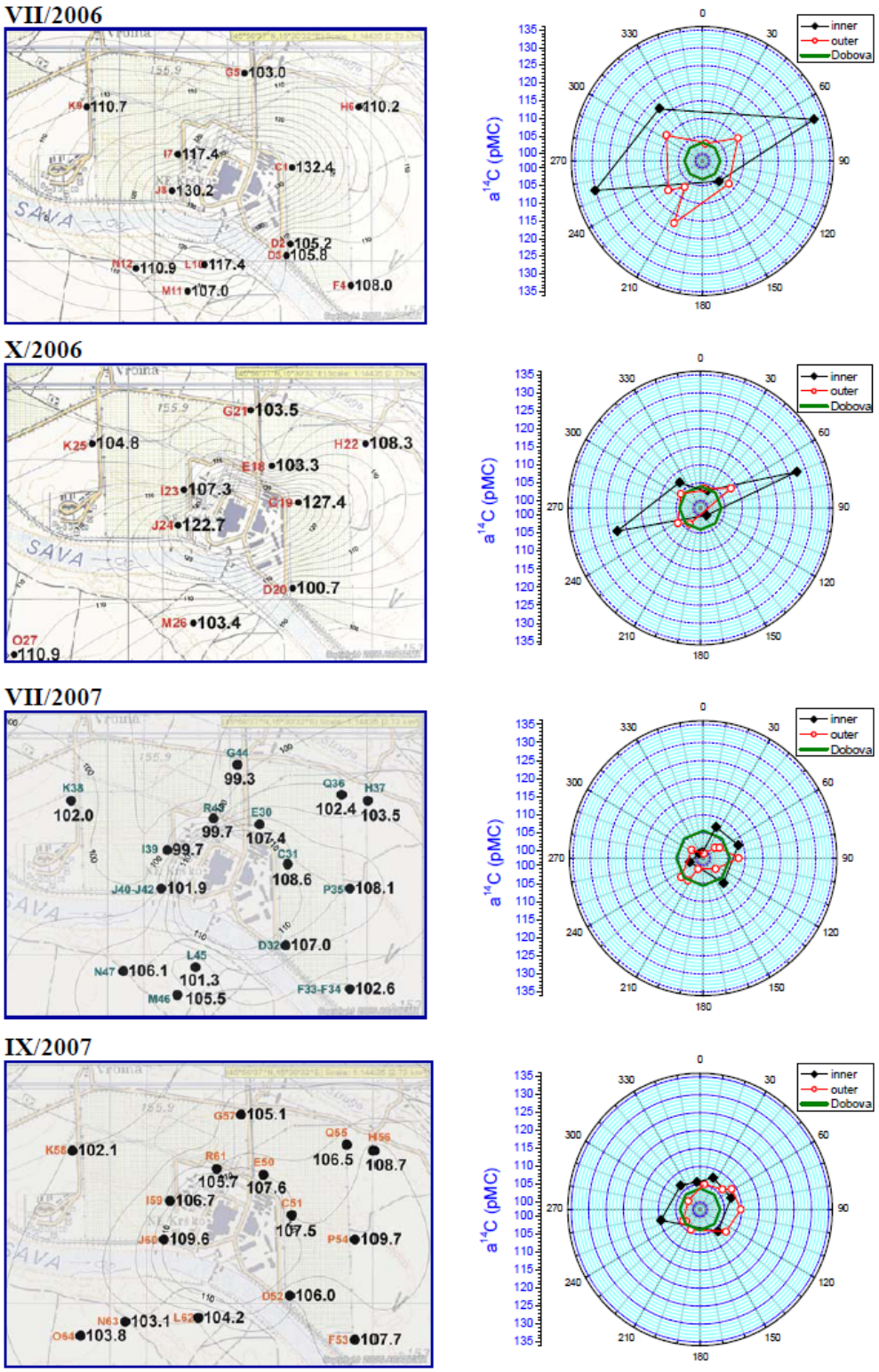


**Figure 4. Spatial distribution and polar diagrams of relative specific $^{14}C$ activity (expressed in pMC).**

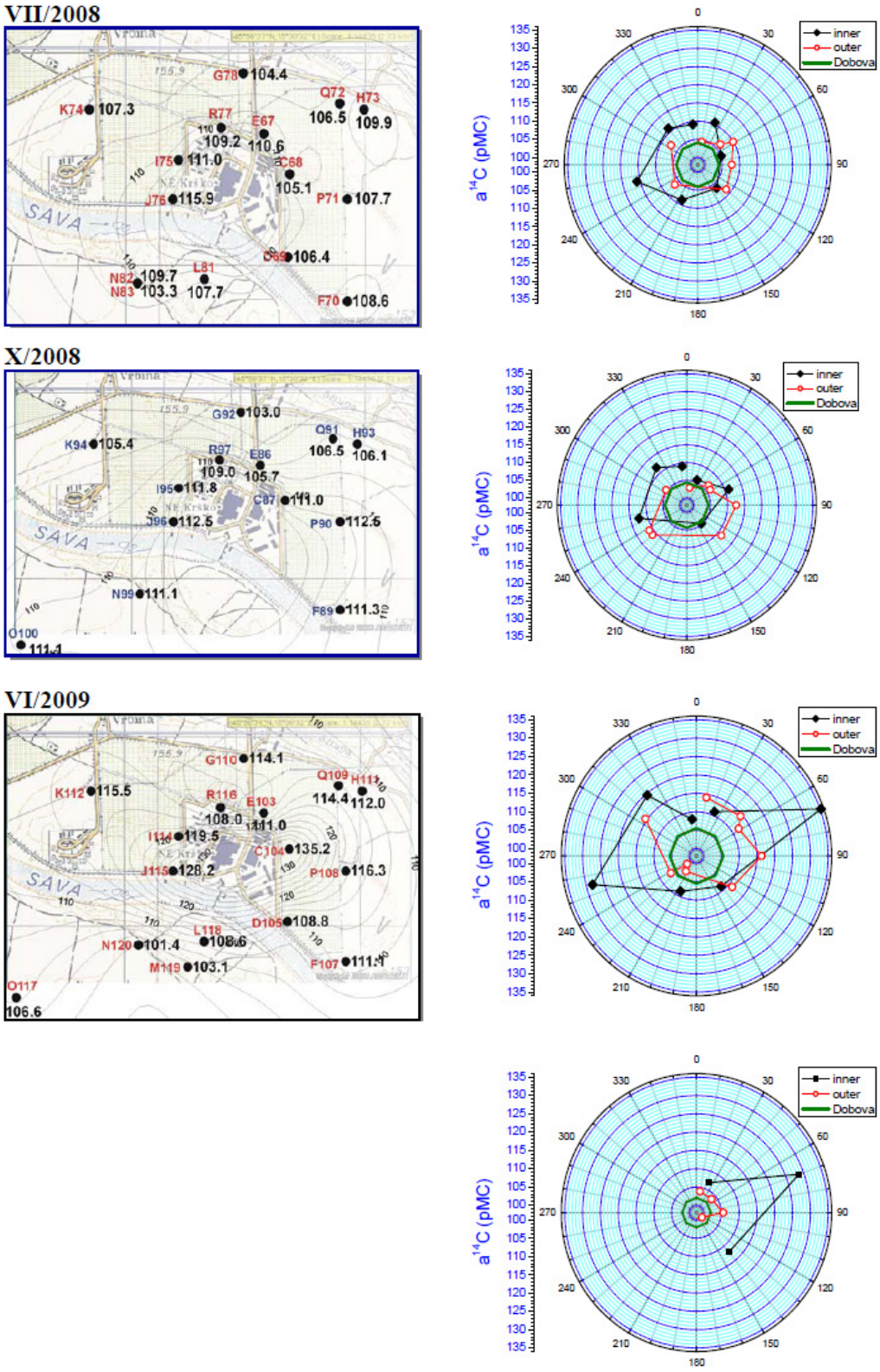


**Figure 4 continued. Spatial distribution and polar diagrams of relative specific $^{14}C$ activity (expressed in pMC). Data for the sampling campaign in September 2009 not yet completed.**

**Table 2. Increase of equivalent $^{14}C$ dose relative to the natural $^{14}C$ dose measured at control point, as well as well as the increase relative to the total natural dose in our country (1.22 mSv).**

| Year | $a^{14}C$ [pMC] NPPK * | $a^{14}C$ [pMC] Dobova | $^{14}C$ dose [µSv] NPPK | $^{14}C$ dose [µSv] Dobova | Increase of $^{14}C$ dose (%) | Increase of total dose (%) |
|---|---|---|---|---|---|---|
| 2006 | 111.6 | 103.5 | 14.95 | 14.86 | 0.65 | 0.0079 |
| 2007 | 105.0 | 104.7 | 15.03 | 15.03 | 0.02 | 0.0003 |
| 2008 | 108.8 | 104.3 | 15.02 | 14.97 | 0.35 | 0.0044 |
| 2009 | 110** | 103.8 | 14.97 | 14.89 | 0.50 | 0.0061 |

* mean value of $^{14}C$ activity in inner and outer circle of NPPK
** data for September 2009 not yet complete

## Conclusion

Monitoring of $a^{14}C$ in biological samples in immediate vicinity and wider environment of the Nuclear Power Plant Krško in Slovenia resulted in spatial distribution of $a^{14}C$ that is clearly determined by the dominant wind directions (SW – NE) and influenced by the outflow of $^{14}C$ from the release point of the plant ventilation system. The difference to the natural present-day $a^{14}C$ is determined relative to the control site Dobova, about 10 km SE from NPPK. At most sites the difference ranges from 0 to several pMC, being the highest 29 pMC at site **J** in July 2006. However, these differences do not affect significantly the total annual dose due to natural radiation sources, according to our model of ingestion.

## Acknowledgments

The presented work was performed within the project 098-0982709-2741 and the project with NPP Krško. We are grateful to A. Volčanšek and V. Bostič (NPPK) for help during sampling and A. Rajtarić for sample preparation.

## References

Breznik B, Volčanšek A, Božnar M Z, Mlakar P, Krajcar Bronić I, Obelić B. Verification of the dispersion model by airborne carbon $^{14}C$. Proceedings of the 12th IRPA Congress, 2008 Oct 19-24; Buenos Aires, Argentina. (CD-ROM).

Horvatinčić N, Barešić J, Krajcar Bronić I, Obelić B. Measurements of low $^{14}C$ activities in a liquid scintillation counter in the Zagreb Radiocarbon Laboratory. Radiocarbon (2004); 46/1: 105-116.

International Commission on Radiological Protection. Age-dependent doses to members of the general public from intake of radionuclides: Part 5 Compilation of ingestion and inhalation dose coefficients. Ann. ICRP 1996; 26 (1): 1-91.

Krajcar Bronić I, Horvatinčić N, Barešić J, Obelić B. Measurement of $^{14}C$ activity by liquid scintillation counter. Applied Radiation and Isotopes 2009; 67: 800-804.

# Uranium and long-lived decay products in water of the Mulde River

Bister, Stefan[1]; Koenn, Florian[2]; Bunka, Maruta[1]; Birkhan, Jonny[1]; Lüllau, Torben[1]; Riebe, Beate[1]; Michel, Rolf[1]

[1] Institut für Radioökologie und Strahlenschutz, Leibniz Universität Hannover, GERMANY

[2] Fachbereich Chemie und Biotechnologie, Campus Jülich, Fachhochschule Aachen, GERMANY

## Abstract

The Mulde River is a left side tributary of the Elbe River and mainly situated in Saxony. The river system consists of the Freiberger Mulde River and Zwickauer Mulde River, which merge to form the Vereinigte Mulde River. The Zwickauer Mulde River drains the former uranium mining and milling areas in Saxony. This research project was established to quantify the long-term effect of the former uranium mining and milling activities by investigating the content of uranium and polonium of the water of the Mulde River. The specific uranium activity in samples from the Zwickauer Mulde River is still high compared with the natural background. The values measured in the water of the Vereinigte Mulde River are also elevated, but to a lesser extent due to the dilution effect caused by the merging with the Freiberger Mulde River. Furthermore, the level of contamination of the river water decreased by at least a factor of three as compared to the early 1990's. The specific activity of polonium shows no correlation with that of uranium and is generally much smaller.

## Introduction

At the time of the Warsaw Pact, the former German Democratic Republic (GDR), was the third largest producer of uranium in the world and the most important supplier of uranium for the USSR. The Zwickauer Mulde River in Saxony and the Weiße Elster River in Thuringia are the most important river systems draining the uranium mining and milling dominated areas of the western Ore Mountains and its foreland, resulting in accordingly high heavy metal loads. Thus they are of particular interest for radiation protection and radioecology. Today this area is subject to a remediation project which, due to its large scale, can be characterized as pioneer work.

The Mulde River is a left side tributary of the Elbe River and mainly situated in Saxony. The river system consists of three main rivers: Zwickauer Mulde, Freiberger Mulde and Vereinigte Mulde. The Muldenberg Reservoir in the western Ore Mountains is deemed to be the source of the Zwickauer Mulde River. Four kilometers downstream of the dam, which is used as a drinking water reservoir, the river already receives contaminated water from the mine Schneckenstein. On its way through the Ore Mountains the river flows through the uranium mining area Aue and Bad Schlema. Downriver of Zwickau the Zwickauer Mulde River passes Crossen and its uranium ore

processing plants and merges with the Freiberger Mulde River at river kilometer 162. The source of the Freiberger Mulde River is located in the Czech Republic, about 5 km from the German border on the ridge of the eastern Ore Mountains. It drains mining areas, however there is no uranium mining in its catchments area. The Vereinigte Mulde River, which is often simply called Mulde River, originates from the merging of the two frontal flows Freiberger Mulde and Zwickauer Mulde and disembogues into the Elbe River north of Dessau at river kilometer 124. At high water-levels the Mulde River is deemed to be the fastest flowing river in Central Europe. Due to its origin in a high-mineral and high-ore affected area it is the most significant reason for heavy metal entering into the Elbe River and thus into the North Sea.

This research project was established to quantify the long-term effect of the former uranium mining and milling activities by investigating the content of uranium and polonium of the water of the Mulde River. It is part of a work package dealing with transport and availability of uranium and its decay products in the Mulde floodplains, which in turn is part of a joint project on radionuclides in the environment and their transport to man via food chains, supported by the German Federal Ministry for Education and Research (BMBF).

## Sampling and analysis

A total of 26 water-samples were collected in April, May and October 2008. 19 samples were collected along the course of the Zwickauer Mulde River and the Vereinigte Mulde River. Water from the Freiberger Mulde River, the headwaters of the Zwickauer Mulde River, a small influent of the Zwickauer Mulde River, and from the Leine River near Hanover, respectively, were used as reference samples. Figure 1 shows the Mulde system and the sampling locations.

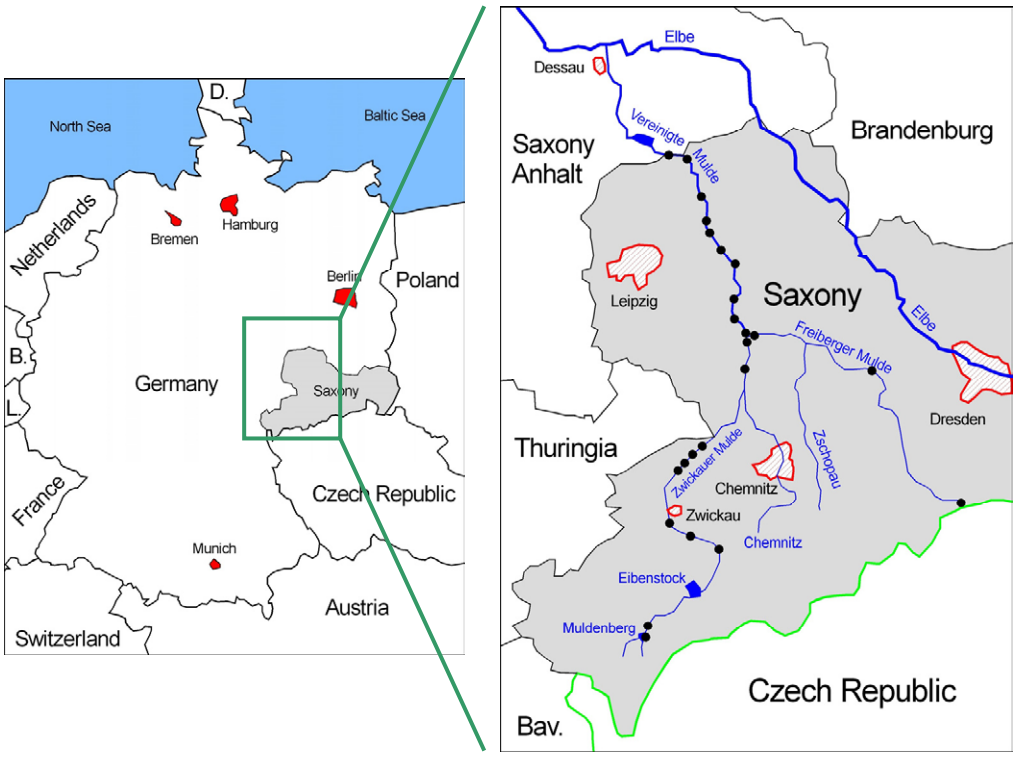


**Fig. 1. The Mulde River system with the sampling locations.**

Generally, four litres of water were collected at each sampling location. In four cases only two litres per sample were taken. The water was filtered on-site using folded filters of a pore size of 7 µm. Subsequently the samples were acidulated with nitric acid to a pH of 1.5 to 2 and stored on ice.

In the laboratory the samples were filtered through cellulose nitrate filters of a pore size of 0.45 µm. As a central step an enrichment of radionuclides via iron hydroxide-coprecipitation was performed. Following this polonium and uranium were separated by solid-phase chromatography using Pb-Resin and UTEVA from Eichrom, respectively. The polonium sample was obtained by means of autodeposition on nickel. The corresponding uranium sample was prepared using electrical deposition on stainless steel. Both samples were measured alpha-spectrometrically by a surface barrier detector. Figure 2 gives an overview of the analytical procedure.

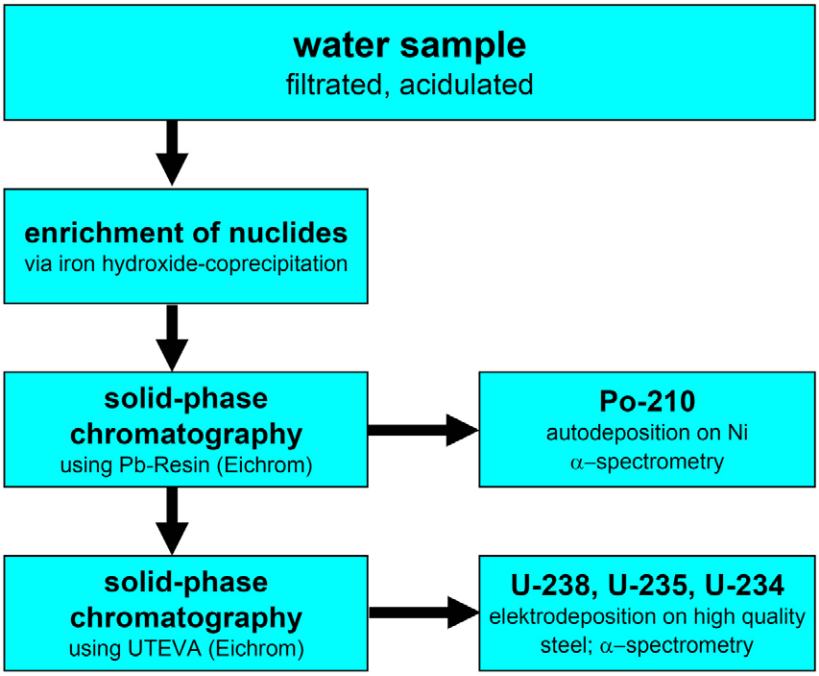


**Fig. 2. Overview of the analytical procedure.**

## Results

Table 1 summarises the measured specific activities of uranium and polonium. The samples are numbered consecutively in flow direction, in which the two letters denote the origin of the sample (”FM“ = Freiberger Mulde River, ”ZM“ = Zwickauer Mulde River, ”VM“ = Vereinigte Mulde River).

Figure 3 shows the variation of the specific activities of uranium and polonium along the course of the Mulde River. Additionally, the arithmetic mean of five polonium blanks and the upper 1σ-interval are plotted. The blank value determination was performed for the overall procedure using ultra-pure water (18.2 MΩ*cm). Determination of five blanks results in an arithmetic mean of 1.75 mBq/kg with a 1σ-interval ranging from 0.26 mBq/kg to 3.24 mBq/kg. The determination of uranium blanks results in a value close to the detection limit.

**Table 1. Specific activities (*a*) and related uncertainties (u(*a*)) for uranium and polonium in the water of the Mulde River; red values marked with ”<“ lie below detection limit.**

| | | U-238 (mBq/kg) | | U-234 (mBq/kg) | | U-235 (mBq/kg) | | Po-210 (mBq/kg) | |
|---|---|---|---|---|---|---|---|---|---|
| | | *a* | u (*a*) | *a* | u (*a*) | *a* | u (*a*) | *a* | u (*a*) |
| 1 | Leine | 13.4 | 1.3 | 26.3 | 2.4 | 0.6 | 0.2 | 4.3 | 0.9 |
| 2 | Bach | 8.4 | 1.0 | 11.8 | 1.3 | < 0.7 | --- | 3.6 | 0.5 |
| 3 | FM1 | 2.6 | 0.3 | 2.7 | 0.3 | 0.2 | 0.1 | 3.0 | 0.3 |
| 4 | FM2 | 2.0 | 0.2 | 2.2 | 0.3 | < 0.1 | --- | 2.8 | 0.6 |
| 5 | FM3 | 12.2 | 1.2 | 16.6 | 1.6 | 0.8 | 0.2 | 1.1 | 0.3 |
| 6 | ZM1 | 2.0 | 0.2 | 3.4 | 0.4 | 0.5 | 0.1 | < 5.0 | --- |
| 7 | ZM2 | 3.0 | 0.4 | 3.5 | 0.5 | < 0.3 | --- | 3.7 | 1.9 |
| 8 | ZM3 | 73.9 | 7.5 | 74.0 | 7.5 | 2.0 | 0.7 | 10.7 | 2.5 |
| 9 | ZM4 | 69.3 | 7.1 | 64.1 | 6.6 | < 1.9 | --- | 13.2 | 3.1 |
| 10 | ZM5 | 63.5 | 6.4 | 68.5 | 6.8 | 1.9 | 0.6 | 3.8 | 0.8 |
| 11 | ZM6 | 79.0 | 6.8 | 84.2 | 7.2 | 2.9 | 0.4 | 10.9 | 1.1 |
| 12 | ZM7 | 85.9 | 8.1 | 86.6 | 8.2 | 3.5 | 0.7 | 2.8 | 0.3 |
| 13 | ZM8 | 83.7 | 7.7 | 95.2 | 8.6 | 4.4 | 0.7 | 4.2 | 0.4 |
| 14 | ZM9 | 82.4 | 7.8 | 87.7 | 8.3 | 3.5 | 0.6 | 4.9 | 0.9 |
| 15 | ZM10 | 69.5 | 5.8 | 80.0 | 6.7 | 4.9 | 0.4 | 4.2 | 0.4 |
| 16 | ZM11 | 74.0 | 6.6 | 78.9 | 7.0 | 3.4 | 0.5 | 2.6 | 0.4 |
| 17 | VM1 | 74.4 | 6.9 | 81.4 | 7.6 | 3.0 | 0.5 | 3.5 | 0.5 |
| 18 | VM2 | 25.2 | 2.6 | 31.6 | 3.2 | 0.6 | 0.3 | 2.6 | 0.5 |
| 19 | VM3 | 38.6 | 3.3 | 46.0 | 3.9 | 1.8 | 0.2 | 2.1 | 0.4 |
| 20 | VM4 | 30.9 | 3.1 | 40.0 | 3.9 | 1.0 | 0.3 | 3.5 | 0.4 |
| 21 | VM5 | 30.8 | 1.4 | 38.6 | 1.7 | 1.3 | 0.3 | 7.3 | 0.6 |
| 22 | VM6 | 33.4 | 1.5 | 34.1 | 1.6 | 1.0 | 0.2 | 3.8 | 0.5 |
| 23 | VM7 | 30.8 | 2.6 | 36.9 | 3.1 | 1.7 | 0.2 | 11.0 | 0.8 |
| 24 | VM8 | 32.4 | 3.1 | 36.8 | 3.4 | 1.3 | 0.3 | 4.8 | 1.1 |
| 25 | VM9 | 30.9 | 2.9 | 36.4 | 3.4 | 1.0 | 0.2 | 2.3 | 0.4 |
| 26 | VM10 | 30.1 | 3.2 | 34.2 | 3.6 | 0.9 | 0.3 | 3.1 | 0.4 |

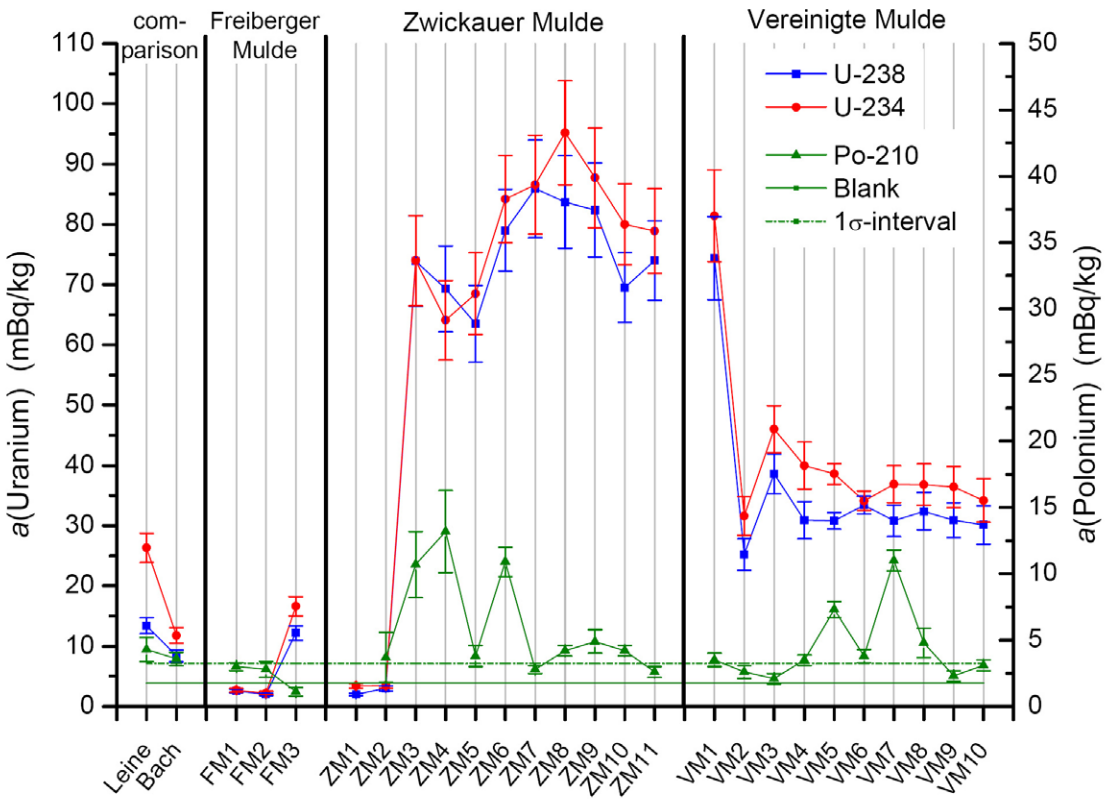


**Fig. 3. Variation of the specific activities of uranium-238, uranium-234 and polonium-210, respectively, along course of the the Mulde River; additionally, the arithmetic mean of five polonium blanks and the upper 1σ-interval is plotted.**

## Discussion

### Uranium

The measured values of the uranium isotopes (U-238, U-234 and U-235) exhibit the composition of natural uranium in almost all of the samples. This is in accordance with the expectation, as isotopic enrichment of uranium was no common practice in Germany.

The values can be divided roughly into three groups (see Fig. 3). The first group represents the reference values, which belong to non-affected areas with regard to uranium mining and milling activities. This includes the samples from the Freiberger Mulde River (FM1, FM2), from the small influent of the Zwickauer Mulde River (Bach) and the Leine River (Leine), as well as the samples ZM1 and ZM2 from the headwaters of the Zwickauer Mulde River. The first contaminated water from the mine Schneckenstein receives the River about 4 km downriver of the dam of the Muldenberg reservoir, which is regarded as the source of the river, and a few hundred meters downriver of the sampling location of ZM2 (see Fig. 4), respectively. The mean specific activity of uranium-238 for the reference samples is 6.2 mBq/kg, which represents a typical background value for unaffected surface water. The second group of values can be attributed to the Zwickauer Mulde River (ZM3 to VM1) – with a mean value of 75.5 mBq/kg for uranium-238. The third group consists of samples from the Vereinigte Mulde River (VM2 to VM10), showing a mean value of 31.5 mBq/kg. The VM1 sample was collected about 400 meters downriver of the rivers' confluence, more

precisely, at the side, where the Zwickauer Mulde River flows in. It can be assumed that at this particular point no considerable mixing of the rivers has taken place.
Along the Zwickauer Mulde River significant variations of the uranium activities can be detected. Hence, Fig. 4 shows the variation of the specific activities of uranium-238 plotted against the river kilometers of the Zwickauer Mulde River extending to a point 15 km downstream of the confluence with the Freiberger Mulde River. Additionally, values from the years 1991 to 1993, determined by Beuge et al. [1], are depicted in order to allow a comparison. The numerical values are listed in Table 2. The determination of the uranium concentration by Beuge et al. [1] was performed employing total-reflection X-ray fluorescence analysis (TXRFA). The results are given as mass concentration in µg/L. The conversion to specific activity of uranium-238 in mBq/kg was performed assuming a density of 1 g/mL. Measurements of samples collected along the Freiberger Mulde River and the Vereinigte Mulde River yielded values, which rarely exceeded the detection limit of TXRFA at ~ 60 mBq/kg (5 µg/L). Thus, they are not considered here.

**Table 2. Comparative values determined by Beuge et al. [1]; samling locations are specified by the corresponding river kilometers; uranium concentration is given as mass concentration (*β*) and as specific activity (*a*) of uranium-238, respectively.**

| sampling location | river kilometer | *β* (U) (µg/L) | *a* (U-238) (mBq/kg) |
|---|---|---|---|
| weir Hartenstein | 55 | 27 | 335 |
| short before Crossen | 80 | 16 | 198 |
| near Glauchau | 94 | 23 | 285 |
| near Sermuth | 161 | 14 | 174 |

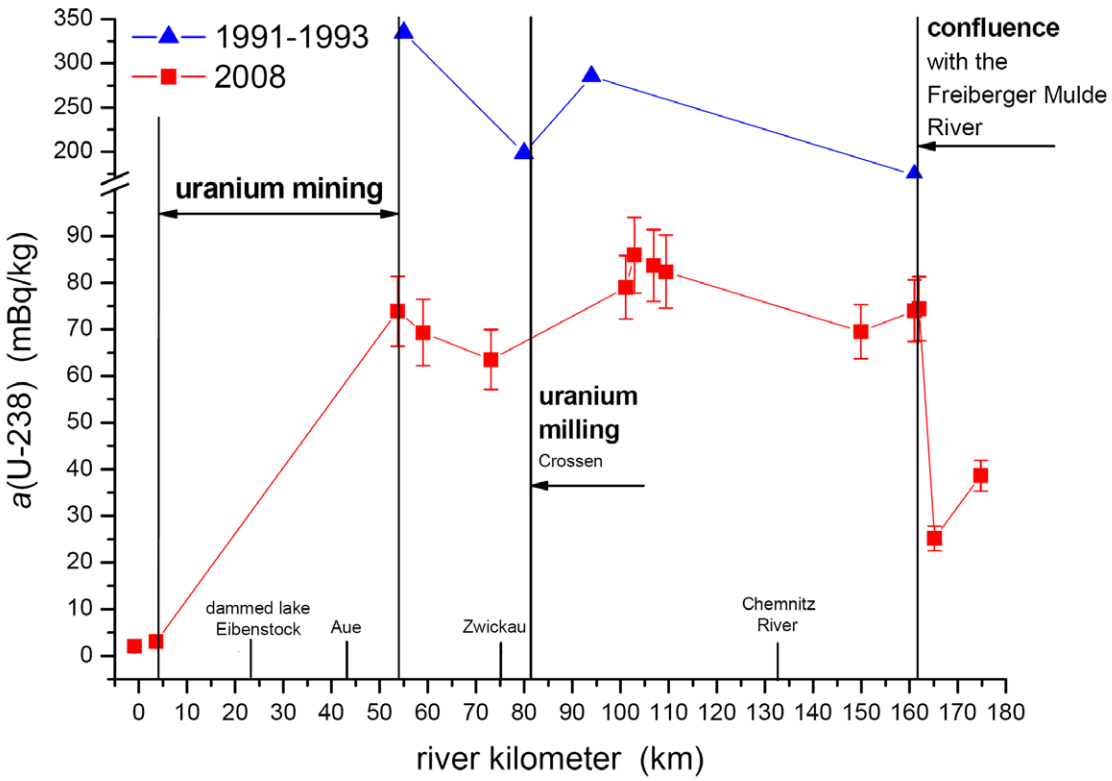


**Fig. 4. Variation of the specific activities of uranium-238 in water of the Mulde River, plotted against the river kilometers; comparative values for the years 1991 to 1993 adapted from Beuge et al. [1]**

As mentioned before, the first two samples taken from the source of the Zwickauer Mulde River represent the natural background of uranium. The next sample (ZM3) was collected at Hartenstein, where the river has already passed the uranium mining area around Aue and Bad Schlema. According to this position, the sample shows a high uranium activity. Following the course of the river to Zwickau (ZM5), the specific activities seem to decrease slightly. This effect can be explained by dilution with less contaminated water from tributaries. Downstream of Zwickau the specific activity of uranium in the water increases again. This increase results from the effluents of the uranium milling industry near Crossen. In the further course of the Zwickauer Mulde River, the activity remains approximately constant until the confluence with the Freiberger Mulde River. Due to measurement uncertainties, the values are in agreement with a slight decrease of the specific activity corresponding to dilution effects caused by tributaries, especially the Chemnitz River, largest tributary of the Zwickauer Mulde River. In contrast, the confluence of the Zwickauer Mulde River with the uncontaminated Freiberger Mulde River reveals a clear dilution effect, and correspondingly a significant decrease of the specific uranium activity.

The measurements from the early 1990's show the same characteristics, but at a much higher (activity) level. During the last twenty years, the contamination of the Mulde River decreased considerably, on average by a factor of 3.4. This effect decreases in the course of the Zwickauer Mulde River. At the upper reaches of the river, at Hartenstein, the difference between the values measured in 2008 (73.9 mBq/kg) and

in the 1990's (335 mBq/kg) is considerably high, resulting in a decrease by a factor of 4.5. At Sermuth, which is located close to the confluence of the Freiberger Mulde River, the difference between the current value (74 mBq/kg) and the one from the 1990's (174 mBq/kg), yield a decrease by a factor of 2.3. This indicates that the decrease of the contamination mainly results from the decreasing emission of the uranium mining and milling industry and accordingly can be attributed to the remediation activities.

The specific uranium activity remains constant along the Vereingte Mulde River, showing an arithmetic mean of 31.5 mBq/kg. The variations of the first three measured values show a correlation between the side of the river on which these samples were taken and the confluence of the Zwickauer and Freiberger Mulde River. This has already been explained in the case of sample VM1. For the samples VM2 and VM3 an incomplete mixing of the water of the two rivers can be assumed as well. The sample VM2 was taken on the right-hand side in flow direction, and thus a stronger influence of the Freiberger Mulde River can be assumed. In contrast, the samples VM3 and VM1 were taken on the left-hand side, which causes a stronger influence of the Zwickauer Mulde River. At the same time the convergence towards the mean value shows the progressive mixing of the water. A decrease of the uranium activity along the Vereinigte Mulde River due to the dilution by smaller tributaries cannot be observed, because the influence of the tributaries decreases with enlarging of the river.

### Polonium

The specific activities of polonium-210 are much lower than those of uranium. A large number of the measured values are well below 5 mBq/kg, and thus those data are relatively difficult to distinguish from the background. There is no apparent correlation with the specific activities of uranium. The low specific activities of polonium in the water can be explained by its very strong affinity to adsorption. Due to the strong adsorption to sediments the variations of the polonium activities are expected to change within a short distance. Only five samples exhibit specific activities above 5 mBq/kg. The samples ZM3 and ZM4 are the first two samples after the Zwickauer Mulde River passed the uranium mining region of the Ore Mountains. Consequently, the river water shows higher values for the polonium activities than the uncontaminated headwaters. The high activities of the other samples cannot be explained yet.

### *Radioecological relevance*

The uranium and polonium concentrations found in river water are insignificant from the radioecologically point of view. The recommended value for uranium in drinking water given by the Federal Environment Agency (UBA) is < 10 µg/L [2]. This corresponds to a specific uranium-238 activity of 123.5 mBq/kg. None of the samples shows a uranium activity exceeding this value. In its recommendation from 2001 the EURATOM states 0.1 Bq/kg as maximum specific activity for polonium in drinking water [3]. Again, none of the analysed samples reaches such a high polonium activity.

## Conclusions

During the last 20 years, the contamination of the Mulde River decreased by at least a factor of three. This effect mainly results from the decreasing emission of the uranium mining and milling industry and accordingly can be attributed to the remediation activities. On the other hand, an influence of the former uranium mining and milling activities can still be detected. The specific uranium activity in samples from the Zwickauer Mulde River is still high compared with the natural background. The values measured in the water of the Vereinigte Mulde River are also elevated, but to a lesser extent due to the dilution effect caused by the merging with the non-affected Freiberger Mulde River. The specific activity of polonium shows no correlation with that of uranium and is generally much smaller.

## References

[1] Beuge P. et al., Die Schwermetallsituation im Muldesystem – Abschlussbericht an das BMBF. Bände I-III, ISBN 3-924330-28-X, in self-publishing of University Hamburg, 1999

[2] Dieter H. H., Schulz C., Telegramm: Umwelt + Gesundheit, Information des Umweltbundesamtes, issue 03/2008 from 18 August 2008

[3] Empfehlung 2001/928/Euratom der Kommission vom 20. Dezember 2001 über den Schutz der Öffentlichkeit vor der Exposition gegenüber Radon im Trinkwasser, published under reference number K(2001) 4580; ABl. Nr. L 344 from 28 Dezember 2001, page 85

# $^{129}$I in Finnish waters

Räty, Tero[1]; Lehto, Jukka[1]; Hou, Xiaolin[2]; Possnert, Göran[3];
Paatero, Jussi[4]; Flinkman, Juha[5]; Kankaanpää, Harri[5]
[1] University of Helsinki, Laboratory of Radiochemistry, FINLAND
[2] Technical University of Denmark, DENMARK
[3] University of Uppsala, SWEDEN
[4] Finnish Meteorological Institute, FINLAND
[5] Finnish Environment Institute, FINLAND

## Abstract

$^{129}$I is a long-lived beta-emitting ($E_{max}$ 154,4 keV) radioisotope of iodine. Its half-life is 15,7 million years. $^{129}$I is produced mainly by human nuclear activities and especially it has been released to the environment from the spent nuclear fuel reprocessing plants. In the pre-nuclear era $^{129}$I/$^{127}$I ratios in the environment were approximately $10^{-12}$. Nowadays $^{129}$I/$^{127}$I ratios have reached values from $10^{-10}$ to $10^{-4}$.

In this study, activity concentrations of $^{129}$I and its distribution into various chemical species (iodide I-, iodate IO3- and bound in organics) were analyzed from four lakes in Finland and from four different sea locations on the Gulf of Finland, the Bothnian Sea and the Bothnian Bay. $^{129}$I was also analyzed from four rainwater samples.

After filtering the 0.3 l water samples, separation of various iodine species was done by anion exchange chromatography: $^{129}IO_3^-$ passes through an anion exchange resin bed in $NO_3^-$ form while $^{129}I^-$ absorbs into the bed. $^{129}I^-$ is eluted from resin with NaClO. Finally samples were precipitated by $AgNO_3$ to form AgI and $^{129}$I was measured by accelerator mass spectrometry (AMS). Stable iodine ($^{127}$I) was analyzed by inductively coupled plasma mass spectrometry (ICP-MS).

First results from a lake in the southern Finland and from sea water taken from the Finnish Bay in front of Helsinki show that levels of $^{129}$I in lake water are around $1 \times 10^9$ atoms per litre while in sea water the levels are 4 – 5 times higher. $^{129}$I occurs both in lake and sea water mainly in iodide form and the fraction of iodate form is only about 5%. The $^{129}$I/$^{127}$I ratio is clearly elevated compared to natural levels, and are approximately the same in sea and in lake, $14 \times 10^{-8}$ and $8 \times 10^{-8}$, respectively. These results are only preliminary and a better picture of the situation will be obtained after finalizing the project. The results obtained so far are, however, at the same level as obtained in Swedish studies at the same latitudes.

# Monitoring and assessment of radioactivity in the Baltic Sea coordinated by HELCOM

Nielsen, Sven P.[1]; Ikäheimonen, Tarja K.[2]; Outola, Iisa[2]; Vartti, Vesa-Pekka[2]; Herrmann, Jürgen[3]; Kanisch, Günter[4]; Suplinska, Maria[5]; Zalewska, Tamara[6]; Vilimaite-Silobritiene, Beata[7]; Stepanov, Andrey[8]; Osokina, Anna[8]; Lüning, Maria[9]; Osvath, Iolanda[10]; Jakobson, Eia[11]

[1] Technical University of Denmark, Risø DTU, DENMARK
[2] STUK – Radiation and Nuclear Safety Authority, FINLAND
[3] Federal Maritime and Hydrographic Agency, Marine Chemistry, GERMANY
[4] Johann Heinrich von Thünen-Institute, Institute of Fishery Ecology, GERMANY
[5] Central Laboratory for Radiological Protection, POLAND
[6] Institute of Meteorology and Water Management, Maritime Branch, POLAND
[7] Environmental Protection Agency, Environmental Research Dept., Radiology Divis, LITHUANIA
[8] V.G. Khlopin Radium Institute, RUSSIAN FEDERATION
[9] Swedish Radiation Safety Authority, SWEDEN
[10] IAEA, Marine Environment Laboratories, MONACO
[11] Environmental Board, Radiation Safety Department, ESTONIA

## Abstract

The Baltic Marine Environment Protection Commission (HELCOM) works to protect the marine environment of the Baltic Sea from all sources of pollution through intergovernmental co-operation between Denmark, Estonia, the European Community, Finland, Germany, Latvia, Lithuania, Poland, Russia and Sweden. Investigations of radioactivity in the Baltic Sea has been part of the HELCOM work since 1986 and carried out by the MORS project (Monitoring of Radioactive Substances) with participation from laboratories and institutes in the countries and organizations mentioned above including the IAEA.

The objective of the MORS project is to implement the Helsinki Convention on matters related to monitoring and assessment of radioactivity in the Baltic Sea. The Contracting Parties to the Convention carry out basic monitoring programmes and transfer the data to the HELCOM database. The monitoring is carried out according to guidelines which are revised annually. The guidelines give details on sampling locations, sample types covering seawater, sediment, fish, aquatic plants and benthic animals, and radionuclides to be determined in the samples. The guidelines furthermore specify the format for reporting the data to the database. High quality of the data is ensured through participation of the MORS laboratories in frequent group intercomparisons of analytical data from laboratory analyses as well as from evaluation

of the reported data at the annual meetings of the MORS group. Intercomparisons cover laboratory analyses of radioactivity in seawater, sediment and biota.

The data collected is summarized in indicator fact sheets that present results of radioactivity in seawater and fish from the Baltic Sea. More comprehensive assessments of radioactivity in the Baltic Sea are made by the group at larger intervals. The assessments include summaries of sources and inputs of radioactivity into the Baltic Sea, environmental levels and model-assisted estimates of radiation doses to man.

# Results obtained in monitoring programmes and environmental studies carried out during more than 40 years in the sea areas surrounding the Finnish NPPs

Ilus, Erkki
STUK – Radiation and Nuclear Safety Authority, FINLAND

## Abstract

Environmental effects of thermal and radioactive discharges from the Loviisa and Olkiluoto NPPs in the recipient sea areas were assessed. The effects of cooling water on the temperatures in the sea were most obvious in winter. The formation of a permanent ice cover has been delayed, and the break-up of the ice has been advanced. The prolonging of the growing season has been the most significant biological effects of thermal pollution. At Loviisa, the thermal discharges have increased the production of organic matter in the discharge areas, which has led to more organic bottom deposits. The depletion of oxygen has caused remobilization of phosphorus from the bottom sediments, and contributed to deterioration of benthic macrofauna. Phytoplankton primary production has doubled in the area, and the thermal discharge has contributed to a stronger increase in the discharge area than in the intake area. The eutrophication of littoral vegetation has been the most obvious and unambiguous biological effect of the heated water in both areas.

Small amounts of local discharge nuclides were regularly detected in environmental samples taken from the discharge areas: tritium in seawater, and activation products in suspended particulate matter, bottom sediments and in indicator organisms. Discharge nuclides from the local nuclear power plants were almost exclusively detected at the lower trophic levels of the ecosystem. The concentrations of local discharge nuclides in the environmental samples have noticeably decreased in both areas in recent years. The radiation doses caused by the radioactive discharges to the population and to the biota were very low, practically insignificant. The effects of the thermal discharges were more significant, at least to the wildlife in the discharge areas of the cooling water, although the area of impact has been relatively small. The results show that the nutrient level and the exchange of water in the discharge area of a nuclear power plant are of crucial importance.

## Introduction

During recent decades, thermal and radioactive discharges from nuclear power plants into the aquatic environment have become the subject of lively debate as an ecological concern. Recently, an increasing demand for facts has appeared in context with the Environmental Impact Assessment procedures that are being in progress for planned new nuclear power units in Finland. This paper is based on a thesis examined in University of Helsinki in September 2009 (Ilus 2009). The target of the thesis was to summarize the large quantity of results obtained in extensive monitoring programmes and studies carried out in recipient sea areas off the Finnish nuclear power plants at Loviisa and Olkiluoto during more than four decades.

Especially in the conditions specific for the northern Baltic Sea, where biota is poor and adapted to relatively low temperatures and to seasonal variation with a cold ice winter and a temperate summer, an increase in temperature may cause increased environmental stress to the organisms. Furthermore, owing to the brackish-water character of the Baltic Sea, many organisms live there near the limit of their physiological tolerance. On the other hand, the low salinity increases the uptake of certain radionuclides by many organisms in comparison with oceanic conditions.

The sea areas surrounding the Finnish nuclear power plants differ from each other in many respects (efficiency of water exchange, levels of nutrients and other water quality parameters, water salinity and consequent differences in species composition, abundance and vitality of biota). In addition, there are differences in the discharge quantities and discharge design of the power plants. In the thesis the environmental effects of the two power plants on the water recipients are compared and their relative significance is assessed.

There are four nuclear power plant units in Finland: two 488 $MW_e$ units at Loviisa and two 840 $MW_e$ units at Olkiluoto. The units at Loviisa were commissioned in 1977 and 1980, and those at Olkiluoto in 1978 and 1980. Environmental studies were initiated at Loviisa about ten years and at Olkiluoto six years before the start of operation of the power plants. Thus, 40-year-long time-series of results are available from the hydrographical, biological and radioecological studies carried out for monitoring the environmental effects of the thermal and radioactive discharges from the power plants in the recipient sea areas.

Brackish water from the Baltic Sea is used for cooling in the Finnish nuclear power plants, and both the thermal and liquid radioactive discharges are let out into the sea. Each of the power plants use cooling water at a rate of about 40–60 $m^3s^{-1}$, and the temperature rises in the condensers by about 10–13ºC. Loviisa NPP is located on the coast of the Gulf of Finland and Olkiluoto NPP on that of the Bothnian Sea. The state of the Gulf of Finland is clearly more eutrophic: the nutrient (total phosphorus and total nutrient) concentrations in the seawater are about 1½–2 times higher at Loviisa than at Olkiluoto, but the total phosphorus concentrations have still increased in both areas, even doubling at Loviisa between the early 1970s and 2000 (Fig. 1). The salinity is generally low in the brackish-water conditions of the northern Baltic Sea. However, the salinity of surface water is about 1‰ higher at Olkiluoto than at Loviisa (varying at the latter from near to 0‰ in early spring to 4–6‰ in late autumn). Thus, many marine and fresh-water organisms live in the Loviisa area close to their limit of existence, which makes the biota sensitive to any additional stress. The characteristics of the discharge

areas of the two sites differ essentially from each other in many respects: the discharge area at Loviisa is a semi-enclosed bay in the inner archipelago, where the exchange of water is limited, whereas the discharge area at Olkiluoto is more open, and the exchange of water with the open Bothnian Sea is more effective.

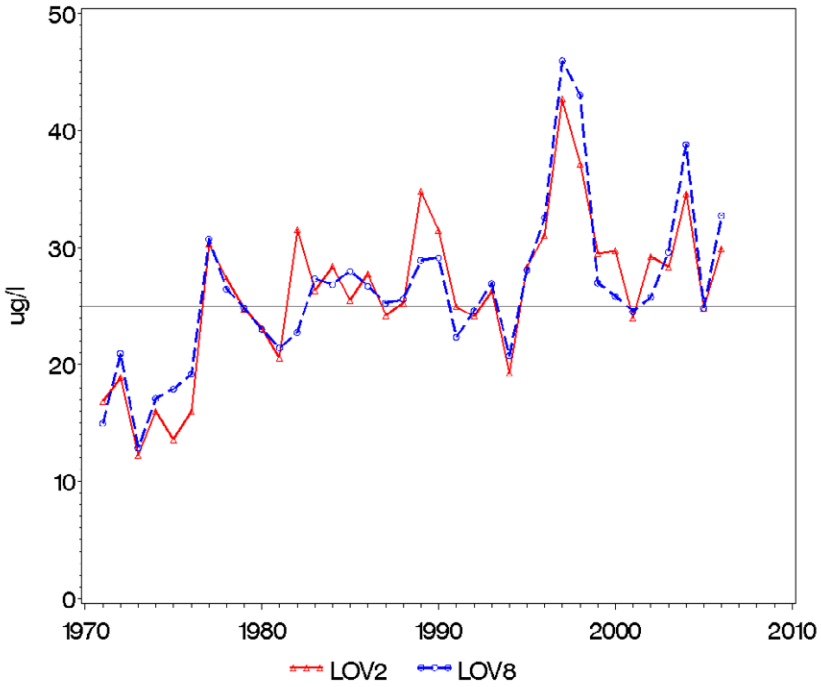


**Fig. 1. Average total phosphorus concentrations (µgP $l^{-1}$) of surface water during the growing seasons (May–October) in the intake (Station 8) and discharge area of cooling water (Station 2) at Loviisa in 1971–2006.**

## Results and discussion

### Environmental effects of cooling water

The effects of the cooling water on the temperatures in the sea were most obvious in winter, when the conditions also most fundamentally differed from those of the natural state. Thermal discharges have significantly affected the ice conditions in the vicinity of the power plants. The formation of a permanent ice cover in the discharge areas has been delayed in early winter. On the other hand, the break-up of the ice occurs earlier in springs so that the growing season has been prolonged at both ends. From the biological point of view, the prolonging of the growing season and the disturbance of the overwintering time, in conditions where the biota has adjusted to a distinct rest period in winter, have been the most significant biological effects of the thermal pollution. Aquatic organisms in the northern Baltic Sea are acclimatized to a distinct annual winter period. The shortening of the ice winter or a total lack of ice cover has led to a blurring of the limits between the growing season and the winter season.

**Table 1. Change in mean surface water temperature of the growing season at eight sampling stations off Loviisa during 1976–2006. Station 8 is located in the intake area of cooling water and considered as a reference station.**

| Area | Hästholmsfjärden | | | Vådholms-fjärden | Klobb-fjärden | Orren-grunds-fjärden | Hudöfjärden | |
|---|---|---|---|---|---|---|---|---|
| Station | 5 | 2 | 3 | 4 | 1 | 7 | 8 | 10 |
| Waterway distance from outlet [km] and direction | 0.4 E | 1.0 NE | 1.7 E | 2.8 SE | 3.4 NE | 5.4 SE | 3.0 SW | 3.4 SW |
| Change in mean surface water temperatureof growing season (May-October) in 1976-2006: | | | | | | | | |
| Probability $p_F$ | <.0001 | 0.0002 | 0.0005 | 0.0017 | 0.0034 | 0.0527 | 0.0628 | 0.1343 |
| | | | | | | | | |
| Average difference to Station 8 in 1997-2001 [ºC] | 4.3 | 2.6 | 3.1 | 1.3 | 2.4 | -0.3 | 0 | -0.1 |
| Average difference to Station 8 in 2002-2006 [ºC] | 4.9 | 2.6 | 3.3 | 1.2 | 2.4 | -0.3 | 0 | -0.3 |

During the growing season, the cooling water has raised the mean surface water temperatures at Loviisa by 4–5ºC at a distance of 0.4 km from the outlet and by 2.5–3ºC at a distance of 1–2 km in the discharge area, Hästholmsfjärden (Table 1). The rise in temperature has also been statistically significant at Station 4 in Vådholmsfjärden (distance 2.8 km) and at Station 1 in Klobbfjärden (distance 3.4 km), but not at Station 7 in Orrengrundsfjärden (distance 5.4 km).

A temperature rise generally increases the metabolic activity and growth rate of aquatic organisms. This means an increased production of organic matter, and thus, thermal pollution promotes the eutrophication process in eutrophied environments. The raised temperature also increases the rate of decomposition of organic matter in the receiving water bodies and leads to depletion of oxygen in deep water layers.

The hydrographical and biological results in the Loviisa area indicated a clearly higher level of eutrophy, which was based on the state of the whole Gulf of Finland. Thus, it was a challenge to distinguish the local effects of thermal discharges from the general eutrophication process of the Gulf of Finland.

During the past 40 years the soft-bottom macrofauna has steeply deteriorated at many sampling stations, at some to the point of almost complete extinction. A similar decline of the macrozoobenthos has been reported over the whole eastern Gulf of Finland. However, the local eutrophication process seems to have contributed into the decline of the bottom fauna in Hästholmsfjärden at Loviisa (Fig. 2). Thermal discharges have increased the production of organic matter, which again has led to more organic bottom deposits. Furthermore, these have increased the affinity of the isolated deeps for a depletion of oxygen, which has in turn caused a strong remobilization of phosphorus from the bottom sediments to the water phase.

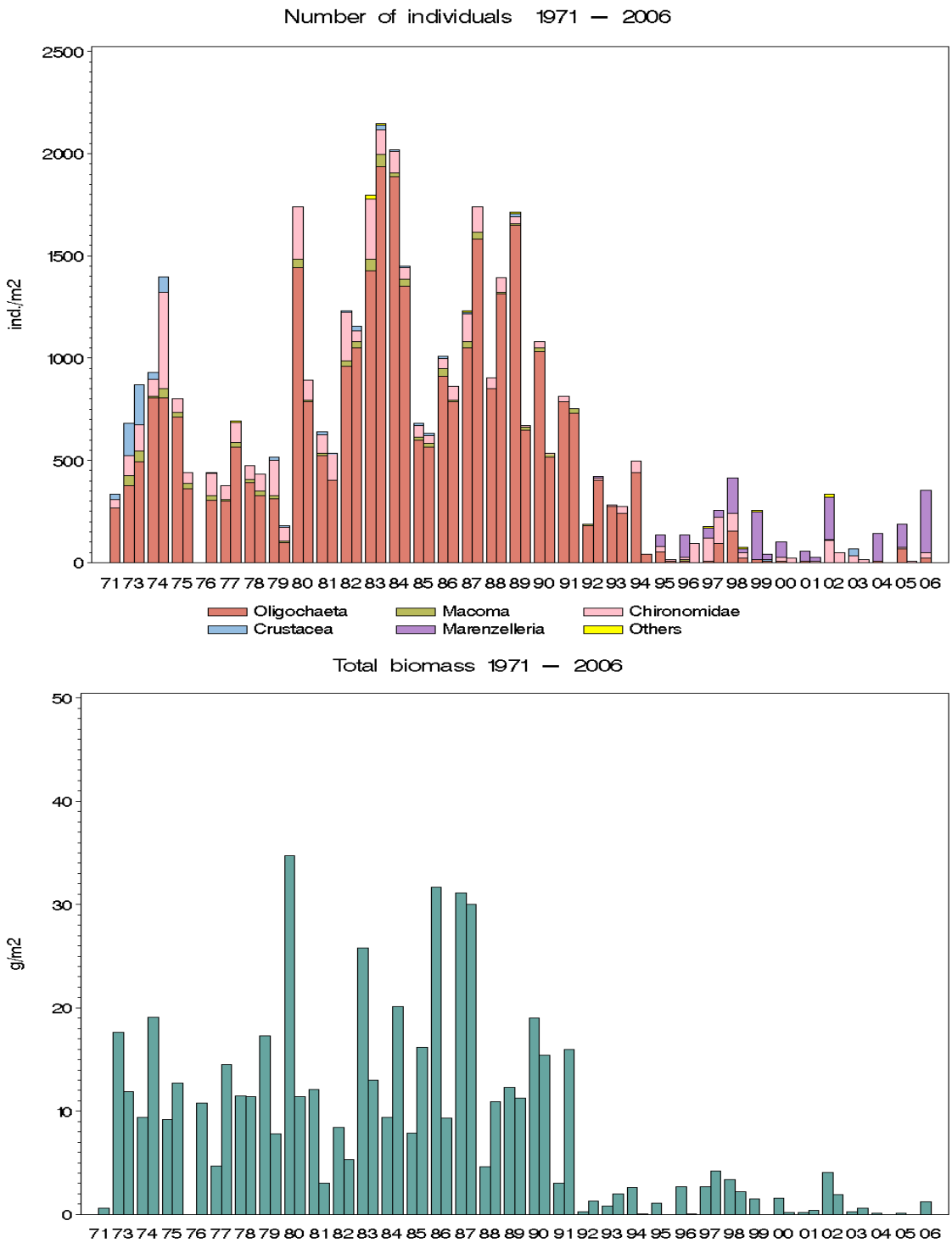


**Fig. 2. Abundance of main species or taxonomic groups (ind. $m^{-2}$) and total biomass of macrozoobenthos (g $m^{-2}$) at a sampling station situated 0.4 km off the cooling water outlet at Loviisa.**

Phytoplankton primary production and primary production capacity doubled in the whole area between the late 1960s and the late 1990s, but started to decrease a little at the beginning of this century. The focus of the production shifted from spring to mid-

and late summer. The general rise in the level of primary production was mainly due to the increase in nutrient concentrations over the whole Gulf of Finland, but the thermal discharge contributed to a stronger increase of production in the discharge area compared to that in the intake area of the cooling water (Fig. 3).

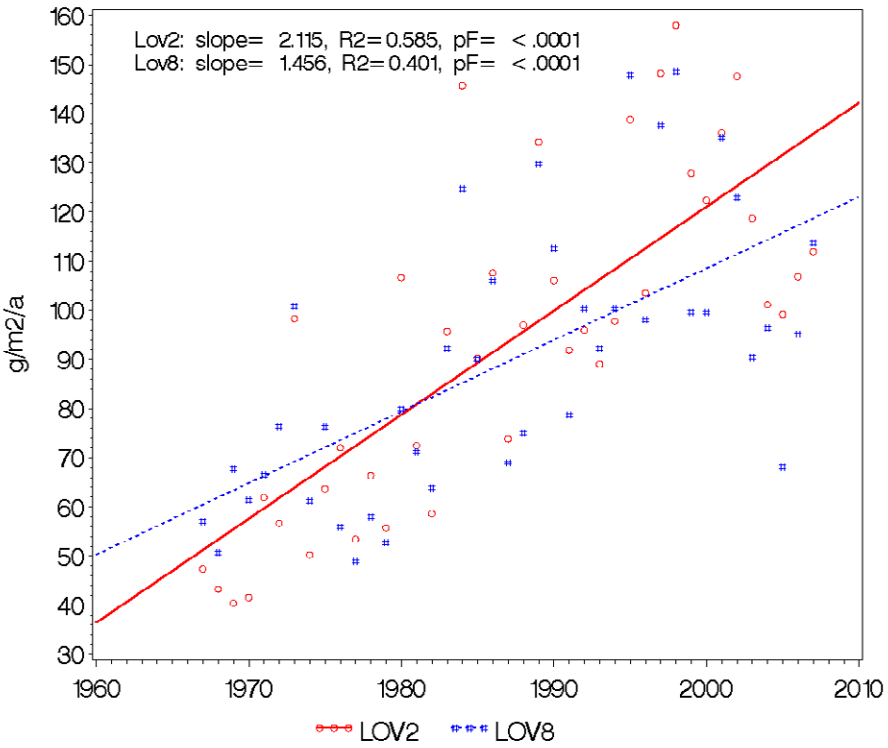


**Fig. 3. The regression lines of annual primary production at the Loviisa 2 (discharge area) and Loviisa 8 (intake area) stations between 1967 and 2006.**

The eutrophication of littoral vegetation in the discharge area has been the most obvious, unambiguous and significant biological effect of the heated water. Spiked water milfoil *Myriophyllum spicatum,* the pondweeds *Potamogeton perfoliatus* and *Potamogeton pectinatus* and the vigorous growths of numerous filamentous algae as their epiphytes have strongly increased in the vicinity of the cooling water outlet, where they have formed dense populations in the littoral zone in late summer (Fig. 4). However, the strongest increase of phytobenthos has extended only to a distance of about 1 km from the outlet, i.e., the changes in vegetation have been largest in those areas that remain ice-free in winter. A weaker eutrophication of littoral vegetation appeared in the whole area of Hästholmsfjärden Bay, but outside this area the phenomenon was slighter and observed only locally.

**Fig. 4. Dense vegetation on the south coast of Häst-holmsfjärden at Loviisa. (Photo by Anna Weckman).**

At Olkiluoto, the studies focusing on the effects of warm water discharge were more concise. Similar trends to those noticed in the Loviisa area regarding to increasing eutrophication were also discernible at Olkiluoto, but to a clearly smaller extent; this was due to the clearly weaker level of background eutrophy and nutrient concentrations in the Bothnian Sea, and to the local hydrographical and biological factors prevailing in the Olkiluoto area. The level of primary production has also increased at Olkiluoto, but has remained at a clearly lower level than at Loviisa. In spite of the analogous changes observed in the macrozoobenthos, the benthic fauna has remained strong and diversified in the Olkiluoto area.

## Environmental radioactivity

Radioactive discharges into the sea from the Finnish NPPs have been on average below 10% of the statutory limits. The discharged amounts of tritium were the most abundant, but those of other discharge nuclides were only a few percent of the limits, and still significantly decreased during recent years (during the last ten years to below 0.5%). Small amounts of local discharge nuclides were regularly detected in environmental samples taken from the discharge areas: tritium in seawater samples, and activation

products, such as $^{60}$Co, $^{58}$Co, $^{54}$Mn, $^{110m}$Ag, $^{51}$Cr, among others, in suspended particulate matter, bottom sediments and in several indicator organisms (e.g., periphyton and the bladder-wrack *Fucus vesiculosus*) that effectively accumulate radioactive substances from the medium.

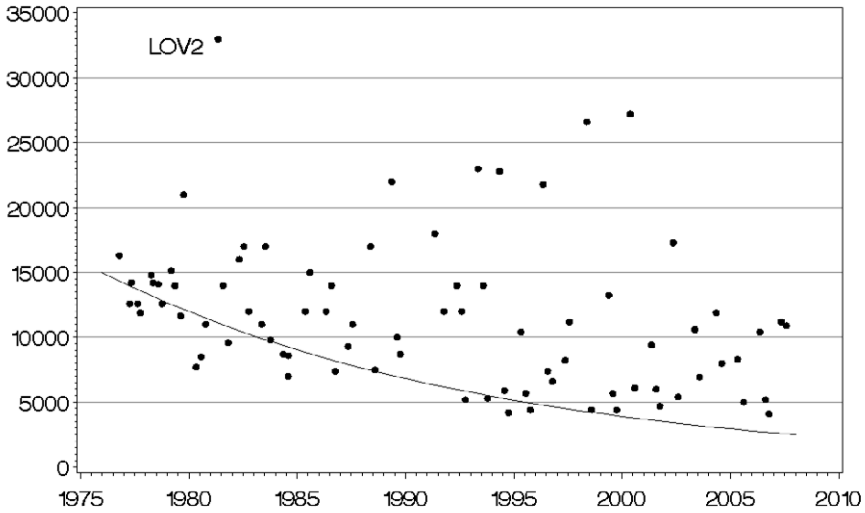


**Fig. 5. Tritium concentrations in surface seawater (Bq m$^{-3}$) in Hästholmsfjärden (discharge area) at Loviisa in 1976–2007. The curve in the graph indicates the decay of weapons-tests tritium in Finnish coastal waters during the monitoring period.**

The tritium discharges and the consequent detection frequency and concentrations of tritium in seawater were higher at Loviisa (Fig. 5), but the concentrations of the activation products were higher at Olkiluoto, where traces of local discharge nuclides were also observed over a clearly wider area, due to the better exchange of water than at Loviisa, where local discharge nuclides were detected outside the Hästholmsfjärden Bay only quite rarely and in small amounts. At the farthest, an insignificant trace amount (0.2 Bq kg$^{-1}$ d.w.) of $^{60}$Co originating from Olkiluoto was detected in *Fucus* at a distance of 137 km from the power plant (Fig. 6).

Discharge nuclides from the local nuclear power plants were almost exclusively detected at the lower trophic levels of the ecosystems (Fig. 7). Traces of local discharge nuclides were very seldom detected in fish, and even then only in very low quantities, but not at all in birds nor in the inner organs and reproductive products of fish and birds.

The best indicators for $^{60}$Co were periphyton, the spiked water milfoil *Myriophyllum spicatum* and the bladder-wrack *Fucus vesiculosus*, whereas the intake of, e.g., Chernobyl-originated $^{137}$Cs was highest in predatory fish, perch and pike. As a consequence of the reduced discharges, the concentrations of local discharge nuclides in the environment have decreased noticeably in recent years at both Loviisa and Olkiluoto (Fig. 8). Radioactive substances that originated from the Chernobyl accident and weapons-tests fallout (e.g. $^{137}$Cs, $^{90}$Sr, $^{239,240}$Pu) were still being detected in the environmental samples; the concentrations of $^{137}$Cs and natural radionuclides (e.g., $^{40}$K, $^{7}$Be) were in general higher than those of the local discharge nuclides.

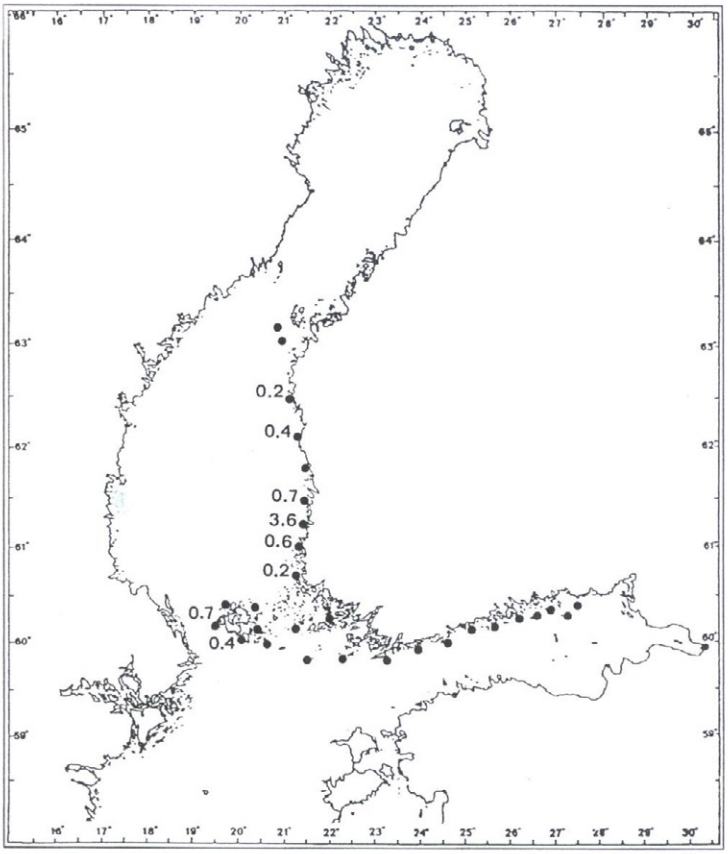


**Fig. 6. Activity concentrations of $^{60}$Co (Bq kg$^{-1}$ d.w.) in *Fucus vesiculosus* collected from 29 sampling sites along the Finnish coast in 1995. A dot without a number means that the concentration was below the detection limit of 0.1 Bq kg$^{-1}$ d.w.**

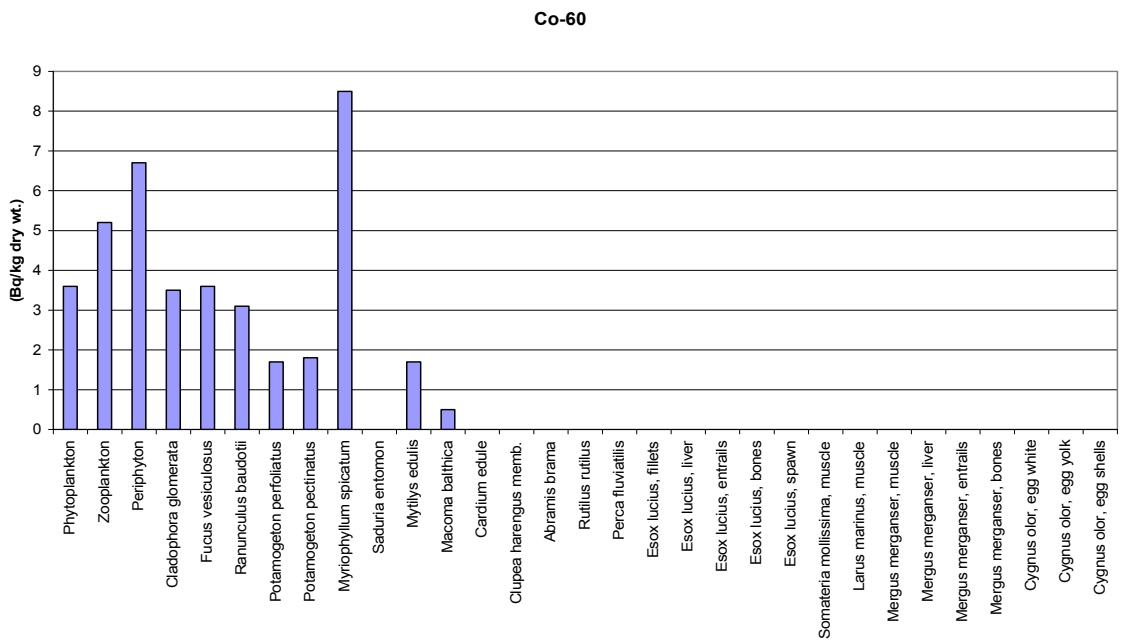


**Fig. 7. $^{60}$Co mean values (Bq kg$^{-1}$ d.w.) in some indicator samples in the sea area off Olkiluoto in 2001.**

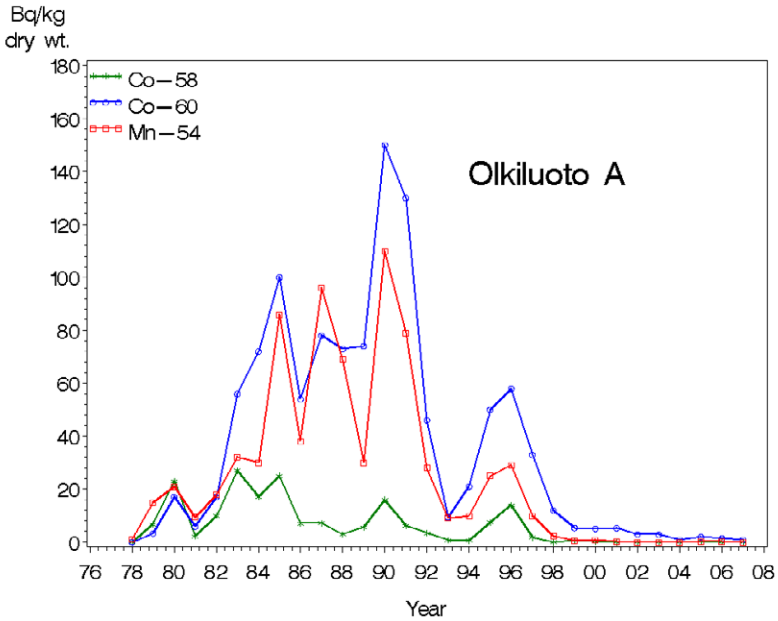


**Fig. 8. Annual mean concentrations of $^{58}$Co, $^{60}$Co and $^{54}$Mn in *Fucus vesiculosus* (Bq kg$^{-1}$ d.w.) at a sampling site nearest to the cooling water outlet at Olkiluoto in 1987–2007.**

The radiation doses to the public caused by discharges of radioactive substances from the Finnish nuclear power plants were small. The dose limit set for members of the public from the normal operation of Finnish nuclear power plants is 0.1 mSv a$^{-1}$. This is approximately 1/40 of the average radiation dose received by Finns from different sources during one year. During the whole operational history of the power plants, the effective dose commitments of the critical groups have been at their highest less than 4%, and during more recent years clearly below 1% of the set limit. In general, the minor doses of local origin to the critical groups have been due to liquid discharges of $^{60}$Co and people's shore occupancy. The environmental risk caused by the ionizing contaminants discharged from the Loviisa and Olkiluoto power plants was negligible: the doses to organisms were far below the conservative screening level of 10 µGy h$^{-1}$.

## Conclusions

Although the concentrations in environmental samples, and above all, the discharge data, are presented as seemingly large numbers, the radiation doses caused by them to the population and to biota are very low, practically insignificant. The effects of the thermal discharges have been more significant, at least to the wildlife in the discharge areas of the cooling water, although the area of impact has been relatively small. The results show that the nutrient level and the exchange of water in the discharge area of a nuclear power plant are of crucial importance.

## References

Ilus E. Environmental effects of thermal and radioactive discharges from nuclear power plants in the boreal brackish-water conditions of the northern Baltic Sea. Report STUK-A238, 2009, 380 pp.

# Tritium level along Romanian Danube river sector

Varlam, Carmen; Stefanescu, Ioan; Vagner, Irina; Faurescu, Ionut; Faurescu, Denisa
National Institute for R&D for Cryogenics and Isotopic Technologies Rm. Valcea, ROMANIA

## Abstract

Danube River is the eleventh longest river in the world, and is one of the important rivers from Europe. Tritium activity concentration from 12 locations distributed along Romanian Lower Danube River was determined by means of low level liquid scintillation counting. The three sampling campaigns were conducted between 2006 – 2007, on 975 km. The average concentration value registered for tritium activity for the studied area was around 15.4 TU, with higher values for Bechet and Seimeni locations. Special attention was accorded to Turnu Severin location, where tritium activity concentration from monthly Danube water was compared with monthly tritium concentration in precipitation. The behaviour of tritium concentration in the Danube water, at the begging of studied area, doesn't follow the behaviour of tritium concentration in precipitation, but the established values are far from any concern from radiological point of view.

## Introduction

The Danube River Basin is the second largest river basin in Europe covering 801463 km$^2$ [ICPDR, 2005]. From its source in the Black Forest at height of 1000 m above sea level, to its three-armed delta on the Black Sea, the Danube flows through eights countries and drains a total of eighteen. Due to its geologic and geographic conditions the Danube River Basin can be divided into 3 main parts: Upper Danube Basin, Middle Danube Basin and Lower Danube Basin. 65% of Lower Danube Basin is the natural border between Romania and Bulgaria.

During the 80's the contribution of nuclear power to total primary energy supply as a percentage of fuel mix has increased significantly, from 9% in 1985 to 15% in 1995 [EC, 2000]. Nuclear power generates between 10% and 45% of electricity in the Danube Space countries. Nuclear electricity has been, on a variable cost basis, cheaper than other options, and consequently used in preference to coal, oil and gas. Two important nuclear objectives for both countries are situated in this region: Kozloduy NPP and Cernavoda NPP. Nuclear energy is considered by the two countries an option for the future development, so Romania already built a new CANDU type unit in Cernavoda, which has been operating since September 2007, and Bulgaria started negotiations for a new nuclear power plant in Belene.

The knowledge of tritium in the Romanian Lower Danube offers two important information: first in the environmental radioactivity monitoring program (Cernavoda is

a CANDU type reactor, where tritium is the most important radioisotope evacuated in the environment) and second a primary estimation of river discharge signature for the end part of Danube by comparing the tritium level from precipitation and river water.

## Material and methods

The Danube typology represents a harmonized system developed by the countries sharing the Danube River [ICPDR, 2005]. The most important factors used for this system are mean water slope, substratum composition, geomorphology and water temperature. Lower Danube Basin contains four ~~types of~~ sections: Iron Gates Danube, Western Pontic Danube, Eastern Wallachian Danube and Danube Delta.

Iron Gates Danube section (A, fig. 1) has an average width of about 750 m and runs in a canyon or through valley form. Dominant main channel has numerous rocks situated directly under the surface water. Sampling point chosen was Ieselnita (1, fig.1), location with easy access to the left side of the Danube. Next sampling point was from Cerna, Danube tributary, at Toplet location (2, fig. 1). Cerna is a small mountain river without industrial activity. The end of this section was Turnu Severin (3, fig.1) another sampling point.

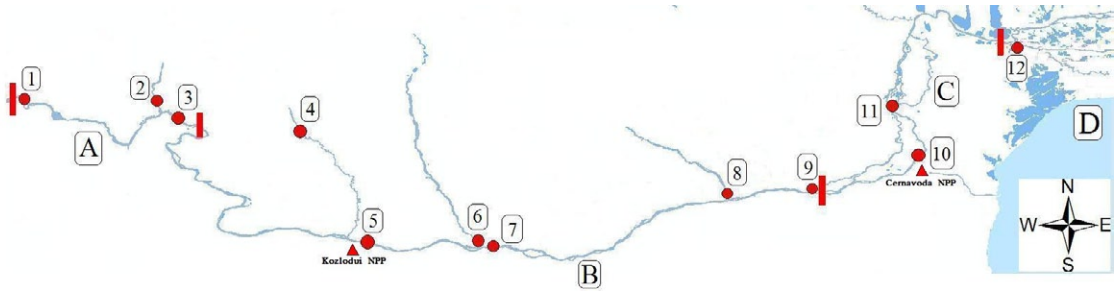


**Fig. 1 Section type and sampling locations from Lower Danube Basin; A - Iron Gates Danube; B - Western Pontic Danube; C – Eastern Wallachian Danube; D – Danube Delta.**

Western Pontic Danube section (B, fig.1) contain floodplain landscape with higher plains of terraced accumulation in a meander and plain floodplain valley. The Romanian bank is low and terraced with wide floodplains. The main channel has an average width of 830 m and mean depth of 8.5 m. The diversity of water bodies in this area close to the stream is large, but we focused on the main course and on few tributaries with important mining industry, Jiu river (4, fig.1), and chemical industry Olt river (6, fig. 1) and Arges river (8, fig.1). Bechet location (5, fig.1) from main course is important due to its location downstream ~~the~~ Kozloduy NPP. Another sampling point was Turnu Magurele (7, fig.1) which is located downstream to jonction to Olt river, approximately in the middle of this section. The end of this section is Chiciu-Silistra (9, fig.1) another important sampling point, before Danube splits in two branches: Old Danube and Borcea.

The Danube changes its watercourse northward in Eastern Wallachian Danube section (C, figure 1). There are two large isles, Balta Ialomitei and Balta Brailei, and many natural lakes. The main channel has an average width of 650 m, and a mean depth of 10.5m. The section is characterized by slow current velocities of 0.8 m/s. The first sampling point of this section was established in Seimeni (10, fig.1) downstream of

NPP Cernavoda discharge channel and the second in Giurgeni (11, fig.1), a point between the two isles were Danube has one main branch for a short distance.

The Danube Delta section (D, figure 1) is the Danube's youngest teritory. There are three main water channels: Chilia, Sulina and Sf. Gheorghe, with numerous canals and floating islands. This section is characterized by an average current velocity of 0.7 m/s. The shape of the delta is triangular, and at mean water levels, 60% of this area is covered by waters. The point from this section was only Tulcea (12, fig.1), due to difficult access to this part of the Danube.

Precipitation sampling was made on a monthly basis in a typical rain water collector [IAEA, 1989] in Drobeta Turnu Severin location and our Institute, starting with January 2007, and ending with October 2007. At the end of the month the container was shaken thoroughly and a sample of 1 liter was filled for shipment to the analytical laboratory. Special attention was given for collection and preservation of water sample [APHA-AWWA-WEF, 2005]. Type of section, water body, and sampling location are in the table 1.Water samples for tritium measurement were collected one meter from the left bank of Danube, 10 cm from the water surface, in glass bottle. pH, conductivity and temperature for water sample were measured in sampling location using portable apparatus WTV pH/cond 340i.

**Table 1. Geographical coordinates of sampling locations.**

| Location number | Location name | Section type | Water body | Latitude | Longitude |
|---|---|---|---|---|---|
| 1. | Ieselnita | A | Danube | $44^0$48'31" | $21^0$24'11" |
| 2. | Toplet | A | Cerna | $44^0$47'58" | $22^0$23'26" |
| 3. | Drobeta Turnu Severin | A | Danube | $44^0$40'2" | $22^0$32'51" |
| 4. | Filiasi | B | Jiu | $44^0$34'8" | $23^0$27'19" |
| 5. | Bechet | B | Danube | $44^0$44'56" | $23^0$57'14" |
| 6. | Islaz | B | Olt | $43^0$44'38" | $24^0$46'46" |
| 7. | Turnu Magurele | B | Danube | $43^0$42'45" | $24^0$53'25" |
| 8. | Oltenita | B | Arges | $44^0$05'51" | $26^0$38'12" |
| 9. | Chiciu/Silistra | B | Danube | $44^0$07'56" | $27^0$16'19" |
| 10. | Seimeni | C | Danube | $44^0$23'31" | $28^0$03'28" |
| 11. | Giurgeni | C | Danube | $44^0$45'2" | $27^0$52'17" |
| 12. | Tulcea | D | Danube | $45^0$10'58" | $28^0$48'25" |

As tritium is a soft beta emitter (5.72 keV mean energy), liquid scintillation is the most appropriate technique for its measurement. In this work, the low-background liquid scintillation spectrometer Quantulus 1220 (Wallac) has been used to determine tritium in water samples. The analytical method used to determine tritium in water samples was, briefly, the following: samples were filtered through slow depth filters; 250 ml of filtrate was distilled using ISO method [ISO, 1989]; 8 ml of distillate was mixed with 12 ml of scintillation cocktail OptiPhase Hisafe 3 in polyethylene vials; three background samples and tritium standards were simultaneously prepared. Samples, backgrounds and tritium standards were counted using Quantulus 1220 during

1000 min/samples. The tritium standards were internal standard capsules containing a tritium-labeled organic compound [fructose-1-$^3$H] provided by PerkinElmer. Tritium-free water (blank water) was deuterium-depleted water with a D/(D+H) value of 15 ppm (Varlam et al. 2009). The counting efficiency at the best factor of merit was between 24.84% and 25.02%, and the background between 0.714 ± 0.016 CPM (counts per minute) and 0.748 ± 0.017 CPM, following a minimum detectable activity of around 4 TU (confidence level of 2). The uncertainty due to the statistical nature of radioactive decay and background radiation was reported at 1σ.

## Results and Discussion

The average fallout during the year 2007 in Romania was ~~with~~ 13.33% higher than the normal climatologic average (NRMA, 2007): for months of April, May, June and July it has been recorded a deficit in precipitation monthly average with an important negative deviation for April (75%), whereas for the month of October there was a significant excess in monthly average (124.9%).

Tritium concentration during the year 2007 at Turnu Severin location had a mean of 10.2 ± 2.1 TU (one Tritium Unit, TU, one tritium atom corresponds to $10^{18}$ hydrogen atom). The same value was recorded in our Institute, 10.7 ± 2.1 TU. We recorded a minimum tritium concentration of 4.6 ± 2.1 TU in January 2007 for Turnu Severin location (table 2) and a minimum tritium concentration of 6.1 ± 2.1 TU in February 2007 for our Institute. The maximum tritium concentration of 16.1 ± 2.1 TU was measured in July for Turnu Severin location, but we recorded for our Institute two months with the higher values of 17.2 ± 2.2 TU and 16.8 ± 2.2, May and August. Comparing published values for tritium in precipitation in Austria [Kralic et al., 2005] with measured values for the monitored locations we can conclude that annual tritium concentration average has had the same trend for the past years: 10.4 TU for 2000, 10.5 TU for 2001 and 10.46 TU for 2002. There are no other influences and tritium behaviour in precipitation has the same tendency to decrease in the environment.

**Table 2. Tritium concentration during observation period of 2007 in Turnu Severin location and our Institute.**

| Period of sampling | Tritium concentration [TU] Turnu Severin | Tritium concentration [TU] Our Institute |
|---|---|---|
| January 2007 | 4.6+/-2.1 | 7+/-2.1 |
| February 2007 | 7.3+/-2.1 | 6.1+/-2.1 |
| March 2007 | 4.8+/-2.1 | 8.1+/-2.1 |
| April 2007 | 8.9+/-2.1 | 12.7+/-2.2 |
| May 2007 | 15.3+/-2.2 | 17.2+/-2.2 |
| June 2007 | 12.7+/-2.2 | 8.8+/-2.1 |
| July 2007 | 16.8+/-2.2 | 14.7+/-2.2 |
| August 2007 | 15.9+/-2.2 | 16.8+/-2.2 |
| September 2007 | 8.8+/-2.1 | 9.5+/-2.1 |
| October 2007 | 7.2+/-2.1 | 6.8+/-2.1 |

A special behaviour regarding tritium concentration was recorded in the Danube water at Turnu Severin location, table 3. The average tritium concentration in the Danube water for this location was 13.7 ± 2.2 TU, higher than that of precipitation, without seasonal variation normally expected for surface water. The measured average for tritium concentration is far from any radioprotection concern (aprox. 1.6 Bq/l comparing with 100 Bq/l recommended by Council Directive 98/83/EC for drinking water), but is important for Danube River discharge signature at the beginning of Lower Danube Basin.

**Table 3. Tritium concentration in Danube water and precipitation at Turnu Severin location.**

| Period of sampling | Tritium concentration [TU] Danube | Tritium concentration [TU] Precipitation |
|---|---|---|
| January 2007 | 11.5 +/- 2.2 | 4.6 +/- 2.1 |
| February 2007 | 17 +/- 2.2 | 7.3 +/- 2.1 |
| March 2007 | 13.7 +/- 2.2 | 4.8 +/- 2.1 |
| April 2007 | 15.3 +/- 2.2 | 8.9 +/- 2.1 |
| May 2007 | 14.8 +/- 2.2 | 15.3 +/- 2.2 |
| June 2007 | 11.2 +/- 2.2 | 12.7 +/- 2.2 |
| July 2007 | 16.3 +/- 2.2 | 16.8 +/- 2.2 |
| August 2007 | 14.9 +/- 2.2 | 15.9 +/- 2.2 |
| September 2007 | 10.6 +/- 2.2 | 8.8 +/- 2.1 |
| October 2007 | 11.4 +/- 2.2 | 7.2 +/- 2.1 |

Tritium sampling campaigns were performed in August 2006, March 2007 and October 2007, table 4.

**Table 4. Tritium concentration along Romanian Danube Sector for sampling campaign of August 2006, March 2007, and October 2007.**

| Location number | Location name | Water body | Tritium concentration August 2006 [TU] | Tritium concentration March 2007 [TU] | Tritium concentration October 2007 [TU] | Mean tritium concentration [TU] |
|---|---|---|---|---|---|---|
| 1. | Ieselnita | Danube | 17.6 +/- 2.2 | 7 +/- 2.1 | 15.7 +/- 2.2 | 13.4 +/- 2.2 |
| 2. | Toplet | Cerna | 11.9 +/- 2.2 | 8.3 +/- 2.1 | 10.7 +/- 2.2 | 10.3 +/- 2,2 |
| 3. | Drobeta Turnu Severin | Danube | 14.8 +/- 2.2 | 6.2 +/- 2.1 | 16.7 +/- 2.2 | 12.6 +/- 2,2 |
| 4. | Filiasi | Jiu | 12.7+/- 2.2 | 9.3 +/- 2.1 | 10.5 +/- 2.2 | 10.8 +/- 2.2 |
| 5. | Bechet | Danube | 27.9 +/- 2.3 | 29.2 +/- 2.3 | 24.7 +/- 2.3 | 27.3 +/- 2.3 |
| 6. | Islaz | Olt | 11.6 +/- 2.2 | 6.8 +/- 2.1 | 13.2 +/- 2.2 | 10.5 +/- 2.2 |
| 7. | Turnu Magurele | Danube | 12.8 +/- 2.2 | 8.9 +/-2.1 | 13.2 +/- 2.2 | 11.6 +/- 2.2 |
| 8. | Oltenita | Arges | 12.2 +/- 2.2 | 11.6 +/- 2.2 | 11.8 +/- 2.2 | 11.9 +/- 2.2 |
| 9. | Chiciu/Silistra | Danube | 9.7+/- 2.1 | 12.2 +/- 2.2 | 8.3 +/- 2.1 | 10.1 +/- 2.2 |
| 10. | Seimeni | Danube | 32.4 +/- 2.3 | 33.5 +/- 2.3 | 28.7 +/- 2.3 | 31.5 +/- 2.3 |
| 11. | Giurgeni | Danube | 15.9 +/- 2.2 | 7.4 +/- 2.1 | 7.2 +/- 2.1 | 10.2 +/- 2.2 |
| 12. | Tulcea | Danube | 11.6 +/- 2.2 | 10.8 +/- 2.1 | 16.5 +/- 2.2 | 13 +/- 2.2 |

Two higher values than the tritium concentration average of 16.2 ± 2.2 TU were recorded for Bechet and Seimeni, 27.3 ± 2.2 TU and 31.5 ± 2.2 TU respectively. The two locations have nearby two different nuclear power plants, Kozloduy and Cernavoda, with important tritiated effluents discharged in the Danube. Tributaries had lower mean tritium concentration (between 10.3 ± 2.2 TU for Cerna River and 11.9 ± 2.2 TU for Arges River) than the tritium concentration average of the Danube. Tritium level in the Danube water is continuously decreasing from 20-25 TU in 1995 [Rank et al., 1999] to precipitation level, even if ~~the~~ nuclear objectives are in the monitored areas.

## Conclusions

The tritium level in precipitation during the monitoring period was 10.2 ± 2.1 TU for Turnu Severin location. Tritium concentration in the Danube water in the same location had higher values than that of precipitation, the mean value calculated during the monitoring period being 13.7 ± 2.2 TU. This value is far from any concern from radiological point of view, but the behavior of tritium concentration during the cold months of the year (January, February) with values higher than 10 TU proves the influence of nuclear activity developed along the Danube. Tritium concentration average in the Danube water along the Lower Danube Basin was 16.2 ± 2.2 TU. Two higher values than the tritium concentration average were recorded for Bechet and Seimeni. The two locations have nearby important nuclear power plants. The highest mean tritium concentration measured during the three sampling campaigns for the Danube water was recorded in August 2006 with a value of 16.6 ± 2.2 TU. The lowest mean tritium concentration measured during the three sampling campaigns for the Danube water was recorded in March 2007 with a value of 13.8 ± 2.2 TU. Tributaries had lower values than tritium concentration average due to their different basins with strong groundwater components. Tritium level in the Danube water is continuously decreasing, from 596 TU in September 1966, to 12.6 TU in December 2005 (GNIR, Vienne Station). Environmental values recorded confirmed that precipitation is the primary source of tritium in the Danube water, in spite of the existence of the two important nuclear power plants in the monitored area, as previously mentioned.

## Acknowledgements

This paper was prepared in connection with work done under National Program for Research and Development AMCSIT CEEX, contract number 63/2005, and PN09190501, contract number 019N/2010.

## References

APHA-AWWA-WEF, Section 7500- 3H B. Liquid Scintillation Spectrometric Method. Standard Methods for the Examination of Water and Wastewater 1995; 19: 7-39.

Council Directive 98/83/EC of 3 November 1998 on the quality of water intended for human consumption, OJ L 330, 5.12.1998, 32–54.

EC, European Commission DG: Region Policy, Danube Space Study – Regional and Territorial Aspects of Development in the Danube Countries with Respect to Impact on the European Union, ANr. A 22404.00, Vienne, 2000.

GNIR, Global Network for Isotopes in Rivers, Vienne Station (Austria), Available on web at http://nds121.iaea.org/wiser.

ICPDR, International Commission for Protection of Danube River, The Danube River Basin District Part A - Basin wide Overview, 2005, http://www.icpdr.org/DANUBIS.

IAEA, International Atomic Energy Agency, Measurement of Radionuclide in food and the environment, Technical Reports Series no. 295, Vienna, 1989.

ISO, International Standard Office, ISO 9698:1989, Water Quality - Volumic activity determination of tritium - Method by counting of scintillation in liquid medium, IDT ISO9698:1989E first edition, 1989.

Kralik, M., Hummer, F., Stadler, E., Scheidleder, A., Tesch, R., Papesch, W. Tritium Osterreich Jahresbericht 1997 bis 2002. Available on web at http://www.umweltbundesamt.at 2005.

NRMA, National Romanian Meteorology Administration, http://www.inmh.ro/, 2006.

Rank, D., et. al., Oxygen-18, deuterium and tritium in the Black Sea and the Sea of Marmara. Journal of Environmental Radioactivity 1999; 47: 77-87.

Varlam, C., Stefanescu, I., Faurescu I., Popescu, I., Dobrinescu, D., Applying direct liquid scintillation counting to low level tritium measurement, Journal of Applied Radiation and Isotope 2009, volume 67, Issue 5, 812:817.

# Radioactivity monitoring of sediments in rivers in Serbia during the period 2005–2009

Eremic-Savkovic, Maja; Pantelic, Gordana; Vuletic, Vedrana;
Tanaskovic, Irena; Javorina, Ljiljana
Serbian Institute of Occupational Health "Dr Dragomir Karajovic", Belgrade, SERBIA

## Abstract

In this paper we present radioactivity monitoring results of the sediments in Serbian rivers from 2005 through 2009. Sediment samples have been collected at eight sites on six Serbian rivers, usually during spring and autumn.

We have applied gamma spectrometry, gross alpha beta activity and radiochemical method of 90Sr separation as measurement methods.

Our results show that activity concentration of natural radionuclide in sediments (mean annual values in Bq/kg) is within the average values limits for the territory of Serbia. Activities of long living radionuclide of artificial origin have tendency of mild decrease as a result of dissolution, leaching and changes in river flow.

## Introduction

Sediment is an essential dynamic component of aquatic systems due to the strong tendency towards bonding the tank of toxic and persistent compounds of anthropogenic origin. Sediment is composed of organic and mineral components. Organic component of the plant and animal material from the river and the watershed area and discharge of industrial waste water utilities. Mineral component contains erosive material from the surface of the entire river basin.

Sediment monitoring and assessment of its quality is usually conducted to determine the extent to which sediment tank and a secondary source contaminenata in surface waters. The aim of this monitoring was conducted in determining the status of the quality of sediment and its impact on the environment and human health through the study of various interactions in the sediment-water system.

## Material and methods

Radioactivity control of sediment in the territory of Serbia is done in the following rivers:

– Danube river (sampling is done on Bezdan near the border with Hungary, in Belgrade and in Prahovo near Romania border)
– Sava (sampling is done at the Belgrade)
– Tisa (sampling is done at Kanjiza)

– Nisava (sampling is done near Pirot)
– Timok (sampling is done at Zaječar)
– Drina (sampling is done at Loznica)

Sediments of the Danube and Sava rivers were taken four times durnig the year, while sediments from other rivers were taken in the spring when water level is the highest and in the fall when water level is the lowest.

One by one kilogram of river sediment was taken by sampler and placed in to plastic containers. Sediment was dried at $105^0$C to constant weight, sieved trough sieve and the fraction less than 250 µm is taken.

Gammaspectrometry is carried out on pure germanium detector manufactured by EG&G ″ORTEC″, which is connected with multichannel analyzer (8192 channels) produced by the same manufacturer and with adequate computer facilities. Energetic calibration, as well as calibration of detector efficiency is performed by means of Amersham radioactive standard (Debertin K. et al.1988, Pantelic G. et al. 1996)

The measurement of gross beta activity is carried out by alpha-beta proportional gas counter PIC-WPC-9550. The level of basic radiation is 0.4 imp/min. The size of planchet is 5cm. The performance of counter is 47% and is determined by $^{90}$Sr standard.

Radiochemical method of $^{90}$Sr separation is based on oxalate isolation of Ca and Sr, ignition to oxides and usage of aluminum as $^{90}$Y carrier. The equilibrium is achieved in 18 days, and after that time $^{90}$Y is isolated on Al $(OH)_3$ carrier (Brnovic 1972), which is then ignited to oxide that is subsequently measured by alpha-beta proportional gas counter

## Results and discussion

Table 1 shows gross beta activity results with standard deviation. The scope of a monitoring program included gross beta activity measurements of river Danube at sites Bezdan and Belgrade as well as river Sava near Belgrade.

During the observation period 2005-2009 there was no significant variations of sediment measurement results of river Danube on both locations.

During the observation period 2005-2009 there was no significant variations of sediment measurement results of river Danube and river Sava obtained on a location near Belgrade.

**Table 1. Gross alpha beta activity in sediments Danube and Sava river (mean annual values).**

| Year | | 2005 | 2006 | 2007 | 2008 | 2009 |
|---|---|---|---|---|---|---|
| | | Activity (Bq/kg) | | | | |
| Danube | Bezdan | 708 ± 65 | 470 ± 140 | 658 ± 170 | 473 ± 92 | 573 ± 70 |
| | Belgrade | 520 ± 140 | 508 ± 100 | 520 ± 180 | 503 ± 86 | 460 ± 220 |
| Sava | Belgrade | 480 ± 180 | 580 ± 140 | 590 ± 220 | 530 ± 120 | 487 ± 95 |

Table 2 illustrate the results of activity concentration of natural radionuclide in river sediments in Danube and Sava (mean annual values in Bq/kg with standard deviation).

**Table 2. Activity concentration of natural radionuclide in river sediments Danube (Zemun) and Sava (Belgrade).**

| Year | River | $^{40}K$ (Bq/kg) | $^{232}Th$ (Bq/kg) | $^{226}Ra$ (Bq/kg) | $^{238}U$ (Bq/kg) | $^{235}U$ (Bq/kg) | $^{7}Be$ (Bq/kg) |
|---|---|---|---|---|---|---|---|
| 2005 | Danube | 480 ± 22 | 34.5 ± 0.4 | 40.4 ± 2.2 | 50.0 ± 8.4 | 2.3 ± 0.3 | < 7.2 |
| 2006 | | 464 ± 14 | 30.8 ± 5.2 | 40 ± 13 | 41 ± 21 | 1.8 ± 0.8 | < 8.7 |
| 2007 | | 411 ± 84 | 26.4 ± 8.7 | 30.3 ± 6.3 | 28 ± 13 | 1.5 ± 0.6 | < 7.2 |
| 2008 | | 589 ± 60 | 36.5 ± 5.0 | 51.2 ± 4.5 | 56.5 ± 5.2 | 2.7 ± 0.6 | < 11 |
| 2009 | | 480 ± 160 | 35 ± 16 | 34 ± 15 | 43 ± 15 | 1.8 ± 0.5 | 37 ± 16 |
| 2005 | Sava | 465 ±31 | 32.3 ± 2.6 | 35.9 ± 5.8 | 39.5 ± 4.9 | 1.7 ± 0.3 | < 7.0 |
| 2006 | | 477 ± 46 | 28.7 ± 6.5 | 40 ± 14 | 35.3 ± 7.6 | 1.6 ± 0.4 | < 8.9 |
| 2007 | | 400 ± 120 | 25 ± 11 | 26 ± 11 | 19.8 ± 1.2 | 0.9 ± 0.1 | < 11 |
| 2008 | | 600 ± 100 | 39.8 ± 4.8 | 51.4 ± 5.6 | 48.1 ± 1.9 | 2.2 ± 0.1 | < 8.2 |
| 2009 | | 460 ± 120 | 14.9 ± 5.0 | 37± 12 | 40 ± 17 | 1.9 ± 0.8 | < 20 |

The average natural radionuclide concentration with standard deviation for sediments in other Serbian rivers (Nisava, Timok, Tisa and Drina) in table 3 is shown.

Activities of natural radionuclides measured in all sediment samples are within the average values for the territory of Serbia. Activity concentration of cosmogenic radionuclide $^{7}Be$ is below the limit of detection.

**Table 3. Activity concentration of natural radionuclide in river sediments Danube (Zemun) and Sava (Belgrade).**

| Year | River | $^{40}K$ (Bq/kg) | $^{232}Th$ (Bq/kg) | $^{226}Ra$ (Bq/kg) | $^{238}U$ (Bq/kg) | $^{235}U$ (Bq/kg) | $^{7}Be$ (Bq/kg) |
|---|---|---|---|---|---|---|---|
| 2005 | Timok | 320 ± 11 | 21.1 ± 1.2 | 23.2 ± 4.0 | 25.2 ± 5.2 | 1.1 ± 0.2 | 24 ± 4 |
| 2006 | | 397 ± 79 | 24 ± 11 | 25 ± 11 | 26 ± 12 | 1.2 ± 0.5 | < 25 |
| 2007 | | 450 ± 140 | 22 ± 13 | 27 ± 14 | 45 ± 10 | 1.7 ± 0.3 | < 6.1 |
| 2008 | | 471 ± 56 | 23.7 ± 5.7 | 32.2 ± 3.9 | 32.1 ± 0.9 | 1.4 ± 0.3 | < 13 |
| 2009 | | 384 ± 13 | 17.4 ± 2.7 | 23.3 ± 1.8 | 22.8 ± 4.8 | 1.1 ± 0.1 | 16 ± 9 |
| 2005 | Nisava | 390 ± 12 | 23.3 ± 0.9 | 22.7 ± 2.6 | 25.1 ± 2.6 | 1.0 ± 0.1 | 8 ± 2 |
| 2006 | | 362 ± 42 | 29.1 ± 1.8 | 35.1 ± 3.5 | 30 ± 10 | 1.5 ± 0.3 | 30 ± 6 |
| 2007 | | 364 ± 87 | 20.1 ± 0.4 | 20.8 ± 2.0 | 13.8 ± 3.1 | < 1.2 | < 3.9 |
| 2008 | | 423 ± 7 | 27.9 ± 6.4 | 31.9 ± 8.6 | 29.3 ± 8.1 | 1.2 ± 0.2 | < 7.2 |
| 2009 | | 482 ± 91 | 28.1 ± 8.9 | 32.3 ± 13.1 | 45 ± 23 | 2.0 ± 1.2 | < 5.5 |
| 2005 | Tisa | 492 ± 16 | 35.6 ± 1.9 | 36.4 ± 5.5 | 54.1 ± 5.2 | 2.4 ± 0.3 | < 12 |
| 2006 | | 390 ± 2 | 19.9 ± 0.4 | 24.2 ± 1.4 | 20.9 ± 5.6 | 1.1 ± 0.1 | < 12 |
| 2007 | | 557 ± 24 | 39.5 ± 0.4 | 36.9 ± 1.6 | 30.4 ± 6.6 | < 2.0 | < 9.8 |
| 2008 | | 555 ± 52 | 32.8 ± 1.3 | 36.2 ± 3.2 | 41.1 ± 1.4 | 1.9 ± 0.1 | 8 ± 2 |
| 2009 | | 443 ± 16 | 34.5 ± 7.9 | 39 ± 10 | 42 ± 14 | 2.1 ± 0.8 | < 6.1 |
| 2006 | Drina | 406 ± 19 | 28.0 ± 1.8 | 27.5 ± 2.9 | 28.8 ± 4.7 | 1.4 ± 0.2 | 24 ± 16 |
| 2007 | | 340 ± 170 | 22 ± 15 | 26 ± 23 | 21 ± 12 | < 1.8 | 9 ± 5 |
| 2008 | | 450 ± 200 | 28 ± 16 | 31 ± 14 | 31 ± 13 | 1.5 ± 0.6 | 6 ± 1 |
| 2009 | | 288 ± 15 | 18.4 ± 5.4 | 19.9 ± 3.7 | 23 ± 12 | 1.0 ± 0.2 | < 8.9 |

The most important source of artificial radionuclides in the environment in Serbia is nuclear accident in Chernobyl Nuclear Power Plant. Results of gamma spectrometric measurement $^{137}Cs$ in sediments of Danube river in tree sites Bezdan, Belgrade and Prahovo shows descreasing during the period 2005-2009 (figure 1). Maximum activity 137Cs was mesured in 2009 in site Prahovo (figure 1).

The sediment was sampled in high water level season. At the actual sampling time, the river flooded the area outside banks, so the sampling of nearby soil has been performed as well.

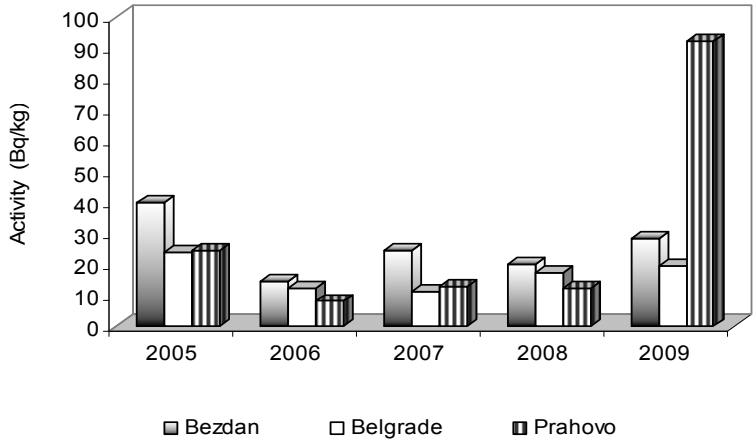


**Fig. 1. $^{137}$Cs activity concentration in sediment of Danube River (mean annual values).**

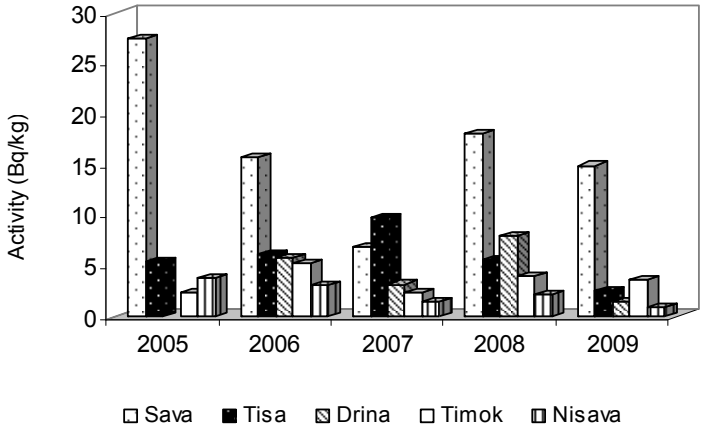


**Fig. 2. $^{137}$Cs activity concentration in sediments Sava, Drina, Tisa, Timok and Nisava (mean annual values).**

Maximum activity of $^{137}$Cs was in 2005. in Sava river sediment (figure 2).

Figure 3 shows 90Sr activity in Danube sediment during the period 2005-2009 at sites Bezdan and Belgrade. Average annual values in 2005 was 0.41Bq/kg at site Belgrade. Average annual values in 2007 was 0.12Bq/kg at site Bezdan. In 2009 90Sr activity in Danube sediment at site Prahovo was not measured.

During the period 2005-2009 90Sr activity was less then 1Bq/kg on all rivers at all sites and tends to decrease, as figure 4 illustrates.

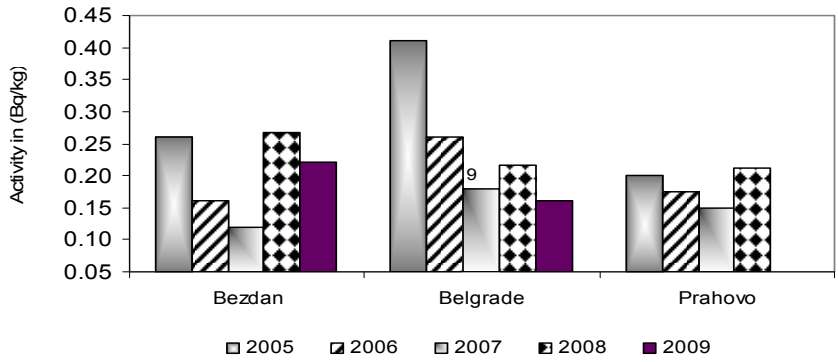


**Fig. 3. $^{90}$Sr activity concentration in sediments Danube river (mean annual values).**

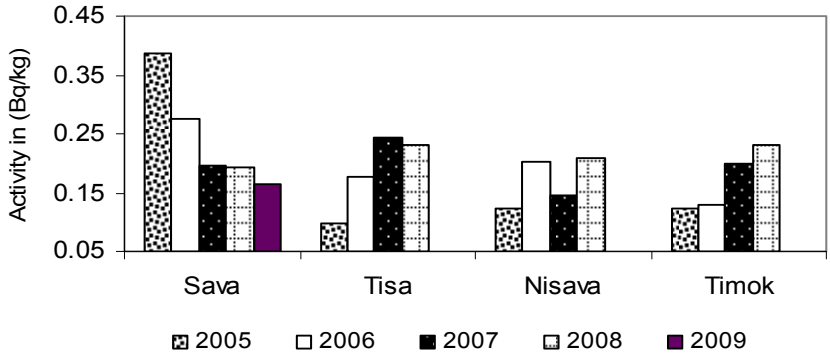


**Fig.4. $^{90}$Sr activity concentration in sediments Danube river (mean annual values).**

## Conclusions

By means of gamma spectrometry measurements of natural and artificial radionuclide as well as gross beta and $^{90}$Sr activity in sediments of rivers in Serbia it is possible to assess the sediment quality and its impact on the environment. The results of the measurements conducted during the period 2005-2009 are within normal limits. Artificial radionuclide activity tends to decrease as a result of dissolution, leaching and river flow changes.

## References

Brnovic R. $^{90}$Sr in the Environment, master thesis , Belgrade, 1972, in Serbian

Debertin K., Helmer R.G. Gamma and X-ray spectrometry with semiconductor detectors, North-Holand, Amsterdam-Oxford-New York-Tokyo, 1988

Pantelić G. Gamma spectrometer calibration with natural radioactive materials Nuclear Instrument and Methods in Physics Research, A 369, 1996, 572-573

# Radiocarbon and tritium activity in the environment of the National Park Plitvice Lakes

Horvatinčić, Nada; Barešić, Jadranka; Krajcar Bronić, Ines; Obelić, Bogomil
Rudjer Bošković Institute, Department of experimental physics, CROATIA

## Abstract

The disturbance of natural distribution of tritium ($^{3}H$) and radiocarbon ($^{14}C$) caused by thermonuclear weapon tests in the sixties of the last century made these isotopes very important tracers in environment. Their concentration can be also locally affected by fossil fuel combustion (decrease of $^{14}C$) or by various nuclear facilities (increase of $^{14}C$ and $^{3}H$). In our comprehensive study of the environment in the Plitvice Lakes National Park we measured $^{14}C$ in monthly samples of atmospheric $CO_2$ and $^{3}H$ in monthly precipitation in period 2003 – 2006. $^{14}C$ activity was also measured in the beech leaves and needles of spruce and abies collected as 1-year composite samples in the woods of the Plitvice Lakes area in 2005 and 2006. $^{14}C$ activity of monthly $CO_2$ samples vary between 101.5 and 109.6 percent of modern carbon (pMC) with slightly lower $^{14}C$ activities in winter months due to the influence of $CO_2$ from fossil fuel combustion. The values are similar to those measured in the city of Zagreb, which is a densely populated industrial center. The $^{14}C$ activities of tree leaves and needles are slightly higher than mean yearly atmospheric $^{14}C$ activities: the highest values have needles of abies (111 pMC, 110 pMC) and spruce (110 pMC, 109 pMC), followed by beech leaves (106 pMC, 105 pMC) and atmospheric $CO_2$ (104 pMC, 105 pMC). Higher $^{14}C$ activities of coniferous wood indicate that the collected needles represent an average of several years period while the $^{14}C$ of leaves of deciduous wood represent the mean $^{14}C$ from the growing period (spring-summer). $^{3}H$ activities of monthly precipitation showed seasonal fluctuations with maximum in summer (13 – 18 TU) and minimum in winter (0 – 5 TU), and are in good correlation with $^{3}H$ in the Zagreb precipitation. In conclusion, $^{14}C$ and $^{3}H$ in the atmosphere of the Plitvice Lakes area reflect the global trend of these isotopes in the atmosphere, and are at the same level as in highly populated area of Zagreb.

# $^{137}$Cs concentrations in Saimaa ringed seals during 2003–2009

Ylipieti, Jarkko; Solatie, Dina
[1] STUK – Radiation and Nuclear Safety Authority, Research and Environmental Surveillance, Regional Laboratory in Northern Finland, Lähteentie 2, FIN-9600 Rovaniemi, FINLAND

## Abstract

The Saimaa ringed seal (*Phoca hispida saimensis*) became isolated in Lake Saimaa at the end of the last ice age ca. 8000 years ago when the connection between Lake Saimaa and the Baltic Sea was broken. The Saimaa ringed seal is one of the very few seal species that live in inland waters. Due to climate change, however, the lack of an ice cover on the lake threatens to drastically decrease the seal population. The Saimaa ringed seal is an endangered species, with an estimated population of 260 seals, and it is protected by law.

As top predators in the aquatic food chain, fish-eating seals are vulnerable to the accumulation of contaminants. Seals are also important indicator species, which provide information about the current state of the environment. The aim of this study was to provide baseline data on radionuclide $^{137}$Cs concentrations in Saimaa ringed seals. Altogether 54 seals were collected in Lake Saimaa by the Metsähallitus Natural Heritage Services between the years 2003 and 2009. The seals had died of natural causes or accidentally by drowning. The seals were sampled under the supervision of the Finnish Food Safety Authority EVIRA. Concentrations of $^{137}$Cs were analysed in muscle, liver, kidney, bone, spleen and pancreas by the Radiation and Nuclear Safety Authority -STUK in Finland.

The mean radionuclide $^{137}$Cs concentrations in muscle, liver and kidney, bone, spleen and pancreas were 76.2, 65.3, 63.5, 75.4, 90.0 and 83.3 Bq/kg f.w., respectively. The highest $^{137}$Cs concentration, 180 Bq/kg f.w., was measured in 2004 and the lowest, 28.8 Bq/kg f.w., in 2009 in muscle tissue. The results indicate that the $^{137}$Cs concentrations in Saimaa ringed seals decreased consistently not only in muscle, but also in liver and kidney, during the study period. A similar trend was found in the correlation between seal weight and the $^{137}$Cs concentrations, which indicates high accumulation of $^{137}$Cs in this species.

## Introduction

The seals (*Phocida*) belong to high trophic level feeders that bioaccumulate many contaminants to a considerable extent. As top predators in the aquatic food chain, fish-eating seals are exposed to the accumulation of contaminants. Seals are also important indicator species, which provide information about the current state of the environment.

From the radiation protection point of view, $^{137}$Cs is the most significant anthropogenic radionuclide because of its 30-year half life and mobility in the environment and subsequent accumulation in food chains. The Chernobyl accident in Russia in 1986 deposited $^{137}$Cs fallout over large areas of Europe (AMAP 1998; Hamilton, 2004), including Lake Saimaa (Ylipieti et al.2008). The content of $^{137}$Cs varies clearly in different parts of Lake Saimaa, the amount of fallout in 1986 ranging between 3-6 kBq/m$^2$ (Saxen, 2001).

In this study the concentration of $^{137}$Cs in Saimaa ringed seals were analysed. The seal samples were collected in Lake Saimaa, which is a 4 400 square kilometer large freshwater lake situated in South East Finland (Fig. 1. ). Lake Saimaa is the largest lake in Finland. All 54 seals were collected by Metsähallitus from different sites in Lake Saimaa: Haukivesi, Orivesi, Puruvesi, Pihlajavesi and Saimaa between the years 2003 and 2009 (Fig. 2.). All the seals had died of natural causes or accidentally by drowning.

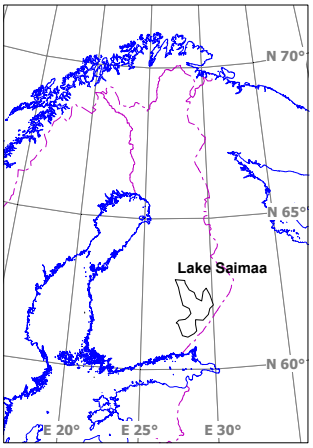


**Fig.1. Location of Lake Saimaa.**

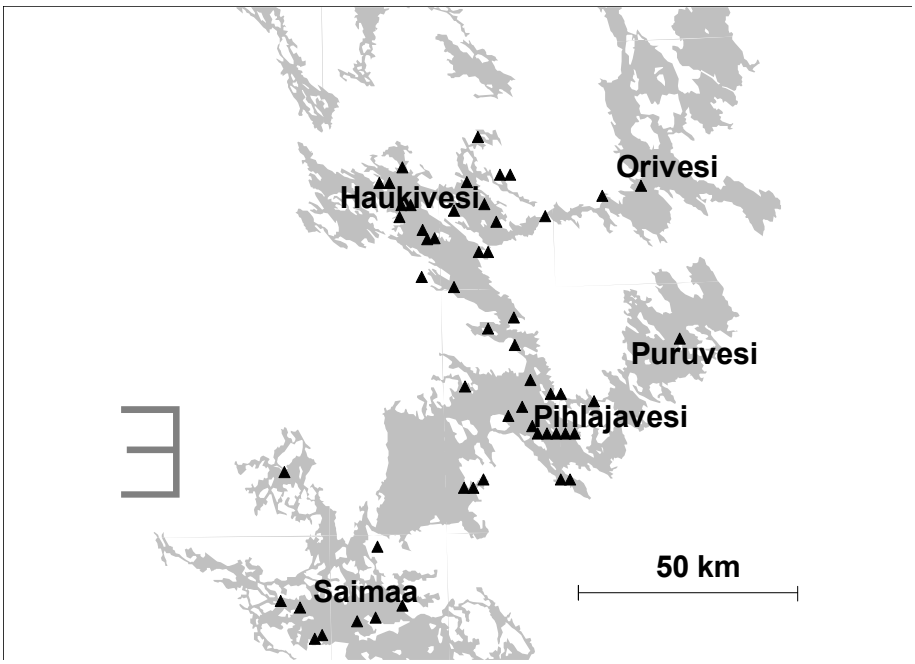


**Fig. 2. Locations of the sampled seals.**

## Material and methods

The seals were divided into two groups according to their age. Adult seals (n = 35) were over one year old and pups (n = 19) under one year, most of the pups being only a few months old (Kokkonen, 2006). Preparation of the seals was carried out under the supervision of personnel from the Finnish Food Service Authority EVIRA. $^{137}$Cs were analysed in muscle, liver, kidney, bone, spleen and pancreas by the STUK's Regional Laboratory in Northern Finland. A High-Purity Germanium (HPGe) detector with 30% relative effective was used in the analysis. The radioactivity concentration was determined using Gamma-99 software developed by STUK (Rantavaara et al., 1994).

## Results

### Muscle

$^{137}$Cs activity concentrations in muscle in adult and pup seals are presented in Table 1 and in the box plot in Fig. 3. Excluding 4 outlier points (2, 10, 11 and 23), the results show that the pups had almost similar $^{137}$Cs concentrations in muscle than adult seals. In general, $^{137}$Cs activity concentrations were below 100 Bq/kg f.w. Chernobyl-specific, short-lived $^{134}$Cs was still detectable in small amounts in two muscle samples (0.23 and 0.38 Bg/kg f.w.). The correlations between $^{137}$Cs concentrations and seal weight in adult seals are shown in Fig. 4.

**Table 1. $^{137}$Cs activity in muscle in adult and pups seals.**

**Descriptive Statistics**

| | N | Minimum | Maximum | Mean | Std. Deviation |
|---|---|---|---|---|---|
| adult_muscle | 35 | 31,0 | 180 | 78,1 | 36,0 |
| pup_muscle | 19 | 28,8 | 154 | 72,7 | 30,4 |

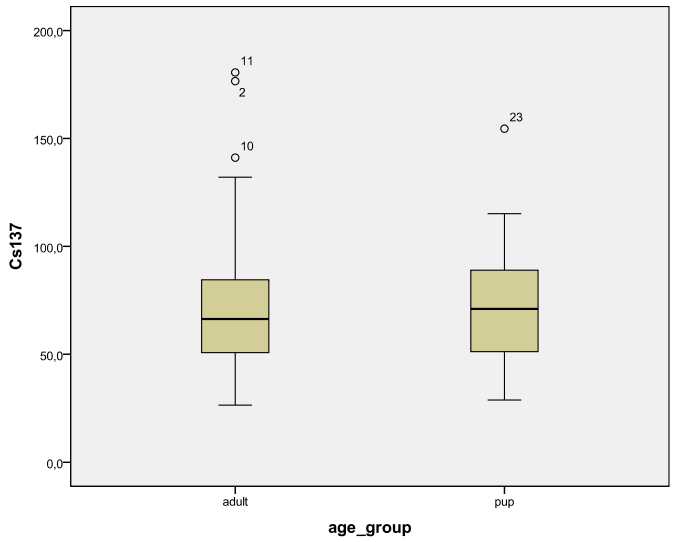


**Fig. 3. $^{137}$Cs concentrations in seal muscle in the two different age groups.**

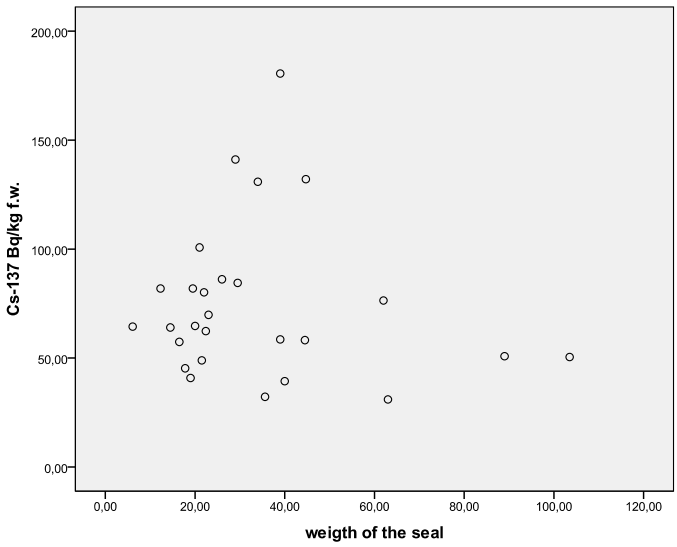


**Fig. 4. Correlations between $^{137}$Cs concentrations and seal weight in adult seals.**

## Liver

$^{137}$Cs activity concentrations in the liver samples were analysed in the same seals except for four adult seals and one pup seal. The results were at the same level and the same trend was observed as in the muscle samples Table 2. Pups were found to have almost similar $^{137}$Cs activity concentrations than adults, as seen in Fig. 5.

**Table 2. $^{137}$Cs activity in seal liver in adult and pup seals.**

**Descriptive Statistics**

| | N | Minimum | Maximum | Mean | Std. Deviation |
|---|---|---|---|---|---|
| adult_liver | 31 | 23,4 | 179 | 66,1 | 34,2 |
| pup_liver | 18 | 17,4 | 123 | 64,0 | 24,5 |

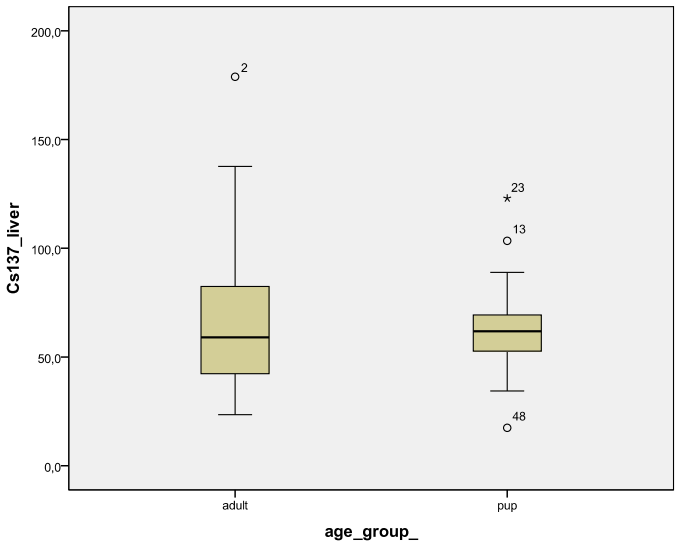


**Fig. 5. $^{137}$Cs concentrations in seal muscle in the two different age groups.**

### Kidney

$^{137}$Cs activity concentrations in the kidney samples are presented in Table 3. A small amount of Chernobyl-specific radionuclide $^{134}$Cs was still detected in one kidney sample (4.6 Bq/kg f.w.).

**Table 3. $^{137}$Cs activity in adult and pup seal kidney.**

**Descriptive Statistics**

| | N | Minimum | Maximum | Mean | Std. Deviation |
|---|---|---|---|---|---|
| adult_kidney | 31 | 21,0 | 167 | 60,1 | 31,9 |
| pup_kidney | 18 | 30,2 | 147 | 69,2 | 27,7 |

### Bone, spleen and pancreas

Some bone, spleen and pancreas were also analysed. The results are presented in Table 4. $^{137}$Cs concentrations in the spleen were at the same level in both adult and pups seals.

**Table 4. $^{137}$Cs activity in bone, spleen and pancreas in adult and pup seals.**

**Descriptive Statistics**

| | N | Minimum | Maximum | Mean | Std. Deviation |
|---|---|---|---|---|---|
| adult_bone | 4 | 25.9 | 92.1 | 66.2 | 29.3 |
| pup_bone | 1 | 112 | 112 | 112 | |
| adult_spleen | 14 | 33.8 | 159 | 89.6 | 40.5 |
| pup_spleen | 16 | 34.1 | 159 | 90.4 | 33.9 |
| adult_pancreas | 1 | 117 | 117 | 117 | |
| pup_pancreas | 1 | 50.0 | 50.0 | 50.0 | |

### Geographical distribution of the $^{137}$Cs in seal muscle in Lake Saimaa

The geographical distribution of $^{137}$Cs in seals muscle is presented in Fig. 6. Red bars indicate the mean concentrations in adult seals and yellow the mean concentrations in pups during 2003-2009. The fallout situation in 1986 and the $^{137}$Cs activity in seal muscle are combined in the same geographical context. Intensity of the gray shading indicates the magnitute of the fallout. (Arvela et al., 1990).

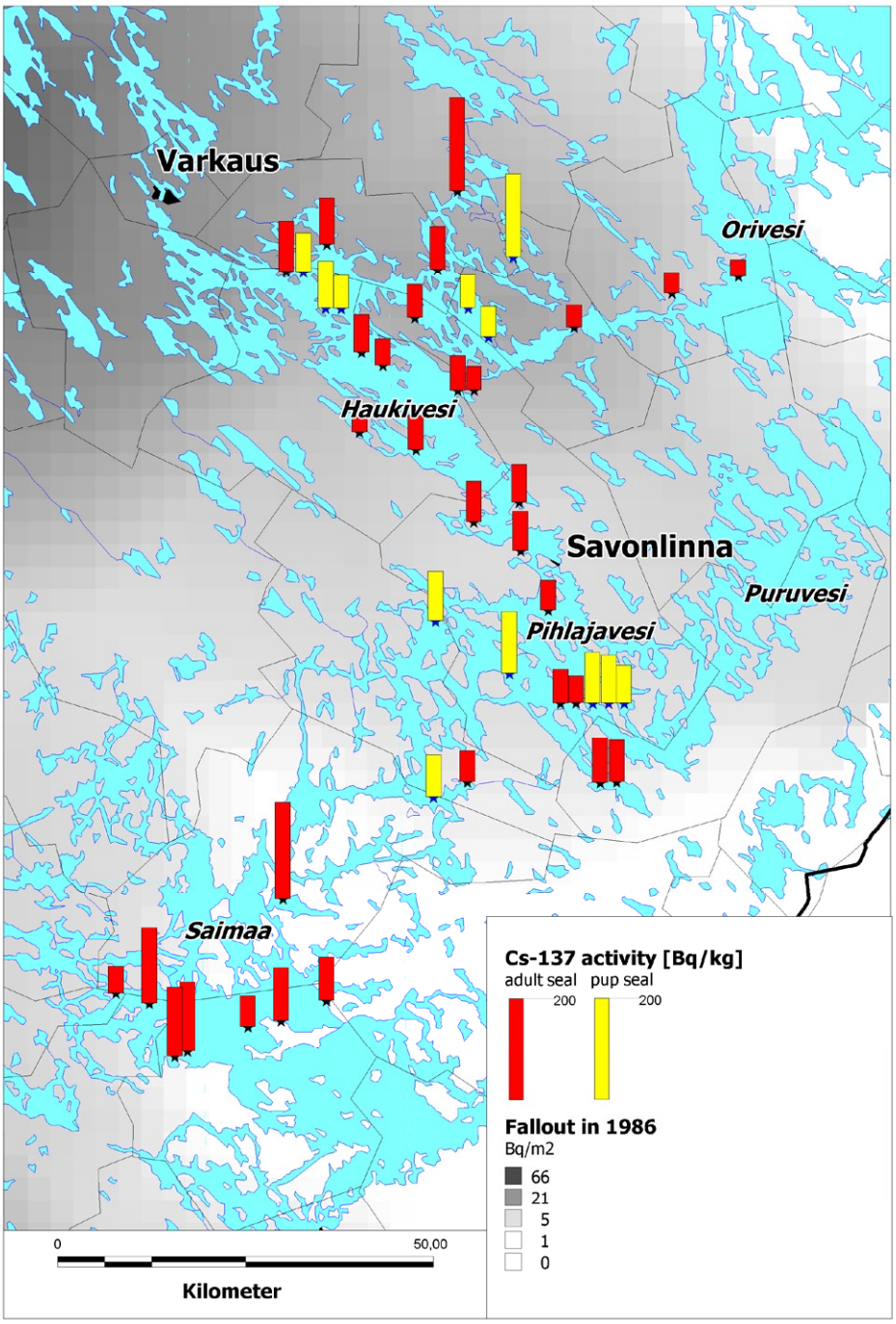


**Fig. 6. $^{137}$Cs activity in seal muscle and the level of Chernobyl fallout in 1986.**

### Changes in $^{137}$Cs concentrations over time

Changes in the $^{137}$Cs concentrations in time were observed in three tissues: muscle, liver and kidney (Fig. 7). One bar symbolizes the average minimum and maximum concentration per year. The $^{137}$Cs concentrations in adults and pups were combined.

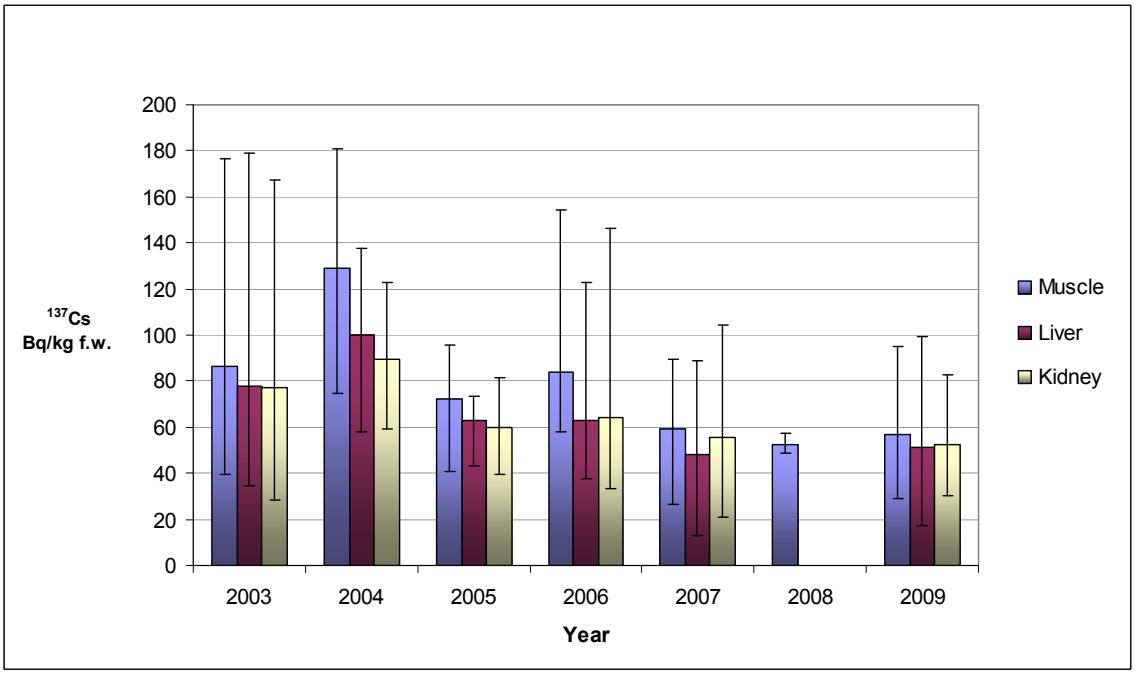


**Fig. 7. $^{137}$Cs concentrations in muscle, liver and kidney during 2003-2009.**

## Conclusions

Pups were found to have almost similar $^{137}$Cs activity concentrations in their tissues (muscle, liver and kidney) than adult seals. No clear correlation was found between seal weight and $^{137}$Cs activity in adults seals. This may be because the seals had been lying dead in the field for days or weeks before collection, with subsequent losses in their body weight. $^{137}$Cs activity concentrations were found to decrease regularly over time in the tissues.

The highest $^{137}$Cs concentration, 180 Bq/kg f.w., was found in muscle in adults seal. The mean concentration in muscle samples was 76.2 Bq/kg f.w, which is much higher than that in ringed seals from the Arctic Ocean, 0,21 Bq/kg f.w. (Carroll et al., 2002). This is due to the higher deposition from Chernobyl into Lake Saimaa than in the Arctic. The large variation in the $^{137}$Cs contents is due to the uneven fallout from Chernobyl. A small amount of Chernobyl-specific radionuclide $^{134}$Cs was detected in the same area where the fallout in 1986 was the highest, but the current $^{137}$Cs activity concentration does not seem to correlate with the geographical distribution of the fallout in the southern part of the lake.

## References

AMAP, 1998. AMAP assessment report: Arctic pollution issues. Arctic monitoring and assessment programme, (AMAP), Oslo, Norway, xii pp. 859.

Arvela H, Markkanen M, and Lemmelä H. Mobile survey of environmental gamma radiation and fallout levels in Finland after the Chernobyl accident. Radiation Protection Dosimetry 1990; 32, 3: 177-184.

Carroll JL, Wolkers H., Andersen M., Rissanen K., Bioaccumulation of radiocesium in Arctic seals. Marine Pollution Bulletin 2002; 44:1366-1371.

Hamilton, T.F., Linking legacies of the cold war to arrival of anthropogenic radionuclides in the oceans through the 20th Century. In Livingston, H.D. (Ed.), Marine Radioactivity 2004; 6 : 30-87.

Rantavaara A, Klemola S, Saxén R, Ikäheimonen T K, Moring M. Radionuclide analysis of environmental field trial samples at STUK, Report on Task FIN A 847 of the Finnish Support Programme to IAEA Safeguards. STUK-YTO-TR 75. Finnish Centre for Radiation and Nuclear Safety, Helsinki, Finland, 1994.

Saxen R., Koskelainen U. Effect of Site-Specific Parameters on the Transfer of 137Cs and 90Sr into Freshwater Fishes. Radichemistry 2001; 43, 5: 487-491.

Kokkonen Tuomo, personal communication, 2008

Ylipieti J., Rissanen, K., Kostiainen E., Salminen R., Tomilina O., Täht K., Gilucis A., Gregorauskiene V. Chernobyl fallout in the uppermost (0-3cm) humus layer of forest soil in Finland, North West Russia and the Baltic countries in 2000-2003. Science of The Total Environment 2008; 407, 1: 315-323.

# Radioactivity of $^{210}$Po in oysters collected in Taiwan

Lee, Hsiu-wei; Wang, Jeng-Jong; Chang, Bor-Jing
Institute of Nuclear Energy Research, Atomic Energy Council No. 1000, Wunhua Road, Jiaan Village, Longtan Township, Taoyuan County 32546, TAIWAN, R.O.C.

## Abstract

The Uranium-238 series decay product, polonium-210($^{210}$Po), exists widely in the environment and is well known to be enriched in the tobacco, animal's viscera and suspension particles in surface sea-water. Oysters are cultivated in great quantity along the coast of Taiwan, and it is one of the most favorite foods for the Taiwanese. The oysters intake the suspension particles in surface sea-water, and the $^{210}$Po is accumulated indirectly in them. It is necessary to evaluate the internal effective dose of $^{210}$Po coming from the intake of oysters by Taiwanese. In this study, oysters around the coast of Taiwan were collected, dried, spiked with a $^{209}$Po tracer for yield, and digested with concentrated $HNO_3$ and $H_2O_2$, and finally dissolved in 0.5 N HCl. The polonium was then spontaneously deposited onto a silver disc, and the activity of $^{210}$Po was measured using an alpha spectrum analyzer equipped with a silicon barrier detector. Meanwhile, the internal effective dose of $^{210}$Po coming from the intake of oysters by Taiwanese was evaluated.

## Introduction

Natural environmental radioactivity arises mainly from primordial radionuclides, such as $^{40}$K, and the radionuclides from the $^{232}$Th and $^{238}$U series. The major contribution to the radiation exposure received by mankind comes from natural sources. These include external sources such as cosmic rays and radiation from primordial radionuclides ($^{238}$U and $^{232}$Th) and their decay products in the environment. Information on the levels of naturally occurring radionuclides is important as they also contribute a substantial fraction of the radiation dose to the natural ecosystems (Holtzam, 1966).

A large contribution to the radiation dose received by humans comes from the naturally occurring uranium series radionuclides accumulated in the body, namely alpha-emitting $^{210}$Po (of physical half-life 138.4 days) and $^{210}$Pb (precursor of $^{210}$Po with physical half-life 22.2 years) (UNSCEAR, 1993). $^{210}$Po is reported to account for up to 75% of the alpha-radiation dose in marine organisms (McDonald, Fowler, Heyraud, & Baxter, 1986) and up to 50% of the internal alpha-radiation dose in people (Holtzman, 1966). In 1988, a report of the United Nations Scientific Committee on the Effects of Atomic Radiation indicated that $^{210}$Po is estimated to contribute about 7% of the total effective dose to man from ingested natural internal radiation (UNSCEAR, 1988). The polonium isotopes are amongst the most radiotoxic nuclides to human beings

(McDonald et al., 1986). The maximum permissible human body-burden for ingested $^{210}$Po is only $1.1\times 10^3$ Bq (CRC, 1982).

The main source of $^{210}$ Po in the environment is the gaseous $^{222}$ Rn, which escapes from the earth's crust into the atmosphere. The daughter products of $^{222}$ Rn are removed from the atmosphere with aerosol particles wet and dry deposition on the land surface and oceans (Skwarzec et al., 2001; Ladinskaya et al., 1973).

The main sources of $^{210}$Po in the human body are food and cigarette smoke (Parfenov, 1974; Holtzman, 1978; UNSCEAR, 1982). Intake of $^{210}$Po by food strongly depends on dietary habits. Polonium has an affinity for protein, enabling it to pass in significant quantities up the food chain. Thus, increased $^{210}$Po burdens are found in people who consume high-protein diets of meat or fish and other seafood(Watson, 1985; Carvalho, 1995; Skwarzec, 1995). UNSCEAR (2000) quotes a worldwide average annual intake of 58 Bq of $^{210}$Po in the diet. The value for annual $^{210}$Po intake in the typical European diet is 40 Bq; however, this is based on data from only five countries (Italy, Poland, Romania, Russia and the UK).

The radioactivity of $^{210}$Po had been measured in drinking and mineral water (Desideri et al., 2007a,b; Forte et al., 2007; Skwarzec et al., 2003, 2004; Vesterbacka, 2007)and cigarette but there are not much data for seafood , like oysters. The oyster is cultivated in great quantity along the coast of Taiwan, and it is one of the most favorite foods for the Taiwanese. The oysters intake the suspension particles in surface sea-water, and the $^{210}$Po is accumulated indirectly in them.

The aim of the present study was to provide information on the levels of natural radionuclides $^{210}$Po in samples of oysters products in different regions of Taiwan. The purpose of this work is to calculate the internal effective dose from $^{210}$Po for the individual local public through oysters ingestion.

## Experiment

### Sampling and pretreatment

The samples of oysters sampling from 6 Taiwanese regions, as shown in Fig. 1, were purchased from traditional consumer markets.

The fresh oysters were dried at 110 ℃ for 24 hours in the oven. A weighted dry oyster sample was transferred into a beaker, then a known activity of $^{209}$Po was spiked into the sample as a yield tracer. The oyster sample was digested with conc. $HNO_3$ and $H_2O_2$ solution. After the digested solution was evaporated to near dryness, the residue was then dissolved in 6 M HCl. The solution was filtered and the filtrate solution was then evaporated to near dryness. Finally, the residue was dissolved in 0.5 M HCl for deposited spontaneously. The process for the $^{210}$Po analysis is shown in Fig. 2.

### Spontaneous deposition

Polonium was spontaneously deposited onto a silver disk, from the 0.5 M hydrochloric solution in the presence of 1 g ascorbic acid (reduction of $Fe^{3+}$), at 90–95 ℃ in continuous for 4 hours. The spontaneous deposition plating apparatus for Po is shown in Fig3. The activities of $^{209}$Po and $^{210}$Po on the silver disk were measured by an alpha spectrometer equipped with semiconductor silicon detectors of surface barrier type. The

counting efficiency of the silicon detectors for $^{209}$Po and $^{210}$Po was about 40%. The polonium yields from the analyzed oysters samples ranged from 50% to 65% for 80000 s counting time.

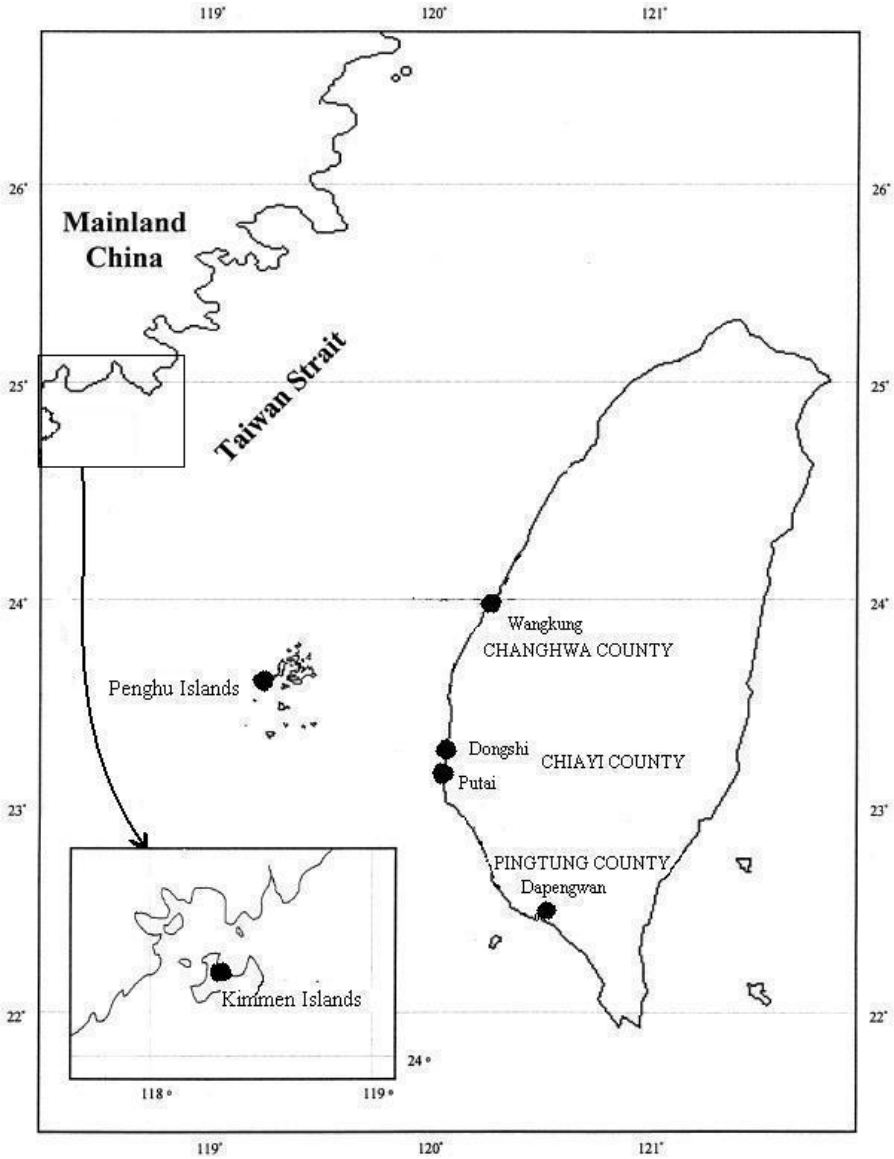


**Fig. 1. Sampling locations(● ) of oysters collected from different coastal areas in Taiwan.**

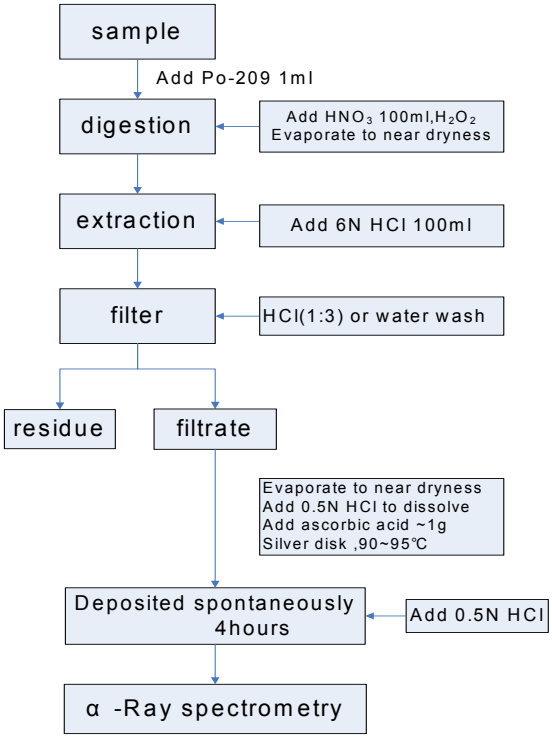


**Fig. 2. process for Po-210 Analysis.**

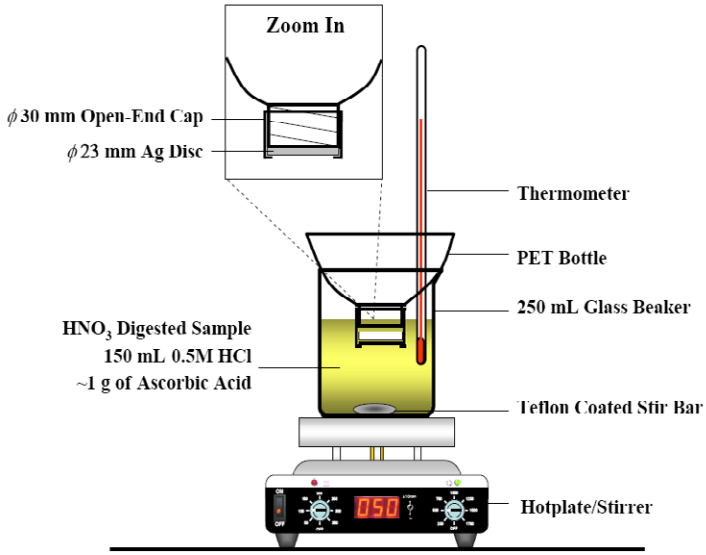


**Fig. 3. Po spontaneous deposition plating apparatus.**

## Results and discussion

### Radionuclide activity concentration

The $^{210}$Po activity concentrations for oysters sampling from 6 regions of Taiwan in our study are listed in Tables 1. The mean value of $^{210}$Po activity concentrations for all oyster samples studied is 50.1 Bq kg$^{-1}$ .The minimum activity concentration of $^{210}$Po (16.9 Bq kg$^{-1}$) was found for sample in Dongshi region. And, the maximum activity concentration of $^{210}$Po(193 Bq kg$^{-1}$) was found for sample in Penghu island region.

The annual production of oysters in Taiwan was about 30420 metric ton(Fisheries Agency,R.O.C. 2006,2007,2008), among which the production of oysters in Kinmen and Penghu islands regions were only 1.3%. The main 98.7% of oysters are produced around the Taiwan coastal areas. However, according to the study results in Table 1, the oysters coming from the Penghu islands and the Kimmen islands have the higher $^{210}$Po activity concentrations.

**Table 1. $^{210}$Po activity Concentration(BgKg$^{-1}$)in oysters.**

| Sample | $^{210}$Po Concentration(BgKg$^{-1}$) |
|---|---|
| Wangkung | 23.3 – 24.3 |
| Dongshi | 16.9 – 18.8 |
| Pudai | 28.8 – 31.5 |
| Dangpenwan | 27.6 – 29.5 |
| Penghu islands | 59.6 – 193.1 |
| Kimmen islands | 69.5 – 78.4 |
| Mean | 50.1 |

### Dose assessment

The internal effective dose of Taiwanese via ingestion of $^{210}$Po present in the oyster was calculated. Annual individual effective doses were calculated using the dose per unit ingestion conversion factors(ICRP-72, 1996) of 1.2 μSv Bq$^{-1}$for $^{210}$Po in the body. Based on the $^{210}$Po daily intake from oysters ingestion. The oysters consumption quantity was calculated by the average product of oysters in Taiwan from 2006 to 2008. The average product for three years of oysters in Taiwan was 30420 metric ton.

The internal dose of the ingestion for $^{210}$Po in oyster for Taiwanese can be calculated by Eq. (1) :

$$D = K^{\cdot} \quad G^{\cdot} \quad C \qquad (1)$$

where D is the effect dose via ingestion(Sv); K is the ingesting dose conversion factor of the $^{210}$Po radionuclide(1.2 μSv Bq$^{-1}$) (ICRP-72, 1996); G is the oysters consumption per year; here is 1.32 kg y$^{-1}$, which is calculated from the annual production of oyster in Taiwan divided by population of Taiwanese; and C is the mean activity concentration of the $^{210}$Po radionuclide(50.1 Bq kg$^{-1}$).

The annual ingestion (Bq y$^{-1}$) and the effective doses(mSv y$^{-1}$) of $^{210}$Po in oyster for Taiwanese were estimated and listed in Table 2. The annual ingestion and effective

dose of Taiwanese due to the $^{210}$Po in oysters were found to be in the range from 22.3 to 254.9 Bq $y^{-1}$ and $2.68\times10^{-2}$ to $3.06\times10^{-1}$ mSv $y^{-1}$, and the mean values of the annual ingestion and the effective dose for Taiwanese were 66.1 Bq $y^{-1}$ and $7.94\times10^{-2}$ mSv $y^{-1}$, respectively.

Taiwan Radiation Monitoring Center indicated that the annual effective dose for adults from natural background radiation in Taiwan is 1.62 mSv $y^{-1}$, including 0.90 mSv from external radiation exposure and 0.72 mSv $y^{-1}$ from internal radiation exposure. The natural radiation dose level is only about 2/3 of the global average(2.4 mSv $y^{-1}$) quoted in the UNSCEAR 1993 Report. The mean annual effective dose of Taiwanese due to the ingestion of $^{210}$Po in oysters was $7.94\times10^{-2}$ mSv $y^{-1}$; which is 11.0 % of the ingestion dose(0.72 mSv $y^{-1}$) and 4.9 % of the total effective dose(1.62mSv $y^{-1}$) of the Taiwanese.

**Table 2. Annual effective dose(mSv $y^{-1}$) of Taiwanese due to the ingestion of $^{210}$Po in oyster.**

| Locations | Annual ingestion of $^{210}$Po in oyster (Bg $y^{-1}$) | Annual dose (mSv $y^{-1}$) |
|---|---|---|
| Wangkung | 30.8 – 32.1 | $3.69\times10^{-2}$ – $3.85\times10^{-2}$ |
| Dongshi | 22.3 – 24.8 | $2.68\times10^{-2}$ – $2.98\times10^{-2}$ |
| Pudai | 38.0 – 41.6 | $4.56\times10^{-2}$ – $4.99\times10^{-2}$ |
| Dangpenwan | 36.4 – 38.9 | $4.37\times10^{-2}$ – $4.67\times10^{-2}$ |
| Penghu | 78.7 – 254.9 | $9.44\times10^{-2}$ – $3.06\times10^{-1}$ |
| Kimmen | 91.7 – 103.5 | $1.10\times10^{-1}$ – $1.24\times10^{-1}$ |
| Mean | 66.1 | $7.94\times10^{-2}$ |

## Conclusion

The $^{210}$Po activity in the different Taiwan regions were determined. The results indicated that the oysters coming from Penghu island and Kinmen island regions contain higher concentrations of $^{210}$Po in comparison with oysters from other regions, in spite of the oyster production of these two regions were just about 1.3 % of the total amount of Taiwanese oysters.

The mean annual ingestion and effective dose of Taiwanese due to the ingestion of $^{210}$Po in oysters were 66.1 Bq $y^{-1}$ and $7.94\times10^{-2}$ mSv $y^{-1}$; which is 11.0 % of the ingestion dose(0.72 mSv $y^{-1}$) and 4.9 % of the total effective dose(1.6mSv $y^{-1}$) of the Taiwanese.

## References

CRC Handbook of Chemistry and Physics. (1982). In: R.C. Weast, M.J. Astle (Eds.), (62nd ed.) Boca Raton, FL: The Chemical Rubber Company Press Inc. Gairola, C. G., Wu, H., Gupta, R. C., & Diana, J. N. (1993). The mainstream and sidestream cigarette-smoke induced DNA adducts in C7B1 and DBA mice. Environmental Health Perspective, 99, 253–261.

Desideri, D., Roselli, C., Feduzi, L., Meli, M.A., 2007a. Radiological characterization of drinking waters in Central Italy: methods and results. Microchemical Journal 87, 13–19.

Desideri, D., Meli, M.A., Feduzi, L., Roselli, C., Rongoni, A., Saetta, D., 2007b. $^{238}$U, $^{234}$U, $^{226}$Ra, $^{210}$Po, concentrations of bottled mineral waters in Italy and their dose contribution. Journal of Environmental Radioactivity 94, 86–97.

Forte, M., Rusconi, R., Cazzaniga, M.T., Sgorbati, G., 2007. The measurement of radioactivity in Italian drinking waters. Microchemical Journal 85 (1), 98–102.

Fisheries Agency,R.O.C.,Taiwan Fisheries Yearbook,2006.(In Chinese).

Fisheries Agency,R.O.C.,Taiwan Fisheries Yearbook,2007.(In Chinese).

Fisheries Agency,R.O.C.,Taiwan Fisheries Yearbook,2008.(In Chinese).

Holtzman, R. B. (1966). Natural levels of lead-210, polonium-210 and radium-226 in humans and biota of the arctic. Nature, 210, 1094–1097.

International Commission on Radiological Protection,1996. Age-dependent doses to the members of the public from intake of radionuclides. Part 5, Compilation of Ingestion and Inhalation Coefficients, 72

Ladinskaya L.A., Parvenov Y.D., Popou D.K., Fedorova A.V., $^{210}$ Pb and $^{210}$ Po content in air, water, foodstuffs, and the human body, Archives of Environmental Health, Volume: 27, (1973), pp. 254-258

McDonald, P., Fowler, S. W., Heyraud, M., & Baxter, M. S. (1986). Polonium-210 in mussels and its implications for environmental alpha-autoradiography. Journal of Environmental Radioactivity, 3, 293–303

Parfenov, Y. D. (1974). Polonium-210 in the environment and in the human organism. Atomic Energy Review, 12, 75–143.

Skwarzec B., Ulatowski J., Struminska D.I., Borylo A., Inhalation of $^{210}$ Po and $^{210}$ Pb from cigarette smoking in Poland, Journal of Environmental Radioactivity, Volume: 57, (2001), pp. 221-230

Skwarzec, B., Struminska, D.I., Borylo, A., 2003. Radionuclides of $^{210}$Po, $^{234}$U and $^{238}$U in drinking bottled mineral water in Poland. Journal of Radioanalytical and Nuclear Chemistry 256 (2), 361–364.

Skwarzec, B., Struminska, D.I., Borylo, A., Falandysz, J., 2004. Intake of $^{210}$Po, $^{234}$U and $^{238}$U radionuclides with beer in Poland. Journal of Radioanalytical and Nuclear Chemistry 261 (3), 661–663.

UNSCEAR (1982)–United Nations Scientific Committee on the effects of atomic radiation. Ionizing radiation: sources and effects. New York: United Nations.

UNSCEAR (1988)–United Nations Scientific Committee on the effects of atomic radiation. Source, effect and risk of ionizingradiation. New York: United Nations.

UNSCEAR (1993)–United Nations Scientific Committee on the effects of atomic radiation. Source and effects of ionizingradiation. New York: United Nations.

UNSCEAR (2000)–United Nations Scientific Commettee on the Effects of Atomic Radiation, 2000. Ionizing: Sources and Effects of Ionising Radiation, New York. Report to the General Assembly with Annex.

Vesterbacka, P., 2007. Natural radioactivity in drinking water in Finland. Boreal Environment Research 12 (1), 11–16.

# Natural alpha emitting radionuclides in bottled drinking water, mineral water and tap water

Benedik, Ljudmila; Jeran, Zvonka
Jožef Stefan Institute, Jamova 39, SI-1000 Ljubljana, SLOVENIA

## Abstract

Quantitative information about the activity concentrations of critical alpha- emitting radionuclides in food and drink is important in the study of cumulative radiation effects on human health. In most countries there is an increasing tendency to replace tap water by consumption of commercial bottled natural and mineral water. Furthermore, various beverages as well as dietary supplements are also prepared from mineral water, not ordinary tap water. In this work tap water and bottled drinking and mineral water were collected in Slovenia and analysed in order to assess the radiation doses from $^{238}U$, $^{234}U$, $^{226}Ra$ and $^{210}Po$. On the basis of radionuclide activity concentrations the internal radiation doses to individuals were assessed and are discussed together with the contribution of each particular radionuclide to the dose.

## Introduction

In most European countries, there is an increasing tendency in population to replace tap water of satisfactory quality for human consumption with commercial bottled natural and mineral water. Moreover, various beverages are also prepared from mineral water, not ordinary tap water. Systematic studies on radiological characterisation of drinking water started after 1993, when the recommendations of the Guidelines for drinking water quality, issued by the World Health Organisation were published (WHO, 1993). These guidelines state that drinking water is safe from the radiological point of view if within the range of normal consumption (2 L per day), the annual dose rate originating from the presence of radioactive nuclides does not exceed 0.1 mSv. UNSCEAR reports (UNSCEAR, 1998, 2000) estimated that exposure to natural sources contributes more than 98 % of the radiation dose to the population (medical treatment is not taken into account). The main contribution to dose is largely due to the presence of naturally occurring radionuclides of both the uranium and thorium decay series. Due to their high radiotoxicity, the contributions of $^{210}Po$ and $^{228}Ra$ to the dose are more pronounced. The dose contributions of the radionuclides are in the order: $^{210}Po > {}^{228}Ra > {}^{210}Pb > {}^{226}Ra > {}^{234}U > {}^{238}U > {}^{224}Ra > {}^{235}U$. Increased concerns concerning the radiological quality of drinking water has led to an increased demand for real data assessment. The old drinking water regulation 980/778/EEC from 1980 (EC, 1980) in which neither radioactivity nor uranium were mentioned, were replaced by the European Directive 98/83/EC in 1998 (EC,1998). In this Directive, the reference dose level of committed annual effective dose

due to drinking water consumption is 0.1 mSv. The Directive points out that the total indicative dose must be evaluated excluding tritium, $^{40}K$, $^{14}C$, radon and its decay products, but including all other radionuclides of the natural decay chains. The maximum values for radon and long-lived radon decay products such as $^{210}Pb$ and $^{210}Po$ are proposed in the European Commission Recommendation 2001/928/Euratom (EC, 2001). Uranium is covered by the Directive, although its contribution to the dose is minor due its small dose conversion factor. However, uranium is a toxic heavy metal and therefore has to be regulated and controlled. The WHO set the most stringent limitation of 2 µg/L in its 1998 report (WHO, 1998), but later (WHO, 2004) changed this limit to 15 µg/L; the USA (EPA, 2000) set the limit to 20 µg/L. Recently, Germany set the uranium limit of 2 µg/L for mineral water considered suitable for infants (Bundesgesetzblatt, 2006). Considering the importance of water for human consumption, its quality has to be assured and regularly controlled. The assessment of the radiological quality of natural or bottled drinking and mineral waters is also important in view of assessment and reduction of the radiation exposure of the population. For practical purposes, the recommended screening levels for drinking water below which no further actions are required are 0.1 Bq/L for gross alpha activity and 1 Bq/L for gross beta activity. If these values are exceeded, determination of particular radionuclides dissolved in drinking water needs to be performed. In 2004, the WHO published the third edition of its guidelines for drinking water (WHO, 2004) in which the recommended screening level for gross alpha activity was increased from 0.1 to 0.5 Bq/L. Due to the increasing tendency in the consumption behaviour of the population to replace surface tap water of sufficient quality for human consumption with commercial bottled drinking natural and mineral water, several studies to assess the radioactivity levels in bottled drinking and mineral water were performed around Europe. The report of Weknow (Weknow, 2005) gave a good overview of radioactivity levels found in drinking water across Europe, while data on drinking water quality in Slovenia are very scarce.

The experimental design of our study was to determine the activity concentrations of the alpha emitters $^{238}U$, $^{234}U$, $^{226}Ra$ and $^{210}Po$ in Slovenian bottled drinking and mineral water, as well as in tap water. The studied samples included bottled drinking and mineral water purchased in the period from October 2009 to March 2010, on the market in Ljubljana. All water samples originated from Slovenia. There are many companies in Slovenia producing natural drinking and mineral water from bedrock aquifers of different depths. Tap water was collected from chosen cities in Slovenia.

## Materials and methods

For this study we analysed three of the most frequently sold mineral waters and eight bottled drinking waters “from the shelf”. We also analysed six tap waters (Fig.1). All reagents used in the analysis were of analytical grade. The tracer solutions ($^{232}U$, $^{209}Po$, $^{133}Ba$) used in the study were prepared from calibrated solutions purchased from Analytics, Inc. (Atlanta, GA, USA). The producer maintains traceability to NIST standards.

An alpha spectrometer (EG&G ORTEC) with a passivated implanted planar silicon (PIPS) semiconductor detector with an active area of 450 $mm^2$ and 28% efficiency for a 25 mm diameter disc was used for alpha-particle spectrometric measurements. The calibration of the detector was made with a standard radionuclide source, containing $^{238}U$, $^{234}U$, $^{239}Pu$ and $^{241}Am$ (code: 67978-121), obtained from Analytics, Inc. A coaxial HP Ge detector was used for measurements of the gamma emitting nuclide $^{133}Ba$.

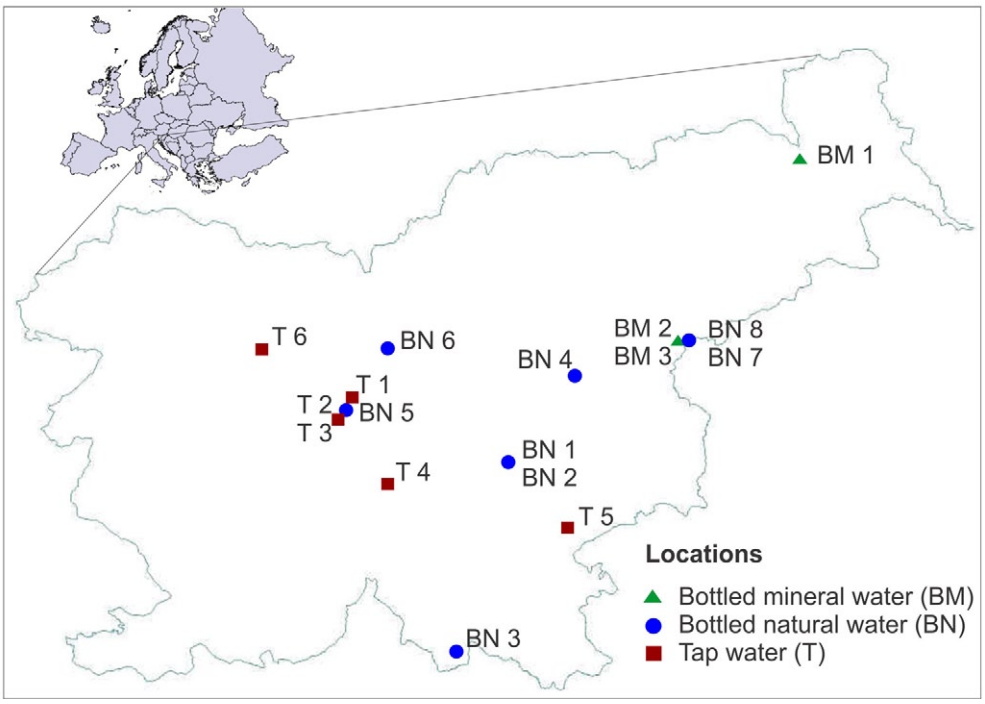


**Fig. 1. Locations of tap water and bottling facilities of selected natural and mineral waters from Slovenia.**

For determination of uranium radioisotopes a known amount of $^{232}U$ tracer (~ 0.5 Bq) was added to the water sample which was acidified with concentrated $HNO_3$ (3mL of acid per 1L of sample). Uranium was preconcentrated from the water samples by coprecipitation with iron(III) hydroxide at pH 9-10 using an ammonia solution. The precipitate was separated by centrifugation, washed with distilled water and dissolved in concentrated nitric acid. The solution was adjusted with distilled water to 3M $HNO_3$ and loaded onto a UTEVA column (Eichrom Industries Inc.) (Horwitz et al., 1993) pre-conditioned with 5 mL 3M $HNO_3$. The column was then washed with 3M $HNO_3$. Thorium radioisotopes were stripped from the column with 9M and 5M HCl. Uranium radioisotopes were eluted with 15 mL 1M HCl. The microcoprecipitation method with neodymium fluoride was used for thin source preparation in the alpha spectrometric determination (Hindman, 1983, Sill and Williams, 1981). The neodymium fluoride suspension was filtered through a 25 mm diameter 0.1 µm polypropylene filter. The dry filter was mounted on a stainless steel disc.

The analytical scheme for determination of $^{226}Ra$ was adapted from Lozano et al. (Lozano et al., 1997). The procedure is based on coprecipitation of $Pb(Ra)(Ba)SO_4$. The water sample was transferred to a glass beaker and acidified with concentrated $H_2SO_4$ (10 mL of sulphuric acid per 1L of sample). After addition of $^{133}Ba$ tracer together with Ba-carrier, the sample was stirred for approximately 30 min. With stirring, 30 mg $Pb^{2+}$ was added in portions to allow good coprecipitation of radium and barium. After settling, the suspension was centrifuged and washed with distilled water. The $PbSO_4$ precipitate containing radium and barium was dissolved in 4 mL 0.1M EDTA, prepared in 0.5M NaOH. For $^{226}Ra$ determination 250 µg of 0.3 mg/mL $Ba^{2+}$ solution was added together with 4 mL of saturated $Na_2SO_4$ solution. With stirring, 1:1

acetic acid solution was added until pH 4–5 was reached, thus precipitating $BaSO_4$, while $Pb^{2+}$ ions remained in solution. Immediately after, 0.2 mL of a 0.125 mg/mL $BaSO_4$ suspension was added, acting as a seeding precipitate to obtain small particles. The suspension was allowed to settle for 30 min and filtered through a 25 mm 0.1µm polypropylene filter. The filter with $BaSO_4$ deposit was dried and mounted on a stainless steel disc and measured by γ–ray spectrometry for $^{133}Ba$ yield determination and by α–particle spectrometry for determination of $^{226}Ra$.

For determination of $^{210}Po$ in water, $^{209}Po$ (~ 0.3 Bq) tracer was added to 9 L of water. After sample acidification with concentrated HCl (2 mL of acid per 1 L of sample), the radionuclides were coprecipitated with $MnO_2$. Precipitation of $MnO_2$ was achieved by adding $KMnO_4$ and $MnCl_2$ and adjusting the pH to 9 with ammonia solution. The precipitate was then dissolved with a mixture of HCl and $H_2O_2$, and adjusted with distilled water to pH 1. To prevent co-plating of other potentially interfering ions ($Fe^{3+}$, $Mn^{6+}$), 0.5 g of ascorbic acid was added. The spontaneous deposition of polonium on a 19 mm diameter silver disc was carried out at 90 °C for 4 hours. The Ag disc, covered on one side, was fixed in a holder and immersed in the solution (Benedik and Vreček, 2001). Polonium radioisotopes were then measured by alpha spectrometry.

Based on the results of activity concentrations of the four alpha emittors in drinking water presented in Table 1, the internal doses (committed effective dose) for an adult were estimated using an annual consumption rate of 730 L/year accoording to the WHO Guidelines for Drinking Water Quality (2004) and the dose coefficients of the relevant radionuclides from the "International Basic Safety Standards for Protection against Ionizing Radiation and for Safety of Radiation Sources" (IAEA, 1996).

## Results and discussion

In Table 1 the results of the activity levels of $^{238}U$, $^{234}U$, $^{226}Ra$ and $^{210}Po$ in three different groups of drinking water, natural and mineral bottled water and tap water, are given. As seen the activity concentrations of uranium in the water samples analysed ranged from 1.1–57 mBq/L and 2.8–173 mBq/L for $^{238}U$ and $^{234}U$, respectively. These values, except for the mineral water BM2 (57 and 173 mBq/L for $^{238}U$ and $^{234}U$, respectively) were relatively low, comparable with some literature data from Italy (Jia and Torri, 2007) and well below the limit values (98/83/EC, 2004, WHO,2004). The lowest absolute values were found in tap waters; however, somewhat elevated levels were measured in three bottled natural waters originating from the east (BN1, BN2) and south (BN3) of the country.

$^{226}Ra$ (Table 1) was in the range between 0.14–31.7 mBq/L and like uranium, can be regarded as low and comparable with data reported for Europe (Weknow, 2005). The highest absolute level of 32 mBq/L was found in a bottled natural water (BN1) which also had an elevated uranium level. Elevated activity concentrations higher than 10 mBq/L were found in two mineral (BM2, BM3) and two bottled natural waters (BN7, BN8) coming from the same region in the eastern part of the country (Fig.1), known for its thermal and mineral springs and spas. With the exception of one sample (T4), tap water had low levels of $^{226}Ra$ in a narrow range between 0.3-and 1.4 mBq/L.

**Table 1. Radionuclide activity concentrations (mBq/L) in natural and mineral bottled water and tap water collected in Slovenia.**

| Sample | Type of sample | U-238 | U-234 | Ra-226 | Po-210 |
|---|---|---|---|---|---|
| BN1 | **Natural water** | **28 ± 3** | **71± 8** | **32 ± 4** | 1,1 ± 0,4 |
| BN2 | | 18 ± 1 | 57 ± 6 | 11 ± 1 | 2,1 ± 0,3 |
| BN3 | | 13 ± 2 | 15 ± 2 | 1,7 ± 0,2 | 0,9 ± 0,2 |
| BN4 | | 2,2 ± 0,5 | 3,5 ± 0,7 | 2,3 ± 0,3 | 0,43 ± 0,12 |
| BN5 | | 8,3 ± 1,1 | 12 ± 1 | 0,14 ± 0,05 | 2,0 ± 0,4 |
| BN6 | | 2,9 ± 0,5 | 13 ± 2 | 6,8 ± 0,8 | 1,2 ±0,3 |
| BN7 | | 5,1 ± 0,6 | 14 ± 2 | 16 ± 2 | 0,24 ± 0,07 |
| BN8 | | 4,2 ± 0,6 | 8,7 ± 1,2 | 15 ± 2 | 0,6 ± 0,2 |
| BM1 | Mineral water | 1,1 ± 0,2 | 2,8 ± 0,5 | 2,4 ± 0,3 | 0,39 ± 0,11 |
| BM2 | | **57 ± 9** | **173 ± 28** | 12 ± 2 | 1,0 ± 0,3 |
| BM3 | | 5,2 ± 1,8 | 12 ± 2 | 17 ± 2 | 0,6 ± 0,1 |
| T1 | Tap water | 7,2 ± 0,7 | 8,5 ± 0,8 | 1,0 ± 0,2 | 0,25 ± 0,06 |
| T2 | | 4,8 ± 0,9 | 6,9 ± 1,1 | 0,47 ± 0,10 | 1,0 ± 0,2 |
| T3 | | 6,7 ± 1,1 | 11 ± 2 | 1,3 ± 0,1 | 0,77 ± 0,16 |
| T4 | | 8,2 ± 2,8 | 8,8 ± 2,9 | 15 ± 2 | 1,1 ± 0,2 |
| T5 | | 7,0 ± 0,9 | 11 ± 1 | 1,4 ± 0,1 | 1,8 ± 0,4 |
| T6 | | 1,1 ± 0,3 | 3,0 ± 0,5 | 0,30 ± 0,03 | 0,67 ± 0,19 |

Among the alpha emitters analysed $^{210}$Po has the lowest activity concentrations in the range between 0.24-2.1 mBq/L in all three groups of drinking water.

In Fig.2 the results of the calculated total effective doses (µSv/a) for adults drinking different types of water are presented. It is seen that doses are on average very low, in the range of 1-11 (µSv/a) and only by drinking for a whole year one mineral (BM2) or one natural bottled water (BN1) would the person obtain a dose higher than 10 µSv/a, which still represents only one tenth of the recommended reference dose level (RDL) of 0.1 mSv from 1 year´s consumption of drinking water (EC 1998).

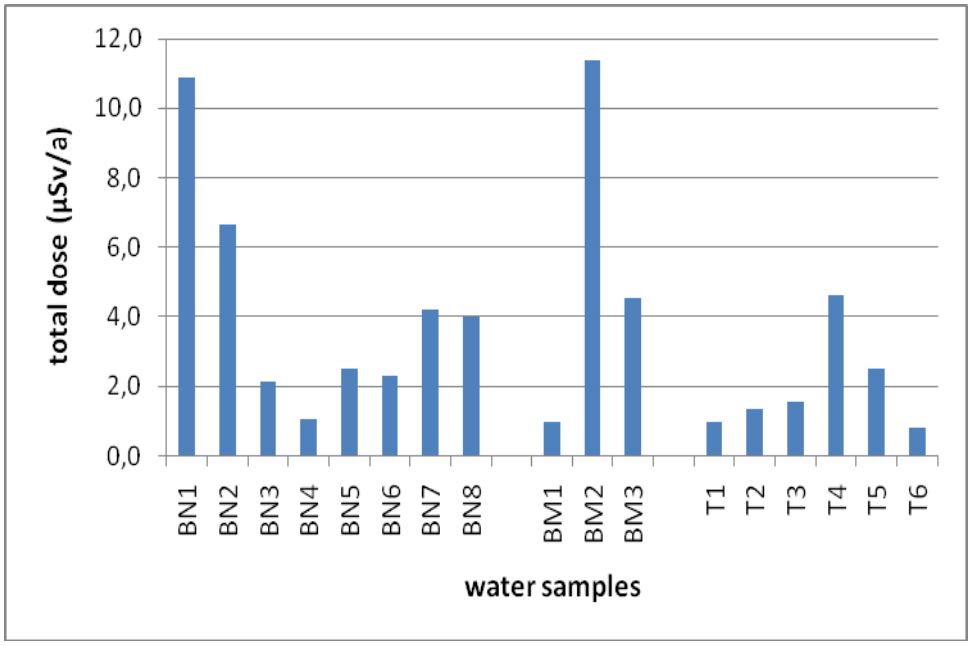


**Fig. 2. Total internal dose ( µSv/a) to adult member of the public due to drinking different types of water.**

The contribution of each analysed radionuclide to the annual total internal dose varies among different types of water samples, but on average in natural bottled waters the contributions were in the order $^{226}$Ra (mean: 46 ± 28%) > $^{210}$Po (27 ± 22%) > $^{234}$U (19 ±8%) >$^{238}$U (8 ± 6%) (Fig.3). In mineral water the order was similar (Fig.3). Only in the mineral water BM2 did $^{234}$U contribute more than 54%, followed by $^{226}$Ra (22 %), $^{238}$U (16%) and $^{210}$Po (8%). In tap water $^{210}$Po (mean: 48 ± 23%) was the main radionuclide contributing to total dose due to its high dose conversion factor.

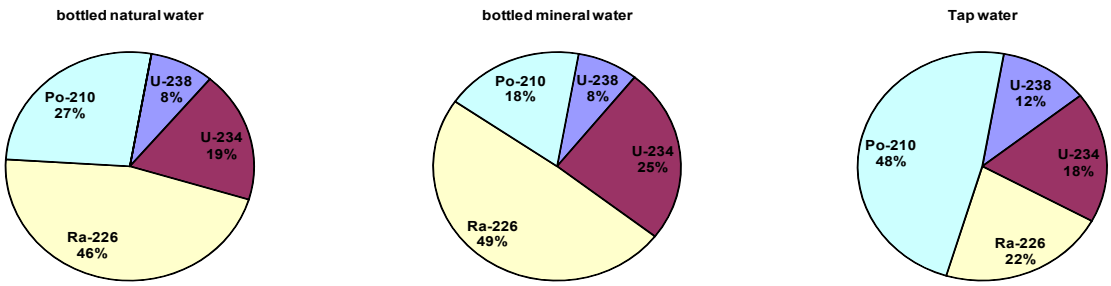


**Fig. 3. The average contribution (%) of alpha radionuclides to internal commited effective doses to adult members of the public drinking different types of water.**

## Conclusions

The present study was a pilot study where only four selected alpha emitters were analysed in different drinking waters from Slovenia. From the survey it is evident that the activity concentrations, with the exception of one mineral and two natural drinking waters, were very low also leading to low calculated internal doses which constitute only a few percent of the recommended reference dose level (RDL) of 0.1 mSv. However, beside the analysed radionuclides there are also some other radio isotopes, namely the long- lived radon decay products $^{210}$Pb and $^{228}$Ra, which both have high dose conversion factors and should be determined and included in dose estimations in the future.

## References

Benedik, L., Vreček, P. Determination of $^{210}$Pb and $^{210}$Po in environmental samples. Acta Chimica Slovenica,2001, 48, p. 199-213.

Bundesgesetzblatt Nr. 56. Seite 2762 (2006) Deutche Mineral und Tafelwasserverordnung, 2006.

Environmental Protection Agency (EPA) December 7, 2000. Proposed drinking water Standards. US EPA 65 FR 76707, 2000.

European Commission (EC), Council Directive of 15 July 1980 relating to the quality of water intended for human consumption. Official Journal of the European Communities L. 229, 30.8.1980, p. 11-29, 1980.

European Commission (EC), Council Directive 98/83/EC of 3 November. The quality of water intended for human consumption. Official Journal of the European Communities L. 330, 5.12.1998, p. 32-54, 1998.

European Commission (EC), Commission Recommendation of 20 December on the protection of the public against exposure to radon in drinking water supplies, 2001/928/EURATOM. L.344, 28.12.2001, p. 85-88, 2001.

Hindman, F.D. Neodymium Fluoride Mounting for Alpha Spectrometric Determination of Uranium, Plutonium and Americium, Anal. Chem., 1983, 55, 2460-2461

Horwitz, E.P., Chiarizia, R., Dietz, M.L., Diamond, H. Separation and preconcentration of actinides from acidic media by extraction chromatography. Anal. Chim. Acta, 1993, 281, p. 361-372.

International Atomic Energy Agency (IAEA). International Basic Safety Standards for Protection against Ionizing Radiation and for the Safety of Radiation Sources. Safety Report Series, No. 115, Vienna, 1996.

Jia, G., Torri, G. Estimation of radiation doses to members of the public in Italy from intakes of some important naturally occurring radionuclides ($^{238}$U, $^{234}$U, $^{235}$U, $^{226}$Ra, $^{238}$Ra, $^{224}$Ra and $^{210}$Po) in drinking water. Applied Radiation and Isotopes 65 (2007) 849-857.

Sill, C.W., Williams, R.L. Preparation of Actinides for Alpha Spectrometry without Electrodeposition, Anal. Chem., 1981, 53, p. 421-415.

United Nations Scientific Committee on the Effects of Atomic Radiation (UNSCEAR), Sources and Effects of Ionising Radiation, United Nations, New York; 1998.

United Nations Scientific Committee on the Effects of Atomic Radiation (UNSCEAR), Sources and Effects of Ionising Radiation, United Nations, New York; 2000.

WEKNOW/ENDWARE, (Weknow, 2005), Radioactivity in European Drinking Water and Sources Designated for the Production of Drinking water, Available from: http://www.weknow-waternetwork.com/uploads/booklets/04__radioactivity_eu_drw_verjuni2005.pdf, 2005.

World Health Organization (WHO), Guidelines for Drinking Water Quality, Recommendation, second edition, vol. 1. WHO, Geneva; 1993.

World Health Organisation (WHO), Health Criteria and Other Supporting Information. In: Guidelines for Drinking-Water Quality, second ed., Addendum to vol. 2, WHO, Geneve, 1998.

World Health Organisation (WHO), Guidelines for Drinking Water Quality. WHO, Geneve, Available from: http://www.who.int/water_sanitation_health/, 2004.

# Radiation protection of the public and the environment: long-term, large-scale radioecological monitoring by spruce needles

Seidel, Claudia[1]; Gruber, Valeria[1]; Maringer, Franz Josef[2]
[1] University of Natural Resources and Applied Life Science, Low-Level Counting Laboratory Arsenal, AUSTRIA
[2] BEV – Federal Office of Metrology and Surveying, AUSTRIA

## Abstract

In a two years radioecological study spruce needle samples of the Austrian Bioindicator Grid collected between 1984 and 2008 were analysed retrospectively by low-level gamma-ray spectrometry to investigate the geographical and temporal distribution of radionuclides in spruce needles of the last 25 years. Main focus was the development of the radioactive contamination before and after the Chernobyl fallout 1986. Overall more than 750 spruce needle samples of selected locations – well distributed among the area of Upper Austria – were analysed for different natural and anthropogenic radionuclides: Cs-137, K-40, Pb-210, Ra-226, Ra-228, U-238. Additionally soil samples were taken at selected sites to estimate transfer factors to describe the transfer of radionuclides from soil to spruce needles. On the basis of the measured Cs-137 activity concentrations in the spruce needles and soil samples estimations are carried out, how to use the Bioindicator spruce needles for environmental radioactivity monitoring. Hence the detection limits for additional Cs-137 deposits (Bq/m²) in spruce needles samples are estimated at various locations. Furthermore the results have been integrated into an existing environmental surveillance programme in Upper Austria.

# Slovenian experience with inconsistencies in the global contamination monitoring results

Cindro, Michel; Vokal Nemec, Barbara; Križman, Milko
Slovenian Nuclear Safety Administration, SLOVENIA

## Abstract

Introduction Monitoring of the global radioactive contamination due to atmospheric nuclear bomb tests (1951-1980) and the Chernobyl accident (1986) has been carried out in Slovenia since the early sixties. The primary purpose of the monitoring programme is to provide a basis for calculating the exposure of the population due to radioactive contaminants. Secondarily, due to the very long measuring period, it is possible to observe and understand the trends of radionuclide concentrations in different media.
Above all, two long-lived fission radionuclides, $^{137}$Cs and $^{90}$Sr, have been followed in the atmosphere, water, soil and in drinking water as well as in foodstuffs and feeding stuffs. In addition to that, river water contamination with $^{131}$I due to medical use was also monitored. In all samples, other natural gamma emitters are also measured, as well as $^{3}$H in surface water, drinking water and precipitation.

The measurement programme was for years roughly equally divided between two technical support organisations, each organisation always measuring the same type of samples, with few samples duplicated for checking purposes. With the changes in legislation and public procurements, this system had to be changed. As a consequence, the continuity is broken since 2005. The monitoring programme is still divided into 2 roughly equivalent parts, with organisations switching between those parts practically every year.

Both organisations are authorised for performing monitoring by the Slovenian Nuclear Safety Administration. The Slovenian legislation has set the accreditation according to ISO/IEC 17025 standard, used by testing and calibration laboratories, as one of the conditions for this. If we take this into account, the change of monitoring operator should not present a problem and all results should be consistent. Nevertheless, the SNSA have noticed some irregularities in long term trends.

## Material and methods

Programmes for monitoring of levels of radioactivity in the environment as a consequence of global contamination due to nuclear bomb tests and the Chernobyl accident have been continuously carried out since the 1960s. In addition to the data on levels of radioactive contamination of the environment, the SNSA has also gathered data from the Krško NPP, the Žirovski Vrh Mine, the Low and Intermediate Level

Waste Depository and the Reactor Centre at Brinje. Beside regular monitoring programmes, the SNSA orders individual studies of particularly interesting aspects of contamination in the environment. All data from regular programmes and most of the data gathered in individual studies carried out since 1961 have been entered into a single database at the SNSA, named ROKO (the name derives from Slovenian Radioactivity in the Environment).

ROKO is a relational database with a simple user interface, intended for use of the SNSA staff and the whole community (http://www.radioaktivnost.si/ROKO/roko.php). We used data from the database to examine trends and to find inconsistencies in monitoring results that have arisen from changes of sampling locations, different calibrations, possible different sampling procedures or simply unexplained discrepancies.

In Slovenia, there are few organization that are authorised by the SNSA to perform environmental monitoring. The two most important ones are "Jožef Stefan" Institute (IJS) and Institute for occupational safety (ZVD). These two are accredited for measuring radioactivity in all environmental samples and perform yearly monitoring programmes for the SNSA and all nuclear facilities.

## Results and discussion

### Concentrations in air

Radionuclide concentration in air was historically measured by ZVD at Golovec, a small hill in the suburb of Ljubljana. The sampling point was situated in the forest environment, with higher $^{137}$Cs content in upper layer of soil and consequently resuspension of particles with higher activity concentration of $^{137}$Cs. In 2006, as well as in 2008 and 2009, IJS measured air in Podgorica, on flat alluvial ground with lower content of $^{137}$Cs. The 2007 measurements were made by ZVD at Polje, situated also on the flat area of the Ljubljana basin. $^{137}$Cs was measured in monthly samples and averaged over the whole year (
Figure 1). Values measured in Podgorica are systematically lower than the other measurements.

Although these 3 locations are geographically close (few kilometres around Ljubljana), their properties regarding environmental radioactivity are very different, making them unsuitable for following long term concentration trends.

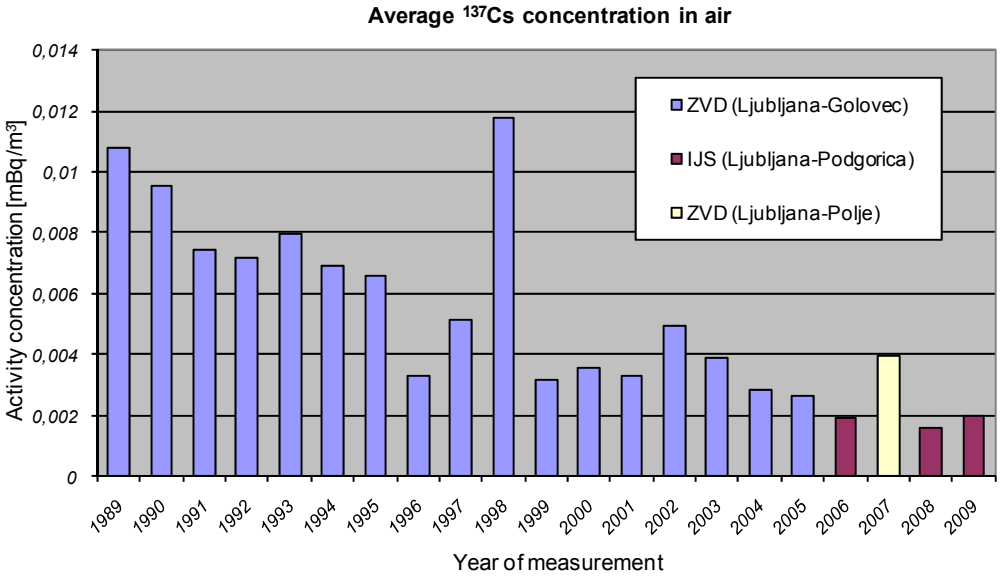


**Figure 1. Average concentration of $^{137}$Cs in air. Elevated values in 1998 are due to the accidental smelt of a $^{137}$Cs source in Algeciras, Spain.**

The activity concentration of $^{7}$Be in air is also interesting. Values, measured by IJS, are obviously higher. Possible reasons for that could be in the difference between locations. Golovec is windswept and elevated, situated in a forest, Ljubljana-Podgorica is flat for several kilometres with no trees so there is no filtration, as shown on Figure 2. The measurements in Polje can not yet be evaluated, since there are not enough data till now.

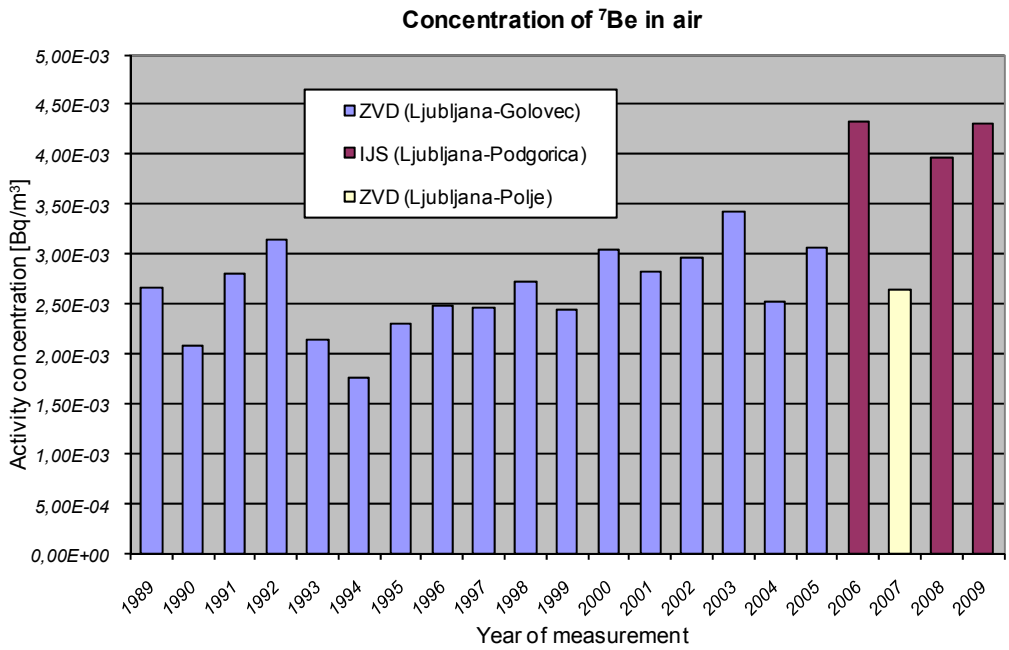


**Figure 2. Average concentration of $^{7}$Be in air. Measurements in Ljubljana (Podgorica) yield higher values.**

## Concentrations in soil

The long-term sampling place for radionuclide concentration measurement in soil was chosen in the 1960s at a big co-operative farm in Barje near Ljubljana (location name Ljubljana), with the intention to follow $^{137}$Cs and $^{90}$Sr along the food-chain. The laboratory that performed soil sampling in 2006 changed the sampling point to Podgorica. As a consequence, clayey soil sampled for four decades was substituted by washed-off alluvial soil with poor $^{137}$Cs content. The measurements (
Figure 3) show lower values for both years when soils was sampled in Podgorica (2006 and 2008), and the value for 2007, sampled again in Barje, is consistent with past measurements. In 2009, the measurements were again done in Barje, but this time by the laboratory that previously used the Podgorica location. The results are consistent with measurements done at the same location in the past, so we can assume that both laboratories have comparable sampling procedures and the past discrepancies were only due to different soil characteristics.

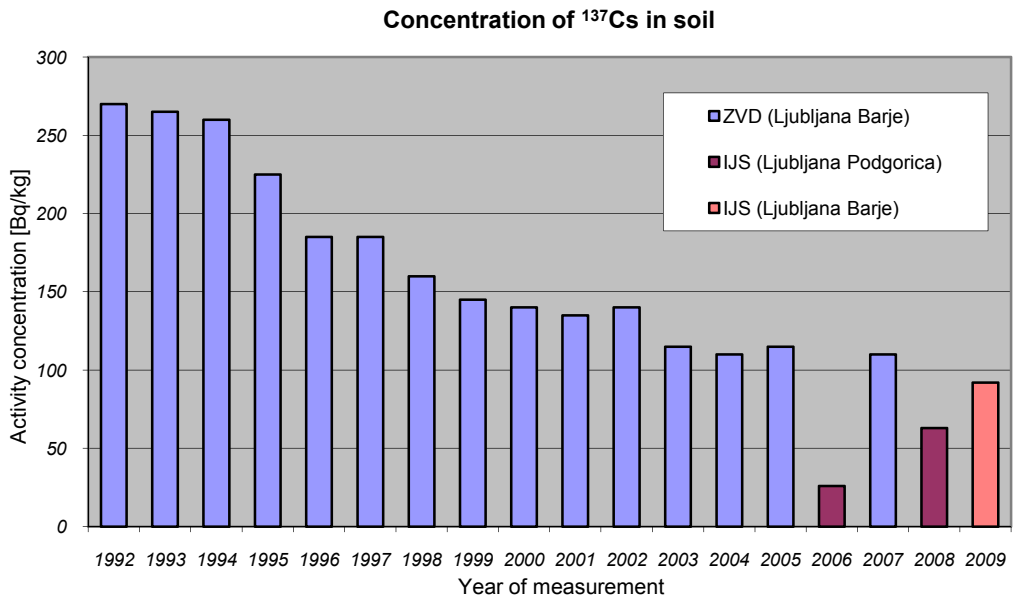


**Figure 3. Activity concentration of $^{137}$Cs in soil. Measurements done on different soil show different $^{137}$Cs content.**

However, such discontinuities in sampling and measurement may also lead to faulty analyses and evaluations. In 2006, the concentration of $^{137}$Cs in soil was generalized for the whole country, and the evaluator omitted any comment on discontinuity of sampling history. As a consequence, the dose to the population calculated from this result was vastly underestimated.

## Concentrations in river water

In the last decade, the content of $^{3}$H in the Sava river showed average yearly concentrations between 1,3 and 1,6 kBq/m$^3$, while in the last 2 years the averages dropped to around 0,8 kBq/m$^3$. Up till the year 2008, the measurements were performed by IJS, department for environmental sciences, the first 9 months of 2008 were analysed by Austrian Research Centre Seibersdorf, and the last 3 months as well as 2009 by IJS again. (Figure 4).

The elevated values in the years before 2008 are explained by the laboratory to be a consequence of faulty calibration of the equipment (roughly 20%), which was later rectified, yet the results since are still not within the expected values. As a comparison, we used data collected by ARC Seibersdorf in rivers in Austria as well as data from Slovenia measured by IJS. The concentrations of $^{3}H$ in all these examples are consistently in the 1,1-1,4 kBq/m$^{3}$ range. $^{3}H$ concentrations measured in precipitation in these cases are slightly higher but also of the same range, so the low values measured in the Sava river at Krško are not expected and can not be easily explained.

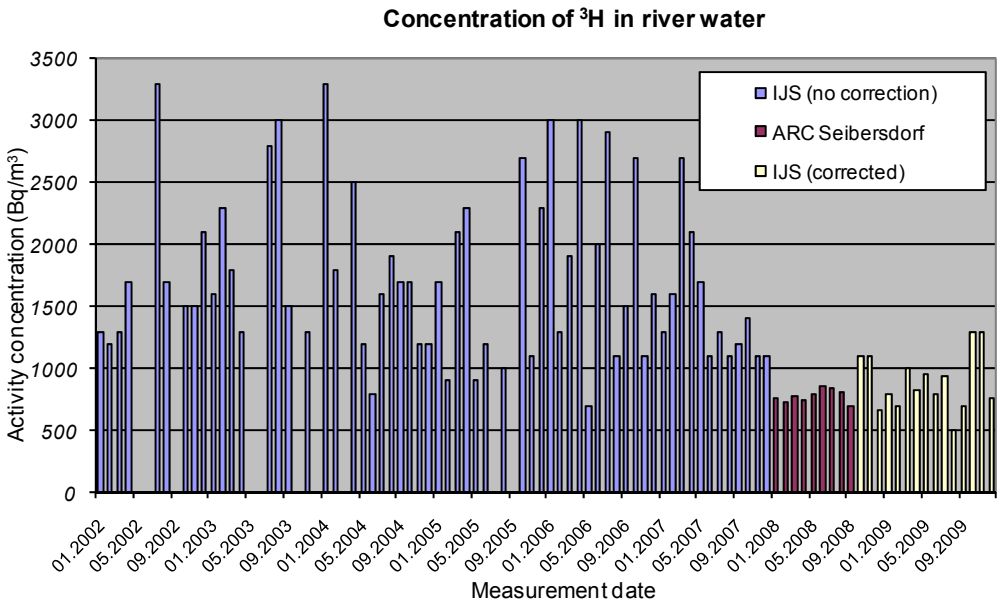


**Figure 4. Activity concentration of $^{3}H$ in river water. Recent measurements show significantly lower values.**

In 2008, the SNSA has started a campaign of independent monitoring programs designed to confirm results obtained thrugh the operational monitoring of emissions and immissionsthat is performed by nuclear facilities. Each year, a number of selected samples are simultaneously measured by an authorised organisation that is not involved in the operational monitoring of those samples. The sampling process is allways witnessed by the SNSA staff.

Among the samples checked in 2009 were grab samples of unfiltered Sava river water. It was measured by IJS in the scope of the operational monitoring program and checked independently by the ZVD laboratory. Measurements of concentrations of some radionuclides in samples simultaneously taken at Krško and Brežice are shown in Table 1.

**Table 1. Measurements of grab Sava river water samples.**

| | $^{210}Pb$ (Bq/m$^{3}$) | $^{131}I$ (Bq/m$^{3}$) | $^{40}K$ (Bq/m$^{3}$) |
|---|---|---|---|
| IJS | <2 to <6 | 8 | 120 |
| ZVD | 14 to 35 | 26 | 43 |

The values differ by up to a decade in worst cases, although the sampling was done simultaneously. Through the analysis of the SNSA photo archive, we were able to pinpoint the possible reason for these discrepancies in different sampling metodology. It is worth mentioning that results from simultaneously taken sediment samples show acceptable agreement. Since sediments are much easier to uniformly sample then unfiltered river water, it only strengthens the premise that sampling procedures must be re-examined and possibly prescribed by the authority in order to obtain relevant and comparable results.

### Concentrations in deposition

In the scope of the yearly environmental monitoring programmes, the SNSA has organized simple intercomparison measurements for radioactive deposition due to precipitation at the sampling point Ljubljana. The measurements show that ZVD has consistently measured order of magnitude higher concentrations for $^{137}$Cs then IJS (Figure 5). Even though the measured values are very low, thus higher variability is expected, the sampling and measuring procedures should be re-evaluated by both organisation to find the cause of this discrepancy.

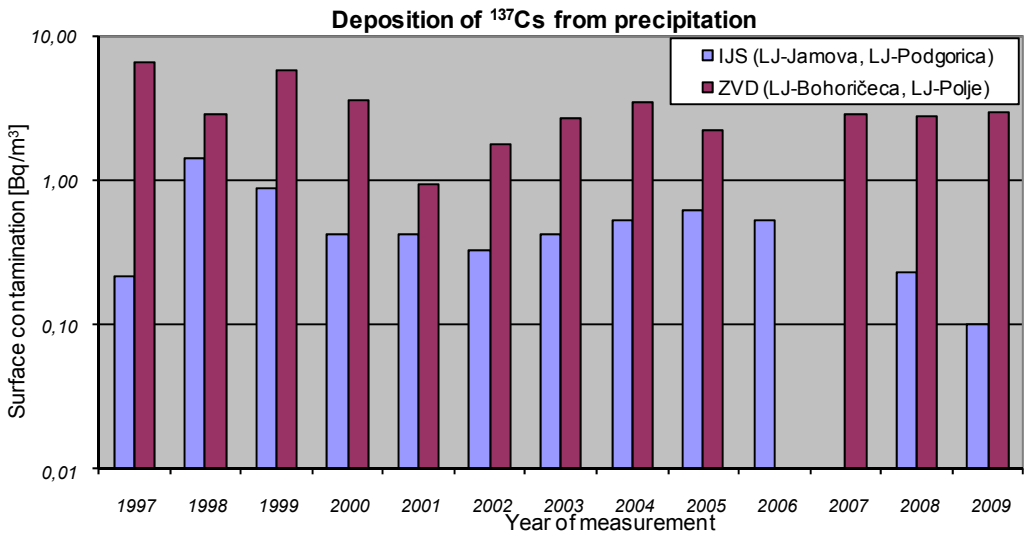


**Figure 5. Activity concentration of $^{137}$Cs in precipitation. Measurements done by ZVD show consistently higher values then IJS. There were no intercomparisons in 2006 and 2007.**

## Conclusions

The examples that are presented in this paper are only a fraction of the overall scope of the results of environmental monitoring, not to mention operational monitorings of different nuclear facilities. It is important to stress that there was no intention to qualify measurements as “right” or “wrong”. In most described cases it would even be impossible, since measurements are done at different locations. The intention was to discuss different influences on monitoring results.

Measurements of concentration of nuclides in air and soil show that location change leads to difficulties in data evaluation. Measurements of concentrations in water and precipitation, on the other hand, show discrepancies that may be due to transport,

different sampling and preparation procedures or some, for now, unexplained reason. It is important to observe that the differences between measurements (50% and more) are much larger than the uncertainties (with the exception of precipitation, in the 10% range).

It is very important, that the contractors continuously analyse and evaluate measured results and compare them to expected values and historical trends. Whenever they find an inconsistency, it is imperative to try to find the reasons for it before reporting the measurements to the consignee.

It would be advantageous for the community if there would be more communication and cooperation between different organizations carrying out monitoring programmes. Due to the nature of the tendering process, it is possible that different organizations switch monitoring programmes from year to year. Especially in that case, it is important that the organizations share their experience and information so the continuity of measurement is preserved.

One of the more important facts that the contractors need to keep in mind is that the Slovenian data can not differ significantly from data of other, geographically similar regions or countries, so this can be used as one of the filters for data when it is needed.

ROKO database, maintained by the SNSA, can be one of the tools for all support organizations for evaluation and comparison of data. It is very important to carefully check all data before entering them into the database, since it is much harder to find mistakes later. Having in mind the number of measurements performed each year through and the number of values (roughly 10000) that are yearly entered into the database, it is a very demanding task.

All organizations performing environmental monitoring of radioactivity in Slovenia are accredited according to ISO17025 standard. This is an important step towards ensuring the uniformity of measurements, but it turns out that there are even more elements that influence results that are not included in the accreditation process.

## References

Annual Reports on the Radiation and Nuclear Safety in the Republic of Slovenia, SNSA, Ljubljana, 1980-2008.

Cindro, Michel et al, Proceedings of the International Conference Nuclear Energy for New Europe 2008, Use of ROKO Database for Analysis of Radiological Data, 2008, p. 905.1-905.7

Measurements of radioactivity in the vicinity of the NPP Krško, Krško, 1979-2008.

Monitoring of the radioactivity in the environment of the Žirovski vrh mine, Ljubljana, 1982-2008

Measurements of radioactivity in the vicinity of the TRIGA research reactor, Ljubljana, 1984-2008

Measurements of radioactivity in the vicinity of the LILW depository in Podgorica, Ljubljana, 1999-2008

Rules on the monitoring of radioactivity, 20. Official Gazette RS, #20/2007, pp. 2509-2518.

Stritar, Andrej et al., Proceedings of the International Conference Nuclear Energy for New Europe 2005, ROKO-database of the environmental radioactivity measurements in Slovenia., 2005, p.129.1-129.6.

# Problems connected to measuring a valid Peak-to-valley ratio in field gamma spectrometry

Östlund, Karl; Samuelsson, Christer
Lund University, Medical Radiation Physics, SWEDEN

## Abstract

During in-situ gamma spectrometry, the ratio between count rates of the full-energy peak and the count rates of an energy region just below the peak, can be used as an indicator of depth of the source below ground level. The peak-to-valley ratio decreases with increasing depth of the source due to forward scattered Compton photons producing counts in the valley. The concept Peak-to-valley ratio used for environmental radioactivity measurements, is connected to a lot of difficulties regarding equipment and measurement geometry. There is great need to keep the ratio as free from disturbance as possible, this because the ratio is always suffering from bad statistics. Tests how changes in measurement geometry changes the ratio in laboratory environment was performed to better understand what to be accounted for in a normal measurement situation. Tests of how dead time might influence the ptv-ratio was conducted with good results for two specific preamplifier types, the resistor feedback and the transistor reset type. The transistor reset preamplifier was showing stability of the ratio for the different settings of the electronics and preserving the ratio to a constant value.

# Interception of wet deposition of radiocaesium and radiostrontium by *Brássica napus*

Rosén, Klas; Bengtsson, B. Stefan
SWEDEN

## Abstract

In this study we examined the effects of $^{134}$Cs and $^{85}$Sr in the form of wet deposition on spring oilseed rape (*Brássica napus* L. 'Joplin'). Simulated rainfall containing the radioisotopes $^{134}$Cs and $^{85}$Sr was applied to the crop on six different occasions during the season. The interception fraction was found to be positively correlated to the leaf area index, with an *r*-value of 0.75 for $^{134}$Cs and 0.77 for $^{85}$Sr and to crop biomass, with an *r*-value of 0.80 for $^{134}$Cs and 0.77 for $^{85}$Sr.

## Introduction

It is important to investigate the direct uptake of $^{134}$Cs and $^{85}$Sr during the first year after wet deposition, when the rate of translocation of these radioisotopes to edible plant parts is high compared with the rate of transfer from soil to plant (Madoz-Escande *et al.*, 2004).

The level of radionuclide capture, or interception, by plant parts is dependent on climate conditions, physico-chemical form of the radionuclides, plant morphology and biomass density (Vandecasteele *et al.*, 2001; Rosén & Eriksson, 2008). The proportion of precipitation that can be hold by the plant declines over time, but after the maximum water retention capacity is reached, the concentration of radioactive particles may continue to increase due to accumulation depending on their physico-chemical properties (Kinnersley *et al.*, 1997). The time from deposition to harvest also has an effect on the total uptake of radio isotopes in plants. This effect, referred to as 'field losses' has been described by Chadwick and Chamberlain (1970).

In the present study, wet deposition of $^{134}$Cs and $^{85}$Sr were applied to spring oilseed rape at different growth stages in order to study interception of $^{134}$Cs and $^{85}$Sr of different development stages of the crop and of plant growth. The crop used was spring oilseed rape (*Brássica napus* L.) and the contaminating isotopes that were used, $^{134}$Cs and $^{85}$Sr, were deposited using simulated rainfall. The study was conducted in the field, on agricultural land under normal cultivation treatments. Biomass samples were dried and activity measured by HPGe detector.

## Materials and methods

### Cultivation of rape

Spring oilseed rape (*Brássica napus* L. 'Joplin') was cultivated on a clay soil (situated at Vipängen, Uppsala, Sweden), with fertilizer supplied at sowing. The field trial consisted of 81 plots (1 m × 1 m) and radionuclides were applied of six plant growth steps.

### Rain simulation

A rain simulator was constructed at the Department of Soil and Environment based on a drip infiltrometer described by Joel and Messing (2001). The water drops hit the crop at a 90° angle and an intensity of 41.6 mm $h^{-1}$. The target amount of precipitation was 1 mm $m^{-2}$. The precipitation consisted of water that was purified and deionised before each deposition event. The appropriate volume of stock solution was added to obtain the desired concentration of radionuclides (20 kBq $m^{-2}$) for both isotopes. The actual content of the radionuclides in the precipitation was measured using an HPGe detector (GMX-13200) after application to the plants.

### Radioisotopes

The radioisotopes used were supplied by Canberra Solution AB on 20 May 2009: $^{85}$Sr in the form of strontium chlorine in a 0.5 M HCl solution at a volume of 2 mL and an concentration of 1.84 MBq $g^{-1}$; and $^{134}$Cs in a 0.1 M HCl solution at a volume of 1 mL and an concentration of 4.991 MBq $g^{-1}$.

### Wet deposition and measurements

The deposition time was equivalent to application of 1 mm of precipitation to the crops. Each plot had three replicates for each treatment and these plots were randomised and plant materials were taken on six different plant growth stages. The plant materials were weighed, dried, re-weighed and milled before measurement of radioactivity. Measurements were made using three HPGe detectors that had an efficiency of 14.2% (GMX-13200), 31.3% (GMX-33210) and 20.5% (GEM-20200) at 1.33 MeV $^{60}$Co. The leaf area index (LAI) was measured on the day of sampling using a LAI 2000 device (LI-COR, Nebraska, USA). Statistical analyses were performed using the statistical computer programme Minitab 15.1.30.0 (Minitab Inc.).

### Interception fraction of $^{134}$Cs and $^{85}$Sr

The percentage of radionuclides intercepted after a wet deposition event was determined by calculating the interception fraction ($f$) as the ratio between the activity in the dry weight biomass of plants directly after deposition had occurred ($A_i$, Bq $m^{-2}$) and the total amount of activity deposited ($A_t$, Bq $m^{-2}$) and multiplying by 100 to get percentage. Modified after Proehl (2009):

$$f = \frac{A_i}{A_t} \times 100 \qquad (1)$$

## Results

### Leaf area index and biomass

The leaf area index increased with growth of the spring oilseed rape up to a maximum at flowering stage and then decreased until harvest. Plant biomass of the spring rape reached its maximum at the stage at development of fruit and then declined until the senescence stage.

### Interception fraction of $^{134}$Cs and $^{85}$Sr

Interception fraction of $^{134}$Cs and $^{85}$Sr was calculated for samples taken on the next day after deposition, or two days after in the case of growth stage leaf development (first leaf unfold) due to weather conditions (Table 1). The interception fractions of $^{134}$Cs and $^{85}$Sr were not statistically different (paired *t*-test *p*-value of 0.132). The interception fraction of $^{134}$Cs and $^{85}$Sr increased over time in line with growth of the spring oilseed rape. The interception fraction was positively correlated to the leaf area index of the spring oilseed rape (Fig. 1) and as well to crop biomass (Fig. 2).

**Table 1. Interception fraction of $^{134}$Cs and $^{85}$Sr deposition for spring rape (mean ± S.D.)**

| Growth stage | Biomass (g dry wt. m$^{-2}$) | LAI* | Total amount deposited ($A_t$) | | Interception on spring rape ($A_i$) | | *f* ** | |
|---|---|---|---|---|---|---|---|---|
| | | | $^{134}$Cs (kBq m$^{-2}$) | $^{85}$Sr (kBq m$^{-2}$) | $^{134}$Cs (kBq m$^{-2}$) | $^{85}$Sr (kBq m$^{-2}$) | $^{134}$Cs (%) | $^{85}$Sr (%) |
| Leaf development (first leaf unfold) | 5 | 0.0 | 16.2 ± 0.13 | 14.8 ± 0.1 | 0.1 ± 0.02 | 0.1 ± 0.008 | 0.3 | 0.5 |
| Leaf development (5 leaves unfold) | 42 | 1.8 | 19.2 ± 4.29 | 17.7 ± 3.9 | 0.4 ± 0.07 | 0.4 ± 0.099 | 2.0 | 2.5 |
| Full flowering | 354 | 4.1 | 17.0 ± 0.24 | 16.7 ± 0.2 | 2.8 ± 1.93 | 2.7 ± 1.821 | 16.3 | 16.2 |
| Development of fruit | 667 | 4.1 | 17.3 ± 0.78 | 16.1 ± 0.7 | 4.5 ± 0.22 | 4.7 ± 0.531 | 17.6 | 29.4 |
| Beginning of ripening | 892 | 2.8 | 16.9 ± 0.32 | 15.3 ± 0.3 | 4.5 ± 0.18 | 4.7 ± 0.521 | 26.6 | 30.5 |
| Senescence | 648 | 1.7 | 16.5 ± 0.06 | 15.1 ± 0.1 | 1.7 ± 0.20 | 2.1 ± 0.140 | 10.4 | 13.8 |

***leaf area index and **interception fraction**

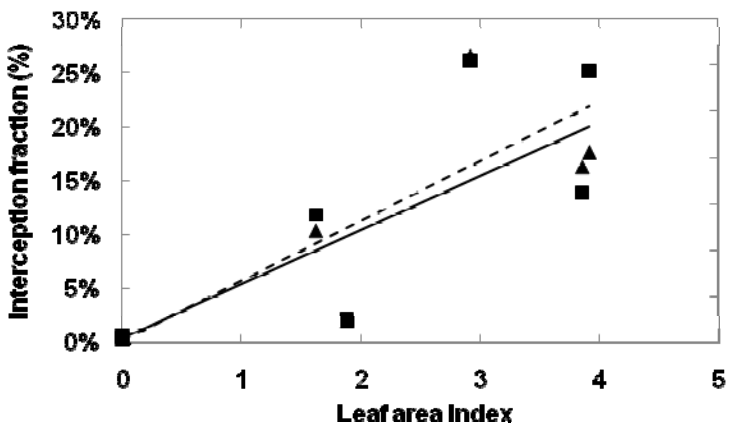


**Fig. 1. Relationship between interception fraction and leaf area index of spring oilseed rape plants during the growing season. Mean values shown for $^{134}$Cs (▲), $^{85}$Sr (■), linear function of interception fraction for $^{134}$Cs (–) and linear function of interception fraction for $^{85}$Sr (−−).**

The interception fraction was positively correlated to the leaf area index of the spring oilseed rape, with high interception of radioisotopes at high values of leaf area index. The data were fitted with a correlation coefficient had an *r*-value of 0.75 for $^{134}$Cs and 0.77 for $^{85}$Sr (Fig. 1). Plotting the interception fraction against biomass density (expressed as kg m$^{-2}$) showed that interception values reached highest at high density of the biomass. The correlation coefficient had an *r*-value of 0.77 for $^{134}$Cs and 0.80 for $^{85}$Sr (Fig. 2).

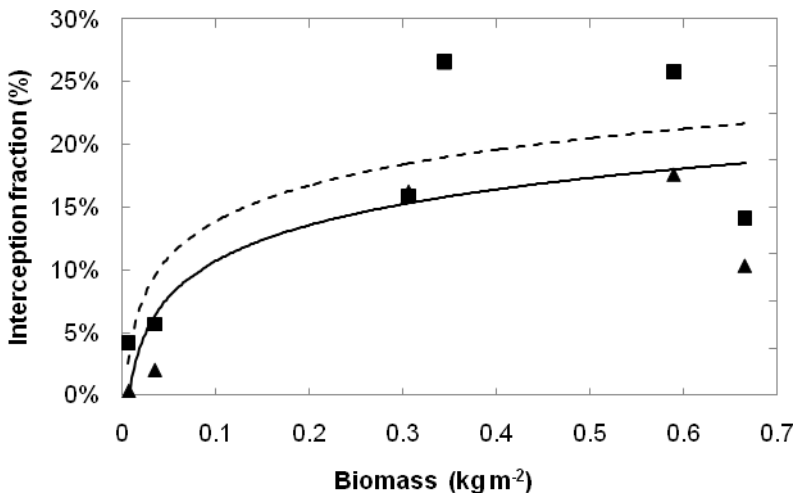


**Fig. 2. Relationship between the interception fraction and dry biomass density (kg m$^{-2}$) of spring oilseed rape during the growing season. Mean values shown for $^{134}$Cs (▲),$^{85}$Sr (■), logarithmic function of interception fraction for $^{134}$Cs (–) and logarithmic function of interception fraction for $^{85}$Sr (−−).**

## Discussion

The interception fraction, which was positively correlated to the leaf area index, followed the same pattern, increasing to a maximum value and then decreasing during ripening of the crop (Table 1, cf. columns LAI and *f*). A similar relationship between interception fraction and LAI, and between interception fraction and biomass, has also been observed for wet deposition on spring wheat (Vandecasteele *et al.*, 2001).

A higher value of interception fraction was observed for $^{85}$Sr in the stage of development of fruit than for $^{134}$Cs and as well in beginning of ripening. This can probably be explained by different physico-chemical form of $^{134}$Cs and $^{85}$Sr or the physiology of the epidermis. The interception fraction by spring oilseed rape was lower when compared to a study performed by Vandecasteele *et al.* (2001) of interception fraction by spring wheat. In the study the interception fraction was up to 84 % for $^{137}$Cs and 88 % for $^{90}$Sr.

## Conclusions

This paper presents the results from the first year of a three-year study. The overall aim is to examine the effects of wet deposition of radioisotopes in 'real' conditions on oilseed crops and the levels of concentration of caesium and strontium in the crop during the season.

These preliminary results showed a positive correlation between the interception fraction for caesium and strontium radioisotopes and the biomass and leaf area index of the spring oilseed rape. There was also found that $^{134}Cs$ intercepted to a maximum level of 26.6 % and $^{85}Sr$ of 30.5 % both at growing stage beginning of ripening.

## References

Chadwick R.C, Chamberlain A.C. Field loss of radionuclides from grass. Atmospheric Environment 1967; 4(1): 51-56.

Joel A, Messing I. Infiltration rate and hydraulic conductivity measured with rain simulator and disc permeameter on sloping arid land. Arid Land Research and Management 2001; 15(4): 371-384.

Kinnersley R.P, Goddard A.J.H, Minski M.J, Shaw G. Interception of caesium-contaminated rain by vegetation. Atmospheric Environment 1997; 31(8): 1137-1145.

Proehl G. Interception of dry and wet deposited radionuclides by vegetation. Journal of Environmental Radioactivity 2009; 100(9): 675-682.

Rosén K, Eriksson J. Motåtgärder i växtodlingen efter ett nedfall av radioaktivt cesium vid olika nedfallsnivåer och årstider. 2008; Jönköping: Jordbruksverket.

Vandecasteele C.M, *et al.* Interception, retention and translocation under greenhouse conditions of radiocaesium and radiostrontium from a simulated accidental source. The Science of the Total Environment 2001; 278(1-3): 199-214

# Variation of dietary intake of radioactive cesium after the Chernobyl fallout in Finland

Kostiainen, Eila; Outola, Iisa; Huikari, Jussi; Solatie, Dina
STUK – Radiation and Nuclear Safety Authority, FINLAND

## Abstract

The deposition of radiocesium after the Chernobyl accident in 1986 was unevenly distributed in Finland. The variation of ingestion doses was studied in three areas, in central Finland with the $^{137}$Cs deposition 50–80 kBq m$^{-2}$ and in southern and northern parts of the country where the deposition was 1–5 kBq m$^{-2}$.

Estimates of dietary intake of radiocesium were made for years 1987, 1997 and 2007 by using the foodstuffs monitoring data and statistics of food consumption. The annual internal radiation doses in the three areas ranged in 1987 from 0.04 mSv a$^{-1}$ to 0.38 mSv a$^{-1}$ and decreased then ranging in 2007 from 0.006 to 0.09 mSv a$^{-1}$. The peak values of radiocesium in agricultural products were found in 1986–87 and the contents of $^{137}$Cs decreased rapidly thereafter. The contribution of wild products to $^{137}$Cs intake in 1987 varied from 32 to 56 percent. Due to the faster decline of $^{137}$Cs in agricultural products the contribution of wild products to the intake increased, and in 2007 their contribution was 77–97 percent of the ingestion dose. Currently the variation in consumption and origin of the wild foodstuffs are the main contributors to the dose variation in Finland.

The ingestion doses calculated via data on foodstuffs were comparable to those received from the whole-body measurements or using data on mixed-diet measurements.

## Introduction

The accident at the Chernobyl nuclear power plant in 1986 gave rise to an unevenly distributed $^{137}$Cs deposition in Finland. In consequence, contamination of foodstuffs varied considerably in various parts of the country. In northern Finland, elevated $^{137}$Cs contents in foodstuffs were found in reindeer meat and a slight increase also in freshwater fish and wild berries and mushrooms, but hardly any change in agricultural products. In central Finland with high $^{137}$Cs deposition, higher levels of radiocesium were measured in all foodstuffs, especially in freshwater fish after the deposition. The variation of radiocesium levels in agricultural products produced in different parts of Finland was largest during the first years after the accident but later on the $^{137}$Cs contents of agricultural products have been rather low and do not differ significantly in various parts of the country. In this work variation of ingestion dose due to radiocesium

was assessed in 1987 and after that in ten year intervals, 1997 and 2007. The ingestion dose depends not only on the contamination level in the area but also on the consumption rates of different types of foodstuffs and the proportion of local foodstuffs in the diet.

Ingestion dose can be estimated by calculating the intakes of radiocesium through various dietary components, when information on the consumption rates and activity concentrations is available. Another way is to analyse whole representative mixed-diet samples instead of the main components of diet. Analysing mixed-diets gives the intake where the food consumption and processing are already included. Disadvantage of this method is that it gives no information on the contributions of different components to the intake. The third way is to estimate internal radiation dose by measuring the body content of $^{137}$Cs in people with whole-body counters. In this work the results of these three different methods are compared.

## Material and methods

The three studied areas, Helsinki, Tampere and Rovaniemi are situated in southern, central and northern parts of Finland (Fig. 1). The $^{137}$Cs deposition in Tampere region after the Chernobyl accident varied from 50 to 80 kBq m$^{-2}$, and in Helsinki and Rovaniemi regions it was less than 5 kBq m$^{-2}$. The map (Fig.1), based on mobile radioactivity measurements of STUK, shows the distribution of $^{137}$Cs deposition in Finland (Arvela et al. 1990). The foodstuffs data originates from the nationwide monitoring data of years 1987, 1997 and 2007 (Rantavaara 1991, Mustonen 1999, 2008, Rissanen 1997, Kostiainen 2007, 2008, Ylipieti 2007, 2008).

The ingredients of the diet included in the study were: vegetables, potato, fruit and berries, cereals, egg, meat (pork, beef, poultry, mutton), milk, fish, reindeer and game meat, wild berries and mushrooms. For the years 1997 and 2007 also data of the preceding and following years were used, if sufficient data for the years in question was not available. The production of vegetables and cereal grains is low in northern Finland, and therefore in our calculations we used $^{137}$Cs concentrations of these products originating from the main production areas. The main local products of diet in Finland are freshwater fish and forest products: various game, moose, wild berries and mushrooms. For game the activity contents of moose were used, because moose meat covers over 70 percent of the game meat annually consumed. All the reindeer meat consumed in Finland originates from the reindeer herding area in northern Finland.

The food consumption data for 1987 is mostly based on the balance sheets for food commodities (Rantavaara 1987, 1991).The consumption data for 1997 and 2007 originates from national Findiet surveys (Finravinto 1997, Paturi et al 2008) and the information on consumption of domestic vegetables and cereals (Penttilä 2000). The national Findiet surveys are based on the results of the 48-hour dietary recall data. The same food consumption rates were used for all the areas. Dietary habits and food choices vary in different parts of the country, and also by gender and age. The consumption rates used in this study are averages for the Finnish adult population, 25- to 64-year-old men and women. The same consumption rates of wild berries and mushrooms were used for all the years in spite of possible variation during the years (Markkula 1997). The statistics of game bags were used for reindeer and game consumption (Saarni et al 2005, Annual Game Bag Statistics 2008). The fish

consumption data for 1997 and 2007 originates from statistics of Finnish Game and Fisheries Research Institute and data for 1987 is based on statistics of fish catches.

In calculations of effective doses the average $^{137}Cs$ concentrations of foodstuffs for each year were used, and the delays in consumption were not taken into account although cereals, potato, root vegetables, cabbages, fruit, berries and mushrooms are harvested in autumn, and consumed until the next harvest. The delays in cereal consumption are even longer. Also the effect of food processing on the intake was neglected. It was assumed that all the foodstuffs consumed were domestic. The consumption of e.g. domestic fruit comprises only a minor part of fruit consumption, and the consumption rate for fruit includes only the domestic fruit.

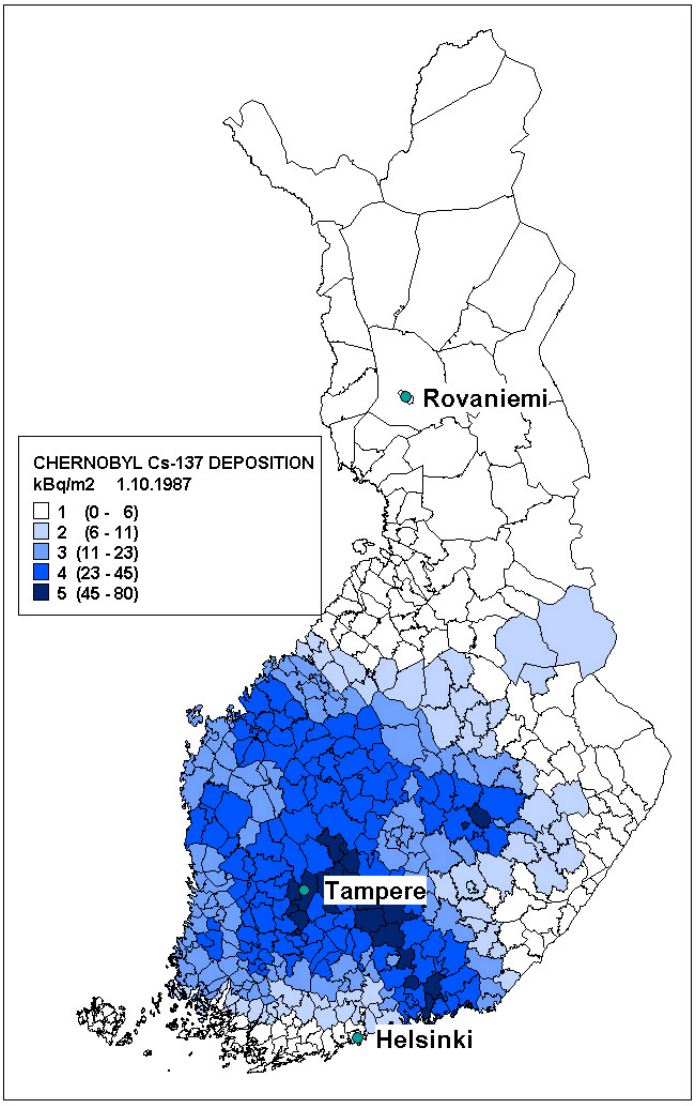


**Fig. 1. Distribution of $^{137}Cs$ deposition kBq $m^{-2}$ in Finland, reference date October 1, 1987. Study sites: Helsinki, Rovaniemi and Tampere.**

## Results and discussion

The consumption rates of foodstuffs are given in Table 1. The consumption rates for 1987 are higher than those for the years 1997 and 2007 due to differences of the methods used in collecting the dietary data. In the consumption of wild foodstuffs, especially of wild berries and mushrooms, there is a lot of variation from season to season caused by the availability of the natural products, which depends on the weather conditions. The mean consumption of mushrooms varies between 0.5 to 2 kg $a^{-1}$.

**Table 1. Annual mean consumption of foodstuffs (kg/year) for Finnish adult population in 1987, 1997 and 2007.**

| Foodstuff | 1987 | 1997 | 2007 |
|---|---|---|---|
| Milk & milk products | 262 | 157 | 145 |
| Eggs | 11.0 | 6.9 | 5.8 |
| Beef | 16.4 | 8.4 | 7.8 |
| Pork | 19.0 | 12.0 | 9.5 |
| Poultry | 4.0 | 6.0 | 10.0 |
| Mutton | 0.2 | 0.3 | 0.3 |
| Wheat | 44.2 | 33.8 | 29.6 |
| Rye | 19.0 | 22.3 | 19.0 |
| Oats | 3.0 | 9.0 | 3.0 |
| Barley | 1.6 | 0.4 | 0.4 |
| Potato | 65.7 | 40.9 | 31.0 |
| Leafy vegetables | 14.6 | 13.0 | 5.2 |
| Fruit vegetables | 16.1 | 20.0 | 23.3 |
| Root vegetables | 18.3 | 8.8 | 11.8 |
| Garden berries | 15.7 | 12.2 | 12.1 |
| Domestic fruit | 5.1 | 0.5 | 0.7 |
| Baltic herring | 1.7 | 0.8 | 0.4 |
| Freshwater fish | 4.1 | 3.7 | 3.5 |
| Game | 1.7 | 1.1 | 2.5 |
| Reindeer | 0.8 | 0.4 | 0.4 |
| Wild berries | 8.3 | 8.3 | 8.3 |
| Wild mushrooms | 1.3 | 1.5 | 1.5 |
| Drinking water | 730 | 730 | 730 |

The average $^{137}Cs$ concentrations for the areas used in dose calculations are given in Table 2. The sampling density and the sampling sites remained not the same during the years for all foodstuffs. This increases variation in $^{137}Cs$ concentrations, and the data in Table 2 shows the level of $^{137}Cs$ contents of foodstuffs in each area based on sample measurements.

The concentrations of $^{137}Cs$ in agricultural products were highest in 1986-87 and have decreased since then rapidly. Since 1997 the average $^{137}Cs$ contents of the agricultural products in all the areas were less than 5 Bq kg-1, whereas those of natural products were remarkably higher, ranging up to some hundreds of becquerels per kilogram. The dose conversion factors used were those reported by ICRP (1996).

**Table 2. Average $^{137}Cs$ concentrations of foodstuffs (Bq kg$^{-1}$) in Helsinki, Rovaniemi and Tampere areas in 1987, 1997 and 2007.**

| Foodstuff | Helsinki | | | Rovaniemi | | | Tampere | | |
|---|---|---|---|---|---|---|---|---|---|
| | 1987 | 1997 | 2007 | 1987 | 1997 | 2007 | 1987 | 1997 | 2007 |
| Milk | 13 | 0.5 | 0.44 | 2.7 | 0.6 | 0.39 | 43 | 1.9 | 0.9 |
| Eggs | 0.5 | 0.13 | 0.02 | 0.5 | 0.13 | 0.02 | 0.5 | 0.16 | 0.02 |
| Beef | 55 | 3.1 | 2 | 12 | 2.82 | 2 | 150 | 3.1 | 2 |
| Pork | 12 | 1.5 | 0.9 | 9.37 | 1.5 | 0.9 | 13 | 1.5 | 0.9 |
| Poultry | 5.2 | 0.5 | 0.5 | 5.2 | 0.5 | 0.5 | 5.2 | 0.5 | 0.3 |
| Mutton | 65 | 5 | 5 | 65 | 5 | 5 | 251 | 30 | 15 |
| Wheat | 0.15 | 0.11 | 0.14 | 0.15 | 0.11 | 0.14 | 0.63 | 0.32 | 0.14 |
| Rye | 2.17 | 0.54 | 0.42 | 4.88 | 0.2 | 0.42 | 5.29 | 0.65 | 0.42 |
| Oats | 0.43 | 0.43 | 0.56 | 5.21 | 0.69 | 0.56 | 2.76 | 2.18 | 0.56 |
| Barley | 1.08 | 0.16 | 0.21 | 0.86 | 0.51 | 0.21 | 1.13 | 0.4 | 0.21 |
| Potato | 1.1 | 0.1 | 0.02 | 0.3 | 0.1 | 0.02 | 2.8 | 0.38 | 0.2 |
| Leafy vegetables | 0.55 | 0.43 | 0.1 | 0.55 | 0.43 | 0.1 | 2.0 | 0.45 | 0.2 |
| Fruit vegetables | 1 | 0.02 | 0.1 | 1 | 0.02 | 0.1 | 16 | 0.47 | 0.1 |
| Root vegetables | 1 | 0.23 | 0.1 | 1 | 0.23 | 0.1 | 0.21 | 0.35 | 0.1 |
| Garden berries | 0.89 | 0.36 | 0.02 | 0.89 | 0.07 | 0.02 | 5.22 | 1.11 | 0.8 |
| Domestic fruit | 0.51 | 0.023 | 0.01 | 0.506 | 0.0227 | 0.01 | 2.15 | 0.27 | 0.01 |
| Baltic herring | 34.0 | 13.7 | 6.8 | 34.0 | 13.7 | 6.8 | 34.0 | 13.7 | 6.8 |
| Freshwater fish | 214 | 101 | 42.0 | 95.0 | 38.0 | 20.0 | 2359 | 763 | 964 |
| Moose | 156 | 74 | 71 | 45 | 36 | 8 | 228 | 352 | 249 |
| Reindeer | 600 | 200 | 100 | 600 | 200 | 100 | 600 | 200 | 100 |
| Wild berries | 70 | 36 | 16 | 40 | 15 | 10 | 232 | 264 | 220 |
| Wild mushrooms | 215 | 107 | 91 | 125 | 100 | 50 | 1347 | 828 | 554 |
| Drinking water | 0.66 | 0.038 | 0.021 | 0.0005 | 0.0005 | 0.0003 | 0.190 | 0.011 | 0.005 |

The annual internal radiation doses for the areas ranged in 1987 from 0.04 to 0.38 mSv a$^{-1}$ and decreased then ranging in 2007 from 0.006 to 0.090 mSv a$^{-1}$ (Fig. 2.).

The contribution of wild products (reindeer, game, fish, berries, mushrooms) to the total internal dose in 1987 was 32 percent in Helsinki area, 56 percent in Rovaniemi and 49 percent in Tampere. By 2007, the contribution of natural products to the dose increased to 77 percent in Rovaniemi, 84 in Helsinki and 97 percent in Tampere. Natural products in the diet only account about 5 percent of the total consumption but their relative contribution to the dose is larger depending on the time after the

deposition. In 1987, the contribution of drinking water to the dose in Helsinki area was 6 percent, and decreased by 2007 to 2 percent. In Rovaniemi and Tampere the doses received via drinking water were less than 0.5 percent of the ingestion doses. The raw water in Helsinki is surface water, in Tampere both surface and ground water, and in Rovaniemi all the raw water is ground water which is well protected against fallout radioactivity (Mustonen 2000).

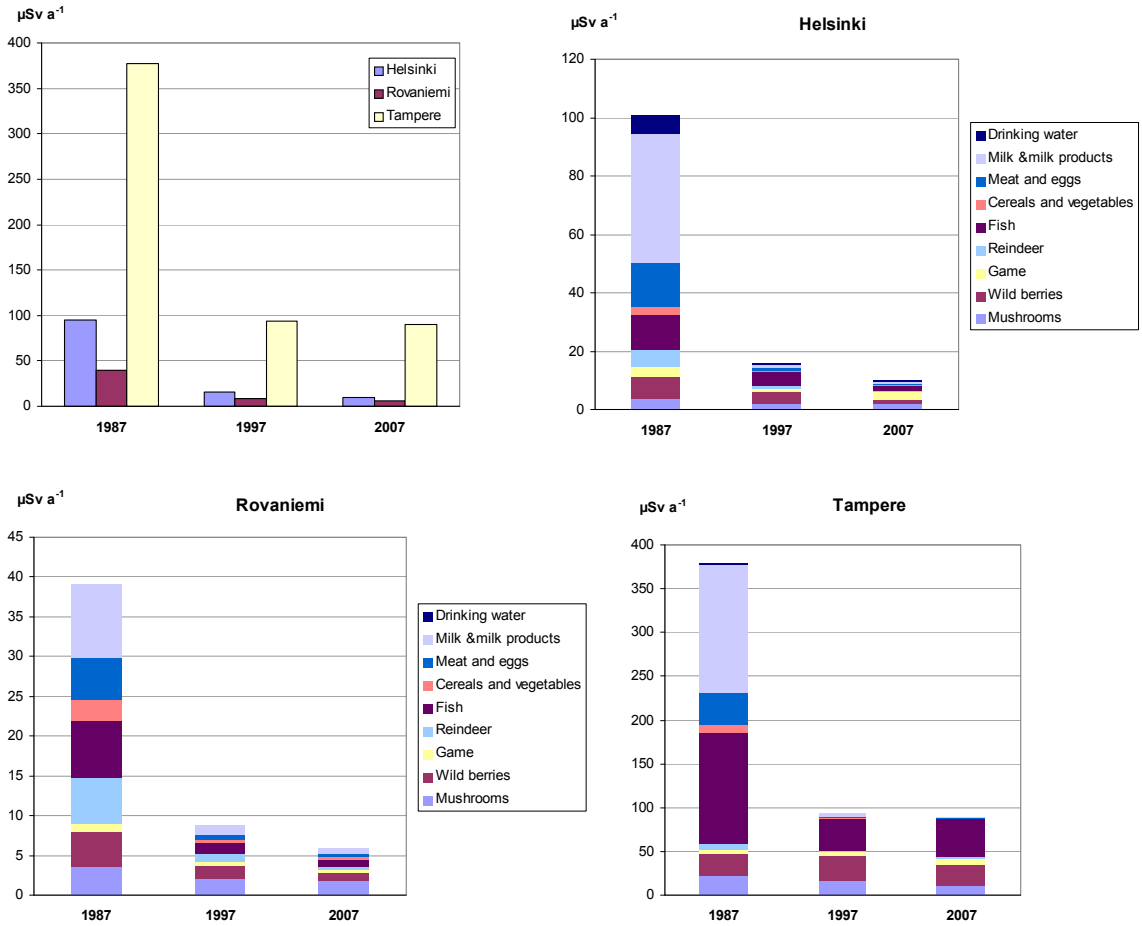


**Fig. 2. Annual internal doses µSv $a^{-1}$ in Helsinki, Rovaniemi and Tampere regions and the distribution of the doses by foodstuff groups in 1987, 1997 and 2007.**

## Discussion

The differences in the radiation doses in the three studied areas reflect the $^{137}Cs$ deposition levels in the areas. The $^{137}Cs$ deposition in Tampere region was more than ten times higher than in Helsinki or Rovaniemi, and this same ratio was seen in the internal doses calculated by using the foodstuffs monitoring data from these areas. The same consumption rates were used in all the areas although it is known there are some differences in consumption rates of northern and southern parts of the country. For example, the consumption of vegetables, fruit and poultry is lower in the northern parts of Finland compared to the central or southern parts of the country (Helakorpi 2002). Also the consumption of cereals and wild berries is highest in northern Finland. The total consumption of foodstuffs for 1987 was about 50 percent higher than that for 2007

due to different origin of consumption data in different years. If consumption data of 2007 were to be used for all the years, the dose due to the agricultural products in 1987 would decrease about 50 percent, but the dose from natural products would remain almost the same.

The average annual doses from ingestion of $^{137}$Cs in Finland have been assessed to be about 0.15 mSv $a^{-1}$ in 1987 and about 0.03 mSv $a^{-1}$ in 1997 (Rantavaara 2008). The results of this study indicate that the average doses received by people living in the most contaminated area were about three times higher in 1987.

The surveillance program on environmental radioactivity run by STUK since 1999 includes regular monitoring of mixed diet samples in Helsinki, Tampere and Rovaniemi (Mustonen 2000, 2008). This monitoring program typifies the food prepared in institutional kitchens, and the level of radioactivity it contains. The deficiencies in this program are minor amounts of natural products included in the diets of institutional kitchens and the contingency of the diet as it is based only on two sampling days. The annual ingestion doses calculated via these mixed diet samples were 6.8–7.6 µSv $a^{-1}$ in 1999 and 3.1–6.7 µSv $a^{-1}$ in 2007. In 1996 the mixed-diet sample meals were studied by analysing the diets of six weeks, in which case elevated $^{137}$Cs concentrations were seen in the meals that included wild products. (Rantavaara 2002). The annual dose calculated from the results of this six week study was 8.7 µSv $a^{-1}$ in 1996 in Helsinki area.

The internal annual doses calculated via the results of whole-body measurements were 0.074 mSv in 1987, 0.011 in 1997 and 0.008 in 2007 in Helsinki area. The doses calculated via mixed-diet in Helsinki were lower, about 60 percent of the doses received via the whole-body measurements. This difference may reflect the absence of wild products in the meals of institutional kitchens. The whole-body measurements for a group of people living in central Finland near Tampere area were 0.42, 0.12 and 0.09 mSv $a^{-1}$ in 1987, 1997 and 2007, respectively. The people in this group consume a lot of natural products like freshwater fish, wild berries, mushrooms and moose meat. The doses calculated from the whole-body measurements are at the same level as the doses calculated via foodstuffs for Tampere area with average consumption rates of natural foodstuffs. We have assumed in our calculations that all the food consumed is produced in the area, although in practice food products are distributed all over the country and only natural products are consumed locally.

**Table 3. Internal doses received by the three different methods.**

| Site | Internal dose, mSv $a^{-1}$, in 1987; 1997; 2007 | | |
|---|---|---|---|
| | **Foodstuffs data** | **Mixed diet data** | **Whole-body measurements data** |
| Helsinki | 0.10; 0.016;0.010 | –[1]; 0.009[2]; 0.005 | 0.074; 0.011; 0.008 |
| Rovaniemi | 0.039; 0.009; 0.0060 | –; –; 0.003 | - |
| Tampere | 0.38; 0.093; 0.090 | –; –; 0.007 | 0.42; 0.20; 0.09 [3] |

[1] No data; [2] Data of 1996; [3] Data from group of people that consume natural products in large quantities

The results of this study were calculated assuming average consumption habits. However, consumption of natural products that contributes most to the ingestion dose in later years after the deposition varies greatly from one individual to another. Among the

critical group that consume natural products in large quantities, the doses can be more than tenfold compared with the average consumer.

The internal doses assessed here do not include the dose increase due to $^{134}$Cs, which was in 1987 about 40 percent. By 1997, the dose from $^{134}$Cs decreased being less than two percent compared to the dose from $^{137}$Cs.

## Conclusions

The different ways to assess internal doses due to $^{137}$Cs in foodstuffs give similar results. When calculating the doses via foodstuffs, the consumption data used affects greatly the results. However, it gives information on the dose distribution by different foodstuff groups which is not extracted from diet measurements or whole-body measurements.

## References

Annual Game Bag 2007. Official statistics of Finland. Riista- ja kalatalous -tilastoja, 5/2008. Finnish Game and Fisheries Research Institute, Helsinki 2008.

Arvela H, Markkanen M, Lemmelä H. Mobile survey of environmental gamma radiation and fallout levels in Finland after the Chernobyl accident. Radiation Protection Dosimetry 1990; 32: 177-184.

Finravinto 1997: the dietary survey of Finnish adults. Publications of the National Public Health Institute; B8/1998, Helsinki 1998.

Helakorpi S, Patja R, Prättälä R, Aro AR, Uutela A. Health Behaviour and Health among Finnish Adult Population, Spring 2002. Helsinki 2002. Publications of National Public Health Institute B12/2002.

ICRP Publication 72. Age-dependant doses to members of the public from intake of radionuclides: Part 5. Annals of the ICRP 26, 1996.

Kostiainen E. $^{137}$Cs uptake of forest berries. In: Nordic Society for Radiation Protection - NSFS. Proceedings of the NSFS XV conference in Ålesund Norway, 26-30 of May 2008. StrålevernRapport 2008:13. Østerås: Norwegian Radiation Protection Authority; 2008. p.135-140.

Kostiainen E. $^{137}$Cs in Finnish wild berries, mushrooms and game meat in 2000-2005. Boreal Environmental Research 2007; 12:23-28.

Markkula M-L, Rantavaara A. Consumption of mushrooms and other wild food products in Finland. In: Proceedings of the 11th Meeting of the Nordic Society for Radiation Protection and the 7th Nordic Radioecology Seminar, (1997) 371–376.

Mustonen R. (Ed.) Surveillance of environmental radiation in Finland. Annual report 1999. STUK-B-TKO 1. Helsinki 2000.

Mustonen R. (Ed.) Surveillance of environmental radiation in Finland. Annual report 2007. STUK-B-91. Helsinki 2008.

Paturi M, Tapanainen H, Reinivuo H, Pietinen P. The National FINDIET 2007 Survey. Publications of the National Public Health Institute; B23/2008, Helsinki 2008.

Penttilä P-L, Siivinen K, Korkka L. Torjunta-aineiden saannin arviointi kasviksista ja viljasta. Helsinki 2000. Elintarvikeviraston tutkimuksia-sarja 10/2000, 22 s. +liitt. Summary in English.

Rantavaara A. Ingestion doses in Finland due to $^{90}$Sr, $^{134}$Cs and $^{137}$Cs from nuclear weapons testing and the Chernobyl accident. Applied Radiation and Isotopes 2008; 66: 1768-1774.

Rantavaara A, Kostiainen E. Samples of 24-hour-meals in monitoring of dietary intake. In: Ilus E (ed.). Proceedings of the 8th Nordic Seminar on Radioecology, 25-28 February 2001, Rovaniemi, Finland NKS-70. Pitney Bowes Management Services Denmark A/S: 111-118, 2002.

Rantavaara A. Radioactivity of foodstuffs in Finland in 1987-1988. Report STUK-A78.STUK, Authority for Radiation and Nuclear Safety, Helsinki, 1991.

Rantavaara, A., Radioactivity of vegetables and mushrooms in Finland after the Chernobyl accident in 1986, STUK-A59, Helsinki, 1987.

Rissanen K, Rahola T. Radioactivity levels in foodstuffs in Finnish Lapland. In: Walderhaug T, Gulaugsson EP (Eds.) Proceedings of Nordisk Selskap For Strålevern. Det 11. ordinære møtet. Det 7. Nordiske Radioøkologi Seminar, 26.-29. august 1996, Reykjavik, Island. 1997; 353-359.

Saarni K, Aikio L, Kemppainen J, Setälä J, Honkanen A. Poronlihatuotteiden markkinat. Kala- ja riistaraportteja nro 364. Riista- ja kalatalouden tutkimuslaitos, Helsinki 2005.

Strand P, Balanov M, Aarkrog A, Bewers MJ, Howard B, Salo A, Tsaturov YS. Chapter 8, Radioactivity. In AMAP Assessment Report: Arctic Pollution Issues. Arctic Monitoring and Assessment Programme (AMAP) Oslo, Norway. xii+859pp. 1998. P. 525-620.

Ylipieti J, Härkönen V, Solatie D. $^{137}$Cs Activity concentrations in mushrooms collected from two different types of habitats in Finnish Lapland. NKS-B Forest Seminar 2008 Oct 7-8; Helsinki, Finland.

Ylipieti J, Solatie D. Changes in $^{137}$Cs activity concentrations with time in various fish species and water in lakes of Finnish Lapland. In: Nordic Society for Radiation Protection – NSFS. Proceedings of the NSFS XV conference in Ålesund Norway, 26–30 of May 2008. StrålevernRapport 2008: 13. Østerås: Norwegian Radiation Protection Authority; 2008. p. 141–145.

Ylipieti J, Solatie D. Radiocesium in wild berries and natural herbs in Northern Finland. International Conference on Environmental Radioactivity. Vienna, Austria April 23-27, 2007.

# Investigation of $^{137}$Cs redistribution within urban ecosystem

Seleznev, Andrian A.; Yarmoshenko, Ilia V.; Ekidin, Alexey A.
Institute of Industrial Ecology, Ural Branch of Russian Academy of Sciences Ekaterinburg, RUSSIA

## Abstract
Contamination of puddle sediments by $^{137}$Cs within the urban ecosystem is studied. The investigation is made on the example of Ekaterinburg city, Middle Ural region of Russia. Contamination density of $^{137}$Cs in the region due to fallouts after atmospheric testing of nuclear weapons and nuclear accidents is assessed about 5.1 kBq/m$^2$, it associates with maximum activity concentration of the upper 15 cm layer bellow 30 Bq/kg. Results of the survey indicate a mean value of $^{137}$Cs concentration in puddle sediments of 70 Bq/kg, with a maximum value of 540 Bq/kg. It is estimated that horizontal migration has led to about fourfold concentration of $^{137}$Cs in puddle sediment.

## Introduction
During the period of atmospheric testing of nuclear weapons and accidents at nuclear facilities the primary attention of researchers was drawn to study radionuclide redistribution patterns in natural ecosystems. The urban ecosystem was not considered as the main object of the research. The aim of the study is to obtain data on levels of accumulation and redistribution of $^{137}$Cs in the city.

The basic hypothesis for the study was the significant redistribution of $^{137}$Cs in the urban environment. Local surface depressed zones where rain water and sediment accumulate in puddles are considered as such deposits. $^{137}$Cs precipitates at the puddle catchments area, which include surrounding soil and ground and roofs of buildings. Radiocaesium is supposed to reach the puddles along with horizontal migration, in soluble (precipitations) and insoluble form (particles of soil and other material such as silt, peat, decomposed plants, domestic and construction wastes on which $^{137}$Cs has adsorbed). In the urban environment routine measures such as cleaning the territory, grass mowing, garbage disposal, land fill, planting and uprooting, adjusting the channels and drainage channels contribute to $^{137}$Cs redistribution as well.

Measurements of activity concentration of $^{137}$Cs at puddle sediments were conducted in Ekaterinburg city, Russia. $^{137}$Cs contaminated the urban ecosystem under study due to the global fallout after atmospheric nuclear weapon's testing and the Chernobyl accident. The study includes the analysis of archive data on $^{137}$Cs

contamination in Ural region, sampling of puddle sediments in Ekaterinburg city, direct measurements of $^{137}$Cs activity concentrations in the samples and data analysis.

## Material and methods

Appropriate depressed zones in the city were selected by visual inspection. Samples were taken at the depressed zones that seemed as the eldest and relatively undisturbed for past years. The samples were taken from the upper 5-cm layer, with a sample mass of about 1.5 kg of dry weight. During the sampling process, domestic wastes and grass were removed. Information on location and site-specific description and photo documentation of puddle and environment were performed. The position of the sampling areas was assigned according to its address and was marked on the city map. The sampling of puddle sediments was carried out during the field study seasons 2007-2009 in 240 locations in 15 districts of the city.

The samples were air-dried under the indoor temperature in the laboratory during one month at least. Dried samples were milled and homogenized. $^{137}$Cs activity concentrations were measured using stationary gamma-spectrometer equipped with NaI(Tl) scintillation detector (crystal size 63 x 63 mm.). Counting time was 3 hours providing detection limit 5 Bq/kg.

## Results and Discussion

Available archive data on $^{137}$Cs contamination were considered as follows:

- results of direct measurements of $^{137}$Cs concentration in fallout by The Federal Service for Hydrometeorology and Environmental Monitoring over the period 1994-2006 presented in the annual reports,
- results of grass contamination measurements over the period 1966-1987 obtained from reports of local agricultural service.

In addition levels of annual deposition of $^{137}$Cs produced in atmospheric nuclear testing over the period 1945-1985 in the northern hemisphere summarized by UNSCEAR (UNSCEAR, 2000) were used.

Analysis of these data allowed reconstructing the $^{137}$Cs contamination in Middle Ural region retrospectively. According to this reconstruction:

- total deposition density of $^{137}$Cs in soils reaches 5.1 kBq/m$^2$ in 2007 with regard to decay;
- over the 20 years after the Chernobyl accident, the $^{137}$Cs activity has increased approximately by 1 kBq/m$^2$;
- the values of the $^{137}$Cs concentration in the 15-cm undisturbed ground in 2007 in dependence on the year of surface formation were modelled under conditions of absence of horizontal migration and suggested median rate of vertical migration <0.5 cm/year (Schuller, 1997; Arapis, Karandinos, 2004);
- the Chernobyl accident contributed up to 30% to the $^{137}$Cs activity concentration in the 15-cm undisturbed ground of Middle Ural region. While the $^{137}$Cs vertical migration rate <0.5 cm/year, the 15-cm layer accumulates more than 70% of total nuclide activity in 2007. The ground surface, which has been formed in the years just before the Chernobyl accident and undisturbed later, are contaminated by $^{137}$Cs in the range of 20-30 Bq/kg, the landscape formed in the period of intensive nuclear weapon testing (1950s and 1960s) possesses higher $^{137}$Cs concentrations,

up to 50-60 Bq/kg. The estimates of contamination obtained by modelling are in agreement with the results of numerous measurements of the upper ground horizon in Ekaterinburg city. $^{137}$Cs surface contamination level of soils below 30 Bq/kg is typical for the city. That level corresponds to the ground formation in period 1970-2000, which is most likely according to direct observations as well.

Fig. 1 presents distribution of $^{137}$Cs activity concentrations in samples of puddle sediments obtained for Ekaterinburg city. The arithmetic mean of $^{137}$Cs concentration is 70 Bq/kg, the maximum value of the $^{137}$Cs concentration is 540 Bq/kg and the minimum value is below the detection limit. The geometric mean of the $^{137}$Cs concentration is 57 Bq/kg. The concentration of $^{137}$Cs exceeds 100 Bq/kg in about 15 % of samples. According to chi-square test, $^{137}$Cs concentrations distribution deviates from lognormal ($\chi 2$=34.80, df=7, p<0.01).

The heterogeneity of data on $^{137}$Cs concentrations was supposed to be associated with features of spatial distribution of contamination. Results of gamma spectrometry measurements of $^{137}$Cs concentration in puddle sediments by the city districts are presented in Table 1.

Process of puddle formation is considered to be similar to forming large water reservoir. Under gravitation transport of water the solid particles are scavenged and transferred to surface depressed zone forming the puddle sediments. $^{137}$Cs concentration in the puddle sediment is supposed to consist of the concentration transferred with solid particles from the surface ground (on which the adsorption in the catchments area surface during the water accumulation in puddle took place) and concentration of water-soluble fraction of $^{137}$Cs in atmospheric precipitation.

The typical activity concentration in the ground's upper layer, $C_{soil}$, for the case under consideration is about 20 Bq/kg, it corresponds to the forming of the catchment area in 1987. The $^{137}$Cs activity concentration of puddle sediments, $C_{sed.}$, is the sum of water-soluble activity concentration of atmospheric precipitation, $C_{water}$, and the activity concentration transferring into the puddle with solid particles from the ground surface, $C_{soil.}$ $C_{water}$ is calculated as

$$C_{water} = I \cdot k \cdot \frac{S}{m}, \qquad (1)$$

where $I$ is the $^{137}$Cs total activity of atmospheric precipitation estimated as $I \approx 1000$ Bq/m$^2$ for period 20 years after the Chernobyl accident; $k$ is the factor of collection of $^{137}$Cs activity within puddle; $S$ is the catchment area, m$^2$; m is the puddle sediment mass, kg. $m/S$ is estimated as 2 kg/m$^2$ for the typical puddle existing for 20 years, i.e. a typical puddle catchment area is about 200 m$^2$ and puddle sediment mass is about 400 kg. Then $C_{sed.}$ is calculated as follows:

$$C_{sed.} = I \cdot k \cdot \frac{S}{m} + C_{soil}, \qquad (2)$$

Accepting $C_{sed.}=70$ Bq/kg and solving equation (2) relative to $k$ we obtain a value $k=0.1$. Thus about 10% of the $^{137}$Cs activity of precipitations are transferred to the puddle in water soluble phase. Water transfer forms about 70% of activity concentration in puddle sediments.

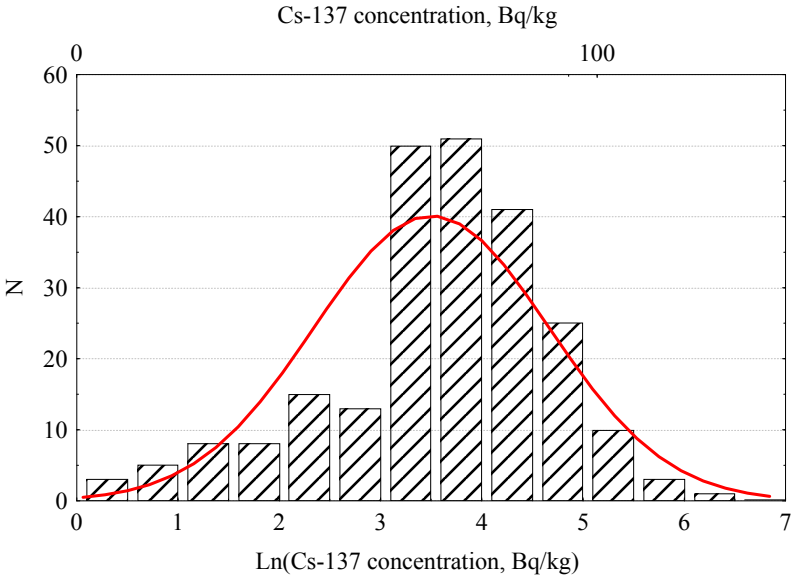


**Fig. 1. Distribution of $^{137}$Cs activity concentrations in samples of puddle sediments obtained for Ekaterinburg city.**

**Table 1. Arithmetic, geometric mean and portion of samples with $^{137}$Cs concentration >100 Bq/kg by districts of Ekaterinburg city. Results based on gamma spectrometry measurements in samples of puddle sediments.**

| District | Arithmetic mean of $^{137}$Cs concentration, Bq/kg | Geometric mean $^{137}$Cs, concentration, Bq/kg | Portion of samples with $^{137}$Cs concentration >100Bq/kg |
|---|---|---|---|
| West | 63 | 30 | 0.16 |
| Centre | 59 | 41 | 0.19 |
| North | 58 | 40 | 0.14 |
| North East Suburb | 67 | 42 | 0.19 |
| East Suburb | 29 | 16 | 0.05 |
| South | 44 | 35 | 0.05 |
| South West Suburb | 64 | 36 | 0.22 |

## Conclusions

The hypothesis that puddle sediments in local depressed zones of the urban landscape are the final deposits of $^{137}$Cs has been proved. $^{137}$Cs contamination levels in puddle sediments are relatively high in comparison with contamination of surrounding soils. The activity concentration of $^{137}$Cs in 14 % of the samples exceeds 100 Bq/kg, with a maximum activity concentration of 540 Bq/kg. Such activity concentrations are comparable with the activity found in bottom sediments of water reservoirs of nuclear

facilities in the region and lakes of the East Ural Radioactive Trace (Trapeznikov, 2007).

Characteristics of the urban environment and ground management can provide suitable conditions for local migration and concentration of radioactive contamination. The observed local surface migration of $^{137}$Cs has led to an approximately fourfold concentration in puddle sediments in comparison with typical activity concentrations in surrounding soils. The study of $^{137}$Cs migration in the urban environment should take into account the influence of anthropogenic processes on radionuclide redistribution.

Puddle sediments are supposed to be prospective object of environmental monitoring in the urban ecosystem. During such monitoring $^{137}$Cs can be applied as a marker of puddle's age. Obtained characteristics of $^{137}$Cs redistribution in the urban environment can be used in investigation of environmental pollution by other metals similar by their properties.

The research has been made under the financial support of RFBR, project: 10-05-96011.

## References

United Nations Scientific Committee on the Effects of Atomic Radiation (UNSCEAR), 2000. Sources and effects of ionizing radiations. United Nations, New York, annex C.

Schuller P., Ellies A., Kirchner G., 1997. Vertical migration of fallout Cs-137 in agricultural soils from Southern Chile. Science of the Total Environment, Vol.: 193, Issue: 3, 197-205.

Arapis G.D., Karandinos M.G., 2004. Migration of 137Cs in the soil of sloping semi-natural ecosystems in Northern Greece. Journal of Environmental Radioactivity 77(2), 133-42.

Trapeznikov A.V., Yushkov P.I., Nikolkin V.N. et al., 2007. Distribution of radionuclides among the main components of Lake Chervyanoe in the Eastern Ural Radioactive Trace. Russian Journal of Ecology, Vol.: 38, Issue: 1, 27-33.

# Radioactivity in the environmental samples around the Cernavoda NPP

Popoaca, Simona; Bucur, Cristina; Simionov, Vasile
SNN – Cernavoda NPP, ROMANIA

## Abstract

The Cernavoda Nuclear Power Plant is dedicated to produce electrical & thermal power in a safe and efficient manner for at least 30 years, from nuclear power using CANDU technology.

The factors presented below ensure that the public health and environment are adequately protected:

- source control;
- effluent control;
- effluent monitoring;
- environmental monitoring.

The Environmental Radioactivity Monitoring Program around Cernavoda NPP is designed to meet the following objectives under normal NPP operating conditions:

- to measure the radionuclide concentrations in environmental media;
- to provide an independent assessment of the effectiveness of the source control, effluent control and monitoring based on measurements in environment;
- to validate the models and parameters used in the calculation of the derived emission limits;
- to provide data to aid in the development and evaluation of models and methodologies which adequately describe the movement of the radionuclides through the environment.

The Environmental Control Laboratory of the Cernavoda Nuclear Power Plant, located in Cernavoda town, is equipped with modern analyzing systems to determine the natural and artificial radionuclide content in the following environmental samples from an area with 30 km radius around the NPP:

- airborne particles, iodine, aqueous vapours and deposition from air;
- surface water, deep ground water, infiltration water, drinking water;
- soil and grass;
- sediment and fish;
- milk, eggs and meat (chicken, pork and beef);
- vegetables, grain, corn and fruits.

The results of the monitoring program are annually compared with the results of The Preoperational Environmental Monitoring Program performed between 1984 and 1994. There were no environmental radioactivity modifications around the Cernavoda NPP comparing to the period before the NPP operation.

## Introduction

The site of the first Romanian Nuclear Power Plant comprising five 700 MWe units was chosen in the Dobrogea area, near the Cernavoda - a town of approximately 20,000 inhabitants. The choice was based on the following main reasons: the Danube river-Black Sea Channel that represents an important source of cooling water, as it provides an easy access route for the heavy and beyond standard equipment, and the low seismicity of the region as compared to other regions of the country.

Cernavoda Nuclear Power Plant is dedicated to produce electrical and thermal energy in a safe and efficient manner for at least 30 years, using CANDU (Canadian Deuterium Uranium) nuclear technology.

Among the activities to be performed during the operational phase of Cernavoda NPP, the following factors are identified which ensure that the public health and the environment are adequately protected: a) source control; b) effluent control; c) effluent monitoring; d) environmental monitoring.

The purpose of the environmental monitoring program is to provide reliable and accurate data, which comprise statistically valid data sets per nuclide/ environmental media combination on an annual basis.

The monitoring program is designed to meet the following objectives under normal nuclear power plant operating conditions:

- to measure the radionuclide concentrations in environmental media;
- to provide an independent assessment of the effectiveness of the source control, effluent control and monitoring based on measurements in environment;
- to validate the models and parameters used in the calculation of the derived emission limits;
- to provide data to aid in the development and evaluation of models and methodologies which adequately describe the movement of the radionuclides through the environment.

## Material and methods

The Environmental Control Laboratory of the Cernavoda Nuclear Power Plant, located in Cernavoda town, at 1.8 km far from the plant, is performing the Environmental Radioactivity Monitoring Program for Cernavoda NPP.

Indicator locations are outside the plant perimeter, and are established depending on emission type, critical groups and pathways used for DEL (Derived Emission Limit) calculation. In addition to these locations, a network of TLD locations was established around the plant beyond the exclusion zone.

Measurements of ambient background are conducted beyond the influence of station emissions. For emissions to air and direct exposure pathway (external irradiation and inhalation) one background location is provided. For water and sediment samples, one background location each is fixed.

The background levels were determined before of first operation of Unit 1 of the Cernavoda NPP, through the Preoperational Environmental Monitoring Program in period 1984 – 1996; all present results are compared to these levels to assess the influence of power plant operation on environment and public health.

The following environmental samples are included in the actual monitoring program, from an area with 30 km radius around the NPP:

- airborne particles, iodine, aqueous vapours and deposition from air;
- surface water, deep ground water, infiltration water, drinking water;
- soil and grass;
- sediment and fish;
- milk, eggs and meat (chicken, pork and beef);
- vegetables, grain, corn and fruits.

The frequency of monitoring or sampling is related to the mean lifetime of the nuclide in a pathway. In the same time for air monitoring, the frequency was established as a function of plant emissions (percentage of DEL/weeks).

**Table 1. Determination of monitoring frequency.**

| Nuclide | Half life ($T_{1/2}$) | Environmental media | Mean residence time | Mean life time | Monitoring frequency |
|---|---|---|---|---|---|
| Tritium | 12.3 years | air | minutes | minutes | continuous |
| | | vegetables-fruits | 3 months | 3 months | quarterly |
| | | milk | 5 days | 5 days | weekly |
| | | water | 1 day | 1 day | daily |

Airborne water vapours are collected by drawing air through molecular sieve. Sampling is continuous with an integration period of one month, during which 4 – 6 $m^3$ of air are passed through the collector. The absorbed water is removed from the sieve by heating at 350ºC. Water samples are prepared by distillation, free water from food samples (milk, fish, vegetables, fruits) is extracted by azeotropic distillation in toluene.

Tritium activity concentration is determined by liquid scintillation counting on sample prepared by mixing extracted water with a scintillation cocktail.

**Table 2. Sample measurements: measurement device used and counting time for tritium.**

| Nr. Crt. | Sample type | Measurement device | Radionuclide assessed | Counting time |
|---|---|---|---|---|
| 1. | Aqueous vapours in air | 20 ml PE vial | Tritium | 400 min |
| 2. | Water – individual and bulked sample | | | |
| 3. | Milk – individual | | | |
| 4. | Deposition – bulked sample | | | |
| 5. | Fish, meat, vegetable, fruit, grain | | | |
| 6. | Soil and sediment | | | |

The frequency of analysis is determined by the following elements:

(1) the minimum required sensitivity;
(2) the analytical sensitivity of the method;
(3) the number of results per nuclide/pathway combination per year required to generate a statistical valid data set;
(4) significance of plant radioactive effluent emissions.

The minimum required detectable specific activity should be such as to detect radionuclides present in the environment as a result of Cernavoda NPP's operations. The Minimum required specific activity was calculated for each specific radionuclide and environmental media with *the following relation:*

$$MDA = \frac{D_a}{C \times DCF}$$

where: MDA = Minimum Detectable Activity; $D_a$ = Maximum additional annual whole body dose above background due to Cernavoda NPP' operations; C = Annual Intake Rate for analyzed media; DCF = Dose Conversion Factor.

**Table 3. Measurement system for tritium.**

| Measurement system | Description | |
|---|---|---|
| Liquid scintillation analyzer | **Manufacturer** | • Wallac |
| | **Type** | • 1220 Quantulus Ultra Low Level |
| | **Calibration procedure** | • Internal departmental calibration procedures |
| | **Maintenance procedure** | • Maintenance and service contract |
| | **Standards used** | • Unquenched H-3, C-14 and background standards for energy calibration and weekly QA verification<br>• Quenched H-3 and C-14 sets of standards for annually efficiency calibration |

## Results

Forteen years of experience in CANDU operation at Cernavoda NPP have shown that tritium is the most significant radionuclide released in gaseous and liquid effluents, mostly as tritiated water, which represents more than 80% of the total radioactivity released. For this reason the environmental monitoring program is heavily weighted toward measurement of tritium.

Air from the radiological area is conducted, after filtration, to the evacuation stack where it is measured for radioactive particulates, gases and tritium water vapours. The total radioactive gaseous effluent emissions are weekly compared with the administrative limits, which are below the approved DELs. An indicator air monitoring station for critical group (Cernavoda inhabitants) is located at 1.8 km (NV) far from the Cernavoda NPP, in the Cernavoda town (ADI-08) and the background station is located at about 30 km (N) far from the NPP (straight line) in Topalu village (ADB-01). Results of tritium measurements ($Bq/m^3$) in the water vapour samples from the two locations, in period 2006 – 2008, are represented in the Figure 1.

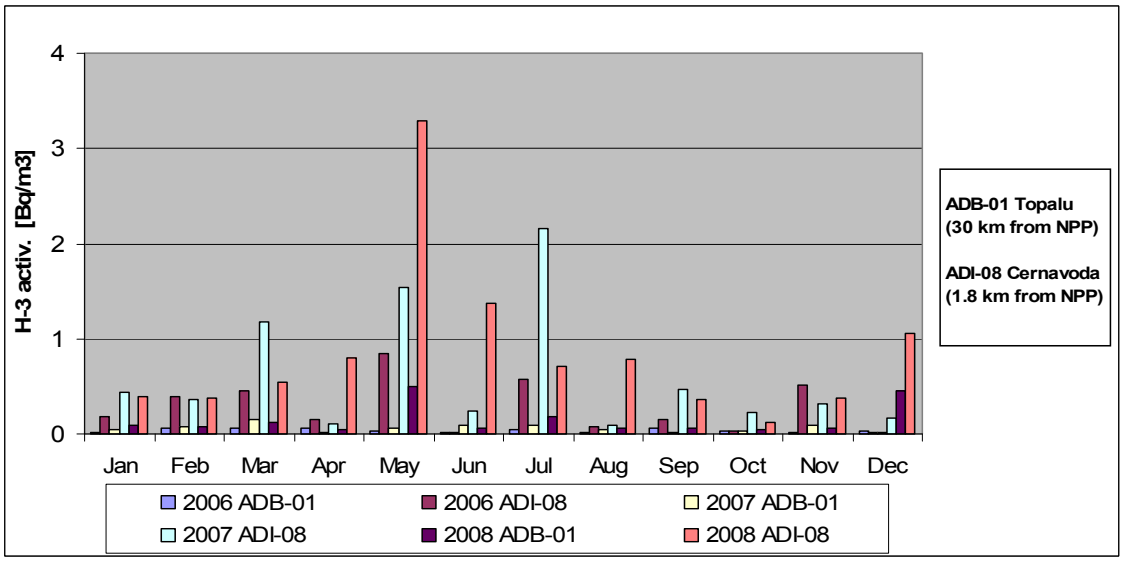


**Figure 1. Tritium concentration activities in air, between 2006 and 2008, around Cernavoda NPP (2 monitoring stations situated at about 1.8 km and 30 km far from NPP).**

Drinking water for the Cernavoda town is coming from the Danube River and after the specific treatments is distributed through the drinking water system. Samples are from the laboratory tap (AII-03, 1.8 km NV). Drinking water for Saligny is supply from underground water and samples are from a drilled well (SSS-03, 5 km SE). Results of tritium measurements (Bq/l) in the drinking water samples, in period 2007 – 2009, are represented in the Figure 2; the legal limit (100 Bq/l) is also represented.

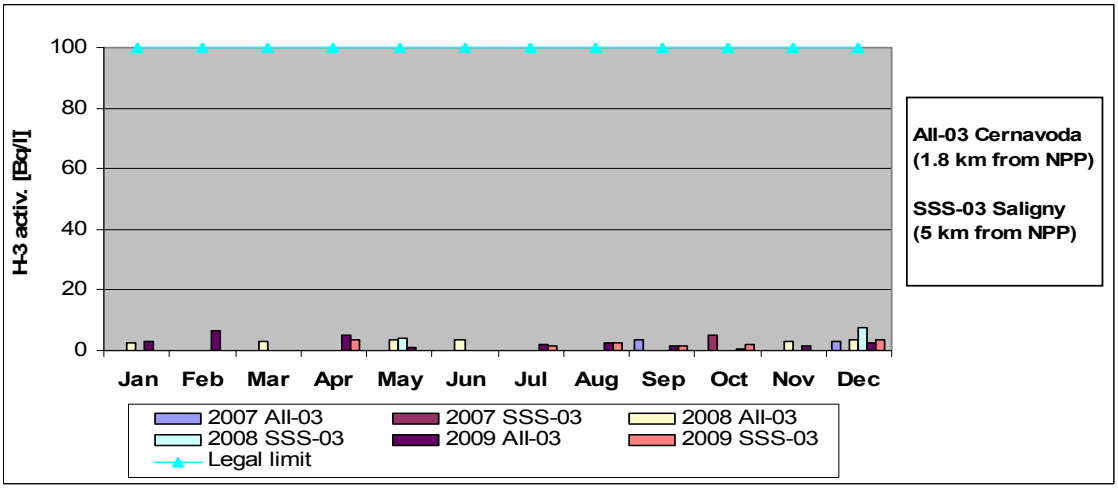


**Figure 2. Tritium concentration activities in drinking water, between 2007 and 2009, around Cernavoda NPP (2 locations situated at about 1.8 km and 5 km far from NPP).**

All food samples are cultivated, grown or produced in the monitoring area and representative for the local diet. Milk samples are provided by a dairy farm located in Seimeni village (AII-02), at about 8 km (NNE) far from the plant. Results of tritium measurements (Bq/l) in the milk samples, in period 2006 – 2008, and the mean value over this period are represented in the Figure 3.

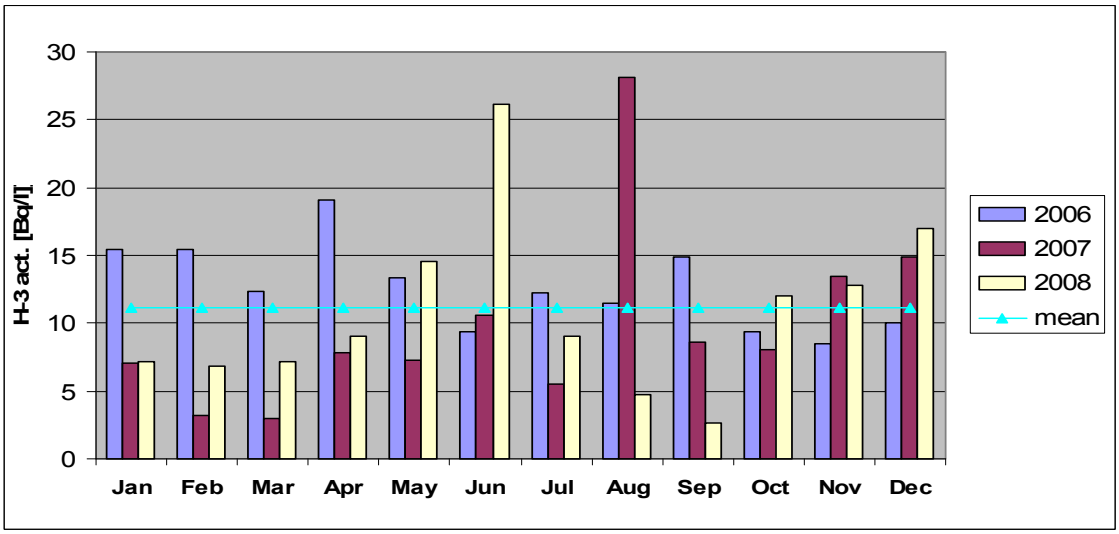


**Figure 3. Tritium concentration activities in milk, between 2006 and 2008, around Cernavoda NPP.**

Fish samples are analysed from Danube River – Cernavoda Harbour (indicator location LII-09, downstream of confluence of evacuation canal with Danube River) and Danube-Black Sea Channel – Cernavoda Harbour Lock (reference location LII-05, upstream of evacuation way) – for liquid emissions in the environment, and 3 pounds: Domneasca (AII-01, 8 km NNE), Baciu (SSS-14, 17 km SV) and Faclia (SSS-15, 8 km SE) – for gaseous emissions in the environment; the last two locations have been introduced in the monitoring program since 2008. Results of tritium measurements (Bq/kg) in the fish samples, in period 2006 – 2008, are represented in the Figure 4.

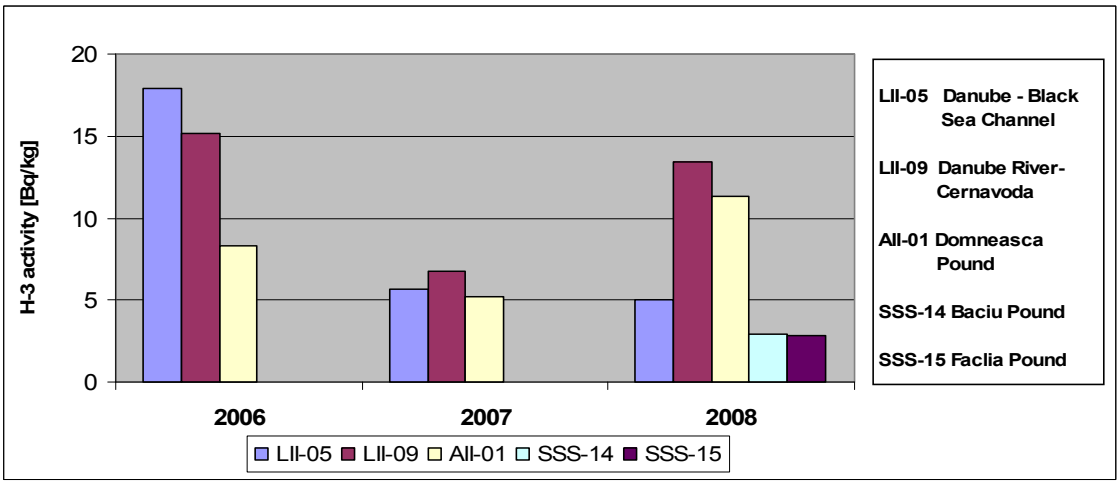


**Figure 4. Tritium activity concentration in fish samples from the Cernavoda NPP monitoring area, between 2006 and 2008.**

## Discussion

Results of tritium measurements in water vapour samples, in period 2006 – 2008, for 2 locations (represented in the Figure 1), are relatively low. For the indicator location – Cernavoda town (ADI-08) results are situated between 0.010 and 3.290 Bq/m$^3$ (mean value: 0.580 Bq/m$^3$) and for background station – Topalu village (ADB-01) results are from 0.010 to 0.050 Bq/m$^3$ (mean value: 0.080 Bq/m$^3$).

Tritium activity concentrations in drinking water sample, represented in Figure 2, are very low comparing with legal limit of 100 Bq/m$^3$. Most of the results are situated below MDA (2.4 Bq/l).

In milk samples, tritium activity concentrations (monthly mean values of weekly sample measurements) in period 2006 – 2008 (represented in Figure 3) are situated between 2.7 and 28.2 Bq/l. Annual mean values of the monthly averages are the following: for 2006 – 12.6 Bq/l, for 2007 – 9.8 Bq/l, for 2008 – 10.8 Bq/l. The mean value for entire studied period is 11.1 Bq/l.

For fish samples, it can be notice that tritium activity concentrations in free water, in the studied period (represented in Figure 4), are lower in the pound water than in the flowing water. The mean value for period 2006 – 2008, for flowing water is 10.7 Bq/kg and the mean value for the same period in pond water is 6.1 Bq/kg.

## Conclusions

The results of the monitoring program are annually compared with the results of The Preoperational Environmental Monitoring Program performed between 1984 and 1996. There were no environmental radioactivity modifications around the Cernavoda NPP comparing to the period before the NPP operation.

In generally, measurements shown that the radiation levels in the external area of a nuclear power plant are around 0.01 mSv per year, comparing with the annual effective dose due to natural radiation sources of 2.4 mSv – the major component coming from the radon (Rn-222, $T_{1/2}$ = 3.8 days) – about 1.3 mSv.

## References

Environmental Radioactivity Monitoring Program for Cernavoda NPP, SI-01365-RP15, 2007.

Annual Environmental Report of Cernavoda NPP, 2007.

Main Findings of Commission's Article 35 verification in Romania – Cernavoda Nuclear Power Plant, European Commission DG TREN, 2007.

Review of the Radiation Protection Programme of the Cernavoda Nuclear Power Plant Control of workers, public and environmental exposure to tritium – Report of the IAEA International Expert Review Service Mission Cernavoda, Romania, 2008.

E. Bobric, C. Bucur, S. Popoaca, I. Popescu, V. Simionov: The impact of tritium emissions from Cernavoda NPP normal operation on environment; "Seventh international conference on nuclear and radiochemistry"; 2008 Aug 25 – 29; Budapest, Hungary.

Information Report – Result of the Environmental Radioactivity Monitoring Program at the Cernavoda NPP in period January – December 2006, IR-96200-023, 2007.

Information Report – Result of the Environmental Radioactivity Monitoring Program at the Cernavoda NPP in period January – December 2007, IR-96200-027, 2008.

Information Report – Result of the Environmental Radioactivity Monitoring Program at the Cernavoda NPP in period January – December 2008, IR-96200-030, 2009.

# Radionuclides activity concentration in soil in Serbia

Pantelić, Gordana[1]; Eremić Savković, Maja[1]; Vitorović, Gordana[2]; Vuletić, Vedrana[1]; Tanasković, Irena[1]; Javorina, Ljiljana[1]

[1] Serbian Institute of Occupational Health "Dr Dragomir Karajović", Deligradska 29, Belgrade, SERBIA

[2] Faculty of Veterinary Medicine, Bulevar oslobodjenja 18, Belgrade, SERBIA

## Abstract

The soil is the basic environment of migration of radionuclides into plants, where from they reach the people and animals through food. The type of soil affects the distribution of radionuclides in the soil itself and their transfer into plants, respectively. Systematic testing of radioactivity of soils in the Serbia is performed after the Chernobyl accident. The periods of sampling were spring and autumn every year. According to collected data, the activity of natural radionuclides was very equal on all locations every year as it was expected because of long half lives of natural radionuclides. High standard deviation and big difference between minimal and maximal $^{137}Cs$ activity concentrations suggested typical artificial pollutant. The activity of long-living radionuclide $^{137}Cs$ is constantly decreasing in the upper layers of uncultivated soil, but because of its long half-life it will remain in ecosystem for a long time.

## Introduction

The primary reason for being concerned about radioactive contamination of the environment is that it results in exposure of humans. External irradiation from radionuclides naturally present in the environment or released from man-made practice or events is usually an important component of the exposure. Most of the food consumed by human beings is grown on land. Contamination of land can occur either from deposition of material originally introduced to atmosphere, or from waste products discharged directly placed in or on the ground, from which they are eventually mobilized by groundwater or erosion.

Soil consists of mineral and organic matter, water, and air arranged in a complicated physicochemical system that provides the mechanical foothold for plants in addition to supplying their nutritive requirements. The type of soil affects the distribution of radionuclides in the soil itself and their transfer into plants, respectively.

Radionuclides deposited on land may enter human food chain in the following ways:

– by direct deposition onto the leaves or exposed parts of plants that are eaten by humans or other animals,

– by persistence in layers of soil from which they are taken up into growing plants through their roots,
– by resuspension as dust from the soil or from other exposed surfaces,
– by being washed of the surface or from deeper ground layers into water sources that are used ultimately for drinking or for irrigation, or as media from which fish or other food are drawn.

The global source of radionuclide contamination in our country is the fallout due to previous nuclear testing and Chernobyl accident, and, in the recent time, after the NATO aggression, depleted uranium content in the environmental samples.

The three naturally occuring radioactive series and $^{40}$K contribute for most of the naural terrestrial radoactivity. Aditionally $^{137}$Cs is the most important radionuclides which contribute to human exposure after nuclear testing and Chernobyl accident.

## Material and methods

Systemic testing of radioactivity of soils is performed on 10 locations in the Serbia (Belgrade- 3 sites, Lazrevac, Obrenovac, Novi Sad, Subotica, Niš, Zaječar, Zlatibor), twice a year during the 20 years period after the Chernobyl accident according to methods defined by regulations (Pantelić et al., 2006).

Additionally to that program undisturbed grassland soils were sampled in 33 different sites in Serbia during 2006-2008. Several sites are located in a mountainous area in the west and central of Serbia (Zlatibor, Kopaonik), several sites in a flat northern Serbia (Vojvodina) and several sites in the south Serbia. In each site 5 cm thick sample layers were separately collected. The periods of sampling were spring and autumn.

The soil samples were purified from plants and rocks. Each sample was dried in an oven at 105$^{o}$C-110$^{o}$C to constant weight during 24-48 h. The dry soil was crushed and sieved (0.5 mm). The resulting sample was weighed and transferred into a Marinelli beaker. Natural and artificial radionuclides concentrations were measured using a high-resolution gamma ray spectrometer (HPGe detector - 30 % efficiency at 1332 keV). Time of measurement was at least 20000 s.

The radionuclide activity of uranium and thorium series and $^{40}$K, as well as the artificial radionuclide $^{137}$Cs was determined.

## Results and discussion

The radionuclide activity of natural uranium and thorium series, and natural radionuclide $^{40}$K was determined in all soil samples. Among fission products, only $^{137}$Cs was measured, while other radionuclides were below detection limit.
The results of measurements are presented in tables 1-4.

Minimum, maximum and average radionuclide concentration measured in 2005 in different regions in Serbia in table 1 is showed. Natural radioactivity in Vojvodina and west and central part of Serbia is very similar, while this activity in south part of Serbia is little bit higher. These results are the same as previos obtained results (during 1987-2004) for the same sites in Serbia because of long half lives of natural radionuclides (Eremić-Savković et al., 2002; Pantelic et al., 2000; Pantelić et al., 2006).

The similar results for natural radionuclide concentration were obtained during 2006-2008 (table 2-4). Maximum activity concentratin for all natural radionuclide is

twice time higher then minimum concentration for the same radionuclide at the same region, but calculated standard deviation is less then 30 % for almost all natural radionuclides.

**Table 1. Radionuclide activity concentration in the soil in Serbia in 2005.**

| Region | | $^{40}K$ (Bq/kg) | $^{137}Cs$ (Bq/kg) | $^{232}Th$ (Bq/kg) | $^{226}Ra$ (Bq/kg) | $^{238}U$ (Bq/kg) | $^{235}U$ (Bq/kg) |
|---|---|---|---|---|---|---|---|
| Vojvodina | Minimum | 306 | 1.5 | 20 | 21 | 18 | < 1 |
| | Average | 420 ± 80 | 7.5 ± 4.5 | 30 ± 9 | 33 ± 11 | 32 ± 13 | 1.5 ± 0.6 |
| | maximum | 523 | 17 | 48 | 54 | 65 | 2,9 |
| West and central | Minimum | 102 | 5.9 | 8.6 | 7.6 | 19 | < 0.6 |
| | Average | 490 ± 200 | 57 ± 47 | 40 ± 16 | 42 ± 17 | 44 ± 19 | 2 ± 1 |
| | maximum | 687 | 172 | 75 | 76 | 103 | 4.2 |
| South Serbia | Minimum | 439 | 0.9 | 37 | 27 | 35 | 1.6 |
| | Average | 590 ± 130 | 36 ± 28 | 42.5 ± 4.3 | 38 ±11 | 75 ± 43 | 2.3 ± 0.5 |
| | maximum | 829 | 68 | 48 | 54 | 153 | 2.9 |

**Table 2. Radionuclide activity concentration in the soil in the Vojvodina region.**

| | $^{40}K$ (Bq/kg) | $^{137}Cs$ (Bq/kg) | $^{232}Th$ (Bq/kg) | $^{226}Ra$ (Bq/kg) | $^{238}U$ (Bq/kg) | $^{235}U$ (Bq/kg) |
|---|---|---|---|---|---|---|
| Minimum | 312 | 1.5 | 28 | 26 | 29 | 1.2 |
| Average | 460 ± 85 | 7.5 ± 4.5 | 38.9 ± 5.8 | 40.4 ± 6.6 | 50 ± 22 | 2.0 ± 0.4 |
| maximum | 612 | 17 | 48 | 49 | 88 | 2.8 |

**Table 3. Radionuclide activity concentration in the soil in the west and central part of Serbia.**

| | $^{40}K$ (Bq/kg) | $^{137}Cs$ (Bq/kg) | $^{232}Th$ (Bq/kg) | $^{226}Ra$ (Bq/kg) | $^{238}U$ (Bq/kg) | $^{235}U$ (Bq/kg) |
|---|---|---|---|---|---|---|
| Minimum | 162 | 6.3 | 7.4 | 11 | 9.4 | 0.5 |
| Average | 440 ± 170 | 69 ± 73 | 35 ± 19 | 36 ± 15 | 45 ±22 | 1.7 ± 0.7 |
| maximum | 586 | 197 | 60 | 55 | 117 | 2.6 |

**Table 4. Radionuclide activity concentration in the south part of Serbia**

| | $^{40}K$ (Bq/kg) | $^{137}Cs$ (Bq/kg) | $^{232}Th$ (Bq/kg) | $^{226}Ra$ (Bq/kg) | $^{238}U$ (Bq/kg) | $^{235}U$ (Bq/kg) |
|---|---|---|---|---|---|---|
| Minimum | 368 | 1.4 | 28 | 28 | 24 | 1.3 |
| Average | 512 ± 83 | 21 ±11 | 43 ± 16 | 46 ± 12 | 74 ± 44 | 2.5 ± 1.0 |
| maximum | 603 | 31 | 70 | 67 | 146 | 4.4 |

Radionuclide $^{137}Cs$ was present in all soil samples. High standard deviation and big difference between minimal and maximal activity concentrations of cesium suggested typical artificial pollutant. Given that its half-life is 30 years, it is distributed deeply into soil by washing out, and it will remain in ecosystem for a long time. Extremely high $^{137}Cs$ concentrations were recorded in the uncultivated soil in the west part of Serbia, that could be explained by first precipitations following immediately the Chernobyl accident. The activity of long-living radionuclide $^{137}Cs$ is constantly decreasing in the upper layers of uncultivated soil comparing with mesurement before 2006 (Pantelić et al., 2006).

## Conclusions

Three years of monitoring the content of natural radionuclides as well as radionuclides of artificial origin in soil samples in the Republic of Serbia indicated that there was no deviations in the natural activity from the average values for the same types of soil samples obtained before 2006. High standard deviation and big difference between minimal and maximal $^{137}Cs$ activity concentrations suggested typical artificial pollutant. The activity of long-living radionuclide $^{137}Cs$ is constantly decreasing in the upper layers of uncultivated soil, which is the result of cesium breakdown and its transport into lower layers.

## References

Eremić-Savković M, Pantelić G, Javorina Lj, Tanasković I, Vuletić V. Radioactivity measurments of soil samples in the Republic of Serbia for the period 1999-2001. Proceedings of the first European IRPA Congress. Towards harmonisation of Radiation Protection in Europe, Florence, 2002, R-137

Pantelic G.K, Petrovic I.K, Javorina Lj.R. Systematic Examination of Radioactive Contamination in Yugoslavia. Procceding of IRPA-10, Hiroshima, 2000, P-4a-253, 1-4

Pantelić G, Eremić Savković M, Vuletić V. Soil investigation in environmental radioactivity monitoring of Serbia. Radionuclide contamination of Serbian soil and remediation possibility. Monograph. Editor Mirjana Stojanović. Belgrade, 2006, 141-164, in Serbian.

# Monte Carlo calculation of ambient dose equivalent and effective dose from natural radionuclides in the soil of Vojvodina district in Serbia

Spasic Jokic, Vesna[1]; Gordanic, Vojin[2]
[1] Faculty of Technical Sciences, University of Novi Sad, SERBIA
[2] Geosci, Belgrade, SERBIA

## Abstract
Presented results are the part of the project financed by Ministry of Science and Technological Development, Republic of Serbia. As the main influences come from uranium, thorium and potassium we measured their concentrations in soil by radiometric techniques. Further we calculate external doses as well as effective doses for particular organs and specified tissues using Monte Carlo code. In this paper only the results for external dose equivalent at 1 m from the surface are presented. Two depths of the soil are taken into consideration, infinite and 15 cm. The results are given for the territory of Bela Crkva and Vrsac in Vojvodina district, Serbia.

## Introduction
The most widely spread radionuclides of natural origin come from uranium and thorium series as well as from potassium (UNSCEAR 2000). Those natural occurring radionuclides are internal or external sources of radiation depending on the position to the organisms. In this survey just radiation originating from the internal exposure is taken into consideration, which arises from intake of terrestrial radionuclides by inhalation and ingestion.

Recently, few researches were carried out on territory of Republic of Serbia in order to determine concentrations of natural occurring radionuclides in surface soil (Bikit et al. 2005; Dragovic et al. 2006). In this study, in addition to measuring concentrations of natural radionuclides in the territory of Bela Crkva and Vršac, the goal was the estimation of effective dose from inhalation and ingestion. The region of interest is located in a northern-east part of Serbia, in the province of Vojvodina. It is mainly oriented to the agriculture, but it is potentially interesting for tourism. Therefore it is important to determine the impact of internal exposure to natural radionuclides (uranium, thorium and potassium). In Figure 1 the location under investigation is shown on the map of Vojvodina.

Eighty soil samples were taken from the area of Bela Crkva and Vršac to evaluate concentration of these natural radioactive sources. The concentrations of radionuclides in the samples were measured by radiometric methods. Based on those measurements

the activities of uranium, thorium and potassium were calculated. Using Monte Carlo simulation the conversion factors were determined in order to estimate the contribution of above-mentioned radionuclides to the effective dose from ingestion and inhalation.

This study was supported by Ministry of Science and Technological Development of Republic of Serbia. The purpose of the project was determining concentration of natural radionuclides in the soil samples and evaluating the radiation doses, received by people living in the area under investigation, resulting from the inhalation and ingestion. The outputs of the project were radiometric maps, which showed the level of the exposure from the radioactive sources.

**Fig. 1. Map of Vojvodina district.**

## Material and methods

### Sampling and radioactivity measurements

For the purpose of this research, eighty soil samples were taken from 13 uncultivated locations in the same geographic area in the vicinity of Bela Crkva and Vršac. They were collected at a depth of (0-5) cm, and each sample weighed 0.5 kg. Geographical coordinates of sampling positions were determined using a GPS tracker. All the samples were air dried, homogenized and sieved to grain size of less than 0.60 mm. They were prepared and placed in cylindrical gas-tight containers with the same geometry as to sample container used for efficiency calibration. The samples were kept for at least three weeks before the measurement to reach secular equilibrium between thorium and radium and their decay products.

Further, gamma-spectrometric measurements were performed with high purity, low energy germanium semiconductor detector (HPGe), manufactured by ORTEC, accompanying electronic equipment and ORTEC software for spectra evaluation. Relative efficiency of HPGe is 28 % and the energy resolution achieved in the measurements is 2 keV, both at the 1.33 MeV reference transition of $^{60}$Co. Calculated minimum detectable concentration (MDC) is 1.1 Bq/kg for $^{238}$U, 1.3 Bq/kg for $^{232}$Th and 2.4 Bq/kg for $^{40}$K. The counting geometry is identical for all radionuclides. The expanded uncertainty of determined radionuclide concentration is 15 % (k = 2) in each case. Detectable energy range of used instrument is up to 2 MeV. Instrument calibration was performed using reference sources:

1) NBL 103 (USAEC), content of U: 0,05 %
2) NBL 107, 0,1 % Th
3) K in form of potassium-chloride
4) Certified mix source, Amersham, 1988 ($^{55}$Fe, $^{60}$Co, $^{137}$Cs, $^{226}$Ra and $^{241}$Am).

## Monte Carlo simulation

In dose estimation, it is assumed that natural uranium contains three isotopes: 99,284 % $^{238}$U +0,711 % $^{235}$U + 0,0058 % $^{234}$U, while other isotopes of uranium neglected.

In order to determine the conversion factors which are needed for calculation of the effective dose due to exposure to radionuclides entered by inhalation or ingestion, Monte Carlo method is used. Firstly, the dose rate conversion factor (absorbed dose rate in air per unit activity per unit of soil mass, nGy/h per Bq/kg) was estimated. For simulation the inscattered and scattered radiation is taken into account.

The main assumption of the problem starts from the polynomial expansion matrix, which solves the transport problem of radionuclides in the soil and between soil and air. Given the gamma lines of radionuclides of interest, the problem of relatively narrow energy range from 1 keV to 2.75 MeV was resolving.

It is assumed that the ground is infinite medium for photon scattering and radionuclides are uniformly distributed over the surface from which the soil samples were taken. Characteristics of soil and cross-sections for photons are taken from existing database.

The code for simulation is written in FORTRAN 77. The simulation is done in $2\pi$ geometry, which was only reasonable solution due to the assumption of indefinite soil thickness. The same density of soil is taken for all the samples, $\rho = 2.6$ kg/m$^3$, which brought additional errors in calculation, but not greater than 2%. The “detector” is 1 m above the soil and is simulated by a square surface with side of 2 m, located in the center of the square slab which represents the soil.

The mechanisms of interaction of photons with matter taken into account were the photoelectric effect, Compton scattering and pair production. Keeping in mind the characteristics of natural radionuclides and its interaction with soil, a cut off the energy range from 50 keV to 2.6 MeV was introduced. This is the reasonable cut off, as the highest important gamma energy of natural radionuclide is 2614 keV and because photons even below 50 keV contribute a negligible amount to the dose rate. ( Clouvas, A. et al 2000)

In order to determine effective dose, voxel phantom was used in Monte Carlo simulation. It enabled solving transport problem of radionuclides entering human body through the respiratory and digestive tract. The effective dose coefficients obtained by Monte Carlo method are expressed in units of Sv/Bq. Effective doses from inhalation and ingestion were determined by multiplying the activities and obtained conversion factors.

## Results

The activity concentrations of $^{238}$U and $^{232}$Th varied from (3.24-57.02) Bq/kg and from (3.4–90.42) Bq/kg, respectively. $^{40}$K was found in higher concentration, it ranges from (84.78–3114.8) Bq/kg. In some samples it was not possible to determine the radionuclide concentration, because it was lower than the minimum detectable

concentration. The mean concentration is 25.23 Bq/kg, 39.03 Bq/kg and 873.69 Bq/kg for $^{238}$U, $^{232}$Th and $^{40}$K, respectively.

The concentrations of $^{238}$U, $^{232}$Th and $^{40}$K analyzed in this research and those reported by UNSCEAR (B) (2000) are presented in Table 1. It is shown that activity concentration of $^{238}$U agrees with one in other countries, and concentration of $^{232}$Th is a bit out of worldwide activity range. In the case of $^{40}$K, the mean activity concentration is much higher that the worldwide average value (400 Bq/kg). It may be explained by either the use of fertilizers or the soil type. (Colmenero Sujo et al. 2004)

The mean concentrations in soil samples from Serbia and Montenegro are 597.96 Bq/kg, 35.697 Bq/kg and 42.12 Bq/kg for $^{40}$K, $^{238}$U and $^{232}$Th, respectively (Dragovic et al. 2006). When the obtained results from are study are compared with these values, it is obvious that concentrations of $^{238}$U and $^{232}$Th are lower, but measured concentration of $^{40}$K is higher in our study.

**Table 1. The comparison of activity concentration ranges of natural radionuclides in soil samples from the present study with the values obtained in other studies conducted worldwide.**

| Concentration (Bq/kg) | $^{40}$K | $^{238}$U | $^{232}$Th | Reference |
|---|---|---|---|---|
| Croatia | 140-710 | 83-180 | 12-65 | UNSCEAR, 2000 |
| Bulgaria | 40-800 | 8-190 | 7-160 | UNSCEAR, 2000 |
| Romania | 250-1100 | 8-60 | 11-75 | Iacob, 1996 |
| Hungary | 79-570 | 12-66 | 12-45 | UNSCEAR, 2000 |
| Poland | 110-970 | 5 -120 | 4 -77 | Jagielak et al., 1992 |
| Median value | 140-850 | 16-110 | 11-64 | UNSCEAR, 2000 |
| Bela Crkva and Vršac | 84.78-3114.8 | 3.24-57.02 | 3.4-90.42 | Present study |

Furthermore, the effective dose was calculated using the determined activity concentrations of $^{238}$U, $^{232}$Th and $^{40}$K and the conversion factors, which the output of Monte Carlo simulation were. The annual effective dose from inhalation of $^{238}$U ranges from (58 - 1100) μSv, the effective dose of $^{232}$Th varies from (39 - 1040) mSv and the effective dose of $^{40}$K varies from (0.53 – 19.5) μSv. On the other hand, the annual effective dose received by ingestion of $^{238}$U ranges from (0.01 – 0.2) μSv, the effective dose of $^{232}$Th varies from (1.25 – 33.3) μSv and the effective dose of $^{40}$K varies from (0.21 – 7.8) μSv.

Using adequate software and based on the GPS coordinate of a taken soil sample, the distribution maps of the activity concentration were generated. The maps are shown in Figures 2-4. It is important to emphasize that distribution of effective dose due to ingestion and inhalation has the same distribution, just the corresponding values are different.

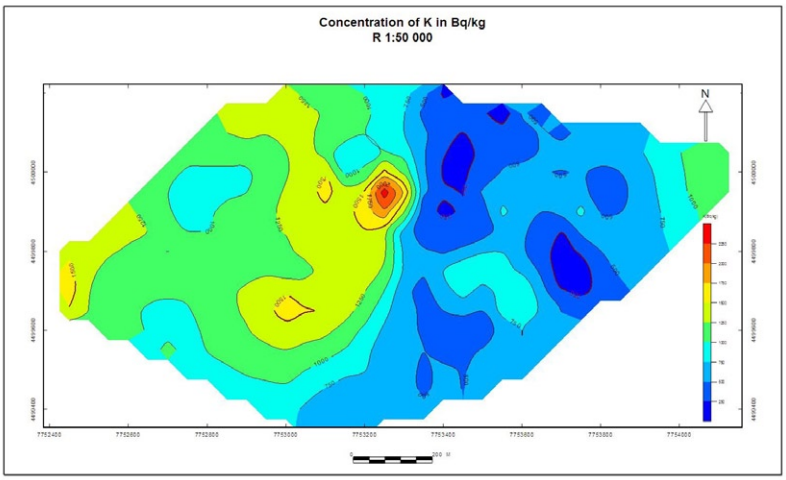


**Figure 1. Activity concentration of $^{40}$K in the area of Bela Crkva and Vršac.**

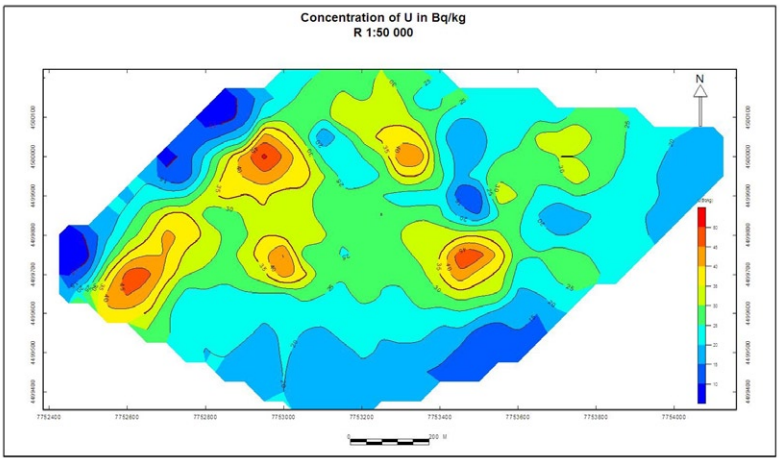


**Figure 2. Activity concentration of $^{238}$U in the area of Bela Crkva and Vršac.**

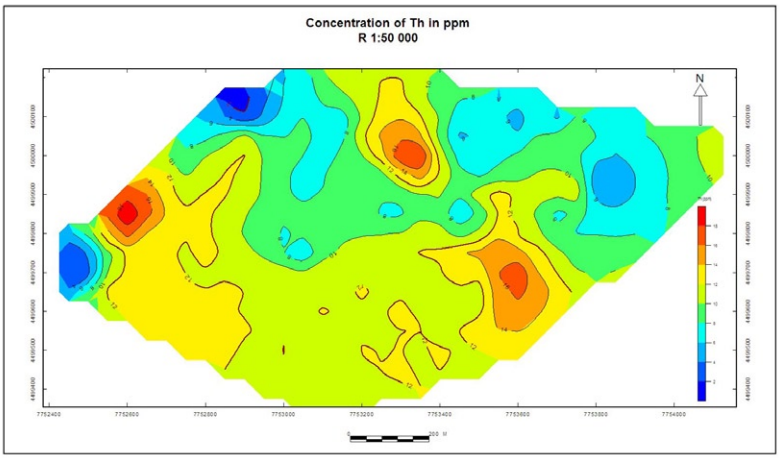


**Figure 3. Concentration of $^{232}$Th in the area of Bela Crkva and Vršac.**

## Discussion

There are two main processes that contribute to internal exposure, the general term used to describe exposures that involve the intake of radionuclides into the body. The two processes are inhalation of contaminated air and ingestion of contaminated foodstuffs. (UNSCEAR 2000) As it is already mentioned, the aim of this research was to determine annual effective dose from inhalation and ingestion of long-lived radionuclides.

**Table 2. Annual effective dose from ingestion of terrestrial radionuclides.**

| Ingestion | Average (UNSCEAR 2000) | Bela Crkva and Vršac (Present study) |
|---|---|---|
| $^{40}K$ | 0.17 | 0.004 |
| U and Th series | 0.12 | 0.017 |
| Total ingestion exposure | 0.29 | 0.021 |

Since $^{238}U$ and $^{232}Th$ are alpha-emitters, when they are ingested or inhaled, they contribute significantly to the radiation dose that people receive. (Colmenero Sujo et al. 2004) Whereas potassium is beta-emitter, its impact is less significant. These facts agree with the output of this research. In Table 2 the obtained effective doses are compared with values reported by UNSCEAR. It is shown that effective dose from ingestion of $^{40}K$ (4 μSv) is lower than the average value (170 μSv). Obtained annual effective dose from ingestion of $^{238}U$ and $^{232}Th$ (17 μSv) is lower than the average value (120 μSv). The total effective dose from inhalation is higher than average value given in UNSCEAR report.

## Conclusions

This paper presents the radioactivity concentrations of $^{238}U$, $^{232}Th$ and $^{40}K$ for 80 soil samples collected in the area of Bela Crkva and Vršac. According to the obtained results, it is shown that activity concentration of $^{40}K$ exceeds worldwide average value. Further investigation should be done in order to give an explanation, but it can be assumed that using fertilizers could contribute to higher potassium concentration. Concentrations of $^{238}U$ and $^{232}Th$ are similar to the reference values provided by UNSCEAR.

Effective dose, an indicator of the stochastic effect of radiation, has been widely used in dose evaluation in the environment. In this research the effective dose from inhalation and ingestion of natural radionuclides is estimated. It is proven that effective dose from ingestion is pretty lower than average values. As regards inhalation, effective dose exceeds average value.

Further research will include using risk assessment.

## References

Bikit I et al. Radioactivity of the soil in Vojvodina (northern province of Serbia and Montenegro). Journal of Environmental Radioactivity 2005; Vol.78:11–19

Clouvas A, Xanthos S, Antonopoulos-Domis M, Silva J.Monte Carlo Calculation of Dose Rate Conversion Factors for External Exposure To Photon Emitters in Soil. Health Physics 2007; Vol.78(3):295-302

Colmenero Sujo et al.Uranium-238 and thorium-232 series concentrations in soil, radon-222 indoor and drinking water concentrations and dose assessment in the city of Aldama, Chihuahua, Mexico. Journal of Environmental Radioactivity 2004; Vol.77:205–219

Dragovic S, Jankovic Lj, Onjia A, Bacic G.Distribution of primordial radionuclides in surface soils from Serbia and Montenegro. Radiation Measurements 2006; Vol.41:611 – 616

Iacob O. Exposure from natural radiation sources in Romania. J. Prev. Med.1996; Vol. 4(2): 73-82

Jagielak J, Biernacka M, Henschke J et al. Radiation Atlas of Poland. 1992; ISBN83-85787-01-1

UNSCEAR Report of the United Nations Scientific Committee on the Effects of Atomic Radiation to the General Assembly 2000; United Nations, New York.

UNSCEAR Annex B: Exposures from natural radiation sources 2000; United Nations, New York.

# Interpretation of radionuclide concentrations near the detection limit for dose calculations

Črnič, Boštjan; Korun, Matjaž; Zorko, Benjamin
Jožef Stefan Institute, Jamova cesta 39, Ljubljana, SLOVENIA

## Abstract

As with many other environmental pollutants, the concentration distribution of various radioactive substances in the environment can be measured. The influence of radioactive releases into the environment, based on these measurements, can then be used in assessments of the radiation doses, so determining the implied risks to the population.

The outcome of a measurement of the activity concentration can be described as a result that is below the decision threshold, a result that has an uncertainty too large to be reported or a definite measurement outcome. In the first case the analyte does not appear in the list of the results, in the second case it appears as an upper limit and in the third case as a measurement result including its uncertainty. A method for consistently treating these three kinds of measurement outcomes is presented.

When the measurement data are used for dose assessments, averaging may be introduced in order to reduce the amount of input data. It has been shown that in order to reduce the systematic influences occurring when calculating averages from sets of data, where measurement outcomes below the decision threshold or measurement results with an unacceptably high relative uncertainty are frequent, the maximal acceptable relative uncertainty should be set as high as possible. Because of the different characteristics of the analytes, however, it is advantageous to use analyte-dependent maximal acceptable relative uncertainties.

## Introduction

Radiological environmental-monitoring programs are carried out in order to survey the radioactivity in the natural and living environment. The purpose of the survey is to assess the impact of the radioactivity on the population, which is performed by evaluating the doses. The radiological impact of nuclear installations in normal operations is commonly considered to have two aspects: the annual dose to a member of the critical group, and the collective dose. This annual dose is compared to the respective regulatory dose limit. To perform the comparison it is useful to know the uncertainty of the dose, which includes the uncertainties associated with the measurement results. Therefore, for a realistic evaluation all the relevant pathways have

to be controlled and the concentrations of the most radiotoxic isotopes have to be measured.

It is important to assess the doses in accordance with the directions of the regulatory bodies and the recommendations of international organisations. If possible, the doses are calculated from the concentrations of materials from the environment. However, doses from discharges in normal operation can accumulate over many years and at distances where the radionuclides are diluted below the detection limit. Therefore, mathematical models and statistical approaches have to be used to evaluate the doses, including the projected doses, correctly.

If the concentrations of the radionuclei of interest are below the detection limit of the measurement methods used, the measurement outcomes may be described as measurement results or concentrations below the decision threshold. Alternatively, some of the radionuclei may be identified in the sample, but the concentrations may be too low to be evaluated quantitatively. In this case the relative uncertainty of the measurement result may approach or even exceed 100%. To treat these results a maximum relative uncertainty is introduced for results reported. The measurement results having a larger relative uncertainty are quoted as a concentration below an upper limit, which is given as the measurement result, increased by its uncertainty, multiplied by a coverage factor, which is determined by the interval of confidence. To arrive at a reliable dose estimate these incomplete data have to be included in the evaluation. However, neither the decision thresholds nor the upper limits are properties of the sample and therefore do not describe the state of the nature but the properties of the measurement process. Therefore, the doses assessed must not depend on them.

It is the aim of this contribution to present a method for how to treat the experimental data in such a way that the assessed doses themselves depend on the sample properties and the uncertainties of the doses on the properties of the analytical process. How to carry out the analytical process in order to minimize the systematic influences arising from converting the measurement results into upper limits is described. This method is used in the evaluation of doses in the program of the off-site radiological monitoring of the NPP Krško (Glavič-Cindo 2006, Glavič-Cindo 2007, Črnič 2008, Črnič 2009, Zorko 2010).

## Material and methods

### The analytical process

The samples that are collected in the annual programs of the radiological survey are usually taken fortnightly, monthly or quarterly. The yearly averages, which are used in the dose assessment, are obtained by averaging the measurement results. Most of the samples, collected in the environment, are measured using gamma-ray spectrometry. For such samples, gamma-ray spectrometry is the method of choice, because of its sensitivity, selectivity and price. Since gamma-ray spectrometry is a multi-nuclide method, the result of a gamma-ray spectrometric measurement is a list of radionuclides identified in the sample and their concentrations.

Within the sample-analysis procedure several operations are made, where the peak count rates or activities are corrected for contributions that do not originate in the material sampled. These operations are a background subtraction, the correction for a

blank and the interference corrections. If the signal from the sampled material is not present or much smaller than the uncertainty of the contribution, which is subtracted, a positive or a negative result is equally probable. In the first case a type-1 error occurs, which occurs in the report as a measurement result with a large relative uncertainty. In most cases this is quoted in the form of an upper limit. Such results are indistinguishable from the results corresponding to samples with a concentration above the decision threshold (critical limit) but having a relative uncertainty exceeding the maximal. It follows that type-1 errors may occur frequently in the measurement outcomes for radionuclei, which are present in the spectrometer background. These are long-lived, naturally occurring radionuclei with their decay products and Cs-137.

If the result of the subtraction is negative, the peak or the radionucleus is deleted from the list of peaks or the radionuclides present in the material sampled (Canberra Industries, 1998). It follows that by the repeated measurements of samples containing a negligible concentration of a radionucleus, one half of the measurements will result in a positive identification. This fraction may be even larger for multi-gamma emitters, if the criterion for the detection allows identification by the recognition of just one of several peaks. For a multi-gamma-ray emitter the activity is calculated as an average over the activities obtained from attributed peaks only, which may result in a considerable systematic influence. The peaks with a negative area are excluded from further analysis and the average calculated corresponds only to the peaks with positive net areas. In the extreme case it may happen that the uncertainty of the average shrinks to a value that results in the average having a relative uncertainty smaller than the maximal. In this case an erroneous result is reported. To decrease the probability of such errors the laboratories maintain maximal relative uncertainties that are much smaller than 100%.

## Presentation of the measurement results

Often the measurement results referring to a specific medium are presented in tables. The measurement results of periodically collected samples of the same medium are presented as records, describing the concentrations of radionuclei at a given sampling time. The measurement outcome can appear in one of three forms:

- as a measurement result: $a \pm u(a)$, where $u(a)$ denotes the uncertainty of the activity concentration $a$,
- as an upper limit: $< q(a)$, where $q(a)$ denotes the decision threshold or the sum of the measurement result and its uncertainty multiplied by the coverage factor
- as an empty space (blank), which implies that the radionucleus was not detected in the sample.

To calculate the yearly averages the three types of entry content have to be converted to the measurement results and their uncertainties. It should be noted that the averaging must not be performed with weights, depending on the uncertainties, in order not to introduce systematic influences into the average.

The uncertainty of the average can be evaluated as the *a-priori* uncertainty, which is given by the uncertainties of the individual measurement results, or as the *a-posteriori* uncertainty, which is given by the spread of the measurement results around the average. Here, care should be taken not to interpret the expected time variations, e.g., seasonal

variations, as deviations from an average, which is assumed to represent a concentration characteristic for the time interval of the averaging. Usually, as the uncertainty of the average, the larger of the *a-priori* and *a-posteriori* uncertainties is used.

Often, the uncertainties are quoted with a coverage factor of unity, defining the interval with a confidence level of 68%. On the other hand, the upper limits are normally calculated for a confidence interval of 95% (ISO 2005). For the one-tailed probability distribution this corresponds to a coverage factor of 1.65 (Hurtgen, 2000). Since the upper values, like the uncertainties, describe the analytical process, they should be treated on the same basis. Therefore, when upper limits are converted to measurement results they are transformed into uncertainties calculated with a coverage factor of unity.

The transformation, which is used for converting the three forms of data in a format that is appropriate for use in the averaging, is the following:

$$\begin{aligned} &a \pm u(a) \Rightarrow a \pm u(a) \\ &< q(a) \Rightarrow 0 \pm q(a)/1.65 \\ &[blank] \Rightarrow 0 \pm 0 \end{aligned} \qquad (1)$$

It can be observed from the Eqs. (1) that the upper limits are transformed to measurement uncertainties. Consequently, the upper limits do not influence the average itself, but its uncertainty.

When performing this transformation, a systematic influence is introduced since all the measurement results having a relative uncertainty exceeding the maximal are replaced by zeros. This effect partially compensates for the effect of false identifications.

If in the spectrum analysis just one peak is used for the calculation of an activity concentration of a radionuclide, and if this peak occurs in the spectrometer background, the probability density distribution for reporting the result $a \pm u(a)$ when the radionucleus is not present in the sample is

$$p(a) = \frac{1}{2u(a)\sqrt{2\pi}} e^{-\frac{a^2}{2u(a)^2}} \qquad (2)$$

giving an average reported activity concentration of $u(a)(\sqrt{2/\pi} \pm \sqrt{1-2/\pi})$ (Korun, 2010). It follows that the relative uncertainty of the average of the wrongly reported activity concentrations, is $\sqrt{\pi/2-1} = 0.76$. Then, in the measurement reports such results are quoted as $< u(a)\sqrt{2/\pi}(1+1.65\sqrt{\pi/2-1}) \approx 1.8u(a)$ and interpreted in the average as $0 \pm 1.8u(a)/1.65$. It follows then that type-1 errors arising from the background subtraction, interference corrections and corrections for blank for the radionuclides that are determined from one spectral peak are, in the averages, properly taken into account with a maximal relative uncertainty of 76%.

It should be noted that the approach described does not comply with the European Commission recommendation on the information on discharges from nuclear installations (Commission recommendation 2004/2/Euratom). Here, the measurement

outcomes below the decision threshold should be substituted by one half of the decision threshold. Only in the case of repeated measurement outcomes below the decision threshold should zeros be assumed to be true values. In our approach the concentration of the radionuclides is reported correctly from the point of view of the analytical process, since the measurement uncertainty is used for determining the measurement outcome.

## Results and discussion

In this section, examples are given in order to illustrate the influence of the maximal relative uncertainty for various types of gamma-ray emitters on the average activity concentration and consequently on the assessed doses.

Let us present the influence of the maximal relative uncertainty on the average over the measurement data, transformed to a form shown in Eqs. (1). In the second row in Table 1 are the hypothetical measurement results, evenly distributed over the interval from 0.7 to 2.7. Since the uncertainties near the decision threshold are dominated by the statistical uncertainty, the measurement uncertainty is a slowly varying function of the measurement result (Weise 2006). Therefore, uncertainties independent of the measurement result are assumed. In these conditions, the *a-priori* uncertainty exceeds the *a-posteriori* uncertainty, and therefore only the *a-priori* uncertainty of the average is presented. For each maximal relative uncertainty in the first row the measurement results, as presented in the measurement report, are given, and in the second row these data are transformed by Eqs. (1) into the form appropriate for averaging. It can be observed that the average value reproduces the average of the measurement results better if the upper limits are calculated for results having a high relative uncertainty, i.e., by using a high maximal relative uncertainty. As it was shown in the previous section, the upper limits for the results with a relative uncertainty exceeding 76% should be quoted. It should also be noted that the difference between the average over the measurement results and the average of the transformed data is covered by the uncertainty in all the maximal relative uncertainties used, but the systematic effect amounts to a factor of 4 when a maximum relative uncertainty of 80% instead of 40% is used.

**Table 1. Comparison between the average over the measurement results (in arbitrary units) and the averages over the measurement data transformed to a form that is appropriate for averaging.**

| Meas. No. | 1 | 2 | 3 | 4 | 5 | 6 | 7 | 8 | 9 | 10 | Av. | Unc. |
|---|---|---|---|---|---|---|---|---|---|---|---|---|
| Results | 0.8±1 | 1.0±1 | 1.2±1 | 1.4±1 | 1.6±1 | 1.8±1 | 2.0±1 | 2.2±1 | 2.4±1 | 2.6±1 | 1.7 | 0.32 |
| Limit of quant.:0.8 | < 2.5 | < 2.7 | < 2.9 | 1.4±1 | 1.6±1 | 1.8±1 | 2.0±1 | 2.2±1 | 2.4±1 | 2.6±1 | | |
| | 0±1.5 | 0±1.6 | 0±1.7 | 1.4±1 | 1.6±1 | 1.8±1 | 2.0±1 | 2.2±1 | 2.4±1 | 2.6±1 | 1.2 | 1.2 |
| Limit of quant.:0.6 | < 2.5 | < 2.7 | < 2.9 | < 3.1 | < 3.3 | 1.8±1 | 2.0±1 | 2.2±1 | 2.4±1 | 2.6±1 | | |
| | 0±1.5 | 0±1.6 | 0±1.7 | 0±1.9 | 0±2.0 | 1.8±1 | 2.0±1 | 2.2±1 | 2.4±1 | 2.6±1 | 1.0 | 1.4 |
| Limit of quant.:0.4 | < 2.5 | < 2.7 | < 2.9 | < 3.1 | < 3.3 | < 3.5 | < 3.7 | < 3.9 | < 4.1 | 2.6±1 | | |
| | 0±1.5 | 0±1.6 | 0±1.7 | 0±1.9 | 0±2.0 | 0±2.1 | 0±2.2 | 0±2.3 | 0±2.5 | 2.6±1 | 0.3 | 1.9 |
| Limit of quant.:0.2 | < 2.5 | < 2.7 | < 2.9 | < 3.1 | < 3.3 | < 3.5 | < 3.7 | < 3.9 | < 4.1 | < 4.3 | | |
| | 0±1.5 | 0±1.6 | 0±1.7 | 0±1.9 | 0±2.0 | 0±2.1 | 0±2.2 | 0±2.3 | 0±2.5 | 0±2.6 | 0 | 2.1 |

For gamma-ray emitters radiating photons at a number of different energies in the identification process, the so-called "abundance limit" parameter is used (Canberra, 1998). This parameter defines for a gamma-ray emitter the minimum ratio of the sum over the emission probabilities for gamma rays identified in the spectrum versus the sum of all the probabilities for the emission of gamma rays for this emitter. It is advantageous to use as many gamma-ray peaks as possible in the activity calculation since interference corrections can then be performed and the average becomes less susceptible to a possible wrong-peak-area evaluation. If the spectrum of a multi-gamma-ray emitter appears in the spectrometer background, it is expected that 50% of the peaks will be identified, providing the concentration of the emitter is well below the decision threshold. With an abundance limit of 50% it is expected that such a radionucleus will be identified in approximately one half of the measurements.

To illustrate the influence of the maximal relative uncertainty on the average a hypothetical example is presented, describing the case of an emitter radiating at several energies with approximately equal probabilities. The case of a multi-gamma-ray emitter radiating at an energy with a much larger probability than at other energies is similar to the case of a radionucleus radiating at a single energy, which was considered in the previous paragraph. The emitter is present in the spectrometer background and radiates at three energies with such probabilities that the uncertainties of the activity concentrations calculated from the areas of the peaks at the three energies are equal. A nucleus, which resembles this example, is U-238, which is in equilibrium with its daughter Th-234 and with U-235 in the natural isotopic ratio. Then, the activity concentrations calculated from the 63-keV, 93-keV and 186-keV peaks have approximately equal uncertainties. The value of the abundance limit parameter of 50% implies that the emitter is identified if any two of the three peaks are identified. Thus, the probability for a false identification is 50%. The average activity concentrations are $u(a)[\sqrt{2/\pi} \pm \sqrt{(1-2/\pi)/2}]$ in the case of two identified peaks (38% of measurements) or $u(a)[\sqrt{2/\pi} \pm \sqrt{(1-2/\pi)/3}]$ in the case of three identified peaks (12% of measurements). The corresponding relative measurement uncertainties are 54% and 44%. To avoid reporting these false results for radionuclei resembling this example, the maximal relative uncertainty should be decreased to below 44%.

Alternatively, increasing the value of the abundance limit parameter can prevent the reporting of false results. A value of 0.7 decreases the probability for reporting false results to 12%, but this is accompanied by an increased probability of type-2 errors.

To present the influence of the abundance limit and maximal relative uncertainty on the frequency of various kinds of measurement outcomes if the activity concentration is near the decision threshold, let us consider again the case of a gamma-ray emitter radiating at three energies. It is assumed that the sample contains an activity concentration that equals its uncertainty if the activity concentration is determined from just one of the three gamma-ray peaks. Since the emitter radiates at three energies, in one measurement three determinations are made and the relative uncertainty of the average activity concentration is $1/\sqrt{3}$. From the probability-density distribution it follows that the probability of the occurrence of type-2 errors is 0.041, the probability for reporting an upper limit is 0.625 (with a maximal relative uncertainty of 80%) and the probability for reporting a positive measurement result is 0.334.

Table 2 presents the probabilities for the type-2 errors and the probabilities for reporting the upper limits if the abundance limits of 50% or 70% were used in the analysis. In the first case the emitter is detected if two of the three peaks in the spectrum are recognized. In the second case the emitter is recognized only in the case when all three peaks are recognized in the spectrum. The probabilities are given for a maximal relative uncertainty of 80% and 44%.

**Table 2. Probabilities for type-2 errors and reporting the upper limits for the case of a gamma-ray emitter radiating at three energies with a concentration corresponding to the statistical uncertainty of one peak area.**

| Abundance limit | Probability of Type-2 errors | Maximal relative uncertainty | |
|---|---|---|---|
| | | 80% | 44% |
| 50% | 0.025 | 0.15 | 0.64 |
| 70% | 0.31 | 0.14 | 0.43 |

It can be observed that at a high abundance limit an unacceptably high probability for measurement outcomes resulting in type-2 errors occurs. These errors occur since the emitter is identified only if all three peaks are identified. At the abundance limit of 50%, at the maximal relative uncertainty of 80%, the minority of measurement outcomes are reported as an upper limit, whereas at the maximal relative uncertainty of 44% the majority is reported in this form. In Table 3 the average over the measurement outcomes resulting in reporting activity concentrations are presented as well as the averages over all the measurement outcomes. In this average activity the concentrations corresponding to type-2 errors and the upper limits are taken into account as zeros.

It can be observed that the systematic influences covered by the uncertainties are smaller at the abundance limit of 50%. At the maximal relative of 44% these influences are larger, since here most of the results are reported as upper limits. It can also be observed that the systematic influences are smaller when a higher maximal relative uncertainty is used.

**Table 3. Average activity concentrations reported and average activity concentrations, calculated over measurement results (in arbitrary units). Here type-2 errors and upper limits have been taken onto account as zeros.**

| Abundance limit | Maximal relative uncertainty | | | |
|---|---|---|---|---|
| | 80% | | 44% | |
| | Average reported activity concentration | Average over all results | Average reported activity concentration | Average over all results |
| 50% | 1.17 ± 0.59 | 0.97 ± 0.64 | 1.56 ± 0.59 | 0.52 ± 0.92 |
| 70% | 1.23 ± 0.58 | 0.68 ± 0.47 | 1.54 ± 0.58 | 0.40 ± 0.58 |

## Conclusions

It can be concluded that systematic influences originating from transforming the measurement outcomes to a form that is appropriate for averaging can introduce substantial systematic influences into the averages, if results near the detection limit are

abundant. To minimize the systematic effects on the average the maximal relative uncertainty, quoted in the reports, has to be optimised. This optimisation has to take into account two conflicting requirements: minimizing the probability of reporting the wrong results and minimizing the systematic influences on the average. Whereas according to the first requirement the maximal relative uncertainty should be set low, the second requirement demands a high relative uncertainty. The smallest systematic influence on the average can be achieved by using a maximal relative uncertainty, which is nuclide dependent. When the measurement outcome is dominated by the information extracted from a single determination, a relative uncertainty of 76% should be used. On the other hand, when the measurement outcome information from more determinations contributes, the maximal relative uncertainty should be set to a smaller value.

If the averages are used in dose assessments, great care should be taken in order to minimize the systematic influences on the calculated doses. Since doses should be assessed realistically, they must be free of impacts originating in the analytical process as well as in the way the measurement results are presented.

## References

Canbera Industries, Genie – VMS Basic User Reference, 1998.

Commission of the European Communities, Commission recommendation on radioactive airborne and liquid discharges into the environment from nuclear power reactors and reprocessing plants in normal operation, Official Journal of the European Union 002, 2004; 36 – 46.

Črnič B, Glavič-Cindo D, Korun M (Eds). Meritve radioaktivnosti v okolici nuklearne elektrarne Krško, Poročilo za leto 2007; Lubljana, Slovenia: Jožef Stefan Institute, 2008.

Črnič B, Glavič-Cindo, Korun M (Eds). Meritve radioaktivnosti v okolici nuklearne elektrarne Krško, Poročilo za leto 2008; Lubljana, Slovenia: Jožef Stefan Institute, 2009.

Glavič-Cindo D, Zorko B (Eds). Meritve radioaktivnosti v okolici nuklearne elektrarne Krško, Poročilo za leto 2005; Lubljana, Slovenia: Jožef Stefan Institute, 2006.

Glavič-Cindo D, Črnič B (Eds). Meritve radioaktivnosti v okolici nuklearne elektrarne Krško, Poročilo za leto 2006; Lubljana, Slovenia: Jožef Stefan Institute, 2007.

Hurtgen C, Jerome S, Woods M. Revisiting Curie – how low can you go?. Appl. Radiat. Isot. 2000; 53: 45 – 50.

ISO11929-7. Determination of the detection limit and decision threshold for ionising radiation measurements- Part 7: Fundamentals and general applications. Geneve: International Standards Organization; 2005.

Korun M, Maver Modec P. Interpretation of measurement results near the detection limit in gamma-ray spectrometry using Bayesian statistics, to be published 2010.

Weise K, et al. Bayesian decision threshold, detection limit and confidence limits in ionising-radiation measurement, Rad. Prot. Dosimetry, 2006; 121: 52 – 63.

Zorko B, Glavič-Cindo D (Eds). Ovrednotenje rezultatov meritev radioakivnosti v okolici nuklearne elektrarne Krško (Poročilo za leto 2009); Lubljana, Slovenia: Jožef Stefan Institute, 2010.

# Environmental tritium monitoring techniques applied for a tritium removal facility

Dobrin, Relu[1]; Dulama, Cristian[1]; Toma, Alexandru[1];
Ciurduc Todoran, Germizara Anca[1]; Varlam, Carmen[2]; Pavelescu, Mihai[3]
[1] RAAN-SCN, Radioprotection, ROMANIA
[2] ICSI – Valcea, ROMANIA
[3] RAAN-SCN, ROMANIA

## Abstract

Nuclear and radiological installations are subjected to the regulatory control throughout their life. A preoperational monitoring program must be designed to assess the background radioactivity level in the area impacted by any future nuclear or radiological activity and shall cover at least one year before the installation will start to be operated. The paper presents the analytical techniques that were developed, optimized and applied during such an environmental monitoring program which addressed the impact area of a pilot tritium removal facility. Since the radionuclide of concern was tritium, a difficult to measure radionuclide, various methods were applied to extract and purify the water from air, vegetation and food products, which are presented in the paper. Due to the low background tritium measurement method applied, a seasonal variability was exhibited as concerns the tritium in air concentration, which confirms the natural origin of tritium background.

# Radioecological studies in the Barents Sea (results of expedition in 2007–2009)

Leppänen, Ari-Pekka[1]; Kasatkina, Nadezda[2]; Matishov, Gennady[2]; Solatie, Dina[1]
[1] Radiation and Nuclear Safety Authority, Regional Laboratory in Northern Finland, FINLAND
[2] Murmansk Marine Biological Institute of the Kola science center of RAS, RUSSIA

## Abstract
The results of radioecological investigations carried out within the framework of the Russian-Finnish high-latitude expeditions in 2007-2009 are presented.

## Introduction
Since 1991, the Murmansk Marine Biological Institute of the Kola science center of RAS (MMBI KSC RAS) has carried out comprehensive investigations of radioactivity of Arctic and Subarctic marine ecosystems, which are based on extensive documentary, geographic, and taxonomic materials. Interest in this region stemmed from the availability of potential regional and local sources of radionuclide emission: atomic fleet bases, nuclear test sites on the Novaya Zemlya Archipelago, and radioactive waste burial sites on the shelf.

MMBI KSC RAS implements annual scientific expeditions to the Barents Sea. In 2007 and 2009, a scientist from Radiation and Nuclear Safety Authority (STUK) joined MMBI expeditions. The objective of collaboration was to study contemporary distribution of radioactive contaminants, anthropogenic and natural (NORMs) radionuclides in the Barents Sea ecosystem.

## Material and methods
The expeditions were carried out with MMBI's research vessel RV Dalnie Zelentsy. The vessel is equipped to carry out extensive marine research for wide field of disciplines. The area and the route of the last three expeditions (2007-2009) covered parts of the Barents Sea which included standard section No. 6 (Kola Section) in the Central Barents Sea and the Franz Josef Land area. The focus of the studies in 2007-2008 was primarily on the Eastern Barents Sea, when sections along the northeastern border of the Sea, the area near the Novaya Zemlya western coast, and section via the trenches in the southeast of the Sea were investigated. In 2009, the focus was on the Western Barents Sea, when investigations along standard sections No. 3 and No. 19 and in the Svalbard/Spitsbergen area were carried out (Fig 1).

Sampling of seawater, bottom sediments, and living organisms was carried out during the expedition. Bottom sediments were sampled by Van-Veen grab where the top layer (0-3 cm) was collected. Cesium isotopes' pre-concentration from 100-litres of

sampled water was performed by the cellulose-inorganic sorbent «Anfezh» on board the vessel. The samples' analysis was carried out jointly at the laboratories in Murmansk (Russia) and Rovaniemi (Finland). The samples were prepared before measurements. The activity concentrations of $^{137}$Cs, $^{40}$K, $^{226}$Ra, $^{228}$Th were measured with low-background gamma-spectrometer. The content of $^{238}$Pu, $^{239,240}$Pu, and $^{210}$Po isotopes was determined by alpha-spectrometric method and the content of $^{90}$Sr was determined by beta-radiometric method after the corresponding radiochemical preparation of the samples.

## Results

Research results of the previous years show very low levels of anthropogenic radionuclides/radioactivity in all components of the Barents Sea ecosystem. The average $^{137}$Cs content in seawater was about 2 Bq/m$^3$, and of $^{90}$Sr − 5 Bq/m$^3$ (Fig. 2). The specific activity of $^{137}$Cs and $^{90}$Sr in bottom sediments varied within the range of 1−8 and 0.2−4 Bq/kg of dry weight respectively (Fig. 3). However, there are some regional differences in radioactivity concentrations. Higher concentrations of radioactivity were found, in bottom sediments and in sea water, in western parts of Barents Sea where Atlantic waters are more dominant. In proportion, areas where Arctic waters are more dominant show clear reduction in radioactivity concentrations. In addition, in bottom sediments increase in radioactivity concentrations were also observed in straights and deep trenches of the Barents Sea were excess radioactivity has accumulated in a sedimentation process (Fig. 2 and 3).The $^{238}$Pu concentrations in bottom sediment along the standard section No. 6 were 0.02-0.04 Bq/kg and $^{239}$Pu concentrations 0.4-1.3 Bq/kg, respectively. Thus the $^{238}$Pu/$^{239}$Pu ratio in the sediment samples was 0.03-0.04 indicating that the Plutonium is of the global fallout origin relating to atmospheric nuclear weapon testing. In addition to water and sediment samples some samples of Barents Sea fauna were also measured. The $^{137}$Cs concentrations in the main commercial fish species were about 0.2 Bq/kg of wet weight. This is very low compared to $^{137}$Cs concentrations of tens of Bq/kg in fresh water fish in Northern Scandinavia (AMAP, 2009). The radioactivity in the Barents Sea nowadays is primarily determined by the presence of natural radionuclides (NORMs) (Table 1).

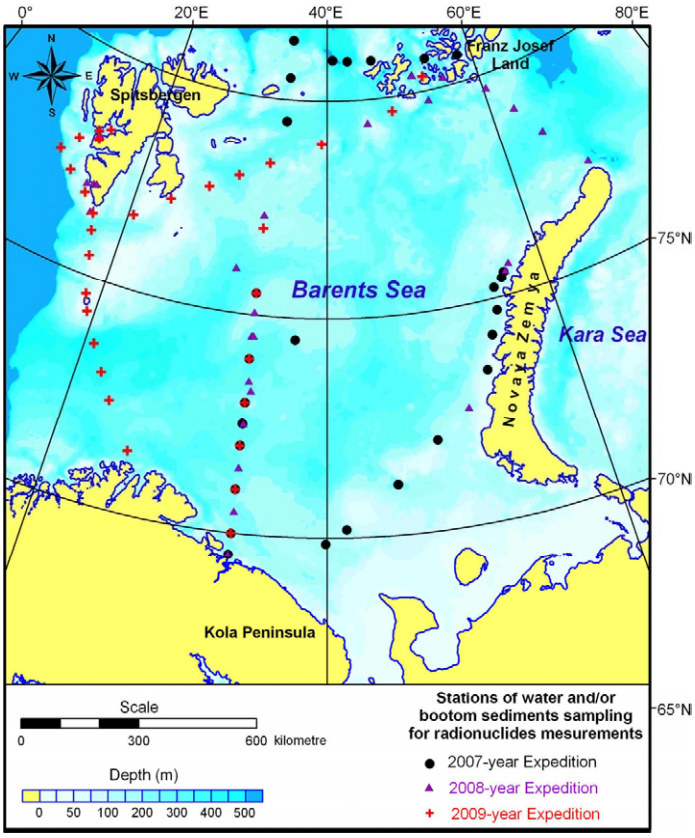


**Fig. 1. Stations of water and bottom sediments sampling during MMBI's annual high-latitude expeditions, 2007-2009.**

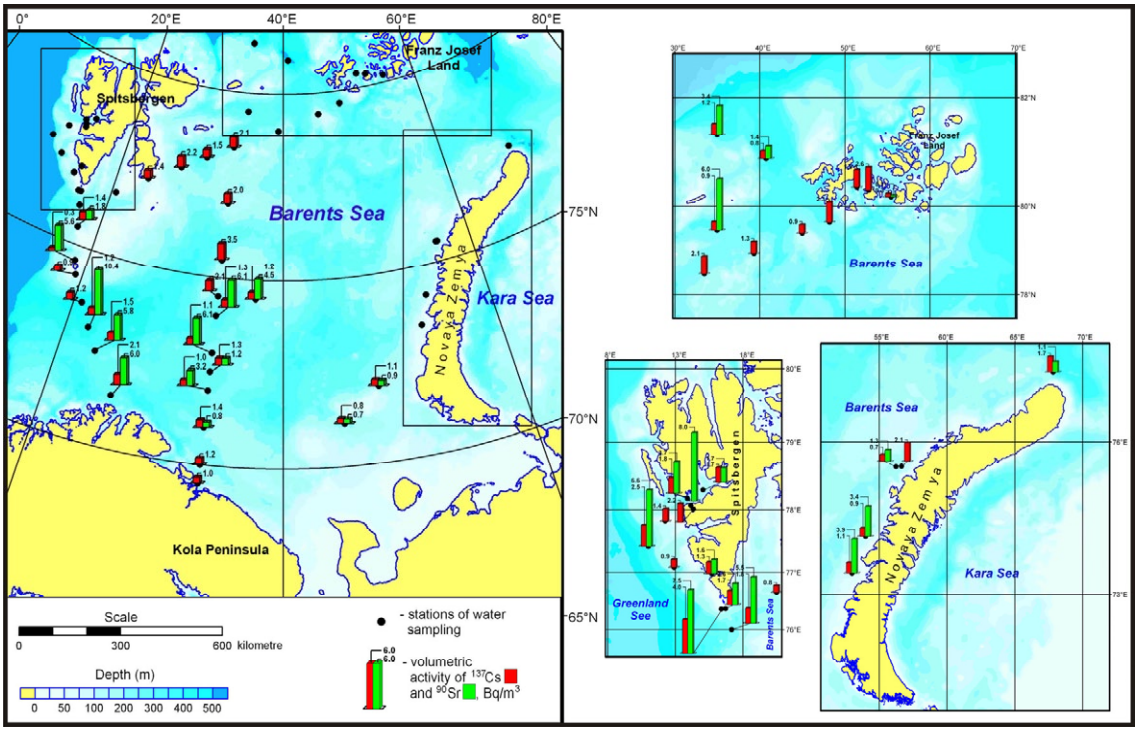


**Fig. 2. Volumetric activity of $^{137}$Cs and $^{90}$Sr in the Barents Sea water masses, 2007-2009.**

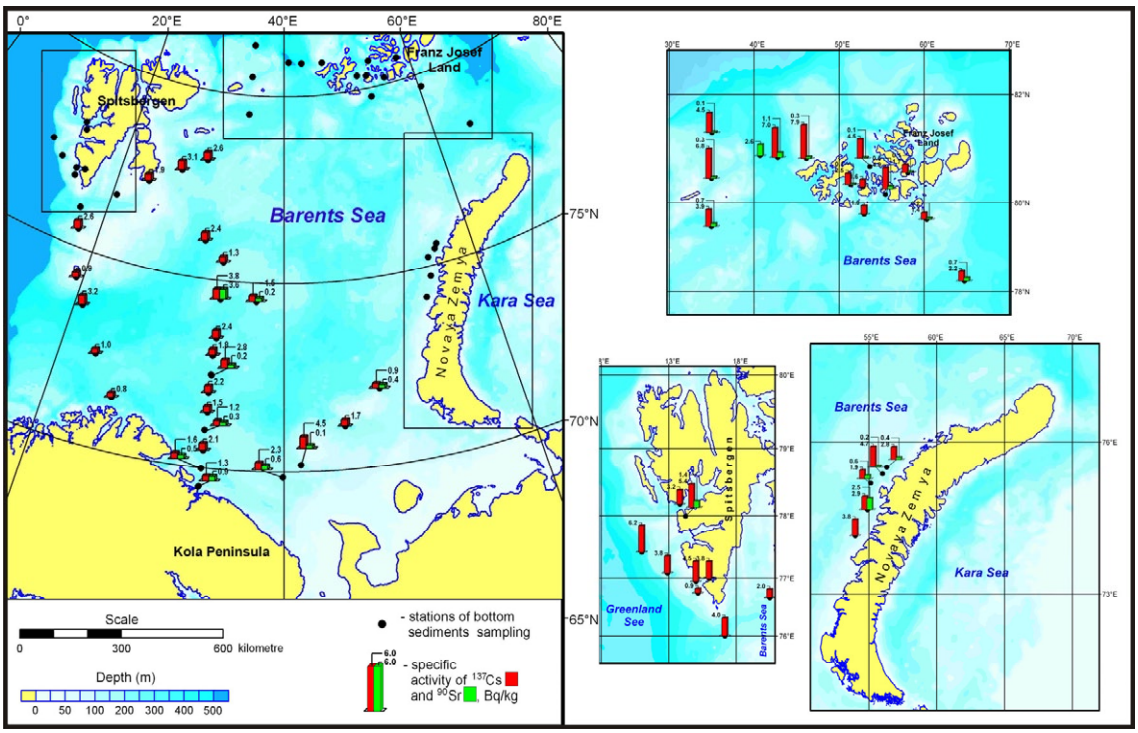


**Fig. 3. Specific activity of $^{137}$Cs and $^{90}$Sr in the Barents Sea bottom sediments, 2007-2009.**

**Table 1. Gamma radionuclides in Barents Sea fish, 2007-2009, Bq/kg wet weight.**

| Species | $^{137}$Cs, Bq/kg wet weight | $^{40}$K, Bq/kg wet weight |
|---|---|---|
| Long rough dab *(Hippoglossoides platessoides)* | 0.10±0.04 | 106±12 |
| Atlantic Cod *(Gadus morhua)* | 0.20±0.08 | 109±12 |
| Atlantic Cod *(Gadus morhua)* | 0.15±0.08 | 116±12 |
| Atlantic Cod *(Gadus morhua)* | 0.15±0.06 | 105±12 |
| Haddock *(Melanogrammus aeglefinus)* | 0.07±0.04 | 116±12 |
| Spotted wolffish *(Anarhichas minor)* | 0.20±0.05 | 115±13 |
| Spotted wolffish *(Anarhichas minor)* | 0.15±0.05 | 99±12 |
| Haddock *(Melanogrammus aeglefinus)* | 0.12±0.05 | 110±11 |
| Haddock *(Melanogrammus aeglefinus)* | 0.12±0.05 | 108±10 |
| Haddock *(Melanogrammus aeglefinus)* | 0.10±0.05 | 116±12 |
| Haddock *(Melanogrammus aeglefinus)* | 0.16±0.05 | 106±10 |

## Conclusions

As a whole, according to the contemporary levels of radioactive contamination, almost the entire Barents Sea may be considered as an area very minor affects of human activity. The local influence of anthropogenic factor was observed mainly in water areas affected by economic activity in bays and inlets of the Barents Sea. Although the radioactivity of the marine environment is generally decreased, it is important to carry out regular monitoring especially in the regions where the potential risk of radioactive pollution is high.

## References

Arctic Monitoring and Assessment Program, 2009. Arctic Pollution. Arctic Monitoring and Assessment Program publications, Oslo, Norway. ISBN 978-82-7971-050-9.

# Experimental study of the radionuclides transport in soil and plants from waste dump

Bragea, Mihaela[1] ; Aldave de las Heras, Laura[2]; Cristache, Carmen[3]; Carlos Marquez, Ramon[2]; Toro, Laszlo[1]

[1] Institute of Public Health, V. Babeş 16, 300226, Timisoara, ROMANIA

[2] European Commission, Joint Research Centre, Institute for Transuranium Elements, P.O. Box 2340, 76125, Karlsruhe, GERMANY

[3] Horia Hulubei National Institute for Physics and Nuclear Engineering, P.O. Box MG-6, 077125 Magurele (Ilfov), ROMANIA

## Abstract

The transport of radionuclides through terrestrial environments is determined by a multiplicity of processes with time-scales ranging from a few minutes to many years. The importance of understanding and predicting the radionuclide migration from soils to vegetation arises from its potential radiological impact: slow migration has as result an increase availability of radionuclides for root uptake and gives rise to external doses for a long time.

The transfer factors (TF) for natural uranium isotopes ($^{234}U$ and $^{238}U$) and $^{226}Ra$ were obtained in vegetation samples growing in granitic soils around disused uranium mine located in the Ciudanovita region in the West of Romania. Affected and non-affected areas of the mine presented large differences in the activity concentrations of radionuclides of the uranium series. We also determined transfer factors for several stable elements (essential and non-essential). A set of statistical tests were applied to validate the data.

## Introduction

It is important to understand the behaviour of natural radionuclides in the environment (distribution pathways, mobility, transfers, etc.) because the information can be used as a natural analogue for the long-term behaviour of materials and processes in developing and testing models, and in obtaining the associated parameter values appropriate for radiological performance assessments [4]. After the exploitation of the mineral, the uranium mine enters a phase of inactivity until its restoration. During both these phases, large amounts of materials, more or less rich in radionuclides, are exposed to environmental agents. In the phase of inactivity, the uranium mine can be regarded as a very appropriate natural laboratory to investigate the mobilization of natural radionuclides by means of their distribution in different compartments (soil, vegetation, water, sediment, etc.), as well as the transfer between them. The soil-to-plant transfer

factor is one of the important parameters widely used to estimate the internal radiation dose from radionuclides through food ingestion. In general, transfer factors show a large degree of variation dependent upon several factors such as soil type, species of plants and other environmental conditions. Due to a predicted long-term transfer of radionuclides in the environment, an understanding knowledge of the geochemical and ecological cycles is also needed as they relate to the behaviour of radionuclides. In addition, the distribution of radionuclides in plant components is beneficial in understanding the dynamics of radionuclides in an agricultural field. Because non-edible parts of agricultural plants are returned to the soil, they may again be utilized in the soil-plant pathway. As a case study, in this work has been considered the uranium waste dump reservoir from the mining perimeter of Ciudanovița.

## Material and methods

The environmental samples like soil and vegetation was collected from the dump of the waste rock of the mine EM Banat, Oravita, Caras-Severin county, in order to evaluate soil to plant radionuclide transfer factors (TF). The definition of TF proposed by the IUR [5] has been used:

$$TF = \frac{concentrationofradionuclideinplant(Bqkg^{-1}drycropmass)}{concentrationofradionuclideinsoil(Bqkg^{-1}drysoilmas\sin theupper20cm)}$$

The vegetation samples at each point were collected from the surface at which the soil sample had to be removed. In all cases, only the aerial fraction was sampled. About 100 g of a representative fraction was obtained by homogenization after drying and chopping. The samples were carefully washed in the laboratory in order to remove all the adhered soil particles. Materials for sampling and pre-treatment of the samples were always cleaned before initiating each procedure in order to avoid cross contamination. Twenty-five sampling campaigns soil and vegetation were performed during a one-year period (2007-2008) in order to take the variability in meteorological conditions into account. The total uranium concentration and the isotopic composition from vegetation and soils samples collected at the same sampling site, were determined by high resolution ICPMS Element 2 after separation and preconcentration of uranium. Content of $^{226}$Ra, $^{234}$U and $^{238}$U from the solid waste and vegetation samples were determined by means of the spectrometric gamma measurement chain HPGe-Oxford, with 40% efficiency. Processing of experimental data was performed using STATISTICA 6.0 software which used methods Quadrat Surface and spleen, with a confidence coefficient set to introduce the experimental values of 95%.

## Results

STATISTICA 6.0 has enabled the distribution of transfer factors for $^{226}$Ra, $^{234}$U and $^{238}$U, depending on the concentrations of both radionuclides in soil and vegetation in 25 point of prelevation. These distributions are show in the graphs in Fig. 1-2-3. Radium is the last member of the alkaline earth metals, a group of metals whose lighter members (Ca and Mg) play a very important role in plant growth and nutrition. The TF values show a very wide variability for $^{226}$Ra. Results have been obtained for radium in grass

with a TF mean value of 4.705, and a range between 0.07-9.34. The statistical analysis of the results indicates that the TF mean values in grass corresponding to the $^{234}U$ are 0,17, and a range between 0.03-0,17, and the TF mean values for $^{238}U$ are 0,355 and a range between 0,05-0,66. It was established correlations: the concentration of $^{226}Ra$ (soil) - the concentration of $^{226}Ra$ (grass) -TF (relationship 1) and the concentration of $^{238}U$ (soil) - the concentration of $^{238}U$ (grass) -TF (relationship 2), which are plotted in Figures 1 and 3.

$$TF\ ^{226}Ra = 61{,}635+2{,}0345x-20{,}434y+0{,}0181x^2-0{,}3817xy+1{,}8685y^2 \quad (1)$$

where: x= the concentration of $^{226}Ra$ in soil [Bq/kg] and y= concentration of $^{226}Ra$ in grass [Bq/kg]

$$TF\ ^{238}U_{nat} = 36{,}9526+1{,}0011x-11{,}5731y+0{,}0088x^2-0{,}1876xy+1{,}0083y^2 \quad (2)$$

where: x= the concentration of $^{238}U$ in soil [Bq/kg] and y= concentration of $^{238}U$ in grass [Bq/kg].

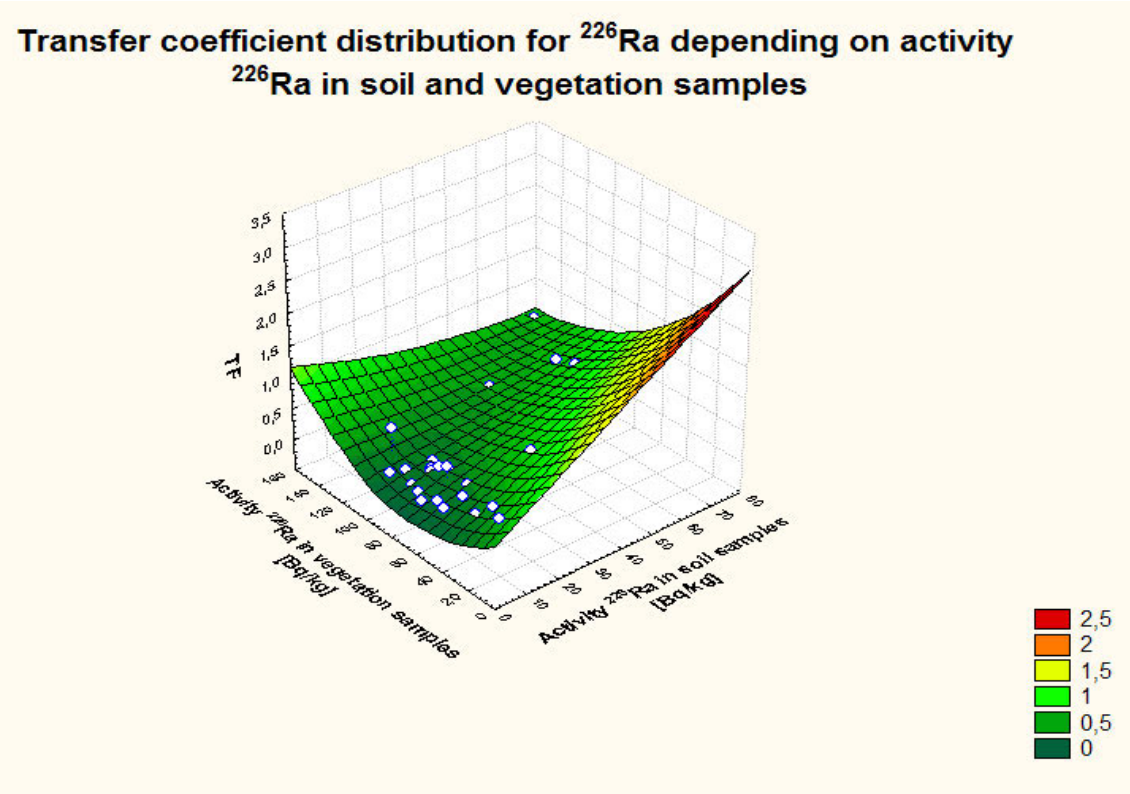


**Fig. 1. Distribution of the TF values for $^{226}Ra$ corresponding of the activity concentrations of $^{226}Ra$ in soil and grass.**

The TF corresponding to $^{226}Ra$ can be considered, at a 95% confidence level, higher (by two orders of magnitude) than uranium isotopes studied. The excess of $^{226}Ra$ in vegetation versus $^{234}U$ and $^{238}U$ must be explained by the higher absorption of radium. From the comparison between the TF values corresponding to the two elements

studied (uranium, and radium), we conclude that the uptake for radium is higher than for the other once element. The fact that uranium is both actinides may explain their more analogous chemical behaviour, whereas this argument cannot be extended to radium which is an alkaline-earth.

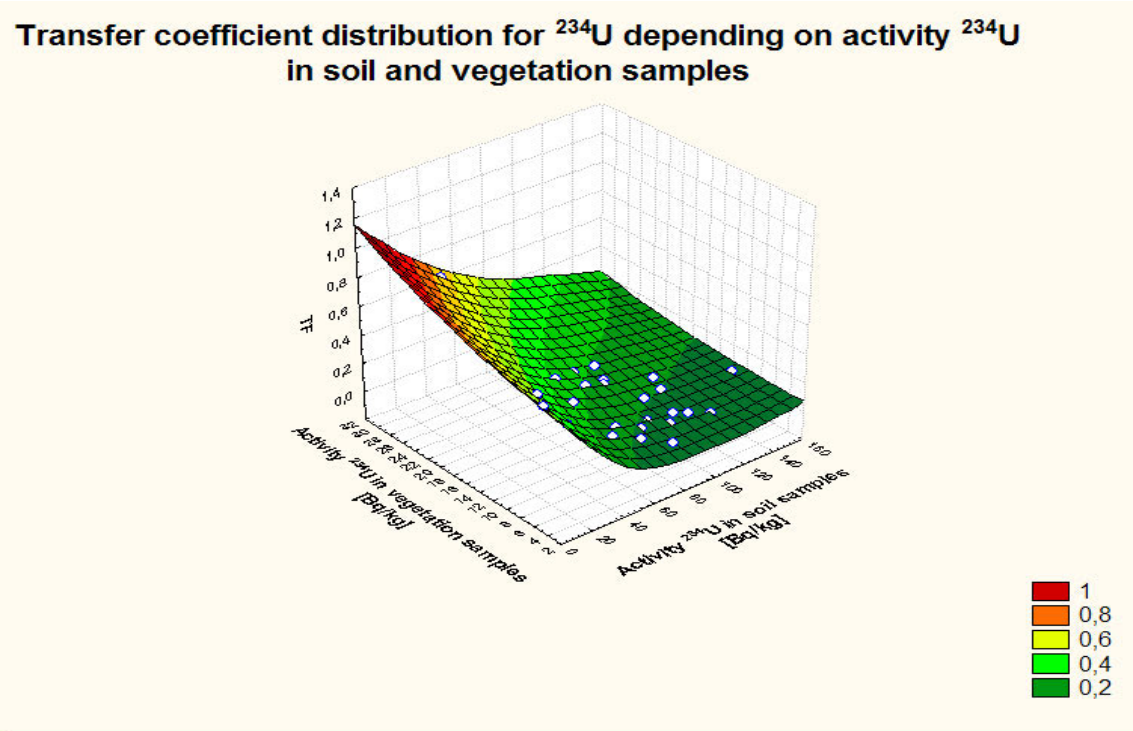


**Fig. 2. Distribution of the TF values for $^{235}U$ corresponding of the activity concentrations of $^{235}U$ in soil and grass.**

This general result is in agreement with other afirmation that TF values for elements in oxidation state +II are almost always greater than for those elements in oxidation state +IV. The results obtained for the soil samples show that the $^{234}U/^{238}U$ atom ratios in all soil samples, are clearly higher than the natural $^{234}U/^{238}U$ atom ratios, 5,54019E-05. Higher $^{234}U/^{238}U$ ratios in soil were observed at 100 and 200m from uranium dump, decreasing with further distance from the uranium tailing dump. When aquatic systems are in contact with minerals, selective leaching processes lead to preferential dissolution and transport of $^{234}U$, resulting in enhancement of $^{234}U/^{238}U$ ratio. The reason underlying the enhancement of the ratio is attributed, as a major cause, to a "recoil induced vulnerability to leaching". The mechanism is view as a creation of defects in the crystal lattice when the parent nuclide ($^{238}U$) recoils during emission of an alpha particle, thus the daughter nuclide ($^{234}U$) is in a microenvironment that is more susceptible to chemical attack than the parent [1]. Electron stripping during the decay process such that $^{234}U$ is more likely to be in more soluble U(VI) state, facilitating the solution of this isotope by a surface etching process [2]. In the vegetation samples collected up to 200 m from the uranium tailing dump, half of the samples analysed presented an enhancement of the ratio $^{234}U/^{238}U$ ratio being always higher in grass than in Tussilago farfara. The mobility of uranium in plant tissues is limited, as it tends to

adsorb on cell wall materials; therefore, concentrations are typically higher in tissues found lower on the plant and are highest on the root surfaces [3].

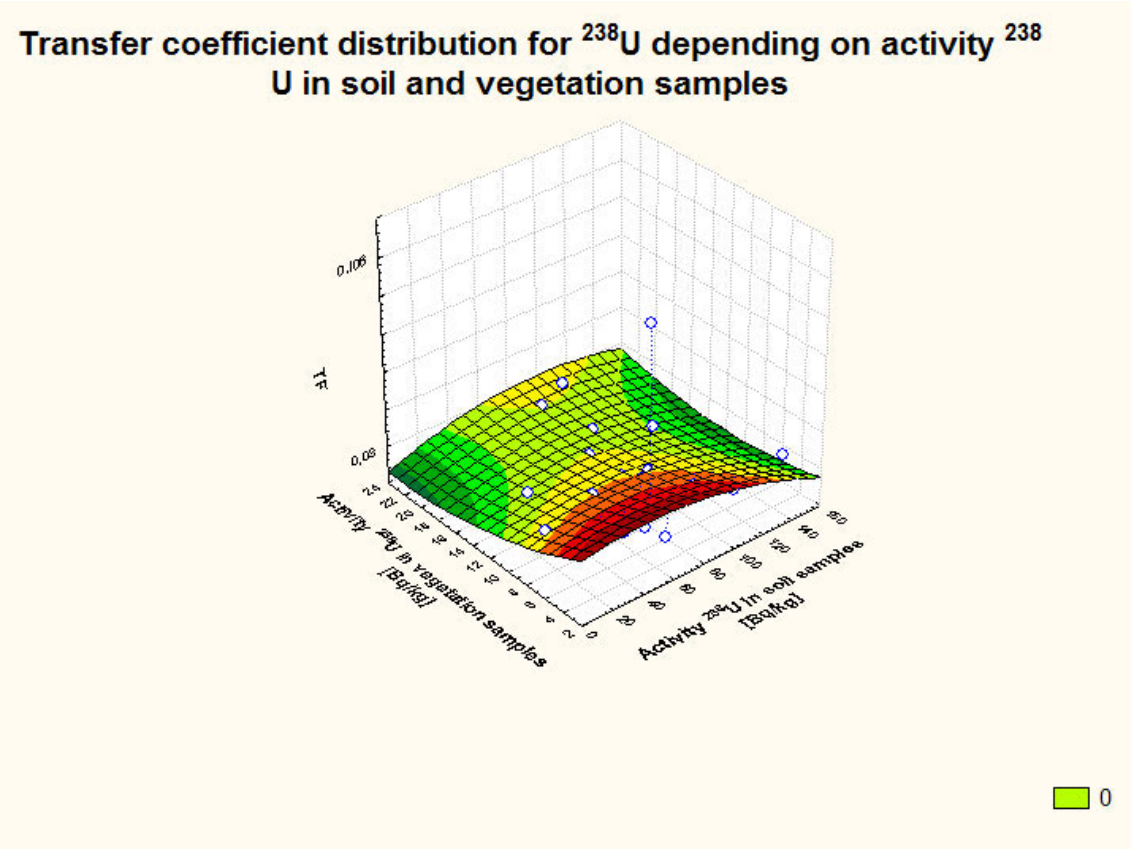


**Fig. 3. Distribution of the TF values for $^{238}U$ corresponding of the activity concentrations of $^{238}U$ in soil and grass.**

In fig.4 is shown correlations between $^{234}U/^{238}U$ ratios in grass and Tussilago farfara and in soil where the plants were grown.

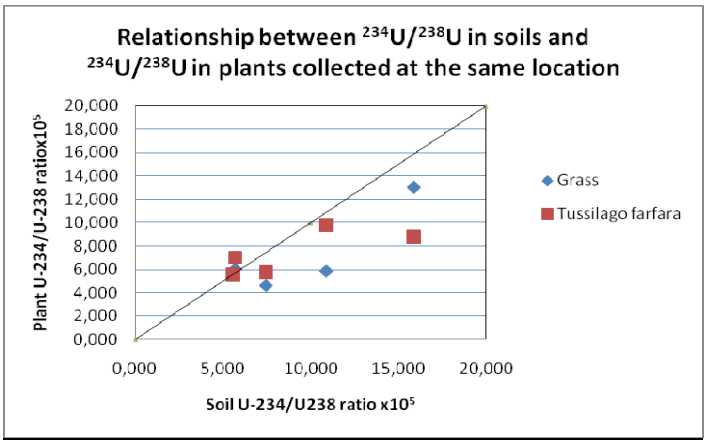


**Fig.4. Relationship between $^{234}U/^{238}U$ ratios in soils and $^{234}U/^{238}U$ ratios in plants collected at the same location.**

Although these plants were grown and harvested simultaneously, we can see that both $^{234}U$ and $^{238}U$ were more easily transferred from soil to roots of grass as compared as compared to transfer of these radionuclides from soil to roots Tussilago farfara.

Plant radionuclide concentrations are not so often linearly related to soil radionuclide concentrations. Nonlinearity can complicate the measurement of bioavailability, because each plant and soil combination may have a unique curvilinear relationship. The study of temporal variations of $^{234}U$ and $^{238}U$ in plant showed that short-term dynamics of radionuclide plant concentrations are rather significant and species-specific.

## Conclusions

Transfer factors (TF) for different natural radionuclides ($^{226}Ra$, $^{234}U$ and $^{238}U$) have been presented for grass samples in an area where a disused uranium mine is located.

The radium uptake is greater than for uranium by about some orders of magnitude. These differences have been attributed to the different solubilities of the elements with oxidation state +II. The Ra-transfer factor depends the plant part concerned, climate conditions, and the physicochemical form of radium. Radium has a high affinity for the regular exchange sites of the soil.

## References

[1] L.Halicz. Determination of the 234U/238U ratio in water samples by inductively coupled plasma mass spectrometry. Analytica Chimica Acta 2000; 422 (2): 203-208.

[2] X. Jiang, Z. Yu, T. Ku, X. Kang, W. Wei, H. Chen. Distribution of uranium isotopes in the main channel of Yellow river (Huanghe), China. Continental Shelf Research 2004, 29 (4): 719-727.

[3] L. S. Morton, C. V. Evans and G. O. Estes. Natural Uranium and Thorium Distributions in Podzolized Soils and Native Blueberry. Journal of Environmental Quality 2002, 31:155-162.

[4] Vera Tome, Soil-to-plant transfer factors for natural radionuclides and stable elements in a Mediterranean area, Journal of Environmental Radioactivity 2003, 65 (2): 161.

[5] H. Velasco, Juri Ayub, J. Sansone,U. Analysis of radionuclide transfer factors from soil to plant in tropical and subtropical environments. Applied Radiation and Isotopes, 2008, 66 (11): 1759 1763.

We acknowledge the “Actinide User Laboratory” program provided by the European Commission, DG-JRC, Institute for Transuranium Elements (ITU) and the financial support from the European Community-Access to Research Infrastructures action of the Improving Human Potential Programme, DG-RTD, Contract No. RITA-CT-2006-026176.

# HYDRUS-computer simulation of radionuclide migration in groundwater due to clearance of low-level waste from decommissioning

Merk, Rainer
BfS Federal Office for Radiation Protection, D-38201 Salzgitter, GERMANY

## Abstract

Bulk amounts of cleared building rubble mainly arise due to decommissioning of nuclear power plants. Depending on the type of clearance, weakly contaminated rubble can be released to be deposited in landfills. Leaching of radionuclides is caused by infiltrating rainwater and may lead to migration of radionuclides through the landfill and the vadose zone into the aquifer where the contaminated seepage is mixed with groundwater. If contaminated groundwater is used for irrigation or direct consumption, the food chain may be affected (water pathway). Clearance levels for radionuclides have to be calculated in such a way that the water pathway is considered and the effective dose for an individual of the public is at most of the order of 10 micro Sievert per year. In the wake of availability of inexpensive and fast computers, the leaching of radionuclides, their transport through the various zones of rubble and soil and eventually the contamination of groundwater can be computed by means of sophisticated mathematical models. The software package HYDRUS constitutes an internationally established standard in contaminant transport modeling. We apply HYDRUS to problems of nuclide transport and water dynamics in landfills, the vadose zone and the aquifer.

## Introduction

Most of the building rubble from decommissioning of nuclear power plants has low radioactivity and can be released for disposal in landfills, provided the activity concentration (in Bq/g) of the material per radionuclide is below the respective clearance level. In Germany, clearance levels are part of the radiation protection ordinance. Following progress in science and technology and adapting to changing conditions concerning, among others, new requirements of new waste legislation, they are continuously updated.

An important radionuclide pathway in the case of low level material contained in landfills is the so-called water pathway. The assumption is that radionuclides contained e.g. in concrete rubble are carried away by rainwater. Radionuclides may migrate through the landfill and the unsaturated vadose zone beneath the landfill. The

contamination may also reach the aquifer and eventually the drinking water and the food chain.

As new approach to estimate groundwater activities resulting from disposal of concrete rubble, the radionuclide transport in the landfill, the vadose zone and the aquifer was calculated in one dimension by means of the computer program HYDRUS (Simunek et al. 1998). With HYDRUS, water transport, leachability of radionuclids and radionuclide migration through the porous structures of rubble, soil and the matrix of the aquifer was simulated numerically. The main equations used within HYDRUS are the Richards equation (water transport) and the convection-diffusion equation (CDE, for the nuclide transport). The computer program HYDRUS represents an internationally established standard tool in the area of groundwater hydrology and contaminant modeling.

With the Richards equation considered here, wetting, drying and the water movement through porous material is adequately described also for non-saturated water contents and precipitation can be varied according to the annual seasons. Physical effects for radionuclide migration considered in our model include the advective transport of radionuclides, their sorption to the background matrix (e.g. rubble or soil), diffusion and dispersion. Also, the radioactive decay is considered as a sink term in the transport equation. Altogether, the HYDRUS code allows for calculation of groundwater activity values. The results are compared with values from the IAEA model of the water pathway suggested for exemption and clearance (IAEA Safety Reports Series No. 44, cf. (IAEA 2005)).

## Material and methods

### Water transport model

The fundamental physical basis used for the water transport is Darcy's equation. It desribes fluid flow through porous media. It is known that soil and the aquifer are best described as porous matrix. The same is assumed for rubble in a landfill.

Usually, Darcy's equation for the water velocity is written as (v: Darcy velocity, K: hydraulic conductivity, h: hydraulic head, l: spatial coordinate, ψ: pressure head, cf. the monograph by Freeze and Cherry (1979) for all details on groundwater hydrology)

$$v = -K(\psi)\frac{dh}{d\ell}$$

In Hubbert's analysis of the fluid potential, the relationship between different pressures within a system of fluid, air and porous medium is expressed in terms of manometer heads and written as $h = z + \psi$, where z (elevation head) measures the vertical distance to the reference point z=0 (datum) and ψ represents the suction effects of the porous material. It is thus the total gradient of both elevation and suction that drives the water flow through a porous medium.

The equation for v was established around 1856 by French engineer Henry Darcy following his engineering work related to water supply. Nowadays, it can be derived from the more general Navier-Stokes equations in case of water flowing through a porous matrix. This is the basic situation in a saturated aquifer. However, physics becomes more involved once the pore space is only partially saturated, which is the

case in the vadose zone and within a landfill consisting of rubble. Besides ψ, the moisture content θ ($0 \leq \theta \leq n$, with n: porosity) becomes an important characteristic of the system.

In unsaturated material, K and θ may be related to ψ. The most commonly used empirical relationship between these quantities for soil material is named after M. van Genuchten and Y. Mualem as van Genuchten-Mualem model (VGM). In principle, this model leads to S-shaped wetting and drying curves saying that conductivity is increasing as moisture content is approaching saturation. The curves have to be inserted into the respective water transport equations with the consequence that a considerable degree of complexity is added to the theory. Furthermore, the main experimental problem is to determine the curve parameters for a given soil type. For example, for concrete rubble, these parameters are usually unknown and hence the water dynamics cannot easily be predicted.

For unsaturated media, the Darcy equation can be coupled with the equation of continuity to yield what is known as the Richards equation (Lorenzo Richards, 1931):

$$\frac{\partial \theta}{\partial t} = \frac{\partial}{\partial x}[K(\frac{\partial \psi}{\partial x} + 1)]$$

In most of the models of the vadose zone, the Richards equation is the starting point for a mathematical analysis of the fluid flow. It can be assumed to hold for concrete rubble as well, at least as long as a sufficient amount of fine-grained material is present.

While hydraulic parameters of the VGM are tabulated for many soil types, available data for rubble is sparse. It is not clear, for example, whether data for coarse-grained sand is sufficient to describe wetting and drying dynamics in a landfill. Therefore, the hydraulic properties of concrete rubble are presently determined by Gesellschaft für Anlagen- und Reaktorsicherheit (GRS) in collaboration with the Technical University Braunschweig as part of a consultant contract with the German Federal Office for Radiation Protection (BfS). A preliminary set of values was calculated from multistep-outflow experiments by means of inverse modeling.

### Radionuclide transport model

Radionuclide transport in water is described by the convection diffusion equation (CDE). In the HYDRUS model, the CDE approach was adopted for radionuclide transport in water flowing through the porous media of concrete rubble, unsaturated soil (vadose zone) and saturated aquifer (Freeze and Cherry (1979). For undisturbed soils, the validity of the CDE approach was demonstrated by Bossew and Kirchner (2004)). The CDE is basically a differential equation expression of mass conservation,

$$\frac{\partial(nC + \rho_b \overline{C})}{\partial t} + \overline{v}\frac{\partial}{\partial x}nC = \frac{\partial}{\partial x}D\frac{\partial}{\partial x}nC - \lambda\rho_b\overline{C} - \lambda nC$$

(C: radionuclide concentration in water, $\overline{C}$: sorbed nuclide concentration, D: dispersion coefficient, λ: decay constant, $\rho_b$: solid material density).

The dispersion coefficient includes both the effects of diffusion and of hydrodynamic dispersion caused by the porous material structure. Initially sharp and

narrow concentration profiles are thus smeared out after travelling through the porous material, resulting in lowered local concentrations.

Sorption is described by a linear relationship between C and $\overline{C}$, which is known as $K_d$ model

$$\overline{C} = K_d C .$$

The CDE can be reduced to an equation for the dissolved fraction C only. However, migration of the dissolved fraction is retarded: high values of $K_d$ therefore result in slowly progressing contamination fronts.

### Modeling the water pathway with HYDRUS-1D

In the HYDRUS numerical code, all of the equations described above are implemented. These differential equations are coupled and usually cannot be solved analytically. HYDRUS attempts a numerical solution of both Richards equation and CDE by applying finite difference and finite elements methods. HYDRUS was validated by BfS against known solutions of the CDE under simplified conditions. The HYDRUS output proved to be in excellent agreement with the known solution. In addition, various test runs were performed before modeling started. For example, in a numerical scheme it can be important to control the (finite) timestep and the resolution of the numerical spatial grid.

We have applied the one-dimensional version of the code to a model situation as depicted in Fig. 1. The landfill is located on top of vadose zone and aquifer, and rain is assumed to infiltrate the landfill. Radionuclides migrate in vertical direction and enter the aquifer where the seepage is diluted by incoming groundwater.

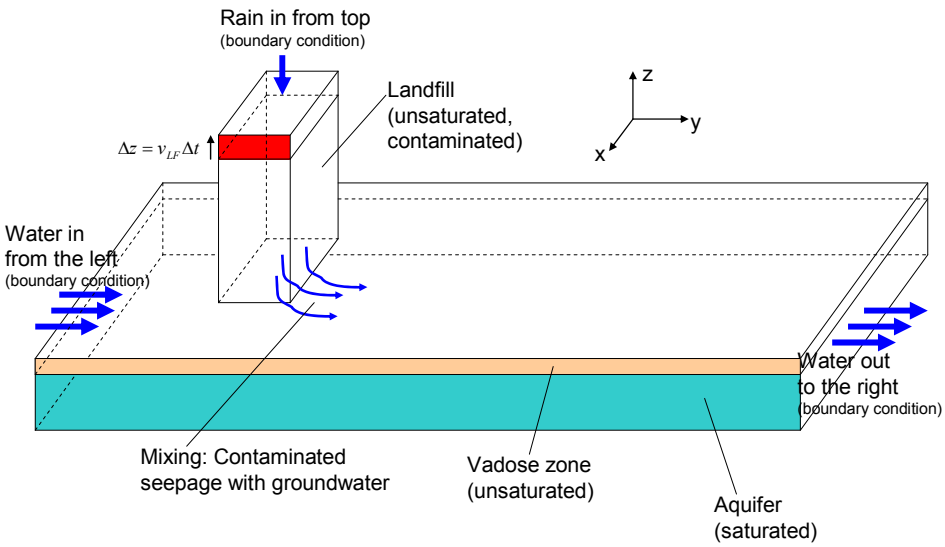


**Fig. 1. 3D-Illustration of the model situation used. Modeling is performed by combining two 1D-Hydrus computer runs, one for the landfill and vadose zone and another one for the aquifer.**

Two one-dimensional computer runs are necessary in the model situation described in Fig. 1, the first one comprising landfill and vadose zone. Dilution with groundwater is performed analytically and the result is inserted into a second simulation for the aquifer.

### The IAEA (SR 44) water pathway model

The IAEA modeling approach is a straightforward analytical method to obtain generic activity levels of contaminated groundwater and was inspired by the RESRAD family of computer codes (Yu et al. 2007). In the IAEA Safety Reports Series No. 44 (IAEA 2005), the water pathway is part of a set of exposure scenarios. Altogether, the exposure scenarios serve to calculate so-called activity concentration (AC) values (in Bq/g). The IAEA suggests to use AC values for exemption and clearance.

The IAEA model is not designed to solve differential equations, rather, it is based on simple estimates and conservative assumptions. It applies the concept of $K_d$ and retardation and directly results in radionuclide concentrations in the seepage and groundwater. Since it does not solve differential equations, the time evolution of the contamination is impossible to follow, which is certainly one of the major drawbacks of this model. Furthermore, dispersion remains unconsidered and the dynamics of the water flow is neglected.

Basically, the model starts with a contaminated zone containing a radionuclide of 1 Bq/g specific activity. It is assumed that the entire inventory of radionuclides is carried away by rainwater at a leach rate of

$$L = \frac{I}{\theta^{cz} z^{cz} R^{cz}} \quad .$$

In this equation, I stands for the infiltration rate, $\theta^{cz}$ stands for the volumetric water content of the contaminated zone, $z^{cz}$ is the thickness of the contaminated zone and $R^{cz}$ is the retardation factor. $R^{cz}$ is largely determined by $K_d$ . Note that the volumetric water content is taken to be a constant, since full water dynamics cannot be modelled with the IAEA model.

The radionuclide concentration in the seepage can be calculated according to the formula

$$C^s = \frac{McL}{IA^{cz}}$$

(M: total mass of contaminated material, c: specific activity of the radionuclide in the contaminated material, $A^{cz}$ is the surface area of the contaminated zone). The explanation of these formulae is in the end straightforward application of proportionalities.

An unsaturated zone is assumed in the model. For this zone, a delay time $t_i$ is inserted into the law for radioactive decay, which considers the time needed to traverse the unsaturated zone. There is no further impact from the assumption of an unsaturated zone. This is a considerable simplification and, in principle could only be justified retrospectively, after a detailed model of the vadose zone has been calculated. The delay time is calculated on the basis of proportionalities from infiltration rate, thickness of the unsaturated zone, retardation factor, saturation ratio and porosity of the unsaturated zone.

In the end, the radionuclide concentration in the well water is calculated from the radionuclide concentration in the seepage by

$$c^{w} = \frac{IA^{cz}}{U^{gw} + IA^{cz}} C^{s} e^{-\lambda t_i} .$$

Here, $U^{gw}$ is the volume of groundwater per unit of time. The first term in the last equation represents dilution by groundwater. There is no detailed modeling of the aquifer and obviously, the well has to be assumed conservatively as being located very close to the landfill.

## Results

In the HYDRUS-modeling approach, two one-dimensional HYDRUS computer runs are combined to calculate the groundwater contamination at a distance of 500 m from the landfill. The first run is for the downward directed water and radionuclide transport through the landfill and the vadose zone.

We have used hydrological data from standard hydrology literature to model in a preferably realistic rather than overly conservative manner (see, for example, the monographs by Freeze and Cherry (1979) and Heath (1988)). Hydraulic data for the vadose zone and the aquifer is provided by HYDRUS (Simunek et al. 1998) within the VGM framework. Respective VGM data for the landfill was determined experimentally by GRS. In the HYDRUS model, an annual precipitation typical for Northern European climate conditions was assumed. An initial activity of 1 Bq/g was taken for the radionuclides contained in the rubble.

Usually, we apply $K_d$ values that are the conclusion of a literature survey within a study performed by a technical consultant of the German Ministry of Environment, Nature Conservation and Reactor Safety (BMU) and published by Deckert et al. (1993). However, note that BfS is also involved in both experimental and theoretical derivation of $K_d$ values. We plan to analyze possible differences in a future investigation. Furthermore, for a preliminary numerical study such as the one sketched here, it is sufficient and easier to analyze if the same $K_d$ is used in all segments of the model.

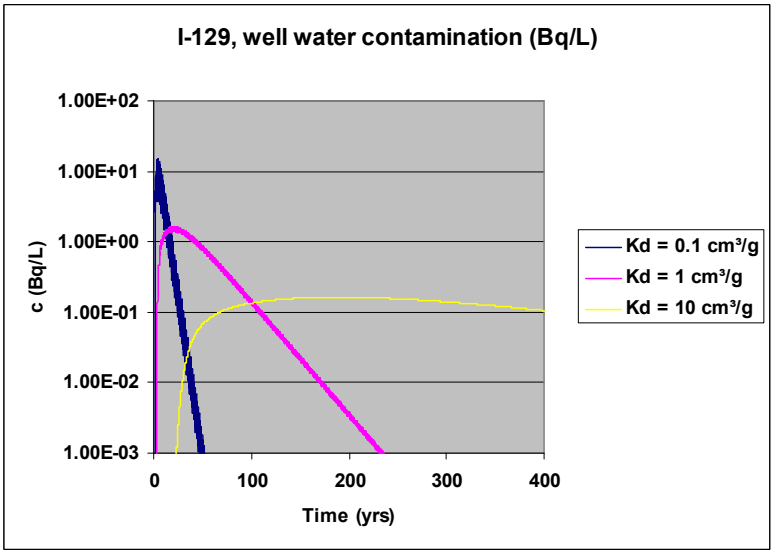


**Fig. 2. I-129 well water contamination time scales (in years) for $K_d$ = 0.1; 1; 10 cm³/g calculated with HYDRUS.**

Fig. 2 shows HYDRUS-modeling results for I-129 (half-life $1.6 \times 10^7$ yrs). $K_d$ was varied between 0.1 and 10 cm³/g, the baseline value being 1 cm³/g. The figure displays the evolution of I-129 groundwater contamination at a model well at a distance of 500 m from the landfill. Obviously, $K_d$ controls the radionuclide transport dynamics to a large extent. Peak contamination levels span three orders of magnitude between around 0.1 and 10 Bq/l and the duration of contamination at the well varies considerably between about 50 yrs ($K_d$ = 0.1 cm³/g) and more than 400 yrs ($K_d$ = 10 cm³/g). Similarly, the arrival times at the well may vary depending on sorption. Although peak contamination levels can often be estimated from a given $K_d$ , reliable contamination time spans are difficult to obtain without numerical analysis. Reasons for this are the dynamics of leaching and the dispersion effects along the path that tend to broaden the contamination peak structure.

In general, it was found that the IAEA modeling results are comparable to our HYDRUS results, provided free parameters are adjusted to ours. It is easier to study how the IAEA model *itself* performs if parameter values vary as little as possible between the models considered. Applying a simplified model can be useful whenever it is intended to get a rough idea of the course of data in a given context. The IAEA model can be programmed as a relatively short computer script and does not consume much computation time.

An example is shown in Fig. 3. Well-water contamination levels were calculated by means of our own computer scripts based on an IAEA model with parameters adjusted to the HYDRUS-model parameters.

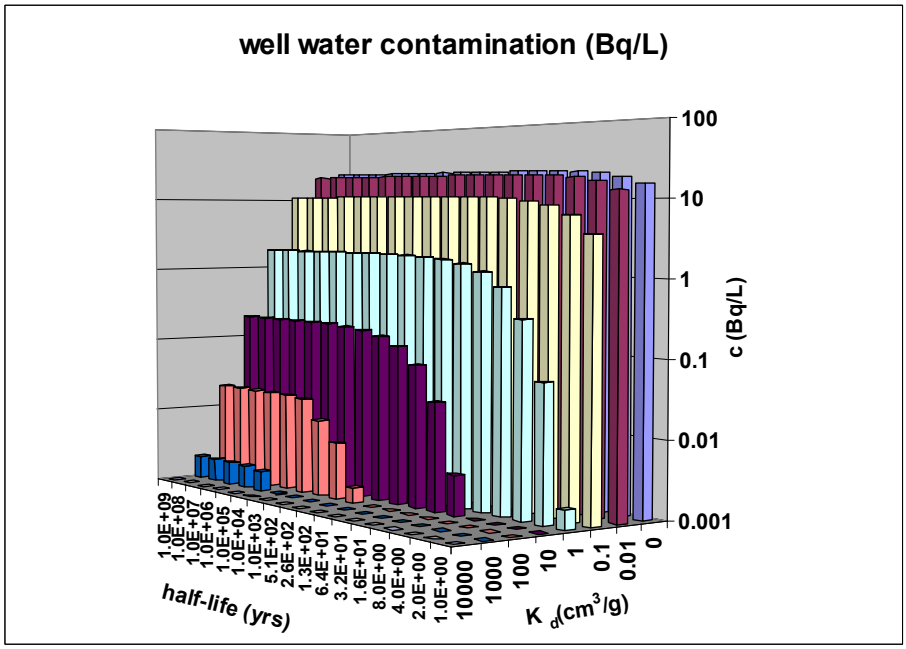


**Fig. 3. The IAEA (SR 44)-modeling approach as applied to the parameter space spanned by $K_d$ and half-life. The columns represent the calculated well water contamination values for a given pair of $K_d$ and half-life. Other free parameters are chosen in accordance with the HYDRUS model (cf. text for details).**

Due to computation time restrictions, general results are sometimes difficult to obtain by performing detailed HYDRUS simulations. For example, the plot depicted in Fig. 3 would require a total number of 272 HYDRUS-computer runs. On the other hand, if a site-specific study of great importance is needed, one should resort to a detailed computer simulation. The same holds if the transport process itself (e.g. the transport through a given segment of soil) is to be studied and compared with experimental data.

## Conclusions

Well water activity levels (in Bq/l) resulting from leaching of radionuclides contained in concrete rubble were calculated by means of HYDRUS computer simulations. The computer program HYDRUS for one-dimensional water and nuclide transport through landfill, vadose zone and aquifer proved to be a robust and modern tool to assess groundwater activity values. Modeling results are similar to values obtained by applying the modeling strategy suggested by the IAEA in the publication (IAEA 2005). The simplified analytical IAEA model for the groundwater pathway appears to be well suited for general-purpose estimates, e.g. to derive generic clearance levels as indicators for a broad class of disposal situations.

In general, the calculation outcome largely depends on $K_d$ . The determination of $K_d$ values, however, was not part of our study so far. In the present approach, $K_d$ is merely an input parameter and was not even varied along the radionuclide path. The same holds for the IAEA study. As the $K_d$ concept appears to control the outcome of water pathway calculations to a large extent, the question may arise whether clearance level calculations based on a generic approach are trustworthy or not. If site-specific parameter values (e.g. $K_d$ ) are available by explicit measurement, detailed computer modeling is therefore to be preferred in site-specific clearance as far as the water pathway is concerned.

## References

Bossew, P. and Kirchner, G: Modelling the vertical distribution of radionuclides in soil. Part 1: the convection-dispersion equation revisited. Journal of Environmental Radioactivity 73 (2004), 127-150.

Deckert, A. et al.: Strahlenexposition durch konventionelle Beseitigung von Abfällen mit Restaktivität. Schriftenreihe Reaktorsicherheit und Strahlenschutz Nr. 393. Bundesministerium für Umwelt, Naturschutz und Reaktorsicherheit (1993).

Freeze, R. A. and Cherry, J. A.: Groundwater. Prentice-Hall, Englewood Cliffs (1979).

Heath, R. C.: Einführung in die Grundwasserhydrologie (German translation of „Basic groundwater hydrology“ U.S. Geological Survey Water-Supply Paper 2220), Oldenbourg Verlag München (1988).

IAEA Safety Reports Series No. 44, Derivation of activity concentration values for exclusion, exemption and clearance, IAEA Vienna (2005).

Simunek, J., Sejna, M. and van Genuchten M. Th.: The HYDRUS-1D software package for simulating the one-dimensional movement of water, heat and multiple solutes in variably-saturated media. U.S. Salinity Laboratory (1998).

Yu, C. et al.: User’s manual for RESRAD-OFFSITE Version 2. U.S. Department of Energy (2007).

# Radioactivity in Trinitite – a review and new measurements

Pittauerová, Daniela[1]; Kolb, William M.[2]; Rosenstiel, Jon C.[3]; Fischer, Helmut W.[1]
[1] Institute of Environmental Physics, University of Bremen, Otto-Hahn-Alle 1, Bremen, 28359, GERMANY
[2] Retired, 2702 Church Creek Lane, Edgewater, MD 21037, U.S.A.
[3] Retired, 2515 E. Jamison St., Anaheim, CA 92806, U.S.A.

## Abstract

Samples of Trinitite and soil from Trinity site were studied in the radioactivity measurements laboratory at the University of Bremen and at the authors' facilities in Anaheim (JCR) and Edgewater (WMK). Gamma spectroscopy was used to identify and quantify radionuclides in Trinitite and to perform a radiometric characterization of soil at the Trinity site. Additionally, a similar material ("atomsite") formed during a soviet test at the Semipalatinsk nuclear test site was investigated. Fission products ($^{137}$Cs, $^{155}$Eu) together with activation products ($^{60}$Co, $^{133}$Ba, $^{152}$Eu, $^{154}$Eu, $^{241}$Am) and $^{239}$Pu were identified. A literature search including some publicly available archive sources was conducted and our data compared to previously published results. Obtained data on Trinitite were also compared to literature data on atomsite formed during atmospheric nuclear tests in Algeria. Variability of radioactivity in Trinitite and relationship of distance from the ground zero and activation were discussed.

## Introduction

### Trinity

The terms Trinitite or atomsite are used for a fused glass-like material formed during the first nuclear test in the desert in White Sands Missile Range, New Mexico, USA, on July 16, 1945. Its colour is usually greyish-green, the top surface (facing the explosion) is smooth and typically more active than the bottom side, which is rougher and contains sand and small stones from the desert surface. The thickness of the Trinitite layer varies usually between 0.5 and 1 cm and the material contains plenty of air inclusions. Trinitite was cleared from the area by the Atomic Energy Commission in 1952, but visitors of the Trinity site can still find small pieces on the ground. Although it is illegal to remove Trinitite from the site now, specimens can be found for sale on the internet and from mineral dealers. The Ground Zero (GZ) of the Trinity test, which is a National Monument since 1965, lies within the military area and can be visited by the public twice a year, always in April and in October (WSMR, 2010).

The physical properties of the glass formed during the first nuclear explosion are described in LA-1126 report (Staritzky 1950). The glass covered an area of about 610 m diameter with a total estimated mass of $17 \cdot 10^5$ kg. A health physics survey more than 20 years after the Trinity test was made to determine the radiological risk for the public visiting the site (Fey 1967). In this study, monitoring of samples of Trinitite carried away from the site for gamma-exposure rates, measurement of surface exposure rate from individual Trinitite pieces and calculation of deposition of radioactivity in the body from ingested Trinitite were performed. In a later report (Hansen, Rodgers 1985), radiological conditions were evaluated for the Trinity site and the associated fallout zone. Here also qualitative data for activity concentrations of selected radioisotopes in the soil at GZ were given.

As for scientific literature easily accessible to the public, Atkatz & Bragg published a Trinitite NaI gamma spectrum in 1995 and from $^{137}$Cs activity they calculated the explosive yield of the device. In a response to the paper, Schlauf et al. (1997) showed advantages of HPGe spectroscopy and identified other gamma emitters in Trinitite. Sixty years after the Trinity test, a comprehensive study of Trinitite radioactivity by means of alpha-, beta- and gamma- spectroscopy was published (Parekh et al., 2006). Among other findings, the authors used $^{152}$Eu as a slow neutron flux monitor and conducted isotopic analyses of Pu in Trinitite samples. In a subsequent study (Semkov et al 2006) based on isotopic data, calculations and modeling, parameters characterizing the Trinity test were determined. Additionally, based on non-radioactive Trinitite properties, Hermes and Strickfaden (2005) devised a new theory on its formation during the explosion. The majority of the Trinitite layer was formed not on the ground, but by a rain of molten glass. After falling to the ground, the surface of Trinitite was further heated by the fireball and developed a smooth surface.

**Fig. 1. A specimen of Trinitite. Left: top side. Middle: edge. Right: bottom side. Mass 3.170 g.**

## Semipalatinsk test site

The USSR conducted its first nuclear explosion at the Semipalatinsk test site in Kazakhstan on August 29, 1949. The Soviets coded it RDS-1 (the acronym is not well understood), while the American intelligence designated it Joe-1, after Joseph Stalin. The tested weapon was a plutonium bomb design similar to that in Trinity, detonated on a tower. The yield was estimated to 20 kt TNT.

Although not much information has been published about radioactivity at the Semipalatinsk test site, there is evidence that the first Russian explosion also created pieces of fused rock at GZ (Kruglov 2002, Hodge and Weinberger 2008). They are called Kharitonchiki in honour of one of the leading Russian nuclear weapons scientists, Yuly Khariton, but are more broadly referred to as atomsite. The authors are not aware of any clean-up involving removal of atomsite, as in the case of Trinity site.

Information on activity concentrations of radionuclides in the upper 2-3 cm of soil at the site of the RDS-1 test at the Semipalatinsk test site has been published by Yamamoto et al. (1996). A mainly in-situ gamma spectroscopic study was performed by Shebell & Hutter (1998).

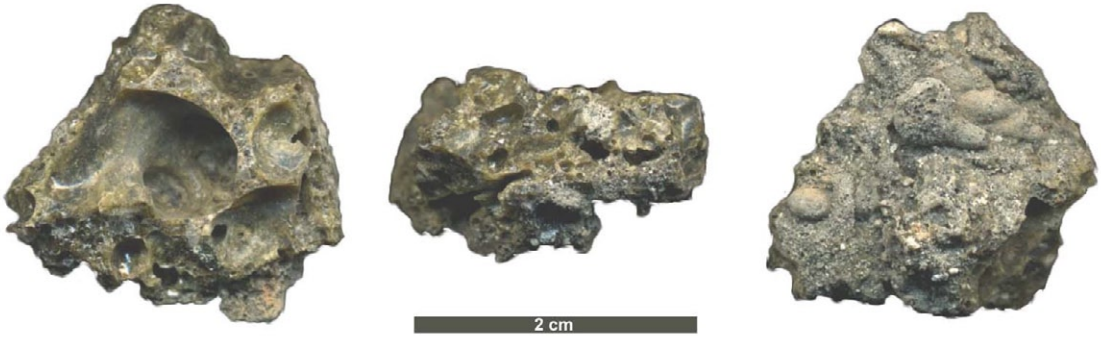


**Fig. 2. A specimen of atomsite from Semipalatinsk test site. Left: top side. Middle: edge. Right: bottom side. Mass: 2,545 g.**

### Algeria

France performed 4 atmospheric nuclear tests in the Algerian part of the Sahara desert between 1960 and 1961 at the Saharan Military Test Centre near Reggane. The first of the tests, conducted on February 13, 1960, was called Gerboise Bleue. The fission device was detonated on a 100 m tower with an estimated test yield of 40-80 kt. In 1999 the IAEA conducted a field expedition with the goal of evaluating residual activity due to the atmospheric nuclear tests (IAEA, 2005, Danesi et al. 2008). The atomsite from Gerboise Bleue test is described as black, vitreous and porous material, typically 100-1000 times more active than unmelted sand.

## Material and methods

Trinitite[1] samples analyzed in the Radioactivity Measurements Laboratory, University of Bremen (Landesmessstelle für Radiaktivität, LMS) included 6 individual larger pieces of 1.4-3.8 g each (one of them in Figure 1), 3 plastic cylindrical containers filled with many small pieces (68, 50 and 14 g each) and 2 samples of powdered Trinitite (1.9 and 1.1 g). Additionally, a 103 g bulk sample of soil from the upper 5 cm of soil collected outside the inner fence, in the distance of approx. 100 m from GZ, was measured. The samples were analyzed by low-level low-background gamma

[1] Most of the Trinitite in the present study is from the Derik Bower collection. Based on personal communications with Ralph Pray (April 2006 to September 2009) and Derik Bower (January 2003 to October 2008), it is almost certain this material was collected by Ralph Pray in the summer of 1951. It would have been located on the south road leading to GZ, possibly between 150 and 220 m from GZ.

spectroscopy using a coaxial HPGe detector (Canberra Industries) of 50% rel. efficiency housed in a 10 cm Pb shielding with Cu, Cd and plastic lining, operated under Canberra Genie 2000 software. Efficiency calibration was performed for each individual sample separately based on its individual size, density and geometry relative to the detector using the Monte-Carlo based LabSOCS Genie 2000 calibration tool (Bronson 2003). Since some of the analyzed gamma emitters have complicated decay schemes ($^{133}$Ba, $^{152}$Eu), the probability of detecting two photons emitted by the same decaying nucleus as one (a phenomenon known as cascade summing), is not negligible (up to 25%), therefore a cascade summing correction has been applied.

Spectra of another piece of Trinitite (#26) purchased from United Nuclear and a sample of atomsite from the Semipalatinsk test site (Figure 2) were obtained using the author's (JCR) Ortec LO-AX-51370/20 coaxial HPGe detector shielded by approximately 7cm Pb, lined with Cu and Sn foil within PVC and acrylic layers. Samples collected by the author (WMK) in October 2006 at Trinity site with known locations around GZ were measured using the author's (WMK) 5" Bicron NaI(Tl) well detector housed in 2 cm of Pb shileding with Cu foil grading. For the two later mentioned setups the efficiency calibration as described above was not achievable, therefore the resulting spectra were used for qualitative and comparative purposes only.

## Results

Gamma spectroscopy of Trinitite enabled identification of several natural and artificial radionuclides, formed as a result of fission and activation or found as remains of nuclear fuel. A gamma spectrum of one of the samples is shown in Figure 3. Radionuclides are listed in Table 1 together with remarks on their origin. Some of the radionuclides ($^{60}$Co and $^{155}$Eu, which were not reported in previous studies) were initially present in very high concentrations; therefore it is possible to detect them, even after more than 10 half-lives. Table 2 gives the specific activity of individual isotopes in Trinitite compared to literature values (Atkatz & Bragg 1995, Schlauf et al. 1997 and Parekh et al 2006).

**Table 1. List of detected artificial gamma emitters artificial in Trinitite and their origin.**

| Isotope | Half-live (yr) | Origin |
|---|---|---|
| $^{60}$Co | 5.3 | Activation of $^{59}$Co – from test tower steel and from soil |
| $^{133}$Ba | 10.5 | Activation of $^{132}$Ba. Baratol - Ba $(NO_3)_2$ - was part of explosive lens system of the Gadget |
| $^{137}$Cs | 30.0 | Fission product (beta decay of $^{137}$Xe and $^{137}$I and also independently) |
| $^{152, 154}$Eu | 13.3 / 8.8 | Activation of stable isotopes $^{151,153}$Eu in soil by slow neutrons |
| $^{155}$Eu | 4.8 | Fission product |
| $^{239}$Pu | 24110 | Principle isotope of nuclear fuel |
| $^{241}$Am | 433 | Mostly present as daughter product of $^{241}$Pu (beta emitter), produced mainly from $^{239}$Pu during the explosion via double-neutron capture. Based on $^{241}$Am ingrowth activity of $^{241}$Pu is possible to determine. |

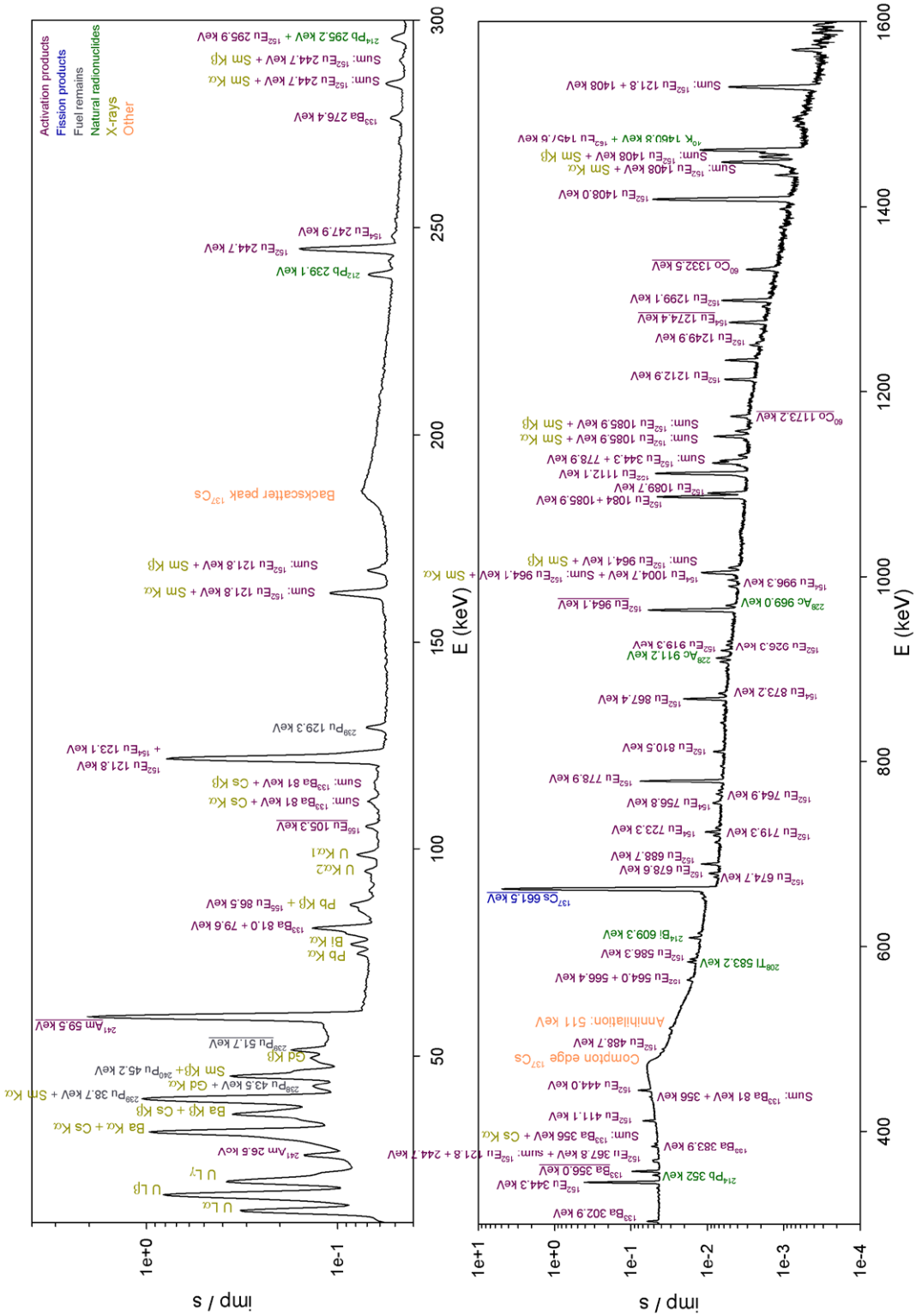


**Fig. 3. A HP-Ge gamma spectrum of a sample of Trinitite measured in LMS (50.2 g, pieces of Trinitite in a plastic cylindrical container, height 20 mm, diameter 70 mm, live-time 423281 s).**

**Table 2. Table of comparison of activity concentrations (Bq/g, uncertainties 1σ) of artificial radionuclides detected in Trinitite and soil from nuclear test sites recalculated to the date of respective nuclear explosions ($^{241}$Am, which is ingrowing from $^{241}$Pu, is reported to the date of analysis - in brackets).**

| Radio-isotope | LMS, 2010 | Atkatz & Bragg, 1995 | Schlauf et al., 1997 | Parekh et al., 2006 | IAEA, 2005 | LMS, 2010 | Hansen & Rodgers, 1985 | Yamamoto et al., 1996 |
|---|---|---|---|---|---|---|---|---|
| | Median, Min - Max | | | Min, Max | Min - Max | Min, Max | Min - Max | |
| | TRINITITE | | | | ATOMSITE ALGERIA | SOIL TRINITY | | SOIL SEMIPALATINSK |
| Bq/g | 11 samples of Trinitite (see text) | Small piece | 8,3 g piece | 3 samples: several small pieces and 2 bigger individual pieces | Black fragments of fused sand | 2 samples of soil (see text) | Samples at GZ area | 2-3 upper mm of soil |
| $^{60}$Co | 47.7 ± 4.6<br><51.8[1] - (72.5 ± 4.8) | - | 44 ± 4 | 44.4 ± 4.6<br>62.0 ± 4.9 | 168.9 | 2.9 ± 0.8<br>20.8 ± 1.3 | 64 - 320 | 1946 ± 43 |
| $^{133}$Ba | 9.10 ± 0.77<br>(5.04 ± 0.51) - (17.8 ± 1.3) | - | 9.9 ± 0.6 | 7.55 ± 0.45<br>9.80 ± 0.26 | 48.9 | 0.104 ± 0.009<br>0.36 ± 0.03 | 0.73 - 1.73 | - |
| $^{137}$Cs | 48.3 ± 1.4<br>(16.26 ± 0.88) - (80.9 ± 2.4) | 83.2 | 90 ± 9 | 27.33 ± 0.08<br>121.8 ± 0.1 | 78.1 | 0.142 ± 0.004<br>0.879 ± 0.026 | 0.38 - 1.87 | 236 ± 2 |
| $^{152}$Eu | 26.0 ± 1.1<br>(14.2 ± 1.3) - (55.5 ± 1.3) | - | 27 ± 1 | 22.61 ± 0.38<br>78.89 ± 0.61 | 54.0 | 7.92 ± 0.19<br>33.42 ± 0.79 | 3.2 - 347 | 998 ± 10 |
| $^{154}$Eu | 7.08 ± 0.24<br><6.03[2] - (12.76 ± 0.36) | - | 4.8 ± 0.6 | 2.45 ± 0.60<br>16.1 ± 1.3 | 27.2 | 1.07 ± 0.08<br>4.80 ± 0.28 | - | 100.8 ± 4.5 |
| $^{155}$Eu | 274 ± 25<br><361[3] - (461 ± 54) | - | - | - | 241.2 | <28.4<br>10.8 ± 2.8 | - | - |
| $^{239}$Pu | 73.6 ± 3.5<br>(25.7 ± 3.6) - (133 ± 25) | - | - | 86.3 ± 2.7 | <230 | < MDA<br>< MDA | - | - |
| $^{241}$Am | 1.870 ± 0.080<br>(0.741 ± 0.048) - (4.47 ± 0.19)<br>(2009) | - | 2.9 ± 0.5<br>(1997) | 1.841 ± 0.053<br>4.137 ± 0.058<br>(2006) | 2.3<br>(1999) | 0.0082 ± 0.0004<br>0.0369 ± 0.0018<br>(2009) | - | 0.52 ± 0.01<br>(1994) |
| $^{241}$Pu[4] | 63.6 ± 2.7<br>(25.2 ± 1.6) - (152.0 ± 6.5) | - | 100 ± 17 | 62.9 ± 1.8<br>141.3 ± 2.0 | 85 | 1.254 ± 0.061<br>0.279 ± 0.014 | - | 18.6 ± 0.4 |

**Several values measured by LMS were below detection limit, mainly due to low sample mass and/or shorter measurement times.**
**[1] 3 values under MDA, minimal value above MDA is 34.5 ± 5.6.** **[2] 3 values under MDA, minimal value above MDA is 2.70 ± 0.07.**
**[3] 5 values under MDA, minimal value above MDA is 115 ± 38.** **[4] Calculated from $^{241}$Am ingrowth**

The spectrum of radionuclides (with exception of $^{239}$Pu) found in Trinity soil was similar to that of Trinitite. The absolute activities of $^{152,154}$Eu and $^{60}$Co, isotopes being formed by activation of elements present in soil itself, were present in the same order of magnitude as in Trinitite. The activity concentrations of $^{137}$Cs, $^{133}$Ba and $^{241}$Am were 1-2 orders of magnitude lower in soil than in Trinitite (Table 2).

## Discussion

### Correlations

Correlation analysis was performed for the set of 11 Trinitite samples measured in LMS using Pearson test (normality was positively tested by Shapiro-Wilk test). Significant positive correlation was found for $^{152}$Eu and $^{154}$Eu (r=0.823;P=0.016). That is in agreement with similar origin of both isotopes (activation of stable Eu isotopes from soil). On the other hand, activation product $^{152}$Eu and fission product $^{155}$Eu are not correlated (r=0,305; P=0,557). $^{239}$Pu and $^{241}$Am, which is present as a decay product of $^{241}$Pu (activation of fuel during the explosion), show strong positive correlation (r=0.967; P=0,000001). Activation product $^{133}$Ba is positively correlated with $^{239}$Pu (r=0,768; P=0,006) and $^{241}$Am (r=0.785; P=0,004). Fission products $^{137}$Cs and $^{155}$Eu were significantly correlated with $^{239}$Pu (r=0,827; P=0,0017 and r=0,836; P=0,038, respectively) and similarly with $^{241}$Am. Positive correlation was also found for $^{137}$Cs and $^{152}$Eu (r=0,703; P=0,0159). $^{60}$Co is not correlated to any other radioisotope.

### Inhomogeneous distribution of radioactivity in Trinitite

The difference of activity at the top surface and the bottom surface of Trinitite is remarkable, mainly for beta activity. Measurements performed on 6 Trinitite specimens collected by WMK in 2006 using a 2" pancake tube inside a plastic bag to stop alpha radiation showed the top/bottom surface ratios ranging between 2.6 and 22.9 (with exception of one sample of unusual appearance showing ratio <1). Gamma measurements do not show such a pronounced difference due to higher penetrability of gamma radiation. A repeated measurement of one piece of Trinitite on a HPGe detector (LMS) top side up and top side down showed top/bottom ratios significantly increased for $^{137}$Cs (1.24±0.05), $^{239}$Pu (1.49±0.11) and $^{241}$Am (1.25±0.08). Top/bottom ratios for $^{133}$Ba and $^{152}$Eu,however, were close to 1 (1.0±0.1 and 0.96±0.09, respectively).

### Variability of radionuclides in Trinitite

While some variation in radionuclide activity (Table 2) can be attributed to sample size and normal variance, differences due to location are also expected and have been observed. Semkow et al (2006) found a power-law dependence between $^{152}$Eu and slant range to the nuclear explosion center. Semkow calculated a least-squares exponent of -6.257 using 1946 data from 300 to 500 m (instruments closer to GZ were destroyed), whereas a spherical spread of neutrons would have resulted in an exponent of -2. Trinitite collected by the author (WMK) in October 2006 from 18 locations between 60 and 260 meters from GZ did, however, exhibit a power-law dependence with an exponent of -2.03 and least-squares correlation of $R^2$=0.777. The activity in counts-per-hour per gram at 1112 keV was found to be 68350 $s^{-2.03}$, where s is the slant range in meters to the top of the 30 m tower. The same specimens showed no significant

relationship between $^{137}$Cs activity (a fission product) and slant range using the 662 keV peak. It is not known how site clean-up activities may have affected the distances measured to GZ but evidence found during the 2006 survey suggests the specimens were probably within a meter of two of their original locations.

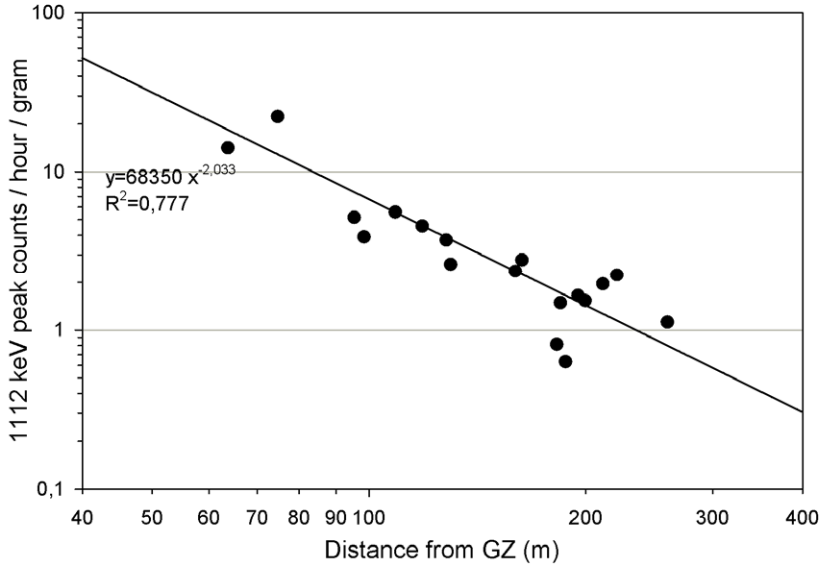


**Fig. 4. $^{152}$Eu activity vs distance from GZ in Trinitite samples collected in October 2006 by WMK measured with 5'' NaI(Tl) well detector.**

### Comparison of Trinitite to atomsite from Semipalatinsk

Gamma activity of a 2.545 g specimen of atomsite (Figure 2) from Semipalatinsk was compared to a typical 6.5 g specimen of Trinitite (gamma spectra in Figure 5). The net peak areas of radionuclides measured in both spectra were corrected by respective masses and decay corrected to the date of explosions (1945 and 1949, respectively). Atomsite from Semipalatinsk showed significantly higher activity than Trinitite. The activity ratios of Semipalatinsk/Trinity atomsite were: $^{137}$Cs: 16.1±0.1, $^{152}$Eu: 23.0±1.5, $^{241}$Am ($^{241}$Pu): 3.4±0.1 and $^{239}$Pu: 3.4±0.6. $^{154}$Eu and $^{60}$Co were under detection limits in Trinitite. $^{133}$Ba was not detected in atomsite from Semipalatinsk. This is surprising due to the fact, that Baratol was also used in explosive lenses in the first Soviet nuclear test (Kruglov 2002).

### Comparison of Trinitite to atomsite from Algeria

Literature values of a sample from Gerboise Bleue atomsite from Algeria (IAEA 2005 – sample No. ALG 4) described as black fragments of fused sand were compared to values of Trinitite measured by LMS (Table 2). Generally, the Algerian atomsite is more radioactive (activities recalculated to dates of explosions). $^{137}$Cs value is about 1.5 times higher than median Trinitite values, $^{152}$Eu 2 times higher, $^{154}$Eu 4 times higher, $^{60}$Co 3.5 times higher, $^{133}$Ba 5 times higher. $^{155}$Eu and $^{241}$Am values are comparable for both Trinitite and atomsite from Algeria. Higher radioactivity in Algerian atomsite is likely due to the higher yield of the tested device.

### Comparison of soil from Trinity to soil from Semipalatinsk test site

Soil data collected from the First Experimental site near the hypocenter where the first Soviet nuclear bomb was tested were published by Yamamoto et al (1996). They were compared to samples of soil from Trinity site. All activities were 1 or 2 orders of magnitude higher in soil from Semipalatinsk site than Trinity. The main difference was the absence of $^{133}$Ba, as the activation product of stable Ba in baratol in Semipalatinsk site.

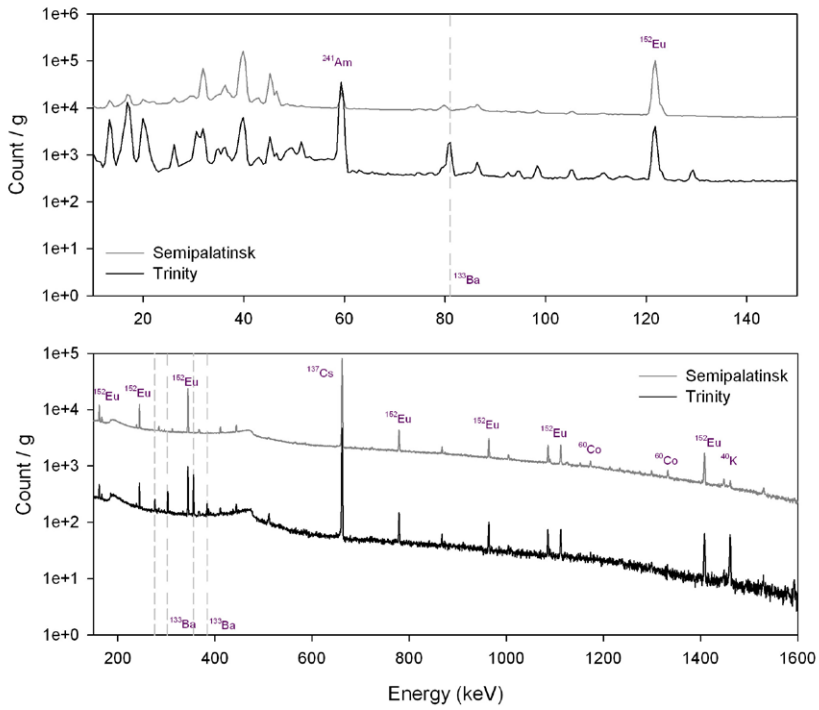


**Fig. 5. 24 hour comparison spectra of atomsite from Semipalatinsk and Trinitite (sample #26) measured by Ortec LO-AX HPGe detector. Dashed lines indicate the main $^{133}$Ba gamma lines in Trinitite and the lack of $^{133}$Ba in the sample from Semipalatinsk.**

## Conclusions

Gamma spectroscopic studies of Trinitite, atomsite from Semipalatinsk and soil from Trinity was conducted. The experimental data were compared to literature data for Trinitite, atomsite from Algeria and soil from Semipalatinsk. $^{133}$Ba (an activation product of Ba in explosive lenses) is present in Trinitite and atomsite from Algeria, but absent in atomsite and soil from Semipalatinsk. $^{155}$Eu, a fission product, was found to be detectable in Trinitite after more than 13 half-lives. Correlations between radionuclides in Trinitite and the inhomogeneous distribution of radioactivity in Trinitite were discussed. Power-law dependence with an exponent close to -2 between $^{152}$Eu and distance from GZ was found.

## Acknowledgements

The authors are grateful to Robert E. Hermes for making it possible to study his specimen of atomsite from Semipalatinsk. Bernd Hettwig's gamma spectroscopy consultations are greatly acknowledged.

## References

Atkatz D, Bragg C. Determining the yield of the Trinity nuclear device via gamma-ray spectroscopy. American Journal of Physics 1995; 63(5): 411-413.

Bronson FL. Validation of the accuracy of the LabSOCS software for mathematical efficiency calibration of Ge detectors for typical laboratory samples. Journal of Radioanalytical and Nuclear Chemistry 2003, 255(1) 137-141.

Danesi PR, Moreno J, Makarewicz M, Louvat D. Residual radionuclide concentrations and estimated radiation doses at the former French nuclear weapons test sites in Algeria. Applied Radiation and Isotopes 2008, 66(11): 1671-1674.

Fey FL. Health Physics Survey of Trinity Site. Report LA-3719, Los Alamos Scientific Laboratory, Los Alamos, 1967.

Hansen WR, Rodgers JC. Radiological Survey and Evaluation of the Fallout Area from the Trinity Test: Chupadera Mesa and White Sands Missile Range, New Mexico. Report LA-10256-MS, Los Alamos National Laboratory, Los Alamos, 1985.

Hermes RE, Strickfaden WB. A new look at Trinitite. Nuclear Weapons Journal 2005; 2, 2-7.

Hodge N, Weinberger S. A Nuclear Family Vacation: Travels in the World of Atomic Weaponry. New York, 2008. 336 pages.

International Atomic Energy Agency. Radiological Conditions at the Former French Nuclear Test Sites in Algeria: Preliminary Assessment and Recommendations. Radiological assessment reports series 2005, 71 p.

Kruglov A. The History of the Soviet Atomic Industry. London, 2002. 280 pages.

Parekh PP, Semkow TM, Torres MA, Haines DK, Cooper JM, Rosenberg PM, Kitto ME. Radioactivity of Trinitite six decades later. Journal of Environmental Radioactivity 2006; 85(1): 103-120.

Semkow TM, Parekh PP, Haines DK. Modeling the Effects of the Trinity Test. In Semkow TM, Pommé S, Jerome S, Strom DJ (Eds). Applied Modeling and Computations in Nuclear Science 2006; Chapter 11, pp 142–159.

Schlauf D, Siemon K, Weber R, Esterlund RA, Molzahn D, Patzelt P. Trinitite redux: Comment on "Determining the yield of the Trinity nuclear device via gamma-ray spectroscopy," by David Atkatz and Christopher Bragg [Am. J. Phys. 63 (5), 411-413 (1995)]. American Journal of Physics 1997; 65(11): 1110-1112.

Shebell P, Hutter AR. Environmental radiation and radioactivity in the vicinity of the Semipalatinsk Test Site. Journal of Radioanalytical and Nuclear Chemistry 1998; 235 (1-2): 133-138.

Staritzky E. Thermal effects of atomic bomb explosions on soils at Trinity and Eniwetok. Report LA-1126, Los Alamos Scientific Laboratory, Los Alamos, 1950.

White Sands Missile Range. WSMR Trinity site web page: http://www.wsmr.army.mil/wsmr.asp?pg=y&page=576. Accessed on 10/4/2010.

Yamamoto M, Tsukatani T, Katayama Y. Residual radioactivity in the soil of the Semipalatinsk nuclear test site in the former USSR. Health Physics 1996; 71(2):142-148.

# External exposure of a representative individual at selected sites of the peaceful underground nuclear explosions in Russia

Ramzaev, Valery; Repin, Victor; Medvedev, Alexander; Khramtcov, Evgeny; Timofeeva, Maria; Mishin, Arkady
Institute of Radiation Hygiene, St-Petersburg, RUSSIA

## Abstract

During the period 2001–2009, eight field expeditions have been conducted to seven selected sites of the peaceful underground nuclear explosions, which were performed in the European and Asian parts of Russia in the last century. Those are: "Crystal" and "Kraton-3" (Yakutia); "Dnepr" (Murmansk region); "Angara" and "Quartz" (Khanti-Mansiysk region); "Globus-1" (Ivanovo region); "Taiga" (Perm region). Evaluation of current doses from the man-made source to a representative individual was one of the main aims of the radiological investigations at the areas. This paper summarizes the key experimental data that are relevant to estimation of external doses.

External doses from the man-made $\gamma$-ray emitting radionuclides to a human were calculated using data of *in situ* measurements and results of laboratory radiometric analyses. Realistic estimations of the location factors were used for model calculations of the doses. The estimated effective doses included contribution from global fallout and Chernobyl debris. It is demonstrated that for some UNE sites the dose of interest may exceed a negligible limit of 10 μSv $y^{-1}$. At the same time, for all these sites the current doses are far below a value of 300 μSv $y^{-1}$, which is the threshold for application of countermeasures, accordingly to the Russian legislation.

## Introduction

Practical implementation of underground nuclear explosion (UNE) technologies in a framework of the National Program "Nuclear Explosions for the National Economy" (Program №7), which had been carried out in the USSR throughout the period 1965–1988 (Ministry of the Russian... 1996), resulted in appearance of a number of sites contaminated by the long-lived man-made radionuclides (Logachev 2001, 2005; Norduke 2000; Yablokov 2003). The majority of the industrial UNE (81 from a total of 124) were conducted in the Russian Federation at the areas located beyond the boundaries of conventional nuclear test sites. The most pronounced contamination of the territory was reported for the UNE Kraton-3 (with $^{137}$Cs, $^{90}$Sr, plutonium) and Globus-1 ($^{137}$Cs, $^{90}$Sr), where accidental releases of the radioactivity had occurred, and for the UNE Crystal ($^{137}$Cs, $^{90}$Sr, plutonium, $^{60}$Co) and Taiga ($^{3}$H, $^{137}$Cs, $^{90}$Sr, plutonium, $^{241}$Am, $^{60}$Co) polluted as a result of the planned technological conditions

(Gedeonov et al. 2002a, 2002b; Logachev 2001, 2005; Lurie 2002; Miretsky et al. 1997). Presently, general public has unlimited access to the sites, and therefore some additional exposure from these man-made sources of the ionizing radiation to a human might be expected.

This paper is devoted to evaluation of the current external $\gamma$-ray dose to a representative individual with respect of the four above mentioned sites of UNE. Three different sites (Dnepr, Quartz-3 and Angara), which did not have significant contamination by the long-lived $\gamma$-ray emitting radionuclides from the local sources, are taken for comparison.

## Material and methods

Table 1 summarises locations and some technological characteristics of the explosions considered. Additional technical details on the UNEs, including geological conditions, may be found in Logachev (2001), Norduke (2000), and Ramzaev et al. (2007, 2009a, 2010b). The sites of selected UNEs are located at forested areas within the moderate or cool climatic zones. Examples are given in Fig. 1 and 2. All selected explosions were carried out in the closest proximity of rivers.

**Table 1. Locations and some technological characteristics of selected UNEs (in chronological order). The geographic coordinates have been recorded during our expeditions to the UNE sites; other data are given accordingly to Logachev (2001).**

| Name of UNE | Year of detonation | Region, geographic coordinates | Depth, m | Power equivalent, kt of TNT | Purpuse |
|---|---|---|---|---|---|
| Taiga | 1971 | Perm region<br>61.3° N, 56.6° E | 127 | 3×15 (45) | Constructing of a canal |
| Globus-1 | 1971 | Ivanovo region<br>57.5° N, 42.6° E | 610 | 2.3 | Deep seismic sounding of the Earth's crust |
| Dnepr-1 | 1972 | Murmansk region<br>67.8° N, 33.6° E | 131 | 2.1 | The breakage of ore |
| Crystal | 1974 | The Republic of Sakha (Yakutia)<br>66.5° N 112.5° E | 98 | 1.7 | Constructing of a reservuar dam |
| Kraton-3 | 1978 | The Republic of Sakha (Yakutia)<br>65.9° N, 112.3° E | 577 | 22 | Deep seismic sounding of the Earth's crust |
| Angara | 1980 | Khanti-Mansiysk AO<br>61.7° N, 67.1° E | 2485 | 15 | Stimulation of oil production |
| Quartz-3 | 1984 | Khanti-Mansiysk AO<br>61.9° N, 72.1° E | 726 | 8.5 | Deep seismic sounding of the Earth's crust |
| Dnepr-2 | 1984 | Murmansk region<br>67.8° N, 33.6° E | 175 | 2×1.8 (3.6) | The breakage of ore |

**Fig. 1. The mountain of Kuel'por (Khibiny, Kola Peninsula) is the site where nuclear explosion technologies were used for the experiments on breakage of the phosphate ore in 1972 and 1984 (project "Dnepr"). The group of tourists and researches is on the road which connects the tourist's camp (to the right) with the site of explosions. July 2008.**

**Fig. 2. A bed for this beautiful lake had been created by a simultaneous detonation of three thermonuclear devices in 1971. The "Taiga" experiment was conducted with the purpose to obtain some field data for the final elaboration of the project on Kama-Pechora canal. The lake "Taiga" has a length of ca. 700 m and a width of (350 to 380) m. The photo was taken from a helicopter in August 2009.**

**Fig. 3. Measurements of γ-ray dose rate in air using the gamma dosimeter EL-1101. The plot is located on the axis of the Kraton-3 radioactive trace at a distance of approximately 1.5 km from the borehole. 100% mortality in the larch tree (*Larix gmelinii*) population is observed. July 2002.**

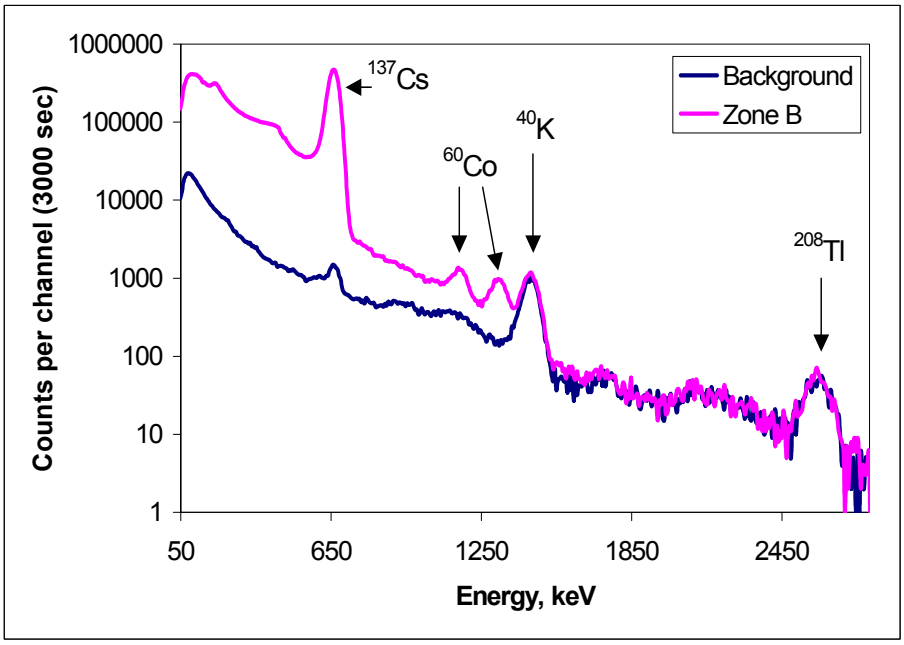


**Fig. 4. The γ-ray spectra were recorded on a background plot in Yakutia and on a plot located within a boundary of the affected forest (zone B) at the Kraton-3 site in July 2002. Note a strong excess the $^{137}$Cs peak on the spectrum from the Kraton-3 site above the background one (actually, 662 keV peak is related to the short-lived meta-stable daughter of $^{137}$Cs – $^{137m}$Ba). Two peaks from $^{60}$Co (1173 keV and 1332 keV) can also be seen here. There is no difference between the background and *on site* spectrum with respect of peaks from the natural radionuclides of $^{40}$K (1460 keV) and $^{208}$Tl (2615 keV).**

Although the experiments (excluding, perhaps, the Crystal UNE) were conducted at remote areas, the sites are frequently used by tourists and local population for

collecting mushrooms and berries, as well as for angling and hunting. The investigators, who conduct field studies, form another group of the exposed individuals.

We suppose that a total duration of a person's staying at the area of an UNE is equal to 14 days in a year. A representative individual was assumed to have stayed within the contaminated site 8 hours each day, totally 112 hours in a year. During 224 hours in a year the person is staying at the background locations: in a camp, forest, on the bank of a river, etc. The scenario is based on our own experience and the results of interviewing other investigators, local citizens and tourists.

For the measurements of γ-ray dose rate (DR) in air at a height of 1 m above the ground, portable γ-ray dosimeters EL-1101, EL-1117 and AT-1121 (ATOMTEX, Belarus) were used (Fig. 3). Technical characteristics of the dosimeters are given in Ramzaev et al. (2006, 2010b). The registered values of DR (Table 2, column 5) include intrinsic noise of the device, cosmic radiation response, contribution from the natural radionuclides, and contribution from the man-made radionuclides. The routine measurements of dose rates in air were supplemented by *in situ* γ-ray spectrometry (Fig. 4) and GPS mapping (Ramzaev et al. 2010b). Soil samples were collected in the plots that might be contaminated as a result of the UNEs and in the "background" plots, which do not lie on sectors affected by the radioactive plume

**Table 2. Mean±standard deviation values of the ground surface contamination with $^{137}$Cs (kBq m$^{-2}$), total measured γ-ray dose rate in air (nSv h$^{-1}$), and calculated external γ-ray dose (μSv y$^{-1}$) to a representative individual. The dose is attributed solely to the man-made radionuclides: $^{137}$Cs and some others, as indicated in column 4. The dose that has been calculated using formula (2) marked (*). Number of sampling plots is given in brackets. The experimental data are obtained from EKORANT (2007), Federal Scientific (2008, 2009), Ramzaev et al. (2007, 2009a) and St-Petersburg Research (2002). The reference date is the sampling date given in the first column.**

| Name of UNE, year | Location | $^{137}$Cs, kBq m$^{-2}$ | Other man-made γ-ray emitters | Total dose rate in air, nSv h$^{-1}$ | Dose, μSv y$^{-1}$ |
|---|---|---|---|---|---|
| Taiga, 2009 | site of UNE | 452 ± 421 (6) | $^{60}$Co, $^{207}$Bi, $^{241}$Am | 274 ± 274 (498) | 22* |
| | background | 1.4 (1) | Not detected | 76 ± 20 (9) | 0.2 |
| Globus-1, 2008 | site of UNE | 17400 ± 19300 (3) | Not detected | 174 ± 240 (189) | 14* |
| | background | 2.5 (2) | Not detected | 46 ± 4 (5) | 0.3 |
| Dnepr, 2008 | site of UNE | 1.9 ± 0.9 (4) | Not detected | 180 ± 202 (60) | 0.1 |
| | background | 2.2 (1) | Not detected | 108 ± 18 (25) | 0.3 |
| Crystal, 2001 | site of UNE | 21 ± 25 (5) | $^{60}$Co, $^{241}$Am | 104 ± 70 (6) | 7.1* |
| | background | 0.8 ± 0.1 (6) | Not detected | 41 ± 8 (8) | 0.1 |
| Kraton-3, 2001-2002 | site of UNE | 955 ± 1870 (14) | $^{60}$Co, $^{241}$Am | 240 ± 230 (332) | 22* |
| | background | 0.8 ± 0.1 (6) | Not detected | 41 ± 8 (8) | 0.1 |
| Angara, 2007 | site of UNE | 1.3 (2) | Not detected | 62 ± 12 (34) | 0.1 |
| | background | 1.3 (1) | Not detected | 57 ± 4 (6) | 0.2 |
| Quartz-3, 2007 | site of UNE | 1.4 ± 0.2 (4) | Not detected | 43 ± 7 (61) | 0.1 |
| | background | 1.4 (1) | Not detected | 34 ± 4 (3) | 0.2 |

trajectories. Between three and seven cylindrical samples, each with a ground surface of 20 $cm^2$, were taken at a plot to determine the man-made radionuclides activity per unit area. The depth of such cores ranged from 10 cm to 40 cm, depending on tasks of sampling and presence of pebbles and stones in the underlying ground. Additional details on the soil sampling procedure may be found in Ramzaev et al. (2006, 2007). Content of the man-made γ-ray emitting radionuclides in soil samples was determined by direct gamma-spectroscopy using shielded high-purity Ge detectors and multi-channel analysers.

## Results

$^{137}$Cs is the only one man-made γ-ray emitting radionuclide detected in the top-soil samples that had been collected at the background plots (Table 2). Levels of $^{137}$Cs deposit in individual plots varied from circa 0.7 kBq $m^{-2}$ in Yakutia to 3.1 kBq $m^{-2}$ in Ivanovo region. Global fallout might be considered as the main source of $^{137}$Cs for background plots in the Asian part of Russia (the UNE Angara, Kraton-3, Crystal and Quartz-3), while for the plots in the European part (the UNE Globus-1, Dnepr, and Taiga) some contribution from Chernobyl source should be anticipated.

$^{137}$Cs ground contamination at sites of the UNE Dnepr, Quartz-3 and Angara did not deviate from the respectful background levels; for the UNE Quartz-3 and Angara there were also no principal difference between the background and *on site* measured DR (Table 2). At the same time, the DR values registered at the Dnepr site, which is located at a mountainous area, were on average somewhat higher than the background values. The *in situ* gamma-spectroscopy indicated that this might be attributed to the local leakage of the underground air, which is enriched with the radon and its daughters. The DR measured near the mouth of one of the tunnels, which connect intramountain cavities with the Earth's surface, was about an order of magnitude higher than levels determined at background plots (Scientific Enterprise… 2008).

Levels of $^{137}$Cs surface contamination at sites of the UNE Kraton-3, Crystal Globus-1 and Taiga exceeded the background values drastically (Table 2). The maximum contamination density (40000 kBq $m^{-2}$) was deduced for the Globus-1 site (Scientific Enterprise… 2008). Some other man-made radionuclides that were found at UNE sites are listed in Table 2, column 4. Elevated levels of DR have been measured at all four sites that had been significantly contaminated as a result of UNE (Table 2). At the Kraton-3 and Taiga sites, the contamination is observed at an area covering more than 1 $km^2$. A smaller spatial contamination may be deduced with respect of the Crystal and Globus-1 sites – about 6 ha and 2 ha, respectively (Ramzaev et al. 2007; Scientific Enterprise… 2008).

The effective external dose ($E_{ext}$) from $^{137}$Cs to a human at a background location can be calculated according to:

$$E_{ext} = T_{loc} \cdot A^{137} \cdot K^{E} \cdot g^{137}, \qquad (1)$$

where

$T_{loc}$ – is duration of staying at a location, h. $T_{loc}$ is 224 h;

$A^{137}$ – is the ground surface contamination with $^{137}$Cs, kBq $m^{-2}$;

$K^E$ – is a coefficient converting the absorbed dose in air to effective dose for a human, Sv $Gy^{-1}$. The numeric value of $K^E$ is 0.71 Sv $Gy^{-1}$ (Golikov et al. 2007);
$g^{137}$ – is a transfer factor from the ground surface contamination by $^{137}Cs$ to absorbed dose rate in air, (μGy $h^{-1}$)/(kBq $m^{-2}$). The numeric value of $g^{137}$ is $0.71 \cdot 10^{-3}$ (μGy $h^{-1}$)/(kBq $m^{-2}$) (United Nations 2000).

Formula (1) has also been applied for calculating the effective dose for a human staying at sites of the UNE Dnepr, Quartz-3 and Angara where no excess of the man-made contamination was observed. Duration of staying at the site of an UNE, $T_{loc}$ has been taken as 112 h. The results of estimation of the external γ-ray dose from the man-made sources are given in the last column of Table 2. As expected, negligible doses (much less than 1 μSv $y^{-1}$) have been calculated for sites of these three UNE and for all background locations.

For calculating the external doses ($E_{ext}$) at contaminated sites, the other approach based on a difference between DR measured *on site* and on background plots was adopted. The equation used for these four sites of UNE is:

$$E_{ext} = T_{site} \cdot (P_{site} - P_{bg}), \qquad (2)$$

where
$P_{site}$ – is the total averaged DR at a site, μSv $h^{-1}$;
$P_{bg}$ – is the total averaged DR at a background location, μSv $h^{-1}$;
$T_{site}$ – is duration of staying at an UNE site, 112 h.

For the three sites of UNE (Taiga, Kraton-3 and Globus-1) the effective dose exceeded a negligible limit of 10 μSv $y^{-1}$ (Table 2).

## Discussion

The legislative status of the peaceful UNEs conducted at the territory of Russia is not yet established officially (Ramzaev et al. 2009b). Nonetheless, the situation of "existing exposure" is, perhaps, the most closely related definition that can be applied for describing general radiological status of the UNE sites nowadays. A short-term staying (during days or weeks in a year) of a very limited number of people on the contaminated areas is a specific feature of the exposure conditions at such sites.

Our estimations of external exposure to a human at the seven sites of peaceful UNEs indicates that for three cases the technogenic dose may exceed a negligible limit of 10 μSv $y^{-1}$. At the same time, for all these sites the current doses appeared to be far below a value of 300 μSv $y^{-1}$, which is the threshold for application of countermeasures, accordingly to the Russian legislation (Federal Service 2009).

The annual effective external dose, which has been calculated according to formula (2), includes contributions from a total suite of the man-made γ-ray emitting radionuclides and some bremsstrahlung radiation from interaction of beta-rays with nuclei in soil and air. The latter source may be of significance at the areas contaminated with $^{90}Sr/^{90}Y$, for example at the Kraton-3 site (Ramzaev et al. 2009a). The direct beta

exposure to the skin and eyes of a person in a radiation field at the UNE sites may somehow contribute to the total dose (see Ramzaev et al. 2009a and references therein). The issue related to the beta-ray exposure requires further studies because relevant quantitative estimations are not presented.

Additionally to the external exposure, which is an inevitable component of the total dose for the UNE situation, a human, in principle, may be exposed from the man-made radionuclides ingested with food products of natural origin and water. Inhalation of the radioactive aerosols may be another pathway of internal exposure at the UNE sites. Contribution of internal exposure to the total may vary significantly. Accordingly to preliminary conservative assessments, the input from internal sources is approximately 20 % at the Taiga, site and it is more than 90 % at the Dnepr site (Scientific Enterprise 2008, 2009).

## Conclusions

The residual levels of the surface ground contamination with $^{137}$Cs at the sites of UNE Kraton-3, Crystal, Globus-1 and Taiga are significantly higher than those detected for background areas.

Our estimations show that, presently, the UNE-relevant effective external dose to a representative individual may exceed a negligible limit of 10 μSv $y^{-1}$ with respect of the Kraton-3, Globus-1 and Taiga sites.

For some sites of UNE, the external gamma radiation may constitute the major contribution to the total technogenic dose.

Periodical monitoring of radiation conditions at the sites of UNE is recommended (Ramzaev et al. 2010a).

## Acknowledgments

The study is supported from the Federal Program “Nuclear and Radiation Safety”. Part of this work received supporting funding from the International Atomic Energy Agency.

## References

EKORANT Scientific and Research Centre. Radiation monitoring at the territories of autonomous okrug in 2007 with the aim of elaborating a radiation passport of the Khanti-Mansiysk AO–Yugra. Vol. 3. Radiological investigations at the sites of the underground nuclear explosions “Taiga” (Oktabr’skiy district) and “Quartz-3” (Surgut district). St.-Petersburg: EKORANT; 2007 (in Russian).

Federal Scientific Organization «Saint-Petersburg Research Institute of Radiation Hygiene after Professor P.V. Ramzaev» of Federal Service for Surveillance on Consumer Rights Protection and Human Well-being. Radiation-hygienic investigation at the territories adjacent to the sites of the peaceful nuclear explosions resulted in ground surface contaminations with radionuclides; development of criteria and conditions to ensure public safety. Scientific research report. St-Petersburg: IRH; 2008 (in Russian).

Federal Scientific Organization «Saint-Petersburg Research Institute of Radiation Hygiene after Professor P.V. Ramzaev» of Federal Service for Surveillance on Consumer Rights Protection and Human Well-being. Development and

substantiation of criteria and conditions to ensure radiation safety of the population living near the sites of application of nuclear explosive technologies; improvement of information activities when addressing general public. Development and substantiation of criteria and conditions to ensure radiation safety for the "Taiga" site. Scientific research report. St-Petersburg: IRH; 2009 (in Russian).

Federal Service for Surveillance on Consumer Rights Protection and Human Well-being. Sanitary rules SR. 2.6.1.2523-09 “Radiation safety standards (RSS-99/2009)”. Moscow: Federal Service for Surveillance on Consumer Rights Protection and Human Well-being; 2009 (in Russian).

Gedeonov AD, Petrov ER, Alexeev VG, Kuleshova IN, Savopulo ML, Burtsev IS, Shkroev VYu, Arkhipov VI. Residual radioactive contamination at the peaceful underground nuclear explosion sites “Craton-3” and “Crystal” in the Republic of Sakha (Yakutia). Journal of Environmental Radioactivity 2002a; 60: 221—234.

Gedeonov A, Petrov E, Savopulo I, Shkroev V. Plutonium-239, 240, plutonium-238 and γ-emitting radionuclides in environmental samples near peaceful underground nuclear explosion site “Taiga” (European North-East Russia). In: P.Børretzen, Torun Jølle, Per Strand (Eds.). Proceedings from the International Conference on Radioactivity in the Environment. 1-5 September, 2002, Monaco. NRPA; 2002b (available on CD).

Golikov V, Wallström E, Wöhni T, Tanaka K, Endo S, Hoshi M. Evaluation of conversion coefficients from measurable to risk quantities for external exposure over contaminated soil by use of physical human phantoms. Radiation and Environmental Biophysics 2007; V. 46 (4): 375—382.

Logachev VA. Peaceful nuclear explosions: guarantees of general and radiation safety. Moscow: Izd.AT; 2001(in Russian).

Logachev VA. Present radioecological situation at the sites of peaceful nuclear explosions at the territory of the Russian Federation. Moscow: Izd.AT; 2005 (in Russian).

Lurje AA. Radioecological study of consequences of the underground nuclear explosions with soil excavation in the north of the Perm Region. Part 1. Surface radionuclide contamination (soil, water, bottom sediments). ANRI 2002; (2): 21—30 (in Russian).

Ministry of the Russian Federation for Atomic Energy. USSR nuclear weapon tests and peaceful nuclear explosions. 1949 through 1990. Russian Federal Nuclear Center – VNIIEF; 1996.

Miretsky GI, Cyganov AS, Bylinkin SV, Popov AO, Ramzaev PV, Chugunov VV. 1997. Hygienic assessment of underground peaceful nuclear explosions in Russian Arctic. In: Extended abstracts from The Third International Conference on Environmental Radioactivity in the Arctic, vol. 2. Tromsø, Norway, June 1–5, 1997. Tromsø: TROMSPRODUCT AS; 1997, p. 152—155.

Norduke MD. The Soviet program for peaceful uses of nuclear explosions. ICRL-ID 124410 Rev 2. USA:US Department of Energy; 2000.

Ramzaev VP, Medvedev AYu, Repin VS, Timofeeva MA, Khramtcov EV. Radiation monitoring of the industrial nuclear explosion sites and evaluation of the doses to

the critical groups of population. Radiatsionnaya Gygiena 2010a; 3 (1): 33—39 (in Russian).

Ramzaev V, Mishin A, Golikov V, Argunova T, Ushnitski V, Zhuravskaya A, Sobakin P, Brown J, Strand P. Radioecological studies at the Kraton-3 underground nuclear explosion site in 1978–2007: a review. Journal of Environmental Radioactivity 2009a; 100, 1092—1099.

Ramzaev V, Mishine A, Golikov V, Strand P, Brown J. Surface ground contamination and soil vertical distribution of $^{137}$Cs around two underground nuclear explosion sites in the Asian Arctic, Russia. Journal of Environmental Radioactivity 2007; 92: 123—143.

Ramzaev VP, Repin VS, Khramtsov EV. Peaceful underground nuclear explosions: current issues on radiation safety for general public. Radiatsionnaya Gygiena 2009b; 2 (2): 27—33 (in Russian).

Ramzaev V, Repin V, Medvedev A, Timofeeva M, Khramtcov E, Yakovlev V. Radiological investigations at the site of the peaceful nuclear explosion “Taiga”: 1. Site description and current γ-ray dose. Submitted to Journal of Environmental Radioactivity 2010b.

Ramzaev V, Yonehara H, Hille R, Barkovsky A, Mishine A, Sahoo SK, Kurotaki K, Uchiyama M. Gamma-dose rates from terrestrial and Chernobyl radionuclides inside and outside settlements in the Bryansk Region, Russia in 1996–2003. Journal of Environmental Radioactivity 2006; 85, 205—227.

St-Petersburg Research Institute of Radiation Hygiene of the Ministry of Public Health of the Russian Federation. Radiation safety of the Republic of Sakha (Yakutia): Estimation of the current and reconstruction of the cumulated doses to the population due to the underground nuclear explosion “Crystal” and “Kraton-3”. Technical report under contract 2/2001, 19.03.2001. St-Petersburg: IRH; 2002 (in Russian).

United Nations Scientific Committee on the Effects of Atomic Radiation. Sources and effects of ionizing radiation, 2000 Report to the General Assembly with Scientific Annexes. Volume 1: Sources. New York: United Nations; 2000.

Yablokov AV. The myth about security and efficiency of the peaceful underground nuclear explosions. Moscow: CEPR; 2003 (in Russian).